7760

II

ANL-7760

Part III

Argonne National Laboratory

RADIOLOGICAL PHYSICS DIVISION ANNUAL REPORT

Environmental Studies

July 1969—December 1970

The facilities of Argonne National Laboratory are owned by the United States Government. Under the terms of a contract (W-31-109-Eng-38) between the U. S. Atomic Energy Commission, Argonne Universities Association and The University of Chicago, the University employs the staff and operates the Laboratory in accordance with policies and programs formulated, approved and reviewed by the Association.

MEMBERS OF ARGONNE UNIVERSITIES ASSOCIATION

The University of Arizona
Carnegie-Mellon University
Case Western Reserve University
The University of Chicago
University of Cincinnati
Illinois Institute of Technology
University of Illinois
Indiana University
Iowa State University
The University of Iowa
Kansas State University
The University of Kansas
Loyola University
Marquette University
Michigan State University
The University of Michigan
University of Minnesota
University of Missouri
Northwestern University
University of Notre Dame
The Ohio State University
Ohio University
The Pennsylvania State University
Purdue University
Saint Louis University
Southern Illinois University
The University of Texas at Austin
Washington University
Wayne State University
The University of Wisconsin

NOTICE

This report was prepared as an account of work sponsored by the United States Government. Neither the United States nor the United States Atomic Energy Commission, nor any of their employees, nor any of their contractors, subcontractors, or their employees, makes any warranty, express or implied, or assumes any legal liability or responsibility for the accuracy, completeness or usefulness of any information, apparatus, product or process disclosed, or represents that its use would not infringe privately-owned rights.

Printed in the United States of America
Available from
National Technical Information Service
U.S. Department of Commerce
5285 Port Royal Road
Springfield, Virginia 22151
Price: Printed Copy $3.00; Microfiche $0.95

ANL-7760
Part III
Biology and
Medicine

ARGONNE NATIONAL LABORATORY
9700 South Cass Avenue
Argonne, Illinois 60439

RADIOLOGICAL PHYSICS DIVISION ANNUAL REPORT

Environmental Studies

July 1969 through December 1970

R. E. Rowland, Division Director
P. F. Gustafson, Associate Division Director

Preceding Report: ANL-7615, July 1968-June 1969

FOREWORD

This is the third and final volume of the Radiological Physics Division Annual Report. It encompasses work done from July 1969 through December 1970. Environmental Studies by nature are dependent upon weather, and the major field effort occurs from April through October. It is intended that Part III of subsequent Annual Reports will cover the calendar year, thus permitting a more complete presentation of the results of that particular field year to appear.

Environmental Studies include Atmospheric Sciences, Terrestrial Ecology, the Radiological Physics Division portion of the Great Lakes Research Program, and Bioenvironmental Studies (formerly entitled Fallout Studies).

Atmospheric Sciences still provide some meteorological support, but the major effort is devoted to research. Areas of emphasis have developed around urban meteorology, atmospheric chemistry, and lake meteorology, the latter being an integral part of the overall Great Lakes program. Terrestrial Ecology has, and will continue to, focus on water balance and nutrient (particularly trace elements) flow through local ecosystems. Particular attention has been devoted to tritium behavior between various trophic levels. The Great Lakes research in Radiological Physics is largely field work including physical measurements of existing thermal discharges into Lake Michigan, and investigations of the distribution of radionuclides from the Big Rock Nuclear Plant in water, sediments, and biota. Use of the Grand River outflow as an analog of a power plant discharge has begun as a joint effort between Argonne (including members of the Chemistry Division) and staff of the Great Lakes Research Division at the University of Michigan. The Bioenvironmental Studies program continues to follow fallout radioactivity in air, soil, food, and man, although part of this program has quite naturally switched over into the Great Lakes work.

In the coming year research in Environmental Studies will become even more sharply focused on the environmental problems attendant on the siting and operations of nuclear power plants.

TABLE OF CONTENTS

Environmental Studies

P. F. Gustafson and Paul Frenzen, Section Heads

GREAT LAKES RESEARCH PROGRAM

Thermal Plume Measurements 1
GERALD P. ROMBERG, WILLIAM PREPEJCHAL, and DONALD M. NELSON

Radionuclide Concentrations Near the Big Rock Point Nuclear Power Station 18
DONALD M. NELSON, GERALD P. ROMBERG, and WILLIAM PREPEJCHAL

Thermoluminescent Dosimetry of Aquatic Life in Transitu through a Reactor Cooling Condenser 26
B. G. OLTMAN, GERALD P. ROMBERG, WILLIAM PREPEJCHAL, and DONALD M. NELSON

The Concentration of Mercury in Fish Taken from Lakes Erie, Michigan, and Superior 30
D. N. EDGINGTON, M. M. THOMMES, A. F. GOSSMAN, and R. M. CUTLER

Minor Element Geochemistry of Lake Michigan Ferromanganese Nodules 39
D. N. EDGINGTON and EDWARD CALLENDER

Micrometeorological Measurements over Lake Michigan 45
PAUL FRENZEN

Eddy-Correlation Measurements of Atmospheric Fluxes over Lake Michigan 50
B. B. HICKS

Refractometer Construction and Testing 60
H. C. MARTIN

Surface Heat Energy Budget over Lake Michigan: A Preliminary Report 65
B. B. HICKS, H. C. MARTIN, and R. L. HART

Wind Stress over Lake Michigan by Variance Reduction Analysis of LIHT Anemometer Measurements 70
PAUL FRENZEN and R. L. HART

METEOROLOGY AND AIR POLLUTION

The Determination of Chimney Plume Rise Theory and Practice 82
HARRY MOSES

Mixing Heights, Ventilation Rates, and Observed Ground SO_2 Concentrations 84
HARRY MOSES, DONALD F. GATZ, ARTHUR C. STRONG, and GUNTHER A. ZERBE

Air Pollution Abatement by Selective Fuel Switching 109
J. E. CARSON, E. W. KLAPPENBACH, and J.-W. LIN

Sulfur Hexafluoride: Atmospheric Background Concentrations. Preliminary Results 111
DONALD F. GATZ and JAMES E. CARSON

Sulfur Dioxide Pollution Characteristics of Chicago Lake Breeze Circulations 121
DONALD F. GATZ

Urban-Rural Differences in Temperature and Dew Point in the Chicago Area 137
BERNICE ACKERMAN

Surface Atmospheric Lead and What Deposits on Human Alveoli 156
S. E. MUNIAK

Wind Tunnel Facility 163
ERICH J. PLATE

The Anatomy of an Air Pollution Episode 165
HARRY MOSES, D. F. GATZ, J. E. CARSON, F. C. KULHANEK and G. A. ZERBE

Meteorological Aspects of Air Pollution Episodes 192
HARRY MOSES, JOHN P. BRADLEY, and EDWARD W. KLAPPENBACH

TERRESTRIAL ECOLOGY

Tritium Studies Quantify Water Movement in an Old Field Ecosystem 223
C. F. JORDAN and J. R. KLINE

Transpiration Measurement in Pines Using Tritiated Water as a Tracer 233
J. R. KLINE, C. F. JORDAN and R. C. ROSE

FALLOUT STUDIES

Recent Trends in Radioactive Fallout 245
P. F. GUSTAFSON, D. M. NELSON, S. S. BRAR, and S. E. MUNIAK

High Altitude Radioactivity Measurements Made from the Argonne Site 249
P. F. GUSTAFSON and R. B. KEENER

METHODS AND TECHNIQUES

A Semiautomatic Method of Neutron Activation Analysis with Application to Environmental Studies 251
D. N. EDGINGTON and H. F. LUCAS, JR.

An Automatic Sequential Rain Sampler 264
D. F. GATZ, R. F. SELMAN, R. K. LANGS, and R. B. HOLTZMAN

Thermal Neutron Activation Analysis of Purified Biological Membranes 265
S. S. BRAR, D. M. NELSON, Y.-E. RAHMAN, and E. A. CERNY

PUBLICATIONS 269

THERMAL PLUME MEASUREMENTS

Gerald P. Romberg, William Prepejchal, and Donald M. Nelson

Introduction

Considerable public concern exists over the possible effects on lake ecology of siting nuclear power plants along the shores of the Great Lakes, particularly Lake Michigan, for which ten new plants are scheduled for completion by 1976. Efficient production of electric power by the steam turbine process requires a vast heat sink, a body of material which will remain at a low temperature regardless of the amount of heat added to it. This is true irrespective of the raw energy source of the plant; that is, nuclear energy, coal, gas, or oil. Experience has shown that large bodies of water constitute the most economically efficient heat sink, though the atmosphere is also usable. A typical plant using lake water for cooling returns this water to the lake heated 6 to 12°C above the intake temperature in the form of a plume of warm water. This thermal input is popularly referred to as "thermal pollution," with the term pollution implying that some damage will be done to the water quality, the biota, or the environment in general.

It is essential to have detailed knowledge of the physical characteristics of a thermal plume before a comprehensive biological effects study program can be formulated. Such factors as the regional increase in temperature of lake water, its extent and degree are extremely important factors in determining what organisms could be affected, and what effects are likely to occur. In addition to supplying information defining boundaries for study of biological systems, measurements of the parameters which affect the plume and the plume configuration are useful input to the plume modeling

effort by J. Asbury and J. Tokar of the Argonne Center for Environmental Studies.

Procedures

Commonwealth Edison's 45-year-old fossil fuel power plant located on the shore of Lake Michigan at Waukegan, Illinois, approximately 40 miles north of Chicago was the area investigated. The water intake and discharge by the plant are through channels at the shoreline and are separated by a breakwater.

In order to measure the size and shape of thermal plumes, it was first necessary to establish known positions on the lake surface. This was accomplished by deploying a grid of identifiable fixed buoys. The location of each buoy was determined from multiple sextant sightings taken to prominent structures in the area. These data were later processed manually or by a computer program developed by I. Abu-Shumays, D. Phillips, and M. Prastein of the Argonne Applied Mathematics Division to yield locations.

Temperature measurements were taken from an 18-foot, outboard powered, fiberglass boat. Thermistor temperature probes were located at depths of 1, 3, 6, and 9 feet along an aluminum boom mounted along the gunwale of the boat. An additional thermistor affixed to a float was used for surface temperature. Temperatures were measured along lines between buoys while the boat was operated at near constant speed. In each minute of running time, each temperature sensor was interrogated sequentially four times, yielding a total of 20 data points, four at each depth, spaced at approximately 100 feet. Lake depth readings were also taken four times each minute. Because of the variable nature of the plume, the maximum measuring time over which a plume is defined was limited to two hours. Data have been recorded manually, but automated equipment is being assembled which should decrease the time required to define the plume. Other relevant parameters such as sea state, wind velocity and direction, wet bulb and dry bulb temperature, lake current velocity and direction, plant intake and discharge water temperature, as well as discharge channel

velocity, were measured and recorded. Power levels and additional operating details were provided by the Commonwealth Edison Company.

Five scaled charts of the buoy grid were constructed, and the observed temperatures plotted for each of the five depths (surface to nine feet). Isotherms were then drawn and used to yield information on surface areas and volumes of the plume at various temperatures and depths.

General Lake Conditions

We have elected to categorize two general lake conditions which we define as stable and upwelling. Stable conditions are typified by a history of onshore wind direction with lake temperature remaining constant or decreasing slightly away from the shoreline. These conditions produce considerable wave action near shore making operation in the plume region difficult. Consequently, fewer plumes have been measured under stable conditions. Upwelling conditions, those produced by a history of offshore wind direction, have been sampled most frequently. During these times the warmer surface waters are moved offshore while the cooler bottom water comes to the surface near shore, resulting in lake surface temperatures which increase with distance from shore. Water temperature inshore can change rapidly as a result of these two types of lake condition, as was observed over a two-day period in July when conditions changed from stable to upwelling and the near shore water temperature dropped 6°C.

To define and evaluate a plume it is necessary to establish the ambient lake temperature (that temperature which would exist in the plume region were the plume not present). Our method of selecting ambient temperature is to use the lowest observed temperature adjacent to the plume. During upwelling conditions this determination is more difficult and indicates that in future work, additional effort must be directed towards obtaining more detailed temperature distribution information in regions near the plume but outside the influence of the plume. In most cases the ambient value selected is within 1 or 2°C below the lowest temperature isotherm that can be closed.

Plumes measured during stable lake conditions have boundaries well defined to within a few tenths of a degree above ambient temperature and consequently tend to be larger in size and heat content than those measured during upwelling conditions. During upwelling, warm water exists offshore and as the heated plume water gets cooler with distance from the plant, a region is eventually encountered where heated plume water merges with the normally occurring warmer lake water at the same temperature (see Figure 8). This then places a limit on the lowest temperature isotherm that can be closed. Because the largest fraction of area and heat content in a given plume exists in the regions of lowest temperature, determinations of total area and heat content for plumes measured during upwelling conditions may be suspect. However, the regions of highest temperature within the plume, which are the regions of greatest potential biological stress, remain well defined.

Field measurements for 1970 were limited to the months of July through September, during which time techniques and procedures were constantly being modified and improved. The relatively restricted time range of the measurements, as well as the developmental nature of our work, must be considered before attempting to draw broad, general conclusions. Also, some data still exist in raw form and have not been presented at this time.

Results

Three example plumes are shown in Figures 1, 2 and 8 to illustrate the variance both in plume direction and lake conditions. These observations were made on August 5, August 12 and September 23, 1970. Detailed characteristics for the three plumes are given in Tables 1-12. Direction of the plume is dominated by lake current and ranged from north to south as shown in Figures 1 and 2. A sharp temperature gradient is seen on the outer edge of these plumes where the lake current and the discharge water meet. The area influenced by water at a given temperature is generally greatly reduced with depth as illustrated in the plotted isotherms for the five depths shown in Figures 2-6. This reduction in area affected is due

to the buoyant characteristics of the warm water as can be seen in the cross-section plots in Figure 7. When large swells are present, however, the plume is mixed to greater depth resulting in a smaller surface area shown in Figure 8. Cross-section plots in Figure 9 show well-mixed lake water to 9 feet and also the existance of upwelling lake conditions.

TABLE 1. General Conditions Existing on 5 August, 1970

Time: 16:27 to 18:04 CST
Lake: Upwelling
Water temperature: 22.3°C
Lake current: Surface 0.5 m/sec to 360°
Air temperature: Dry bulb = 78.7°C, wet bulb = 74.2°C
Wind: 8 mph from 120°
Plant output: 730 megawatts
Plant ΔT: 4.5°C
Discharge volume: 37 m^3/sec
Discharge velocity: 1.4 m/sec
Discharge temperature at plant: 26.7°C

Figure 1 is the surface and 6-foot isotherm plots of the plume for 5 August, 1970, 16:27-18:04 CST. Tables 2-4 give plume characteristics. The assumed ambient temperature is 22.3°C, and the lowest temperature isotherm is 23°C.

TABLE 2. Area of Plumes at Various Depths on 5 August, 1970

Depth in feet	Area (x 10^4 m^2)
0	127
1	120
3	96
6	11
9	3

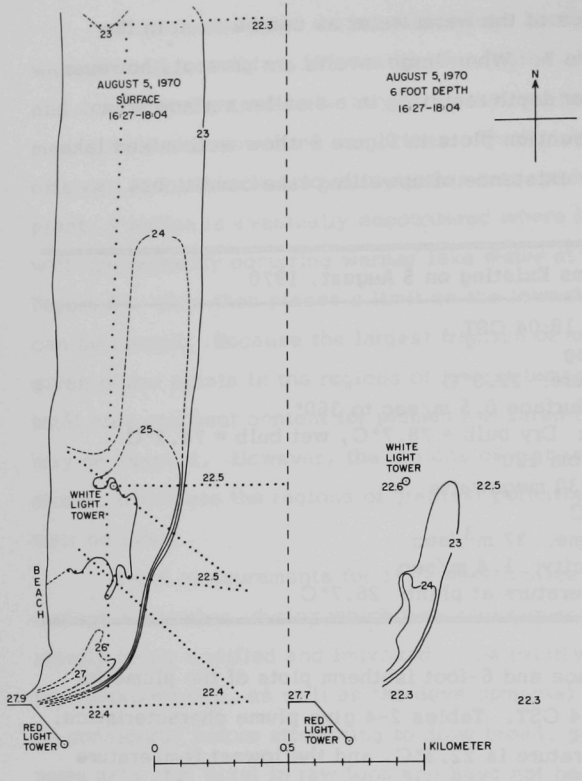

FIG. 1.--Surface and 6-foot depth isotherms for 5 August, 1970. Dots on the surface plot indicate location of data points.

TABLE 3. Volume of Heat Content of Plume as a Function of Depth on 5 August, 1970

Depth in feet	Volume (x 10^4 M^3)	Heat content (x 10^9 kg-cal)
0 - 3	104	1.84
3 - 6	49	0.88
6 - 9	6.4	0.10

TABLE 4. Surface, Volume, and Heat Distribution as a Function of Temperature on 5 August, 1970

Degrees C above ambient	Surface area ($\times 10^4$ m^2)	Volume ($\times 10^4$ m^3)	Heat content ($\times 10^9$ kg-cal)
0.7 - 1.7	72	90	1.07
1.7 - 2.7	31	52	1.13
2.7 - 3.7	21	16	0.52
3.7 - 4.7	2	2	0.08
>4.7	1	0.3	0.02

TABLE 5. General Conditions Existing on 12 August, 1970

Time: 12:00 to 13:26 CST
Lake: Stable
Water temperature: 23.0 - 23.5°C
Lake current: 0.18 m/sec to 180°
Air temperature: Dry bulb = 25.7°C, wet bulb = 23.4°C
Wind: 4 m/sec from 120°
Plant output: 925 megawatts
Plant ΔT: 7.3°C
Discharge volume: 49 m^3/sec
Discharge velocity: 1.6 m/sec
Discharge temperature at plant: 31.1°C

Figures 2-6 represent isotherm plots of the plume for 12 August, 1970 for depths to 9 feet. Figure 7 shows isotherm plots of vertical sections between numbered buoy positions on surface plot. Tables 6-8 give plume characteristics. The assumed ambient temperature is 23°C and the lowest temperature isotherm is 24°C.

TABLE 6. Area of Plume at Various Depths on 12 August, 1970

Depth in feet	Area ($\times 10^4$ m^2)
0	250
1	210
3	180
6	39
9	24

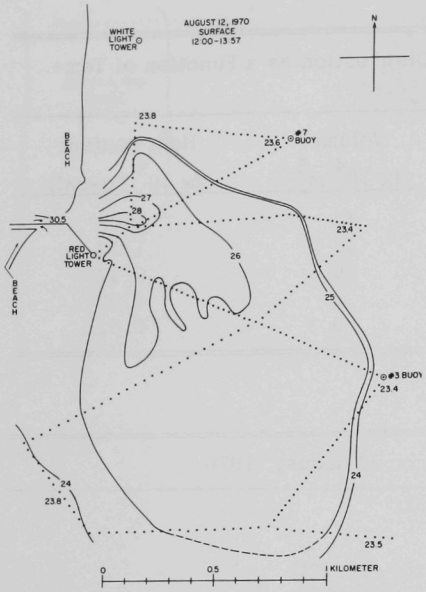

FIG. 2.--Surface isotherms for 12 August, 1970. Dots indicate location of data points.

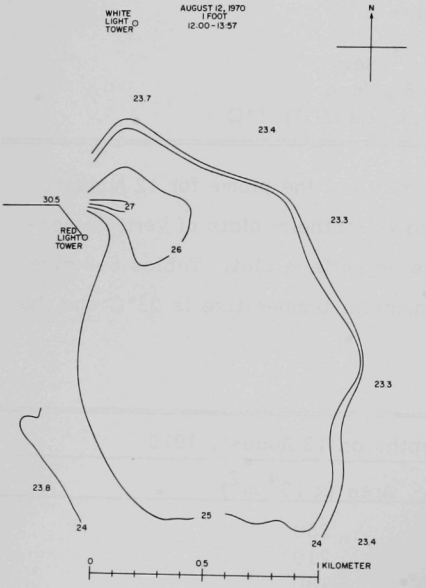

FIG. 3.--Isotherms for 1-foot depth on 12 August, 1970.

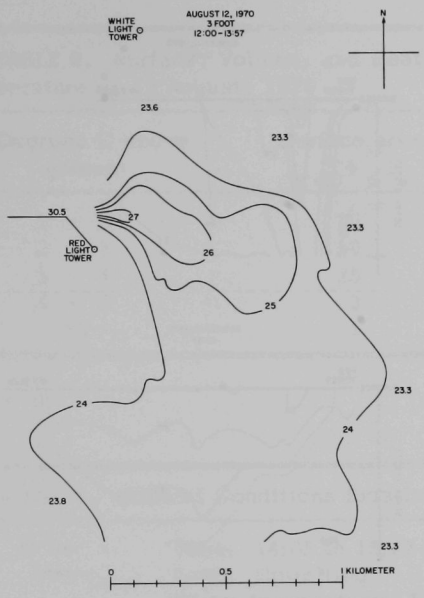

FIG. 4.--Isotherms for 3-foot depth on 12 August, 1970.

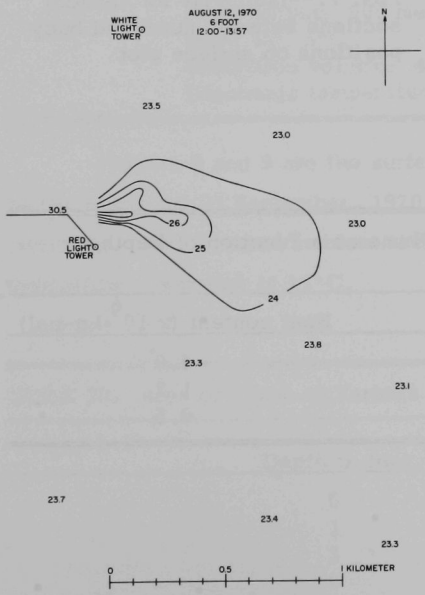

FIG. 5.--Isotherms for 6-foot depth on 12 August, 1970.

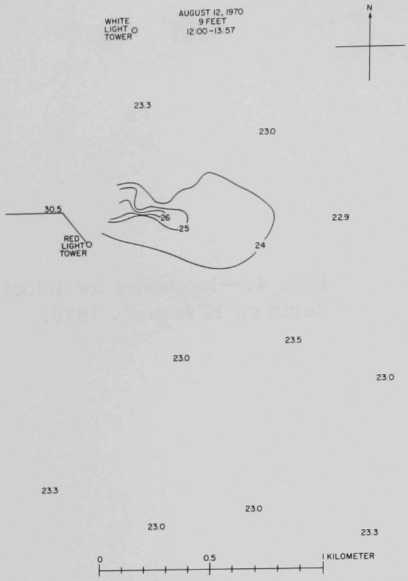

FIG. 6.--Isotherms for 9-foot depth on 12 August, 1970

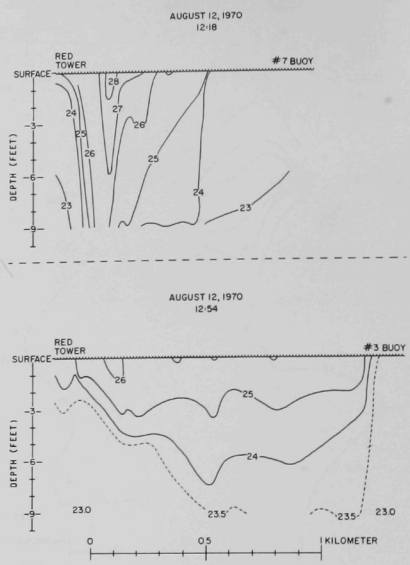

FIG. 7.--Isotherms for vertical sections between numbered buoy positions on surface plot

TABLE 7. Volume and Heat Content of Plume as a Function of Depth on 12 August, 1970

Depth in Feet	Volume (x 10^4 m^3)	Heat content (x 10^9 kg-cal)
0 - 3	190	4.0
3 - 6	100	1.7
6 - 9	30	0.5

TABLE 8. Surface, Volume, and Heat Distribution as a Function of Temperature on 12 August, 1970

Degrees C above ambient	Surface area ($\times 10^4$ m^2)	Volume ($\times 10^4$ m^3)	Heat content ($\times 10^9$ kg-cal)
1 - 2	70	190	2.8
2 - 3	150	110	2.8
3 - 4	25	18	0.6
4 - 5	3	2	0.07
>5	1	0.1	0.01

TABLE 9. General Conditions Existing on 23 September, 1970

Time: 14:05 to 15:27 CST
Lake: Upwelling
Water temperature: 13°C
Lake current: 0.09 m/sec to 60°
Wind: 8 mph from 60°
Plant output: 900 megawatts
Plant ΔT: 5°C
Discharge volume: 49 m^3/sec
Discharge temperature at plant: 19.4°C

Figures 8 and 9 are the surface plume plot and the vertical sections of the plume for 23 September, 1970. Tables 10-12 give plume characteristics. The assumed ambient temperature is 13°C and the lowest temperature isotherm is 15°C.

TABLE 10. Area of Plume at Various Depths on 23 September, 1970

Depth in feet	Area ($\times 10^4$ m^3)
0	21.8
1	19.7
3	19.0
6	9.6
9	4.2

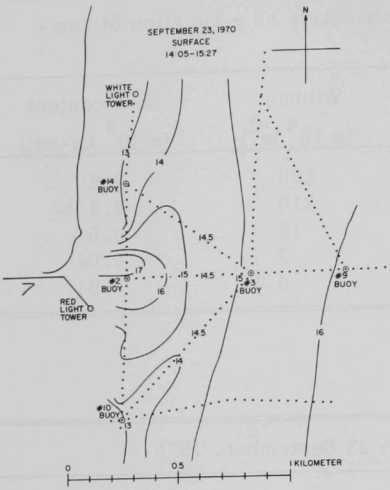

FIG. 8.--Surface isotherms for 23 September, 1970. Dots indicate location of data points.

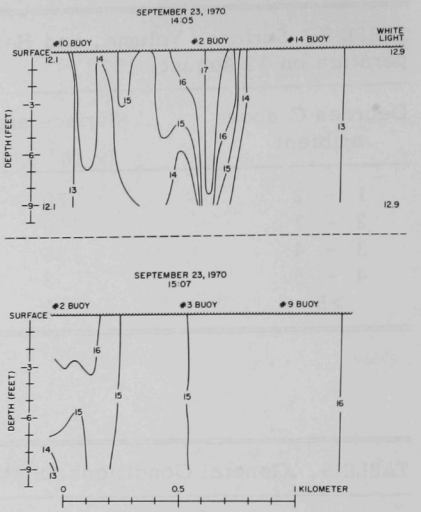

FIG. 9.--Isotherms for vertical sections between numbered buoy positions.

TABLE 11. Volume and Heat Content of Plume as a Function of Depth on 23 September, 1970.

Depth, feet	Volume ($\times 10^4$ m^3)	Heat Content ($\times 10^9$ kg-cal)
0 - 3	18.1	0.53
3 - 6	13.1	0.37
6 - 9	6.3	0.18

TABLE 12. Surface, Volume, and Heat Distribution as a Function of Temperature on 23 September, 1970.

Degrees C above ambient	Surface area ($\times 10^4$ m^2)	Volume ($\times 10^4$ m^3)	Heat content ($\times 10^9$ kg-cal)
2 - 3	13.4	26.5	0.66
3 - 4	6.2	7.8	0.27
>4	2.2	3.2	0.14

The distribution of area, volume, and heat content in all plumes evaluated to date are given in Tables 13-17. Values are expressed as per cent of the total to provide easy comparison under widely varying plume sizes. Median values are included to indicate typical conditions.

TABLE 13. Surface Area of Plume as a Function of Temperature above ambient

Ambient temp., °C	Total enclosed area (x 10^4 m^2)	% of area in given temperature range 1-2°C	2-3°C	3-4°C	4-5°C	>5°C	
17	51	40	53	6	1	<0.1	(a)
12	55	--	66	28	3	2	(a)
12	230	29	41	27	3	0.6	(a)
21.5	40	79	21	<0.1	<0.1	<0.1	
22.3	130	56	24	17	2	0.6	
23	250	28	60	11	1	0.3	
23.5	260	12	60	25	2	1	
23	67	66	30	3	1	<0.1	(a)
23	270	69	25	6	0.4	0.2	
17.5	36	53	41	4	2	<0.1	(a)
18.5	33	90	9	1	<0.1	<0.1	(a)
13	32	47	20	24	9	<0.1	(a)(b)
13	22	--	61	28	10	<0.1	(a)(b)
Median values	55	50	30	11	2	<0.1	

(a) Upwelling.
(b) Large swells.

Pertinent facts shown are that typically 60% of the heat content is in the upper three feet of water and that over 70% of the heat content is in water no warmer than 3°C above ambient. Also of interest is that typically less than 1% of the total enclosed plume volume contains water heated more than 5°C above ambient.

The maximum distances (in meters) that water at given temperatures above ambient extended from the point of discharge are shown in Table 18.

Summary

1. Numerous lake temperature surveys were made near the warm water discharge from a 1100-MW fossil fuel electric generating plant located on the west shore of Lake Michigan at Waukegan, Illinois.

TABLE 14. Volume of Plume Water as a Function of Temperature above ambient

Ambient temp., °C	Total vol. of enclosed plume (x 10^4 m^3)	% of volume at given temperature above ambient					
		1-2°C	2-3°C	3-4°C	4-5°C	>5°C	
17	72	51	40	9	0.1	<0.1	(a)
12	50	--	64	30	4	1	(a)
12	440	64	25	10	1	0.4	(a)
21.5	35	92	8	<0.1	<0.1	<0.1	
22.3	160	56	32	10	1	0.2	
23	320	58	36	6	0.6	<0.1	
23.5	390	52	39	7	1	0.5	
23	77	75	22	3	0.4	<0.1	(a)
23	210	77	18	4	0.5	<0.1	
17.5	63	77	22	1	<0.1	<0.1	(a)
18.5	23	85	14	1	<0.1	<0.1	(a)
13	68	60	22	13	4	<0.1	(a)(b)
13	38	--	70	21	9	<0.1	(a)(b)
Median values	72	64	25	7	0.6	<0.1	

(a) Upwelling.
(b) Large swells.

2. These measurements allowed the construction of isotherms to define the various temperature regions of the plume.

3. Plume configurations ranged from north through south and both stable and upwelling lake conditions were encountered as is illustrated in three representative plumes.

4. Determination of ambient lake temperature, which is necessary to relate the plume to the unperturbed lake, is difficult and especially so during upwelling conditions.

5. The calculated size and heat content of the observed plumes varied by a factor of ten and generally tend to be smaller for upwelling conditions.

6. Mean values for the distribution of heat content for all plumes analyzed to date show that typically 60% of the heat content is in the upper

TABLE 15. Heat Content of Plume as a Function of Temperature above ambient

Ambient temp., °C	Total heat content of enclosed plume (x 10^9 kg-cal)	% of heat content in given temperature range 1-2°C	2-3°C	3-4°C	4-5°C	>5°C	
17	1.5	36	48	15	0.3	<0.1	(a)
12	1.5	--	55	35	7	3	(a)
12	8.8	48	31	17	3	1	(a)
21.5	0.5	91	9	<0.1	<0.1	<0.1	
22.3	2.8	37	39	19	3	0.7	
23	6.2	44	45	10	1	0.2	
23.5	6.5	37	46	12	3	2	
23	1.4	64	29	6	0.7	<0.1	(a)
23	3.8	64	26	9	1	0.6	
17.5	0.9	67	31	2	0.4	<0.1	(a)
18.5	0.7	76	19	4	<0.1	<0.1	(a)
13	1.4	43	26	21	10	<0.1	(a)(b)
13	1.1	--	61	25	13	<0.1	(a)(b)
Median values	1.5	44	31	12	1	<0.1	

(a) Upwelling.
(b) Large swells.

3 feet of water and over 70% is contained in water less than 3°C above ambient.

7. Mean values for the distribution of plume volume show that typically less than 1% of the total enclosed plume volume contains water more than 5°C above ambient.

We are indebted to the many laboratory employees who supplemented our crew and especially to Michael M. Thommes and Paul Siebold* who were our most frequent helpers. Thanks are also due to Peggy Wagner† for endless hours of data plotting which made this contribution possible. The ingenuity and able assistance of

*Summer employee, 1970.

†Neighborhood Youth Corp Program, Summer 1970.

TABLE 16. Volume of Plume as a Function of Distance below Surface

Total enclosed volume (x 10^4 m^3)	Distance below surface, feet 0 - 1	1 - 3	3 - 6	6 - 9	
72	20	33	31	16	(a)
50	29	35	24	12	(a)
440	18	35	30	17	(a)
35	35	40	19	6	
160	24	41	31	4	
320	22	37	32	9	
390	21	40	34	6	
77	11	42	36	1	(a)
210	31	37	25	7	
63	17	28	32	23	(a)
23	31	32	27	10	(a)
68	14	26	38	22	(a)(b)
38	17	31	35	17	(a)(b)
Median values 72	21	35	31	10	

(a) Upwelling.
(b) Large swells.

TABLE 17. Heat Content of Plume as a Function of Distance below Surface

Total heat content of enclosed plume (x 10^9 kg-cal)	Distance below surface, feet 0 - 1	1 - 3	3 - 6	6 - 9	
1.5	21	32	30	17	(a)
1.0	41	49	35	16	(a)
8.8	22	37	27	14	(a)
0.5	35	41	18	6	
2.8	24	41	32	4	
6.2	26	39	27	8	
6.1	26	41	28	5	
1.4	24	38	31	7	(a)
3.8	32	37	24	7	
0.9	19	30	31	21	(a)
0.7	54	24	16	6	(a)
1.4	16	27	37	20	(a)(b)
1.1	18	31	34	17	(a)(b)
Median values 1.4	24	37	30	8	

(a) Upwelling.
(b) Large swells.

TABLE 18. Extent of Heating

	ΔT, °C					
	>1	>1.5	>2	>3	>4	>5
Surface	(a)	1500	1050	750	400	300
3-foot depth	1050	(a)	750	600	350	(a)
9-foot depth	750	(a)	550	400	(a)	(a)

(a) Insufficient data.

Mr. Richard Selman of Central Shops in design and construction of booms, supports, and sundry devices is greatly appreciated.

RADIONUCLIDE CONCENTRATIONS NEAR THE BIG ROCK POINT NUCLEAR POWER STATION

Donald M. Nelson, Gerald P. Romberg, and William Prepejchal

Introduction

One aspect of Argonne's program to study the effects of siting large power reactors on the Great Lakes deals with the release of radioactivity into the aquatic environment and its subsequent uptake into biological systems. The most obvious and most easily measured effect is the increased concentration of certain radionuclides in the vicinity of the plant. The measurement of these isotopes within organisms as a function of distance from their source along with knowledge of the emission rate of the source allows a realistic assessment of any potential radiation hazards under present emission guidelines. Also, knowledge of the fate of low level wastes allows one to make more accurate predictions in the event of any larger unexpected releases.

For these reasons a survey of the gamma-ray emitting nuclides present in the biota near an existing power reactor was initiated by Argonne during 1970. The only operating reactor on Lake Michigan during 1970 was the Big Rock Point station operated by Consumers Power. This 70-MW boiling water reactor near Charlevoix, Michigan, has been in operation since 1963, so that radionuclide concentrations may be at or near their equilibrium values for most isotopes. During 1970 Argonne personnel made three sampling trips to Charlevoix (late June, late July, late October), collecting numerous water, sediment, and biological samples. The gamma-ray emitting nuclides in these samples were determined using low background NaI(Tl) detectors and multichannel pulse height analyzers.

Water

Two types of water samples were collected near the Big Rock reactor: surface water samples to be analyzed for tritium and samples collected with the Battelle Large Volume Ocean Sampler in which approximately 280 liters

of water are forced through a filter and ion-exchange resin bed combination. Only a limited set of these latter samples will be discussed in the present report.

The radioactive effluent from the Big Rock reactor (which is mixed with the cooling water and discharged through a shoreline channel) consists of a very low-level, continuous discharge plus periodic releases of higher activity waste. This variability of source strength in addition to the variable nature of lake currents decreases the usefulness of short duration samples taken at some distance from the source. However, samples taken at the discharge point before and during a release are instructive. Table 1 shows the concentrations of five of the major gamma-ray emitting components (^{134}Cs, ^{137}Cs, ^{95}Zr, ^{65}Zn, ^{60}Co) in three Battelle samples. The first was collected 18 October, 1970 in the discharge channel the day before a

TABLE 1. Radioactivity Concentrations in Lake Water

Sample	Nuclide				
	^{134}Cs, pCi/l	^{137}Cs, pCi/l	^{95}Zr, pCi/l	^{65}Zn, pCi/l	^{60}Co, pCi/l
In channel before release					
Filter	0.01	< 0.01	< 0.005	0.14	< 0.005
Cation resin	0.032	0.048	0.005	<.05	< 0.05
In channel during release					
Filter	5.0	17.0	0.24	33.0	1.1
Cation resin No. 1	16.0	53.0	0.1	0.43	0.04
Cation resin No. 2	26.0	82.0	< 0.1	<0.05	< 0.05
1/4 mile off channel during release					
Filter	0.30	0.87	0.01	1.3	0.05
Cation resin	0.55	1.8	0.01	0.09	< 0.005

scheduled release, the second was collected the following day, also from the channel, but about halfway through an 8-hour release, while the third

was collected about 1 hour later and 1.4 mile out into the lake directly offshore from the discharge point (with the discharge still in progress). From these three samples it would seem that 1) the vast majority of radioactivity is released under controlled conditions, 2) the concentrations decrease rapidly once in the lake, 3) most ^{65}Zn and ^{60}Co (as well as ^{58}Co and ^{54}Mn, which we did not measure quantitatively) are associated with particulates, 4) most ^{137}Cs and ^{134}Cs are present as cations, and 5) cationic values of Cs should be looked upon as lower limits (in the second sample where two cation resin beds were placed in series, it is assumed that the first bed has saturated and the loosely held Cs is being displaced to the second bed).

Near-Shore Organisms

An important part of the present study deals with defining the area of influence of the source, that is measuring concentration in some pertinent organisms as a function of distance from the source. Obviously the only organisms useful for this purpose are those which either are attached to the bottom or have a limited range. The most convenient organisms from a collection standpoint are those living in the near-shore waters which can be gathered by hand.

The near-shore organisms collected in the present study consisted of those which seemed most abundant and easiest to gather. In general, samples of about one hundred grams wet weight were collected. These were counted wet and then oven dried at 100°C to get dry weights. All data are reported on a dry weight basis.

Table 2 summarizes the concentration values for the five radionuclides reported in water as well as potassium (measured by the naturally occurring ^{40}K) in crayfish, water snails, the aquatic macrophytes Potomogeton sp. and Ranunculus sp., the green algae Chara sp., Cladophora sp. and Periphyton. As expected, all species show marked decreases in concentration with increasing distance from the discharge point for most nuclides. Of the five isotopes, only the ^{95}Zr concentrations seem to remain constant, indicating that this nuclide is not primarily coming from the

TABLE 2. Radioactivity Concentrations in Near-Shore Organisms.

Sample	Feet from outfall	^{134}Cs, pCi/g	^{137}Cs, pCi/g	^{95}Zr, pCi/g	^{65}Zn, pCi/g	^{60}Co, pCi/g	K, g/Kg	$\frac{^{65}Zn}{^{60}Co}$	$\frac{^{65}Zn}{^{134}Cs}$	$\frac{^{137}Cs}{^{134}Cs}$
Crayfish[a]	14,000 west	0.25	1.4	<0.4	3.8	<0.2	12	>19	15	5.6
Crayfish	4,000 "	0.57	1.9	<0.4	12.4	0.6	15	21	22	3.3
Crayfish	2,500 "	0.73	2.2	0.2	15.1	0.73	11	21	21	3.0
Crayfish [a]	< 500	4.5	15	1.7	118	2.32	--	51	26	3.3
Crayfish	Outfall	10.1	54	3.8	620	17.4	--	38	61	5.3
Crayfish	Outfall	7.4	35	1.6	365	6.95	--	53	49	4.7
Crayfish	3,000 east	0.73	3.8	0.14	51	0.23	11	222	70	5.2
Crayfish	5,000 "	0.58	3.4	<0.4	61	0.5	16	122	105	5.9
Crayfish [a]	14,000 "	0.35	1.9	0.52	15.6	0.14	9	111	45	5.4
Snails	Outfall	6.37	25.8	2.3	184	13.8	--	13	29	4.0
Snails	1,500 east	0.80	4.92	0.5	47	6.28	13	7	59	6.1
Potamogeton sp.	3,000 west	<0.1	0.18	3.8	6.6	0.59	14	11	>70	>2
Potamogeton sp.	2,500 "	0.32	0.43	3.4	16.3	0.40	13	41	51	1.3
Potamogeton sp.	1,500 "	0.45	0.50	3.4	23.1	0.29	<10	80	51	1.1
Potamogeton sp.	500 "	<0.2	0.63	2.6	20.2	0.20	14	408	>100	>3
Potamogeton sp.	500 east	3.1	6.3	4.2	285	15.6	18	18	92	2.0
Potamogeton sp.	1,500 "	<0.5	1.8	3.2	152	2.95	19	52	>300	>3
Potamogeton sp.	3,000 "	0.47	1.0	3.2	66	2.08	16	32	140	2.1
Potamogeton sp.	4,000 "	0.49	0.77	2.4	46	1.94	11	24	94	1.6
Ranunculus sp.	3,000 east	1.6	4.6	0.6	266	2.14	30	106	141	2.9
Ranunculus sp.	4,000 "	0.6	2.6	<0.4	177	3.70	30	48	295	4.3
Chara sp.	1,500 east	1.8	2.9	<2	178	13.7	<30	13	99	1.6
Cladophora sp.	4,000 west	0.4	1.6	30.8	4.4	0.22	86	20	11	4.0
Cladophora sp.	3,000 "	<0.15	1.7	19.2	2.9	0.16	50	18	>19	>11
Cladophora sp.	2,000 "	2.1	7.1	20	100	3.9	59	26	49	3.4
Cladophora sp.	< 500 east	15.2	39.4	35.2	344	23.0	38	15	23	2.6
Cladophora sp.	500 "	4.3	16.8	15.8	179	6.9	43	26	42	3.9
Cladophora sp.	1,000	1.7	6.3	10.2	58	1.7	49	34	34	3.7
Cladophora sp.	1,500 "	1.0	4.1	14.8	47	1.2	57	39	47	4.1
Cladophora sp.	8,000 "	1.3	3.5	27.2	11.0	0.64	58	17	8	2.7
Periphyton [a]	14,000 west	0.43	1.79	1.4	1.9	0.05	3	38	4	4.1
Periphyton [a]	< 500	38.4	86.5	17.9	1980	124	--	16	51	2.3
Periphyton [a]	14,000 east	1.6	3.4	8.1	22.1	0.77	5	29	14	2.1

[a] Sample supplied by Michigan Department of Natural Resources.

plant, but rather from atmospheric fallout. It could be expected that ^{137}Cs should also have a large input from fallout; however, the constant ^{137}Cs to ^{134}Cs ratio indicates that the primary ^{137}Cs input is from the plant (at least out to distances of a few miles).

Figures 1 and 2 graphically present the concentration versus distance for ^{65}Zn and ^{137}Cs. These composite graphs were constructed by plotting each species on a separate graph and then adjusting the concentration scales by eye until the best fit for all species was obtained. The relative

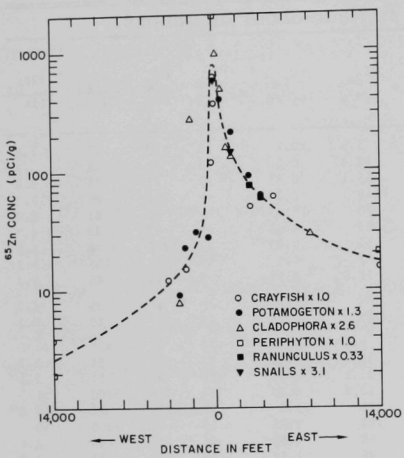

FIG. 1.--Normalized ^{65}Zn concentrations in shoreline organisms as a function of distance from Big Rock Power Station.

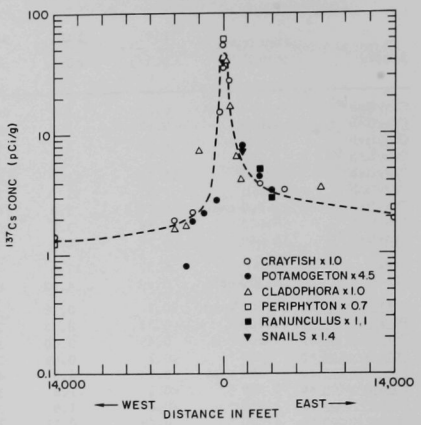

FIG. 2.--Normalized ^{137}Cs concentrations in shoreline organisms as a function of distance from the Big Rock Power Station.

concentration factors (assuming crayfish = 1.0) are also presented. While there are some large gaps in the data as well as rather large statistical fluctuations, the general relationships seem rather well defined and point to somewhat different mobilities for these two nuclides. The more rapidly decreasing concentrations of ^{65}Zn may be due to its having initially been present in particulate form, while ^{137}Cs, as was noted earlier, started primarily as a cationic species.

Sediments

Originally it was hoped that sufficient bottom samples could be obtained to permit an inventory of nuclides on the bottom near the plant. The difficulty of finding sandy patches on the generally rocky bottom, coupled with the limited time allotted for bottom sampling, made this impossible during 1970. A number of samples were taken at various distances directly offshore from the discharge channel as well as along the beach in both

directions from the plant. The samples were taken either with a Ponar dredge mounted on the Argonne boat or by hand if the water was shallow enough. In general, they consisted of a sand and gravel mixture. After air drying, the samples were sieved with the fraction passing through a No. 30 U.S. standard sieve (0.595-mm opening) being taken for gamma counting.

Table 3 summarizes the activity levels found in sand. In addition to the nuclides listed, rather uniform concentrations of uranium (0.5 ppm average) and thorium (1.0 ppm average) were found. The wide variation among samples taken from the discharge channel points up the difficulty of obtaining representative bottom grabs. If the concentrations of ^{65}Zn and ^{137}Cs in bottom sands are graphed and superimposed on Figures 1 and 2, they lead to relative concentration factors X 100 for ^{65}Zn and X 4 for ^{137}Cs.

TABLE 3. Radioactivity Concentrations in Bottom Sands

Feet from outfall	Feet offshore	^{134}Cs, pCi/g	^{137}Cs, pCi/g	^{95}Zr, pCi/g	^{65}Zn pCi/g	^{60}Co pCi/g	K, pCi/g	$\frac{^{65}Zn}{^{60}Co}$	$\frac{^{65}Zn}{^{134}Cs}$	$\frac{^{137}Cs}{^{134}Cs}$
20,000 west	2,000	0.014	0.20	0.006	0.01	0.014	11	10	1	14
4,000 "	< 200	0.065	0.57	0.03	0.20	0.026	7	8	3	9
3,000 "	< 100	0.033	0.39	0.008	0.05	0.010	7	5	2	12
At outfall	100	2.15	6.34	< 0.2	20.1	2.60	7	8	9	2.9
"	100	1.58	5.60	0.1	15.3	3.22	11	5	10	3.3
"	100	0.57	1.97	0.03	2.8	0.36	9	8	5	3.5
"	200	3.32	10.3	0.3	61.4	6.75	8	9	18	3.1
"	500	0.63	2.79	< 0.1	4.8	0.86	7	6	8	4.4
"	500	0.68	2.66	< 0.1	3.1	0.51	5	6	5	3.9
"	2,000	0.40	1.57	0.2	11.2	2.46	13	5	28	3.9
1,500 east	< 100	0.35	2.31	0.12	9.3	0.97	7	10	27	6.6
3,000 "	< 100	0.66	2.68	0.09	3.9	0.45	10	9	6	5.6
4,000 "	< 100	0.10	0.77	< 0.02	0.63	0.09	7	7	6	7.7
5,000 "	< 100	0.08	0.68	0.06	0.15	0.07	8	2	2	8.5
10,000 "	< 200	0.11	0.56	< 0.05	0.46	0.11	9	4	4	5.1

Fish

Undoubtedly the most important organisms from the radiological health viewpoint would be the fishes, especially those potentially useful as food. Their mobility along with the variability of the source makes it

imperative that large numbers of samples be taken before any definite conclusions are drawn. Table 4 summarizes concentration values in the fish samples we were able to collect. In general, the samples are composites of several fish (most below edible size) taken from the discharge channel. Considerable effort went into trying to catch larger fish, with no success. From those samples collected, it would seem that fish in the area have concentrations roughly comparable to other biota, at least for the isotopes we measured. It is hoped that in 1971 samples of larger fish will be obtained near the plant and at more remote locations.

TABLE 4. Radioactivity Concentrations in Fish

Sample	Feet from outfall	^{134}Cs, pCi/g	^{137}Cs, pCi/g	^{95}Zr pCi/g	^{65}Zn pCi/g	^{60}Co pCi/g	K, g/kg	$^{65}Zn/^{60}Co$	$^{65}Zn/^{134}Cs$	$^{137}Cs/^{134}Cs$
Bluegill No. 1	Outfall	1.05	3.95	0.3	34.5	1.21	10	29	33	3.8
Bluegill No. 2	Outfall	1.03	5.44	< 0.05	15.4	0.65	12	24	15	5.3
Bluegill No. 3	Outfall	2.23	8.19	0.1	86	0.89	10	97	39	5.1
Bluegill No. 4	Outfall	1.59	6.27	0.2	51	0.05	13	1020	32	3.9
Alewife No. 1	Outfall	0.92	5.71	< 0.15	138	1.1	13	125	150	6.2
Alewife No. 2	Outfall	0.19	0.91	< 0.05	4.43	0.10	11	44	23	4.8
Alewife No. 3	Outfall	< 0.1	0.67	< 0.05	0.86	0.16	11	5	>9	> 7
Bass No. 1	Outfall	0.22	2.06	< 0.06	6.7	0.07	14	96	26	9.4
Bass No. 2	Outfall	0.30	3.19	0.1	6.0	0.6	14	10	20	10.6
Bass No. 3	Outfall	0.27	1.77	< 0.1	1.3	< 0.06	10	> 20	5	6.6
Sunfish	Outfall	0.33	1.06	< 0.06	4.2	0.2	10	21	13	3.2
Sucker	Outfall	< 0.1	1.03	< 0.05	< 0.3	< 0.03	16	--	--	> 10

An interesting comparison can be drawn between activity levels observed near the Big Rock reactor and maximum daily intakes of radionuclides for non-occupational exposure as recommended in the NBS Handbook 69.[1] The maximum permissible daily intakes (in pCi/day) for ^{134}Cs (20,000), ^{137}Cs (45,000), ^{95}Zr (130,000), ^{65}Zn (220,000), and ^{60}Co (110,000) are of such a level that several hundred grams (dry weight) of typical biological material originating in the discharge channel would have to be consumed in order to exceed them. At distances of about 1/4 mile

the necessary intake would increase to several kilograms (dry weight). Also, it would tentatively seem that daily intakes of fish on the order of several kilograms (dry weight) would be necessary to exceed maximum permissible daily intakes.

Reference

1. Maximum Permissible Body Burdens and Maximum Permissible Concentrations of Radionuclides in Air and in Water for Occupational Exposure, recommendations of the National Committee on Radiation Protection, NBS Handbook 69, National Bureau of Standards, Washington, D. C.

THERMOLUMINESCENT DOSIMETRY OF AQUATIC LIFE IN-TRANSITU THROUGH A REACTOR COOLING CONDENSER

B. G. Oltman, Gerald P. Romberg, William Prepejchal, and Donald M. Nelson

Introduction

An experiment was conducted to investigate the external radiation dose from neutrons and gamma rays that aquatic organisms might be exposed to in passing through a nuclear power plant cooling condenser. The problem was to carry out dose measurements in situ as the water passes through the cooling condenser. Space and buoyancy restricted detector sizes to less than 3/4" in diameter and densities to less than unity. Thermoluminescent dosimetry[1,2] with its high sensitivity and dose rate independence seems to be the most promising technique at this time.

Thermoluminescence is a radiative phenomenon characteristic of certain crystals which have been exposed to ionizing radiation. These crystalline materials, when exposed to radiation, absorb energy and on subsequent stimulation with heat, release it in the form of light. A quantitative determination of the amount of light emitted provides an indirect measurement of the amount of ionizing radiation. The following will be a description of the experimental techniques that were used, and the preliminary results. Some modifications for improving over-all efficiency will be described.

Experimental Procedure

The thermoluminescent materials selected were calcium fluoride (TLD-200) and lithium fluoride (TLD-100) crystals in extruded form. These crystals are 1/8" x 1/8" x 0.035" in size and are commercially available.* Calibrations of dosimeters from the same batch of material indicated good uniformity of response.

---

*Harshaw Chemical Company, Solon, Ohio 44139.

Since the crystals are dense and water soluble, it was necessary to encapsulate them in small lengths of heat shrinkable plastic tubing 1/8" outside diameter by 1/2" long. This convenient technique provided a water tight seal and a means of controlling buoyancy. We could only speculate as to the radiation levels in and around the condenser and the length of time that a detector would be in the system. Thus, the sensitivity of the dosimeter was a critical factor and led us to use two types of materials with different sensitivities. Calcium fluoride is 30 times more sensitive than lithium fluoride, and both materials have stable glow peaks between 200°C and 240°C. This ensures that there will be no undue fading brought about by the normal temperature of the condenser (≈ 38°C).

The Big Rock Point nuclear power station near Lake Charlevoix, Michigan, is operated by the Consumer's Power Company of Michigan. We had their assistance and full cooperation for this experiment. Lake Michigan water is pumped into the condenser at the rate of 50,000 gallons per minute. The condenser consists of 4,618 tubes 26 feet long and 0.777 inches in internal diameter, giving a static water volume of 395 cubic feet. With a flow rate of 50,000 gallons per minute, the full capacity discharge from the condenser is 111 cubic feet per second. Under above flow rate conditions, the time that a small object of neutral buoyancy would remain inside the condenser is 3.5 seconds. We have assumed that the only radiation the dosimeter is exposed to comes from the condenser and that one can essentially neglect any activity that may be in the cooling water except when low level radioactive wastes are being discharged.[3] No such discharges were in progress during this experiment.

Twenty encapsulated dosimeters were placed in the water at the intake point very near the pumps. This was done to avoid straggling in entry into the system. The recovery team in the discharge channel consisted of a spotter on the bridge overlooking the channel, a diver in the water, and the Argonne II power boat. The dosimeters began to appear in the discharge channel 7 to 8 minutes after they were dropped at the intake. They were observed on the surface, but because of turbulence at the discharge pipe,

the last dosimeter recovered was picked up approximately 20 minutes after entry. The recovery team remained on station for an additional 30 minutes but seven dosimeters were not found. The dosimeters were then returned to the laboratory along with their controls.

The apparatus[4,5] used to read out the dosimeters consists of a heat source, photomultiplier tube, high voltage supply, electrometer, and a two-pen recorder and curve integrator. The electronic instrumentation is calibrated for gain by using a non-electronic radium current generator. The gain of the photomultiplier tube is determined by reading a set of pre-calibrated dosimeter standards.

The dosimeters from Big Rock were read out, along with their controls and the data recorded and analyzed.

Results and Conclusions

Twenty dosimeters were introduced at the intake pipe; of this number, thirteen were recovered. Of the thirteen, six were LiF and the remainder CaF_2. The recovery ratio is good, considering the small size and color of the dosimeter, plus the long path and the large area of the outfall.

LiF, being the least sensitive of the two materials, did not show any significant increase over the control dosimeters. CaF_2, however, did show a net difference of 1.4 mrads ± 12% with a confidence level better than 95%. It should be noted that CaF_2 is essentially sensitive only to gamma rays. The power plant was generating 53 MW gross electrical power at the time of the exposure.

A more brilliantly colored heat shrinkable tubing would help reduce the number of dosimeters lost because of poor visibility at the outfall. Also, a factor of two improvement in sensitivity could be attained by using calcium sulfate (manganese activated).

We plan to carry out further experiments with improved techniques and gain more information with regard to both neutron and gamma-ray energy discrimination.

The authors are indeed grateful to Messrs. Hartman, McNamara, Tyson, and Axtell of the Consumer's Power Company of Michigan for their complete cooperation and assistance in this experiment. We are also indebted to Mr. K. Eckerman for useful discussions and advice.

References

1. Cameron, J. R., N. Suntharalingam, and G. N. Kenney. Thermoluminescent Dosimetry. The University of Wisconsin Press, Madison, 1968.
2. Proceedings of the Second International Conference on Luminescence Dosimetry, Sept. 23-26, 1968. U. S. Atomic Energy Commission Report CONF-680920.
3. Nelson, D. M., G. P. Romberg, and W. Prepejchal. This report.
4. Kastner, J., Ramesh Hukkoo, B. G. Oltman, and Y. Dayal. Thermoluminescent Internal Beta-Ray Dosimetry. Radiat. Res. 32, 625-640 (1967).
5. Ashby, W. C., J. N. Beggs, J. Kastner, B. G. Oltman, and H. Moses. Thermoluminescent Dosimetry and Environmental Radiation Studies. Argonne National Laboratory Radiological Physics Division Annual Report, July 1965 through June 1966. ANL-7220, p. 115.

THE CONCENTRATION OF MERCURY IN FISH TAKEN FROM LAKES ERIE, MICHIGAN, AND SUPERIOR

D. N. Edgington, M. M. Thommes, A. F. Gossman, and R. M. Cutler

Introduction

The aquatic environment provides not only a source of food but has been used as a very convenient sink for the dispersal of waste materials from the activities of man. In the last five years concern has been growing about the possible effects of the dispersion and disposal of waste materials in the environment. This is particularly so with respect to the dumping of sewage and industrial wastes into lakes, streams and rivers and their ultimate effect on the biota.

Mercury is one of several elements which is causing grave concern. In addition to occurring naturally in the biosphere, large quantities are used for industrial and agricultural purposes. Mercury in its elemental state is used for electrodes in chlor-alkali plants, where although it is recycled, it may be partially lost with the liquid wastes. Organo-mercury compounds have been extensively used in the paper industry and in agriculture to prevent, for the former, the growth of slime on the paper machines, and for the latter, the deterioration of seed grains.[1]

Until very recently it has been assumed that since most of the inorganic mercury compounds are highly insoluble, any mercury discharged into a lake or river would be rapidly precipitated out and accumulated in the sediment and, therefore, unavailable for concentration in the biota. It appears, however, that the sediments contain microorganisms which are able to convert inorganic mercury compounds into mercury alkyls, and it is in this form that mercury is accumulated and concentrated by fish and other organisms.[2]

In an earlier communication, Lucas et al.[3] reported the concentrations of seventeen trace elements in many different fish caught from Lakes Erie, Michigan and Superior in the summer and fall of 1968.

Mercury was reported to be present in these fish at very low concentrations (≤ 0.004 μg/g tissue). However, in the light of evidence which showed that mercury in fish is present as organo-mercury compounds, the methods of analysis were reviewed as to the possibility of losses of mercury.[4] Mercury losses could have occurred during freeze-drying and low-temperature ashing. Both of these processes are performed under a moderate vacuum which would facilitate the loss of volatile material.

Therefore, it was decided, in view of the tremendous interest in the problem of mercury pollution, to analyze an extensive series of these fish which had been caught in 1968 in order to provide some background information on mercury levels in the Great Lakes and to provide a comparison with the wealth of data available for fish caught in 1970. These samples of fish, were obtained through the cooperation of the Bureau of Commercial Fisheries in Ann Arbor (now the Bureau of Sport Fisheries). Fish were taken from various locations in Lakes Erie, Michigan, and Superior (using trawls or gill nets), and individual samples were selected and deep frozen immediately after landing.

The Determination of Mercury using Neutron Activation Analysis

Mercury has been determined in biological materials by three different techniques: colorimetry, i.e., using dithizone; atomic absorption spectrophotometry; and neutron activation analysis. At the present time the last two methods are being employed extensively. The atomic absorption method utilizes the high absorption of mercury vapor, which permits a sensitivity of <0.0001 μg,[5] but there are real problems in obtaining a complete separation of the mercury vapor from the water, carbon dioxide, and other volatile materials produced in the ignition of the organic material.

Several papers have appeared since 1960 describing the determination of mercury by neutron activation analysis. Irradiation of mercury produces three radioactive nuclides: ^{197m}Hg with a half-life of 24 hours and X rays at 140 keV, ^{197}Hg with a half-life of 65 hours and X rays at

77 and 191 keV, ^{203}Hg with a half-life of 47 days and a 77-keV X ray and 280-keV gamma ray. If the mercury concentration and the neutron flux are both large enough, then after a sufficient time has been allowed for decay of short-lived activation products, mercury may be determined instrumentally by measuring the activity due to ^{203}Hg. For more sensitive determinations chemical separations must be used. After a wet oxidation stage these have included distillation of the mercury followed by either electrolytic deposition,[6] ion-exchange,[7] or absorption of vapor on selenium-impregnated paper,[8] and precipitation.[9,10]

The separation method used in these experiments was anion-exchange following a simple wet oxidation with aqua regia. Mercury is quantitatively absorbed by Dowex 1-X8 anion exchange resin from all hydrochloric acid solutions or nitric acid solutions containing a small concentration of chloride ion, and is not eluted under the conditions required to elute almost all other elements which are likely to interfere.

The fish had been frozen and stored at -10°C until time of analysis. Samples were removed from each fish at the left anterior dorsal side with a surgical steel scalpel and Teflon-coated tweezers. Care was taken to obtain only edible flesh, with skin and bones removed. This portion of the fish was chosen for analysis because it is the most often consumed by humans. Before irradiation, approximately one-gram portions were placed in 0.4-dram snap-top polyethylene vials* and weighed to the nearest 0.1 milligram. Duplicate mercury standards were prepared by micropipetting 50λ of mercury solution (54 μg mercury) into the same kind of vials.

A set of twelve samples together with two mercury standards were placed in styrofoam packing, which served as a thermal insulator and a shock absorber. This in turn was placed in a polyethylene irradiation capsule. Two of these sets were placed in a container of dry ice and taken to the Iowa State University research reactor at Ames, Iowa, where they

---

*Olympic Plastics, Los Angeles, California.

were irradiated for an integrated neutron flux of 7.2×10^{16} neutrons/cm^2. The samples thawed slightly during irradiation, but were immediately refrozen in dry ice.

After irradiation the still frozen samples were transferred to 125-ml Erlenmeyer flasks with 5 to 10 ml 9M HCl; then about 40 ml of aqua regia were added to each. The samples were left to digest overnight at room temperature. A few glass beads were then added to prevent bumping, and the samples were heated to a slow boil for one hour. Ten milliliters of aqua regia were added, and the solutions were allowed to boil somewhat more vigorously for another hour, after which about 30 ml of solution remained. The digested solutions were cooled in an ice bath to solidify the fat, and were then filtered through glass wool into a 50-ml Pyrex centrifuge tube. A 15-ml volume of 9M HCl was used to wash the flasks and filters. Previous studies by Markun[11] have shown that after digestion fat contains less than 3% of the mercury in a sample. A very slight loss of mercury due to volatilization may occur during digestion, although aqua regia rapidly transforms methyl mercury to mercuric chloride.

The resultant solution was then pumped through a 15-cm column containing 10 ml of Dowex 1-X8 (100 mesh), prepared as described previously, at a flow rate of 0.75 ml min^{-1} using a polystaltic pump. The column is then treated with three different eluents in succession, 80 ml 9M HCl, 20 ml water, 120 ml 1M NaCl. The mercury remains quantitatively absorbed on the resin under these conditions together with silver, gold, antimony, and some residual bromine and zinc.

The resin is then transferred to a plastic counting tube. These samples were counted using a NaI crystal and a gamma-ray spectrometer and the ^{203}Hg activity determined by a least squares analysis of the resultant spectra. These procedures have been described in detail elsewhere.[12]

The mercury content in the fish is determined by comparing the ^{203}Hg activity found on the resin to that in the standards irradiated at the

same time. (The gamma-ray spectra obtained 96 days after irradiation for a 50-μg mercury standard and 0.4-μg mercury from a lake perch using these techniques are shown in Figure 1.) Replicate analyses agreed in most cases to better than ±5%.

Results and Discussion

The concentration of mercury found in fish taken from Lakes Erie, Michigan and Superior are summarized by species and collection site in Table 1. The concentrations are given in parts per million wet tissue. Values are given for twenty-nine different species of fish. It should be emphasized that these fish were collected in the open lake and are, therefore, representative of the general lake environment and not any particular polluted area. The concentration of mercury in fish for human consumption is recommended by the U.S.F.D.A. not to exceed 0.5 ppm, and the W.H.O. has recommended that it should be reduced to 0.05 ppm.[13] It is clear from the data presented in Table 1 that if this latter recommendation were accepted, virtually no fish caught in any of these lakes would be suitable for consumption.

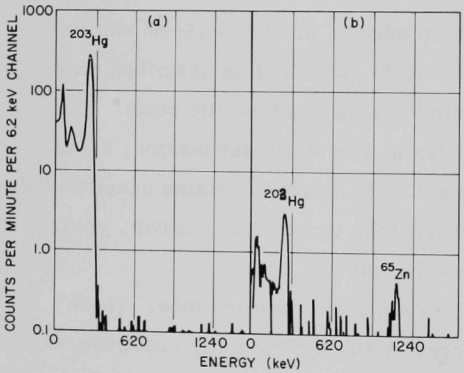

FIG. 1.--Gamma-ray spectra obtained 96 days after irradiation for (a) 50-μg mercury standard and (b) 0.4-μg mercury from a lake perch adsorbed on an anion exchange resin column.

Unfortunately, it is very difficult to catch the same species of fish in each of three lakes. Perch were found in Lakes Erie and Michigan, while comparisons can be made between Lakes Michigan and Superior for whitefish, smelt, and lake trout. The difficulty of finding the

TABLE 1. Results of Analyses of Fish Taken in 1968 from Lakes Erie, Michigan, and Superior

	Concentrations of mercury, ppm wet tissue		
	Lake Erie	Lake Michigan	Lake Superior
Alewife		0.45	
Barbot			0.39, 1.17
Bloater		0.20, 0.17, 0.43, 0.51	0.09, 0.23, 0.21, 0.15, 0.14, 0.22, 0.22, 0.15
Brown-nosed Sucker			0.12, 0.07, 0.09
Bullhead	0.22, 0.18, 0.20		
Carp	0.30, 0.29, 0.12		
Chinook Salmon		0.31	
Chub		0.15, 0.17, 0.18, 0.13, 0.22	
Deepwater Schulpin		0.76, 0.80, 0.82, 0.50, 0.68, 0.56	
Drum	0.37, 0.44, 0.42, 0.20		
Goldfish	0.22, 0.19, 0.09		
Herring			0.42, 0.15, 0.17, 0.20, 0.20
Kiyi			0.15
Lake Trout		0.20, 0.21, 0.25, 0.11	0.31, 0.26, 0.31, 0.58, 0.33, 0.28, 0.20
Menominee Whitefish			0.14, 0.13, 0.13
Northern Pike		(0.31)[a]	(0.48)
Yellow Perch	0.41, 0.41, 0.29, 0.50	0.11, 0.14, 0.13	
Pumpkin Seed			(0.47)
Quill Back		(0.34)	
Rainbow Trout			(0.12)
Shad	0.19, 0.07		
Slimy Sculpin			1.10
Smelt		0.12, 0.14, 0.12, 0.10, 0.17, 0.12	0.31, 0.10, 0.20
Stickleback			0.96
Trout-Perch			0.24
Walleye	0.84		
White Bass	0.38, 0.43		
Whitefish		0.07, 0.11	0.09, 0.11, 0.13, 0.16, 0.08, 0.12

[a] Values given in parentheses refer to fish not caught in the lake. See text for explanation.

same species in each lake reflects the real difference between Lake Erie and the other two: it is basically a warmer lake.

The data overall show that there is very little difference between the three lakes if grand averages are taken of all the data. These averages are: Lake Erie $\bar{x} = 0.32$ ppm for N = 26; Lake Michigan $\bar{x} = 0.29$ ppm for N = 33; and Lake Superior $\bar{x} = 0.26$ ppm for N = 45. However, the average for Lake Michigan is increased significantly by the inclusion of analyses of six samples of deep water sculpin, all of which have a mercury level of greater than 0.5 ppm.

The concentration of mercury in the sculpin is many times greater

than that in any of the other bottom feeders. This may be due in part to this species having an exceptionally high fat content which will concentrate organo-mercury compounds more effectively. It is difficult to freeze-dry these fish completely without obtaining an oily residue. Because of this unusual behavior, the omission of the results for this species can be justified. If the averages are recalculated for Lakes Michigan and Superior leaving out the values for all types of sculpin, they are then, for Lake Michigan $\bar{x}$ = 0.19 ppm for N = 27 and for Lake Superior $\bar{x}$ = 0.24 ppm for N = 44. These averages may be compared to those obtained by various workers in the field for fish taken in 1970. The values are: Lake Erie $\bar{x}$ = 0.38 ppm for N = 454, Lake Michigan $\bar{x}$ = 0.12 ppm for N = 64, and Lake Superior $\bar{x}$ = 0.13 ppm for N = 7.[14] The values given in Table 1 are also in good agreement with those reported by Jervis and coworkers.[15] This comparison of results for fish taken in 1968 and 1970 indicates that there have been no major changes in the mercury contamination of these lakes during this time span. Under these circumstances it would appear that there may be significantly small differences in the mercury levels in the fish taken from these lakes, the order in decreasing average concentration being Erie, Superior, and Michigan. This result would not be surprising as it would reflect the use of mercury in many paper mills discharging water into Lake Superior and the large discharges from various industrial plants at the western end of Lake Erie.

Where it is possible to make interlake comparisons for various species, no definite pattern is recognizable. A comparison of all three lakes using the same species is impossible. For Lakes Erie and Michigan, the only common species is the perch. In this case, the samples taken from Lake Erie contain three times as great a concentration of mercury, 0.40(4), as those taken from Lake Michigan, 0.13(3). (In all cases, the average value is given in ppm, and the number in parentheses is the number of samples analyzed.) In comparisons between fish taken from Lakes Michigan and Superior, the differences are smaller. Giving the values for Lake Michigan first: bloater, 0.33(4), 0.18(8); lake trout, 0.19(4), 0.32(7);

smelt, 0.13(6), 0.20(3); whitefish, 0.09(2), 0.11(6). The bloater is the only species where the concentration of mercury is greater in samples taken from Lake Michigan. For two of the other species, lake trout and smelt, there are significantly higher concentrations of mercury in the fish taken from Lake Superior.

The results given in Table 1 also show that the concentration of mercury is higher in the predators and game fish than in the bottom feeding fish. For the various species of fish taken from Lake Erie, the average mercury concentrations for goldfish, carp, and bullhead, which are bottom eaters, are 0.13, 0.23, and 0.20 ppm, respectively, while for the predator species, drum, perch, white bass, and walleye, the average values are 0.38, 0.42, 0.40, and 0.84 ppm, respectively.

The values given in parentheses in Table 1 indicate that these fish were not taken from the lake in question. The northern pike in the Lake Michigan column was taken from the Kalamazoo River, as was the quillback, and the northern pike under Lake Superior was taken from the Presque Isle River in the Upper Peninsula of Michigan, which flows into that lake. This fish was caught in an area above a dam where there has been no industrial activity other than logging and where there are no towns upstream. It is, therefore, interesting to compare the concentration of mercury in this fish, 0.48 ppm, taken from an unpolluted river to that in the one fish, 0.31 ppm, taken from the Kalamazoo River which drains a large industrial and agricultural region.

The data presented in this paper tend to support a conclusion that, even if it were possible to identify and eradicate all sources of mercury pollutions, its concentration in fish and other marine and aquatic organisms would still be greater than the desirable limit of 0.05 ppm suggested by the World Health Organization. This is not surprising when it is realized that all soils (and, therefore, presumable sediments) contain up to 0.04 ppm, basaltic and granite rocks contain up to 0.09 ppm.[16] seawater contains up to 0.27 μg/liter[17] mercury, and that fish show an enrichment of between 10^4 and 10^5 over seawater.

References

1. Johnels, A. and T. Westermark. Mercury Contamination of the Environment in Sweden. Chemical Fallout, Ed. M. W. Miller and G. G. Berg. Charles C. Thomas, Publisher, Springfield, Illinois, 1969, pp. 221-241.
2. Maximum Allowable Concentrations of Mercury Compounds. Report of an International Committee. Arch. Environ. Health 19, 891-905 (1969).
3. Lucas, H. F., D. N. Edgington, and P. Colby. Concentrations of Trace Elements in Great Lakes Fishes. J. Fisheries (Canada) 27, 677-684 (1970).
4. Westöö, G. Determination of Methyl Mercury Compounds in Foods. Acta Chem. Scand. 20, 2131-2137 (1966).
5. Hatch, W. R. and W. L. Ott. Determination of Submicrogram Quantities of Mercury by Atomic Absorption Spectrophotometry. Anal. Chem. 40, 2085-2087 (1968).
6. Sjøstrand, B. Simultaneous Determination of Mercury and Arsenic in Biological and other Organic Materials by Activation Analysis. Anal. Chem. 36, 814-819 (1964).
7. Samsahl, K. Radiochemical Method for Determination of Arsenic, Mercury, Antimony, and Selenium in Neutron Irradiated Biological Material. Anal. Chem. 39, 1480-1483 (1967).
8. Kosta, L. and A. R. Byrne. Activation Analysis for Mercury in Biological Samples at Nanogram Level. Talanta 16, 1297-1303 (1969).
9. Smith, H. Estimation of Mercury in Biological Material by Neutron Activation Analysis. Anal. Chem. 35, 635-636 (1963).
10. Johansen, O. and E. Steinnes. A Simple Neutron Activation Method for Mercury in Biological Material. Int. J. Appl. Rad. Isotopes 20, 751-755 (1969).
11. Markun, F. (Argonne National Laboratory). Personal Communication.
12. Edgington, D. N. and H. F. Lucas. A System for the Neutron Activation Analysis of Trace Elements in Samples of Biological and Environmental Interest. J. Radioanal. Chem. 5, 233-250 (1970).
13. F.A.O. and W.H.O. Pesticide Residues in Food. W.H.O. Tech. Report Series No. 370 (1967).
14. Moolenaar, R. J. (Dow Chemical Co., Midland, Michigan). Personal Communication.
15. Jervis, R. E., D. Debrum, W. Le Page, B. Tiefenbach. Mercury Residues in Canadian Foods, Fish, Wildlife. Progress Report. Univ. of Toronto. National Health Grant Project No. 605-7-510 (1970).
16. Turekian, K. K. and H. Wedepohl. Distribution of Elements in Some Major Units of the Earth's Crust. Bull. Geog. Soc. Am. 72, 178-192 (1961).
17. Hosohara, K. 1961. Mercury Content of Deep Seawater. Nippon Kagaku Zasshi 82, 1107-1108 (1961).

MINOR ELEMENT GEOCHEMISTRY OF LAKE MICHIGAN FERROMANGANESE NODULES*

D. N. Edgington and Edward Callender†

Samples of ferromanganese nodules and their underlying sediments from several localities in Lake Michigan have been analyzed for their minor element content utilizing neutron activation and gamma-ray spectrometry,[1] atomic absorption, and electron microprobe techniques.

The elemental concentrations and average concentration factors [ppm(sediment)/ppm(water)] are compared with analysis of marine nodules in Tables 1 and 2. In these tables the analytical values are reported for only that part of the nodule or sediment which is soluble in strong hydrochloric acid but are given in terms of total dry weight. Generally, the nodules contained five times as great a fraction of acid soluble material and, therefore, in order to compare the results the sediment values should be multiplied by this factor.

The Lake Michigan nodules, in general, do not contain as large concentrations of trace elements as their marine counterparts and also do not exhibit as large concentration factors. Exceptions however are chromium, which shows approximately double the concentration; barium, which shows approximately a quadrupling in concentration and a doubling of the concentration factor; radium, a five times greater concentration; and arsenic, for which values have not been reported in marine nodules. On the other hand, strontium which occurs in marine nodules at a level of 0.9% has a concentration of <10 ppm. The concentrations of many of the elements tend to be greater in the sediments than in the nodules with the notable exceptions of barium, cobalt, and arsenic.

---

*Abstract of paper presented at the 13th Conf. on Great Lakes Research, Buffalo, New York, April 1970.

†University of Michigan.

TABLE 1. Average Chemical Composition in ppm and Average Concentration Factors for Freshwater and Marine Sediments

Element	ppm(sediment)/ppm(water)					
	Green Bay sediments		Green Bay nodules		Marine nodules	
Antimony	1.43		2.25		30	
Arsenic	25.7	(6,400)[a]	179	(45,000)	--	(?)
Barium	771	(14,300)	9,360	(173,000)	2,500	(83,000)
Bromine	5.3	(26)	7.4	(37)	--	(?)
Cadmium	1.4	(18)	3.3	(40)	10	(90,000)
Chromium	---	(--)	27.5	(15,300)	15	(300,000)
Cobalt	10.0	(11,000)	63	(65,000)	3,500	(1.3×10^7)
Copper	15.1	(1,510)	8.3	(830)	4,300	(1.4×10^6)
Gallium	1.4	(1,400)	0.92	(920)	10	(330,000)
Iron	20,500	(30,600)	104,000	(155,000)	205,000	(2.1×10^7)
Manganese	--	(--)	100,000	(5×10^7)	230,000	(1.2×10^8)
Mercury	0 - 2.95[b]		<0.2			
Radium (pCi)	--	(--)	31.3	(80,000)	6	(100,000)
Thorium	0.21	(10,500)	0.53	(26,500)	3 - 150	(1.5×10^6)
Tungsten	0.74		3.4		90	
Uranium	0.77	(770)	1.27	(1,270)	6 - 10	(2,700)
Zinc	75	(7,500)	174	(17,400)	470	(47,000)

[a] Values in parentheses indicate average concentration factors.

[b] See text.

Preliminary studies of x-ray backscatter from the electron microprobe have shown that most of the nodules examined have an iron-rich crust over a manganese-rich inner area. The whole nodule is formed around a feldspar nucleus. Traces obtained of the various x rays from the electron microprobe scans across sections of the nodules confirm these initial observations. Iron is found at the highest concentration at the edge of the nodule, and in much lower concentrations in bands alternating with the manganese inside the nodule. Barium and calcium are associated with the manganese, and arsenic and silicon are associated with iron.

The experimental data for the rare earths are given separately in Table 2. The values are compared to those found in marine nodules and shales. The values in parentheses refer to the fraction (μg rare earth/ μg lanthanum) gain; the absolute average values are far lower than those found for marine nodules. However, the weight ratios are interesting.

TABLE 2. Concentration of Rare Earths in Green Bay Sediments and Ferromanganese Nodules

Element	Concentration, ppm			
	Nodules	Sediments	Marine Nodules	Shales
Lanthanum	45 (1.0)[a]	15.2 (1.0)	175 (1.0)	20 (1.0)
Cerium	176 (3.9)	61 (4.0)	1460 (8.3)	59 (2.9)
Samarium	13.1 (0.29)	4.6 (0.30)	55 (0.31)	5.6 (0.28)
Europium	1.5 (0.03)	0.5 (0.03)	12 (0.07)	1.1 (0.055)
Terbium	0.95 (0.02)			0.6 (0.03)
Thulium	6.8 (0.15)			0.3 (0.015)
Ytterbium	3.9 (0.09)		35 (0.20)	0.18 (0.09)
Lutetium	0.32 (0.01)			0.33 (0.02)
Scandium	0.8 (0.02)	1.5	11 (0.06)	13 (0.65)

[a] Values in parentheses are fraction gain (μg rare earth/μg lanthanum).

These were compared to those found in various minerals, and it was found that they gave the best match to those found in shale, with the exception of the value for [Tm/La].

The high concentrations of arsenic found in these nodules and their relationship to the underlying sediment is of interest. Samples of nodules were collected from six and sediments from five locations in Green Bay. These locations are shown in Figure 1 as well as the locations where measurements of Ph and Eh(mV) of the sediment were made. The results of the analyses for arsenic are given in Table 3. It can be seen from

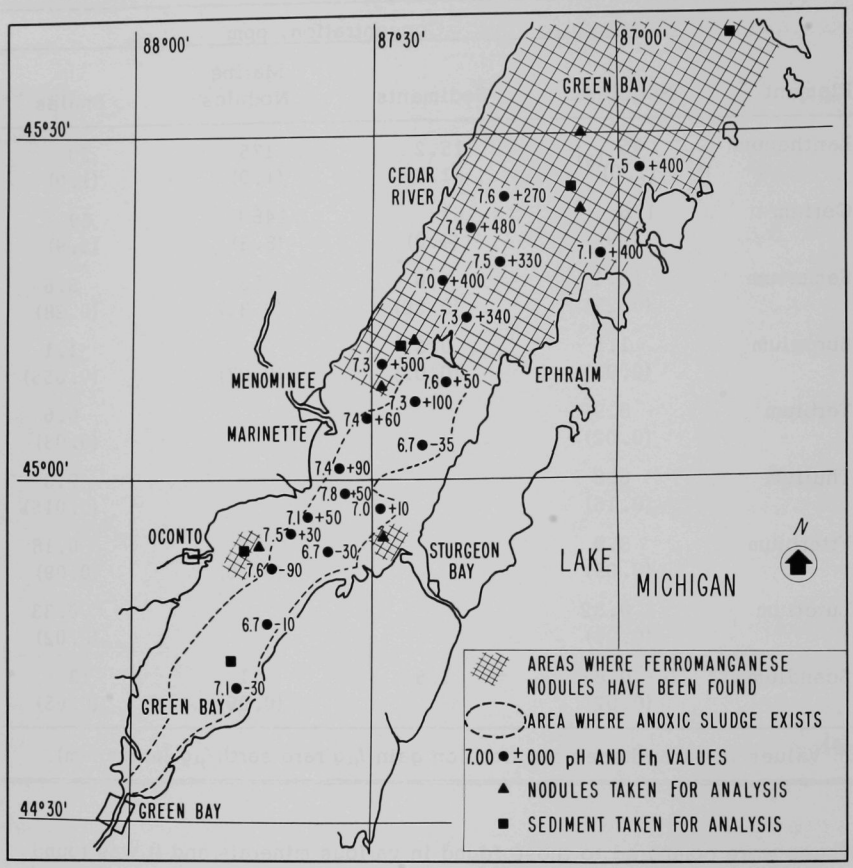

FIG. 1.--Map of Green Bay showing sampling locations and the limits of reduced and oxidized bottom sediments

TABLE 3. Concentration of Arsenic and Mercury (ppm) in Green Bay Sediments and Ferromanganese Nodules

Location	Eh (mV)	Sediment	Nodule
44° 43'N 87° 45'W	- 30	2.4 (1968) 4.5 (1969) [2.95][a]	None
44° 50'N 87° 43'W	+ 30	102	320
44° 54'N 87° 29'W	+ 10	---	164
45° 07'N 87° 29'W	+ 60 + 500	---	138
45° 10'N 87° 24'W	+ 500	15.0	52.0
45° 23'N 87° 05'W	+ 270	24.5	129
45° 30'N 87° 05'W	+ 400	---	173 [0.85]
45° 44'N 86° 47'W	---	3.6 [0.38]	---

[a]Values in brackets are for mercury.

these data that nodules are only found where the Eh of the sediment is oxidizing. Under these conditions the concentration of arsenic in the underlying sediment is also quite large when the difference in solubility and total mass are considered. A major feature of the southern end of Green Bay is the large area of anoxic grey sludge which fans out from where the Fox River enters the bay and extends to well north of Sturgeon Bay. Nodules have not been found in this reducing area, and the analysis of a sample of the sludge showed that the concentration of arsenic is very low in comparison with the values found for this element in the areas where nodules are found. There is a very thick deposit of these nodules off Oconto, where there is a very sharp demarkation between this deposit and the anoxic sludge.

It is evident then that nodules are found in those areas where aerobic conditions exist and the values of the Eh ≥ 100 mV. No nodules are found in the southern end of Green Bay where eutrophication is advanced and anaerobic conditions exist. Where the value of Eh is ≥ 30 mV, the underlying sediments also contain large concentrations of arsenic. In the light of this evidence, two questions remain to be answered. They are 1) is the arsenic found in these nodules due to the local geochemistry or due to pollution in the area, and 2) if the bay continues to be polluted, will the spread of reducing and thereby acid conditions cause the dissolution of these nodules and release the arsenic into the water?

The levels of mercury in these nodules and underlying sediments are of some interest as they may lead to some understanding concerning the base levels of this element in the aquatic environment and also point to possible sources of pollution. Mercury was found in only three of the samples of nodules and sediments analyzed. Mercury was below 0.2 ppm in all samples of nodules except the ones collected 15 miles south of Escanaba (45° 30'N, 87° 05'W), where the concentration was 0.85 ppm. Mercury was found in two samples of underlying sediments; one from the extreme northern end of Green Bay in Big Bay De Noc (45° 44'N, 86° 47'W), where the concentration was 0.38 ppm, and the other from the southern end of the bay in the middle of the area of anoxic sludge (44° 43'N, 87° 47'W) where the concentration was 2.95 ppm. This last value probably reflects the high degree of pollution in the southern end of the bay due to the industrial and agricultural uses of mercury in the Fox River.

Reference

1. Edgington, D. N. and E. Callender. Earth Planetary Sci. Letters 8, 97-100 (1970).

MICROMETEOROLOGICAL MEASUREMENTS OVER LAKE MICHIGAN

Paul Frenzen

Introduction

During the past summer an experimental investigation of the interaction between the lowest layers of the atmosphere and the open water surface of Lake Michigan was begun by this Laboratory. Descriptions of several initial experiments and some preliminary findings are reported in the four papers following this general introduction to the program.

Results of these studies will add to our understanding of the so-called mass-energy balance of the Great Lakes. In the case of such large bodies of water, very few direct measurements of the phenomena which control this balance have been carried out. Rather, what is known (or at least what is thought to be known) has either been inferred from observations of long-term seasonal or annual changes in water level and heat content, or has been based upon extrapolations from results of studies conducted over considerably smaller bodies of water such as artificial reservoirs.

The present investigation uses proven techniques of micrometeorological measurement at a point where observations may be considered representative of conditions over the open lake. The experiments are designed to examine both the normal daily cycle of the several components which make up the air-water exchange (see Fig. 1 of "Surface Heat Energy Budget over Lake Michigan," which follows) and the occasional discontinuous changes in these mechanisms, which should be associated with more or less abrupt changes in meteorological conditions. Such observations of both cyclical and aperiodic short-term variations will improve our understanding of possible irreversible long-term changes which could result, for example, from thermal pollution.

FIG. 1.--The micrometeorological research tower installed 700 m offshore in Lake Michigan. During observation periods, no personnel or unnecessary equipment remained aboard. The vertical 8.0-m extension is not clearly shown since, at the time of the photo, it was in a retracted position.

Field Site and Tower Facility

Measurements were made from the small instrumented tower shown in Figure 1, a facility erected for these experiments and maintained by personnel from the Detroit office of the U. S. Lake Survey. The tower was located some 700 m off the eastern shore of Lake Michigan, just south of the city of Muskegon. This site offers a number of advantages, the most useful to the purposes of the experiment being that winds with westerly components arrive at this point with past trajectories over open water in excess of 100 km. The particular shore location on the north side of the Mona Lake inlet has been used as a temporary field station in previous years by workers from the University of Michigan and the U. S. Lake Survey. At this point the beach is not readily accessible to the general public. Therefore cables crossing the beach and near-shore dunes are not disturbed, and apparatus on the tower as well as recording equipment housed in a small travel trailer on shore remain relatively secure. Finally, the shore location is immediately adjacent to a small, navigable inlet, this aiding small boat operations.

The tower stood in water about 7 m deep with the main, upper cross arm shown in the figure supporting eddy-correlation sensors at a height of 5.5 m above the mean water surface. A slender, vertical extension was used to carry a single fast-response anemometer at an elevation of 8.0 m. The working platform about 3 m above mean water level was reached by climbing the lower tower structure and passing through a small trap door. A trapeze hung about 18 inches below the down-wind edge of the platform, at the point where the boat could most easily approach the tower, assisted personnel in stepping from the bow of the boat to the fixed tower. This transfer became difficult in waves three feet high and impossible in waves of four feet. As a result, the tower was inaccessible whenever onshore winds were stronger than 7 or 8 m sec^{-1}.

A marine power cable laid along the lake bottom brought 117 VAC service to the tower. A six-pair, individually-shielded instrumentation cable was installed in the same fashion to transmit data to shore.

Although not designed for marine service, this cable served adequately for two expeditions. But after several months under water a gradual deterioration of the internal insulation limited its use to only two circuits. By the final expedition of the season, a radiotelemetry link had been placed in operation. This equipment, designed and constructed by the Electronics Division of ANL, was able to transmit three audiofrequency, pulse modulated signals, thus largely replacing the inoperable circuits of the data cable. The transmitter has a nominal output of 5 watts at a licensed frequency in the 215 to 260 MHz telemetry band.

Experimental Equipment

In addition to the fast-response, turbulence sensing devices described in the subsequent papers summarizing initial observations, a number of slower sensors were installed on the tower to record mean values of various meteorological parameters. Perhaps not too surprising in view of the specialized skills and primary interests of the personnel involved, more success was obtained in these first field trials with the turbulence equipment than with the simpler averaging devices. For example, no dependable means of remotely recording lake-surface temperatures at the tower was ever developed, and it was necessary to rely upon bucket temperatures. A ventilated, wet and dry bulb resistance thermometer combination was constructed, but an early failure of the associated electronic circuitry and subsequent deterioration of the data cable to shore required substitution of hand-held Assmann psychrometer readings. When possible, air and lake temperature data were recorded at the tower; but more often psychrometer and bucket temperatures were simply recorded from an exposed point on the beach. Mean wind speeds were obtained by using a scaler or frequency counter to sum the fluctuating, audio-frequency outputs of fast-response cup anemometers over typical run periods of 30 minutes' duration. Wind directions were simply estimated from the orientation of a small pennant mounted on a pole atop the foreshore dune.

Net-radiation measurements were recorded at the tower by a Funk-type, polyethylene-shielded net radiometer. This unit was mounted on an arm extending outward from the working platform level as seen in Figure 1. The constant supply of dry air required to keep this instrument's plastic, hemispherical shields inflated was supplied by a small aquarium pump, which vented through a container of silica gel. Output of the radiometer was connected through one pair of leads in the data cable, directly to the input of a relatively high-impedance, voltage-to-frequency converter (Dymec Model 2210) located in the instrument trailer on shore. Since very little current was drawn by this arrangement, neither the resistance of the long cable nor that of the thermopile within the radiometer itself caused significant loss of signal. The net-radiation signal was continuously recorded on magnetic tape or integrated by summing with a frequency counter over run periods of 30 minutes to one hour.

Future Plans

The observations over Lake Michigan will be resumed in the coming field season; subject, of course, to feasibility estimates by the U. S. Lake Survey, we tentatively plan to install the tower more than twice as far from shore and in water twice as deep. This will avoid the occasional influence of warmer water from the outfall of the Mona Lake Inlet and will enable us to obtain measurements where wind-driven waves (in deeper water) more nearly approximate those found in mid-lake.

Work will also shortly begin on a free-floating, instrumented buoy which, with the aid of the radiotelemetry equipment now being completed, will make it possible to obtain measurements in the open lake. The buoy development is being undertaken as a major portion of our proposed participation in the research program of the International Field Year for the Great Lakes scheduled for the calendar year of 1972 in Lake Ontario.

EDDY-CORRELATION MEASUREMENTS OF ATMOSPHERIC FLUXES OVER LAKE MICHIGAN

B. B. Hicks*

Introduction

The interface between the atmosphere and the earth's surface is the principal source of the atmosphere's sensible heat and, of course, all of its latent heat in the form of water vapor. Also, the interface is a major sink for atmospheric momentum. To a large extent, the fluxes of the first two quantities determine the rate of heat loss by the underlying surface, while that of the last results in lateral stresses which, in the case of water surfaces, generate waves and currents. An important geophysical problem is to increase our understanding of these fluxes and of the way they depend on atmospheric and surface conditions.

Over water, the problem is of considerable practical interest, since we need to know, for example, the rate of heat loss from lakes before possible effects of thermal pollution can be assessed accurately. On the broader scale accurate specification of the turbulent fluxes at sea is considered essential for reliable long-range weather forecasting.

The aim of most investigatory programs is to evaluate the sensible heat flux (H), the flux of water vapor (or evaporation rate, E), and the momentum flux or surface stress (τ) in terms of bulk gradients between the surface and the air of the quantities being transferred: temperature ($\theta_s - \theta_z$), specific humidity ($q_s - q_z$) and wind speed (u_z). The wind speed at the surface is assumed to be zero. The fluxes are then written as functions of bulk aerodynamic transfer coefficients (D_H, D_E and C) which remain to be evaluated.

$$H = \rho c_p D_H u_z (\theta_s - \theta_z) \tag{1}$$

*Permanent address: Division of Meteorological Physics, C.S.I.R.O., Aspendale, Victoria, Australia.

$$E = \rho D_E u_z (q_s - q_z) \tag{2}$$

$$\tau = \rho C u_z^2 , \tag{3}$$

where ρ is air density, c_p is the specific heat of air at constant pressure, and where q_s is the specific humidity of air saturated at the surface temperature, T_s. Two points should be noted here. Firstly, Equation 1 is often written in terms of the absolute temperature (T) rather than the potential temperature (θ), thus neglecting effects of the adiabatic lapse rate ($\approx 0.01°C$/meter). Secondly, the bulk transfer coefficients will be used here in subscripted form so that the height of applicability will be obvious. Thus C_8 indicates a stress transfer coefficient (or drag coefficient) relevant to wind speeds measured at height z = 8 m.

The study described here involves the direct measurement of each of the above fluxes by the eddy-correlation technique, allowing some empirical evaluations of the transfer coefficients. Data were obtained in three experimental periods between August and November, 1970, at a site near Muskegon on the eastern shore of Lake Michigan.

Instrumentation

Turbulent fluxes were measured using up to four "Fluxatrons" of C.S.I.R.O., Division of Meteorological Physics, Australia. These instruments compute the covariance between the vertical wind component (w) and air temperature (to obtain H), humidity (for E), or horizontal wind speed (for τ). Analog techniques are employed, in which capacitive filters are used to remove the mean values of the various parameters.[1] The equations upon which the eddy-correlation method depends are

$$H = \rho c_p \overline{w'T'} \tag{4}$$

$$E = \rho \overline{w'q'} \tag{5}$$

$$\tau = \rho \overline{w'u'} , \tag{6}$$

where the primes denote deviations about mean values and the overbars indicate time averaging (usually over half-hour periods).

In their latest form, the Fluxatrons used at Muskegon employed the following sensors:

w' A vertically oriented propeller anemometer.[2]

u' A six-cup light weight anemometer previously developed at ANL.[3]

T' A small bead thermistor.

q' A hygrometer of the Gjessing type from which fluctuations in relative humidity are obtained.[4]

All these sensors need to be of sufficiently fast response that all flux-carrying eddies are detected.

The eddy-flux sensors, and those for wind speed and net solar radiation (a polyethylene-shielded Funk radiometer), were mounted on a fixed tower erected 700 m offshore in water about 7 m deep.

Whenever possible, surface and air temperatures were measured, the former by using the dipping bucket method in which a mercury-in-glass thermometer gives the temperature of a sample of surface water and the latter by using a hand-held Assman psychrometer usually at a height of about 3.5 m.

Momentum Fluxes

In Figure 1, the average transfer coefficients for momentum obtained at Muskegon are grouped according to wind speed at 10 m (u_{10} being obtained by extrapolation of speeds measured at lower heights) and atmospheric "stability" as indicated by the air-to-water temperature difference. Three "stability" classes are shown: "unstable" [$(T_s - T_z) > 0.5°C$], "neutral" [$0.5 > (T_s - T_z) > -0.5$] and "stable" [$(T_s - T_z) < -0.5°C$]. Because of their uncertain value, no corrections are made for the effects of surface drifts or subsurface currents, which could account, in part, for the large magnitude of the standard errors shown.

The size of the errors is a direct indication of the difficulties inherent in measuring turbulent fluxes of low magnitude to the required accuracy. Typically, momentum fluxes over water are 20% of those found over grass-covered land at the same wind speed.

Wu[5] suggests that $C_{10} = 0.5 \times 10^{-3} \sqrt{u_{10}}$ (when u is in m sec^{-1}), is the best fit to results from open ocean. The present "unstable" and "neutral" data are fitted quite well by Wu's curve, but our "stable" data differ markedly. To illustrate this effect further, the drag coefficients obtained at Muskegon are normalized according to Wu's predicted value and grouped according to the observed surface-to-air temperature difference. The results of this procedure are listed in Table 1. It is seen that as the temperature difference decreases (from highly "unstable"), the drag coefficient ratio drops slowly until a sudden drop is seen at about -0.5°C. The effect is of high statistical significance.

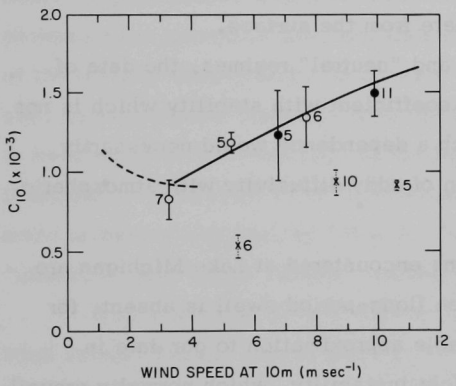

FIG. 1.--Ten-meter drag coefficients obtained using Fluxatrons over Lake Michigan, sorted into classes of atmospheric stability according to the measured surface-to-air temperature differences. Circles represent "unstable" data (surface much warmer than the air), dots are "neutral" (surface and air nearly the same) and crosses are "stable" (air much warmer than the surface). The solid line is Wu's[5] relationship and the dotted line shows the predicted behavior over an aerodynamically smooth surface. The number of observations contributing to each mean is shown.

It is possible, although not likely, that instrumental failure could account for part of this effect. It is known that the principal frequencies associated with flux transfer become higher as stability increases, with a corresponding increase in instrumental difficulties. However, the magnitude of the drop observed

TABLE 1. Ten-Meter Drag Coefficients Obtained over Lake Michigan, Normalized Using the Relationship of Wu[5] and Classified According to Surface-to-Air Temperature Differences, (T_s - T)

	"Unstable"			"Neutral"	"Stable"		
T_s - T, °C	2.52	1.28	0.97	0.00	-0.41	-0.71	-1.44
C_{10}/C_{Wu}	1.11	1.16	0.94	0.96	0.87	0.56	0.57
Error	0.14	0.16	0.07	0.06	0.09	0.11	0.03
No. of runs	4	6	7	9	8	10	11

here and the rapidity of its onset are incompatible with our knowledge of atmospheric turbulence. It seems most likely that the effect is indeed atmospheric, and it seems probable that it indicates some degree of turbulent decoupling of the atmosphere from the surface.

Throughout our "unstable" and "neutral" regimes, the data of Table 1 indicate a variation of drag coefficient with stability which is not contained in Wu's formulation. Such a dependency would necessarily follow from the well-known variation of eddy diffusivity with atmospheric stability.

Even though wave conditions encountered at Lake Michigan are noticeably different from those at sea (long-period swell is absent, for example), Wu's result is an acceptable approximation to our data in conditions of near neutrality and slight instability, which normally prevail over open water. This result is not entirely surprising, since theoretical considerations suggest that small-scale, short-period capillary waves determine the aerodynamic roughness of a water surface.

Sensible Heat Fluxes

Sensible heat fluxes measured at Muskegon were generally low, averaging about 2 mW cm^{-2} (positive indicating an upward flux). As in the case above, such measurements are extremely difficult owing to the low magnitude of the heat transfer over water. For comparison, daytime fluxes over dry land often exceed 20 mW cm^{-2}. Evaluation of the bulk transfer coefficient for heat flux (D_H) is correspondingly difficult,

particularly since the surface-to-air temperature differences found over water are also small, and so each estimate of the coefficient results as the ratio of two inadequately determined values. In this context it has been suggested that the use of the dipping bucket technique for surface temperature measurement contributes an error due to the large temperature gradient likely to exist within the surface water layer. Such an error might be critical to any determination like the one attempted here.

The heat flux data are presented in Table 2, grouped into four wind speed and stability classes. To absorb some of the errors of measurement, average values of the fluxes, wind speeds, and temperature differences are listed in each class, from which best estimates of D_H are obtained. These estimates are generally low, consistent with a systematic overestimation of the surface temperature. If an error of 0.3°C is assumed (attributable, say, to evaporative cooling), then the values listed as D_H' result, more in keeping with our knowledge of the bulk transfer coefficient for heat flux. It should be emphasized that a potential temperature correction has been made in the calculations of Table 2. Had this been neglected, lower "unstable" and higher "stable" values would have resulted.

It is intriguing to note that the most stable data of Table 2, the low wind speed "stable" group, gave an extremely low heat flux. This is precisely the condition under which atmospheric decoupling from the surface was postulated as an explanation for a similarly anomolous result for

TABLE 2. Sensible Heat Flux Data Obtained over Lake Michigan, sorted According to the Surface-to-Air Temperature Difference and u_{10}

	"Unstable"		"Stable"	
Wind speed (u), m sec^{-1}	3.23	6.20	3.85	8.39
Heat flux (H), mW cm^{-2}	0.36	1.33	-0.13	-1.66
T_s - T, °C (T at 3.5 m)	1.11	1.31	-0.57	-0.71
Θ_s - Θ, °C	1.08	1.28	-0.60	-0.74
D_H referred to 10 m (x 10^{-3})	0.77	1.18	0.42	2.08
D_H' (assuming T_s error 0.3°C)	1.14	1.57	0.28	1.45
Number of runs contributing	7	16	3	22

the momentum flux. Neglecting this case, the mean values for the bulk transfer coefficients for sensible heat flux are 1.56×10^{-3} (assuming no surface temperature error) and 1.45×10^{-3} (accepting 0.3°C error). The best estimate from the present data seems to be $D_H \approx 1.5 \times 10^{-3}$, applicable at a wind speed of about 6.3 m sec^{-1}.

There are few published data with which this result can be compared. However, estimates of the comparable coefficient for evaporation, D_E, are available. Since the transfer of heat and that of water vapor in the atmosphere appear to be governed by eddy diffusivities which are identical (to the limits of experimental accuracy in unstable conditions[6]), we would expect the bulk transfer coefficients to differ only by that small amount attributable to the difference in the corresponding molecular diffusivities. It is readily shown that a difference of only a few per cent should result. Values of D_E reported in the literature range from 1.4×10^{-3} to 2.5×10^{-3}. The Lake Hefner study[7] gives, in our units, about 1.6×10^{-3}, in fair agreement with the present result. This value is confirmed by Webb,[8] while Linacre et al.[9] report results which show very little difference from the predictions of the bulk formulation using the Hefner coefficient (actually yielding about 1.5×10^{-3}).

A comparison with semitheoretical considerations involving the known magnitudes of the drag coefficient and thermal conductivity can be made along the line suggested by Swinbank.[10] Using Wu's relationship for C_{10}, it is possible to deduce D_H as a function of wind speed and surface temperature. The results range from 1.3×10^{-3} at 3 m sec^{-1} to 1.6×10^{-3} at 12 m sec^{-1}, for a surface at 15°C in near neutral conditions. At 6 m sec^{-1}, D_H is 1.45×10^{-3}, again in close agreement with our result.

It is tempting to interpret the data of Table 2 as confirmation of such a wind speed effect and, in fact, closer study of the raw data contributing to the table tends to support this conclusion. However, the sensitivity of the present calculations to small errors in temperature

measurement cautions one against any definite statement on this aspect.

Evaporation Rates

During September, some measurements of the latent heat of evaporation were made using the eddy-correlation/Fluxatron approach. Humidity fluctuations were detected using a Gjessing[11] quartz crystal sensor, in which rapid changes in the equilibrium humidity of a thin sensitized surface are measured.

The evaporation rates measured averaged at 10.0 mW cm^{-2}, ranging from 8 to 13 mW cm^{-2} over individual half-hour periods. No measurements of the parameters necessary for the evaluation of a bulk formula estimate of E were obtained during this period, but these were obtained in similar conditions on the following day when the estimate was found to be about 10 mW cm^{-2}. Sensible heat fluxes were about 2 mW cm^{-2} at both times.

Conclusions

The momentum flux measurements reported here suggest that the surface of Lake Michigan behaves essentially as open ocean, since stress measurements at sea yield very similar drag coefficients. However, a strong indication of occasional decoupling of the atmosphere from the lake surface is found, even at moderate atmospheric stabilities.

The sensible heat flux data allow us to estimate the appropriate bulk aerodynamic transfer coefficient $D_H = 1.5 \times 10^{-3}$ referred to 10-m and surface data. Use of the same value in a bulk formula for evaporation (as is supported both by theory and by experimental evidence) leads us to deduce daytime evaporation rates of about 10 mW cm^{-2} during September (i.e., about 4.1 inches per month). This value is verified by direct measurement using the eddy-correlation principle.

An indication of a dependence of D_H on wind speed leads us to suspect a similar variation in D_E. Also, evidence of a change in drag coefficient with atmospheric stability has similar implications for both

D_H and D_E. Thus it is not yet clear whether it is correct to assume, as has become accepted, a constant value for either quantity. In this regard it is important to recognize the possible effects of such relationships on evaporation rates deduced from inland lakes. This situation is basically different from that found at sea, where long over-water fetches assure that the air is generally in near-equilibrium with the surface, leading to an average condition of slight atmospheric instability. For a lake, it is easy to imagine spring and early summer conditions of high stability, particularly during daytime, when both sensible and latent heat fluxes will be much lower than those predicted by conventional application of a bulk aerodynamic formula. The opposite situation would apply during cold weather, and particularly during sudden cold outbreaks.

There is an obvious need for further work of this kind to identify any dependencies of the bulk transfer coefficients on either wind speed or atmospheric stability. Such studies must necessarily involve the direct measurement of the turbulent fluxes and, of the methods currently available, the eddy-correlation technique seems to be well-suited for this purpose.

The Fluxatrons and the Gjessing hygrometry system are on loan to the Radiological Physics Division from C.S.I.R.O., Division of Meteorological Physics, Aspendale, Victoria, Australia.

References

1. Hicks, B. B. J. Appl. Meteorol. 8, 386 (1970).
2. Dyer, A. J., B. B. Hicks, and K. M. King. J. Appl. Meteorol. 6, 408 (1967).
3. Frenzen, P. Argonne National Laboratory Radiological Physics Division Annual Report, July 1966-June 1967. ANL-7360, p. 160.
4. Hicks, B. B. and H. S. Goodman. J. Appl. Meteorol., in press.
5. Wu, J. J. Geophys. Res. 74, 444-455 (1969).
6. Dyer, A. J. Quart. J. Roy. Meteorol. Soc. 93, 501 (1967).
7. Harbeck, G. E. Int. Assoc. Sci. Hydrol. Publ. 3, 437 (1958).
8. Webb, E. K. Commonwealth Sci. and Ind. Res. Org. (Australia), Div. Meteorol. Phys., Tech. Paper No. 10 (1960).
9. Linacre, E. T., B. B. Hicks, G. R. Sainty, and G. Grauze. Agr. Meteorol. 7, 375 (1970).

10. Swinbank, W. C. Studies in Weather Analysis and Forecasting. Air Force Cambridge Res. Center, Mass. Report AFCRC-TR-60232 (1959), pp. B1-16.
11. Gjessing, D. T., C. Holm, T. Lanes, and A. Tangerud. J. Sci. Instr. 1, 107 (1968).

REFRACTOMETER CONSTRUCTION AND TESTING

H. C. Martin*

Among the meteorological variables which describe the state of the atmosphere, the local humidity is perhaps the most difficult to measure, especially when records of fine-scale, fast fluctuations are required. In the lowest layers of the atmosphere, where studies of turbulence require good sensor performance at frequencies as high as 10 to 100 Hz, the problems associated with the determination of the humidity microstructure are perhaps best illustrated by the scarcity of data available.

Several approaches to the problem have met with varying degrees of success. Resistance thermometry has been used to produce fast-response wet bulbs, but these are limited by their susceptibility to contamination and by the need to maintain a carefully controlled rate of water flow to the element. Surface films of various hygroscopic materials have been used in many ways, but these are again subject to contamination when exposed to the real environment. Selective absorption of infrared and ultraviolet radiation by water vapor provides another set of techniques; however, devices using these properties frequently involve mechanical and electronic configurations of unacceptable complexity.

The dependence of the dielectric constant of air (ϵ) on humidity is the physical principle employed by the device known as a refractometer.[1] The dielectric constant of air is related to temperature (T), pressure (p), and vapor pressure (e) by the equations

$$\epsilon = n^2 \tag{1}$$

and

$$(n - 1) \cdot 10^6 = 77.6(p + 4810 \cdot e/T)/T \ , \tag{2}$$

where n is the refractive index.

* Visiting Scientist, Department of Transport, Meteorological Branch, Toronto, Ontario, Canada.

During the summer of 1970, an improved refractometer was designed and built at Argonne. The sensing element is an open air capacitor, the active component in a variable frequency oscillator. The output frequency of this oscillator is mixed with that from a virtually identical circuit in which the air capacitor has been replaced by a stable reference capacitor. In this way the high frequency output of the sensor oscillator (of the order 10 MHz) is reduced to a beat frequency of the order of 3 kHz, and effects of changes in ambient conditions on circuitry components are minimized. Providing the circuits are mechanically and thermally stable to a sufficient degree, the resultant output frequency is dependent on T, p, and e. For operational periods of one hour or less, the pressure dependence can be neglected, and hence humidity measurements may be obtained from the frequency and an independent measurement of T. Moreover, when used over open water surfaces in the manner intended, fluctuations in T are expected to be negligible because of the very low sensible heat fluxes that are obtained in these circumstances. By the same token, the moisture flux is large, and therefore fluctuations in e will be large.

The electronics package was constructed by the Argonne Electronics Division. All components are mounted on a printed circuit board, resulting in a rugged and compact unit which can be easily assembled. The revised circuit design has improved the long-term stability of the instrument.

The sensor capacitor consists of a stack of five invar plates, each measuring about 1.5 x 15 cm, and separated from its neighbor by an air gap of 6.3 mm. The assembly is rigidly mounted on a low temperature coefficient glass plate. All materials used are chosen to minimize the overall temperature sensitivity. The completed instrument is self-contained, weighing 1 kg and with a maximum dimension of 20 cm. Its time constant is about 0.05 sec, and its sensitivity is better than 0.1 mm Hg.

Field tests were conducted on the Lake Michigan tower described elsewhere in this report. Briefly, the tower stood in 6 m of water about 600 m offshore and extended to a height of 6 m above mean water level.

The site affords an upwind water fetch of at least 60 km for prevailing winds from southwest through northwest.

In one test, the refractometer was compared with a Lyman-alpha humidiometer, a commercially available device (Electromagnetic Research Corporation, College Park, Md.) which detects the absorption by water vapor of the Lyman-alpha spectral line of hydrogen. The two instruments were mounted 90 cm apart crosswind, at a height of 4.7 m. A sample variance density spectrum obtained from each instrument is shown in Figure 1. Both spectra closely follow the now well-established -5/3 power law for higher frequency turbulence of sufficiently large Reynolds number. The greater departure of the Lyman-alpha humidiometer curve from the predicted form may have resulted either from interference with the natural wind flow presented by the tower (the humidiometer was mounted only about 35 cm from the tower) or from the somewhat restricted arrangement of the instrument's available sensing volume, a relatively narrow gap between the source tube and the detector. At the time of this test, the water surface was relatively calm, and wind speeds were only about 2 m sec^{-1}. In these circumstances, both humidity instruments appeared to operate satisfactorily.

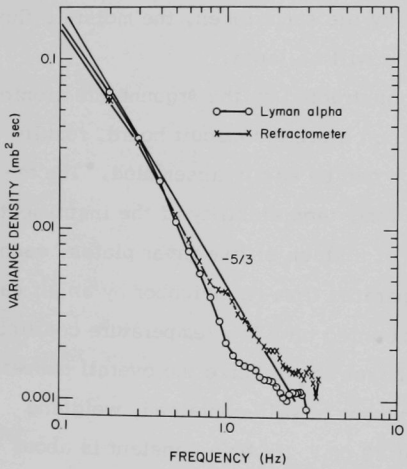

FIG. 1--Humidity spectra obtained from a refractometer and from a Lyman-alpha humidiometer over Lake Michigan on 25 September, 1970. The wind speed was about 2 m sec^{-1}.

Higher winds, about 7.5 m sec^{-1}, prevailed during a second field test, with correspondingly rougher water. Under these conditions it was evident that particular care

must be taken to prevent vibration of the refractometer, since the capacitive sensor is sensitive to its own motions relative to any electrically grounded objects nearby, such as the tower. A slight increase in the low frequency spectral components found during this experiment can be attributed to this type of sensitivity, in this case associated with the oscillating ground plane presented by the large waves. These proximity effects can probably be reduced by improving the shielding of the instrument and by increasing its distance from such sources of error. Further tests to isolate these difficulties are planned.

In neither of the tests was the refractometer signal corrected for the contribution of temperature fluctuations (see Equation 2). Thus, the expectation that the small temperature fluctuations over open water would not distort the result was realized. This is in marked contrast to the situation normally prevailing when refractometers are used over land. The dominance of humidity fluctuations was further confirmed by measurements made of the Bowen ratio (sensible heat flux/latent heat flux) over the lake.

These tests suggest that this type of refractometer should be well suited to the measurement of water vapor fluxes by the eddy-correlation technique, in which fluxes are computed as the (local) covariance between fluctuations of humidity and the vertical component of the wind. For over-water studies, the refractometer may provide sufficiently accurate results without the need for a temperature adjustment of the measured refractive index fluctuations.

The Lyman-alpha humidiometer used in the comparison experiments was made available by the Institute of Oceanography, University of British Columbia, Vancouver. The equipment was brought here and operated by Mr. A. Macklin of the Department of Atmospheric Sciences, University of Washington, Seattle. All arrangements were made with the kind cooperation of Prof. J. Businger of the latter organization. Mr. F. R. George of the ANL Electronics Division improved the refracometer oscillators and constructed the final circuitry.

References

1. Hay, D. R., H. C. Martin, and H. E. Turner. Rev. Sci. Inst. 32, 693 (1961).
2. Bean, B. R. and E. J. Dutton. Radio Meteorology, NBS Monograph 92. U. S. Government Printing Office, Washington, D. C., 1966.

SURFACE HEAT ENERGY BUDGET OVER LAKE MICHIGAN: A PRELIMINARY REPORT

B. B. Hicks, H. C. Martin, and R. L. Hart

Introduction

Measuring rates of change of the total heat content of large bodies of water is fundamental to the investigation of thermal pollution problems. Frequently this is done by comparing temperature-depth soundings distributed in time and space. However, limits on the accuracy of such measurements restrict this procedure to the detection of long-period changes with time scales of the order of weeks or months. Important day-to-day changes associated with varying meteorological conditions, such as wind speed or cloudiness, are lost in the averaging process. The difficulties become especially severe when dealing with the thermal budgets of bodies of water as large as the Great Lakes, where the amplitude of day-to-day fluctuations in the rate of exchange of natural heat with the atmosphere can often exceed the average changes observed from one month to the next.

An alternative approach is via the surface heat balance equation, usually written as

$$R - G = H + LE , \qquad (1)$$

in which the right-hand side represents the rate of heat loss per unit surface area to the atmosphere by diffusive processes: H is the upward sensible heat transfer, and LE is the latent heat of evaporation. Four components comprise the net radiation R: the short wave solar radiation $R_s\downarrow$, the reflected short wave component $R_s\uparrow$, the incoming long wave radiation $R_l\downarrow$ and the long wave radiation $R_l\uparrow$ emitted from the surface. The net radiation is then $R = R_s\downarrow + R_l\downarrow - R_s\uparrow - R_l\uparrow$. The water heating flux is written as G to preserve the terminology used over land, where G is the "ground heat flux."

Using this approach, diurnal cycles of G can be constructed from

measured cycles of R, H and LE. Such measurements were made during the micrometeorological experiment near Muskegon, Michigan. Data obtained during three days in October, 1970 are used here to give an example of the diurnal heat cycle of Lake Michigan.

Data Sources

A net radiometer and several anemometers were mounted on a fixed tower 700 m off the eastern shore of Lake Michigan described earlier in this report. (See "Micrometeorological Measurements over Lake Michigan.") Surface temperatures were obtained whenever possible by measuring the temperature of surface water samples. Air temperatures and humidities were measured with an Assmann psychrometer.

Sensible heat fluxes were measured directly by eddy-correlation instruments (Fluxatrons) mounted on the tower. The turbulent fluxes are considered in some detail earlier in this report.

Evaporation rates are estimated from the bulk aerodynamic formula

$$LE = \rho L D_E u_z (q_s - q_z) , \qquad (2)$$

where L is the latent heat of vaporization of water, E is the evaporation rate (in cm/sec), ρ is the air density, u_z is the wind speed at height z, q_s is the specific humidity of air saturated at the surface temperature and q_z is the ambient specific humidity at height z. D_E is the bulk transfer coefficient for water vapor, for which a value of 1.5×10^{-3} is used here, as indicated by consideration of the eddy flux measurements. It should be noted that this value of the transfer coefficient is similar to, but somewhat smaller than, the figure usually used in formulations of this kind. The value 1.6×10^{-3} often used has been derived from studies of smaller reservoirs (e.g., Lake Hefner). It appears to be somewhat large when compared against measures of evaporation over open water surfaces where the air, to significantly greater heights, is in closer equilibrium with the water surface, thus tending to reduce rates of evaporation.

Results

Data obtained on October 25, 26, and 29 were sufficient to allow an average diurnal cycle to be identified. These days were of similar meteorological conditions, with onshore winds of about 5 m sec^{-1}, average daily air temperatures of about 12°C, scattered clouds by day and mainly clear skies at night. Figure 1 illustrates the results obtained, the broken lines indicating extrapolation of our data on the basis of measurements made on other occasions.

Net incoming radiation is seen to peak at about 48 mW cm^{-2}, significantly higher than would be expected over land but explainable in terms of the extremely low albedo of a water surface. At this time (solar noon) the outgoing sensible heat flux H is 2 mW cm^{-2}, while the evaporation rate corresponds to a latent heat flux LE of approximately 9 mW cm^{-2}. Thus, at the time and in the conditions of the present example, about 77% of the available solar energy at mid-day goes toward water heating.

At night, each flux removes heat from the surface, in this case at rates of about $|R| = 7$, $|LE| = 7$ and $|H| = 2$ mW cm^{-2} on a clear night at this time of year.

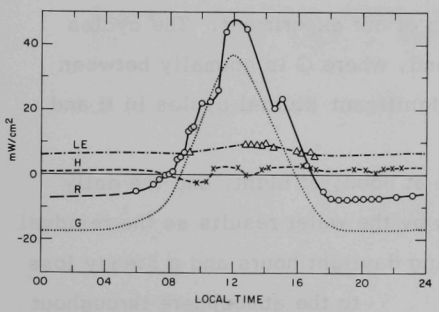

FIG. 1.--Measurements of the components of the heat energy budget over Lake Michigan. Solid lines indicate direct measurement of the plotted quantity; broken lines show interpolated or inferred values. Data obtained on three days are combined.

As a 24-hour average, Figure 1 indicates that the solar energy input amounts to about 5 mW cm^{-2}. The average loss of heat to the atmosphere through turbulent exchange during the same period is $H + LE \simeq 8 + 2 = 10$ mW cm^{-2}. Thus the average flux of heat within the water is upward, with a rate equal but opposite to the solar input (-5 mW cm^{-2}). Assuming complete mixing throughout the 7-m

depth at the base of the observation tower, this loss of heat would correspond to an average water temperature decrease of approximately 1.0°C per week. For comparison, surface temperatures measured through our entire experimental period indicate an average cooling rate of 1.1°C per week.

The mean daily evaporation rate estimated from the diagram is about 3.3 in/month, corresponding to the average latent heat flux LE = 8 mW cm^{-2}. The value 4.1 in/month was obtained on two other occasions in September and October, when the same technique was used. Over these two months, an average evaporation rate of 3.8 in/month results. In comparison, Richards and Irbe[1] obtained 4.0 in/month for Lake Huron during the same months, which we might expect to be comparable with our result considering the similarities in water depth and average latitude of Lakes Huron and Michigan.

Conclusions

The cycles drawn in Figure 1 represent our understanding of the surface flux behavior in the conditions of our experiment. The cycles differ greatly from those found over land, where G is normally between 10 and 20% of R at noon, and where significant diurnal cycles in H and LE are usually found.

Table 1 summarizes the fluxes at noon, at night, and the daily averages. The mean rate of heat loss by the water results as the residual between a large but periodic gain during daylight hours and a steady loss to the atmosphere throughout the entire 24-hour period. In this regard, cloudiness is obviously a critical consideration through its effect upon the net radiation, both by restricting the incoming short wave radiation by day and by reducing the out-

TABLE 1. A Summary of the Surface Heat Fluxes Found over Lake Michigan, October 25, 26 and 29, 1970.

	mW cm^{-2}			
	R	LE	H	G
Noon peak	48	9	2	37
Midnight	-7	7	2	-16
Daily average	5	8	2	-5

going long wave radiation at all times.

The overall average evaporation rate deduced from our data using the technique outlined in this example is 3.8 in/month for the months of September and October.

The case study presented here represents an occasion when the lake, as a whole, was losing heat. However, at other times of the annual cycle large gains occur. In particular, in mid-summer not only does the net radiation maximize at a higher level but also there is an average smaller cloud cover, implying an even greater rate of heat gain than would be expected on simplistic grounds. The net radiation at noon may exceed 60 mW cm^{-2}, possibly leading to a peak water heating flux 30 to 50% greater than we measured in late September. Investigation of this remains a problem for the future, probably best approached using the techniques outlined here.

Reference

1. Richards, T. L. and J. G. Irbe. Proc. 12th Conf. on Great Lakes Research, Ann Arbor, Michigan, May 5-7, 1969. Braun-Brumfield Inc., Ann Arbor, 1969, p. 469.

WIND STRESS OVER LAKE MICHIGAN BY VARIANCE REDUCTION ANALYSIS OF LIHT ANEMOMETER MEASUREMENTS

Paul Frenzen and R. L. Hart

Introduction

One of the aims of the Lake Michigan micrometeorological observation program is to evaluate the constants (i.e., the exchange coefficients) in the parametric relations for the vertical turbulent diffusion of heat, moisture, and momentum. The goal is to express these important but rather difficult to measure exchange rates in terms of the more easily recorded average measures of temperature, relative humidity, and wind speed. In the case of the vertical flux of momentum (which is equivalent to, and frequently simply identified as, the horizontal stress exerted by the wind upon the surface), the problem of parameterization reduces to determination of the drag coefficient C_d in the expression:

$$\tau = -\rho C_d \overline{U}_z^{\,2} .$$

Here τ is the wind stress in dynes per cm^2, while ρ represents air density and $\overline{U}_z$ the mean horizontal wind speed at a given elevation z, each in appropriate cgs units. Although sometimes omitted, the negative sign convention emphasizes that the flux of momentum is normally directed downward, opposite to the gradient of horizontal wind which almost invariably is directed upward.

From the equation it will be seen that the magnitude of C_d is a function of the height chosen for the reference wind $\overline{U}_z$. In work over open sea, the 10-m level is widely used as a standard; hence the coefficient is often written C_{d10}, or simply C_{10}. Since it is simply a proportionality factor, C_d is dimensionless; therefore one can write

$$C_d = (u_*/\overline{U}_z)^2 ,$$

which introduces the familiar scaling parameter, the friction velocity:

$$u_* \equiv \sqrt{\tau/\rho} \, .$$

Wind stress over water can be measured by several methods, each with its own particular problems and advantages. In near neutral stratification, a condition which nearly always obtains sufficiently far from land, properties of the logarithmic wind profile are often utilized. From the observed variation of wind speed with height one has

$$d\overline{U}/dz = u_*/kz; \qquad \text{hence} \quad \tau/\rho \equiv u_*^2 = [kz(d\overline{U}/dz)]^2,$$

where $k \simeq 0.41$ is the von Karman constant. In practice, the measurement of wind profiles over the relatively smooth surfaces presented to the wind even by nominally "rough" water is difficult because the wind stresses are so small that speeds change only very slowly with height. Consequently, quite accurate wind sensors must be used, these mounted at at least three, and preferably four or five, different elevations.

To observe the strongest wind gradients, differences in wind speed fairly close to the surface are required. In addition to all other difficulties presented by this, the wave-top environment, small errors in height at low elevations contribute significant percentage errors to gradient measurements. Successful profile measurements apparently have been made with sensors mounted on free-floating, semistable buoys, notably by the group from the Meteorological Institute of the University of Hamburg. However, results obtained by this last method are distinctly different from our own (see Fig. 1).

The eddy-correlation procedure (some examples of which are described by Hicks[1] in this report) has been suggested as the standard flux measurement over open water to which results obtained by other methods should be compared. This procedure makes no stability assumptions and places no premium upon knowledge of the actual height of the instrument, other than assurance that the device is located within the nominal constant

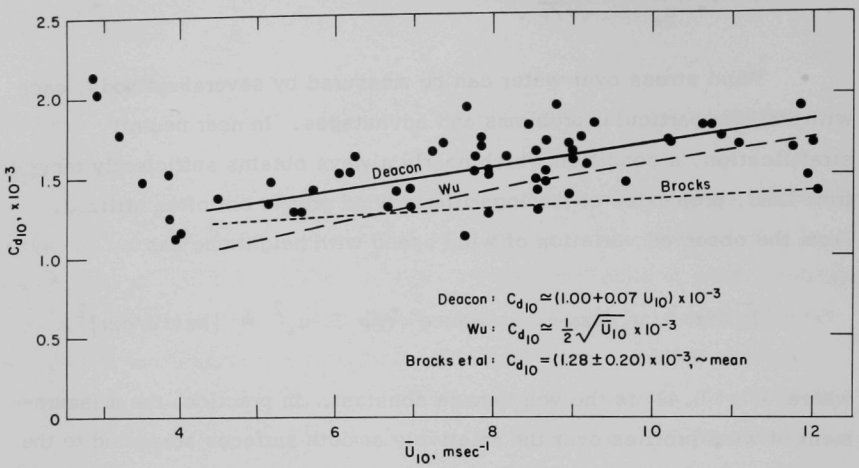

FIG. 1.--Ten-meter drag coefficients obtained by the single dissipation method and variance reduction analysis of winds recorded over Lake Michigan. Solid curves represent empirical relations suggested by Deacon[8] and Wu[9], respectively, while the dashed line represents an approximate mean of results derived from profile observations by Brocks and Krügermeyer.[10] (Also see Ref. 1, Fig. 1.)

flux layer, say no higher than 10 m. For momentum flux, the eddy correlation method requires accurate resolution and simultaneous measurement of moderately high frequency fluctuations in both horizontal and vertical components of the wind. Surface stress is obtained by calculating the covariance of the two wind signals over a relatively wide range of frequencies (Ref. 1, Eq. 6). Properly carried out, the eddy correlation method is a definitive one. In practice, however, its use is limited to rigid-tower installations, since the wind sensors must be maintained in proper orientation to the true vertical in order to resolve the wind components with the requisite accuracy. Alignment errors as small as one or two degrees cause systematically correlated errors in both components which are compounded in the covariance calculation.

A third method based upon the statistical nature of small-scale turbulence is the subject of the present report. Like the profile method, its application both presupposes near-neutral stratification and requires some knowledge of the sensor height. But only a single sensor is used, and that instrument need not operate close to the water surface. However, it must have good dynamic response since higher frequency fluctuations (on the order of 1 or 2 Hz) are to be recorded. Analysis is simplified by the fact that only single-signal variance rather than two-signal covariance is computed. Finally, the use of higher frequency wind speed fluctuations allows the effects of low frequency noise (e.g., that resulting from motions of a semistable platform) to be minimized by appropriate filters. As will be seen, variance reduction analysis used in the present study defines a band pass filter which takes care of this problem automatically.

Theoretical Basis of the High-Frequency Method

The kinetic energy of higher frequency atmospheric turbulence near the ground (to a fair approximation, where $f > \overline{U}/z$) appears to follow the Kolmogorov relation for the inertial subrange, even though conditions specified by the theory are not always fully met. Thus, for the spectral energy density $E(f)$ we have

$$E(f) = \alpha \epsilon^{2/3} \overline{U}^{2/3} f^{-5/3} ,$$

in which $\overline{U}$ is the mean wind speed, f is the frequency, and ϵ represents the rate at which turbulent kinetic energy is dissipated through work done against the viscous stresses. Although the point is not absolutely established, measurements of atmospheric "downwind" or speed spectra (as computed, for example, from data recorded by fast-response cup anemometers) appear to agree on a value of the Kolmogorov constant α very near to that found by our own (unpublished) measurements in Australia, that is $\alpha = 0.49$ for f measured in Hz. At any rate, by measuring the turbulent kinetic energy in an integrated "slice" of the "psuedo-inertial,"

5/3 spectral region detectable by our equipment (which typically sums $E(f) \cdot df$ over $\overline{U}/z$ values between 1 and 2), it becomes possible to determine the dissipation rate ϵ through the Kolmogorov relation.

In steady conditions, the turbulent energy budget can be written as a balance between dissipation and production:

$$\epsilon = \frac{\tau}{\rho} \frac{d\overline{U}}{dz} + \frac{(H + 0.07\ LE)}{\rho c_p} \frac{g}{\overline{\theta}} - D,$$

where, in addition to the previous notation, we represent H as the turbulent flux of sensible heat, L as the latent heat of vaporization, E the rate of evaporation (hence the combination LE represents the flux of latent heat), c_p the specific heat of air at constant pressure, g the acceleration of gravity, and $\overline{\theta}$ as the mean temperature. The first term on the right represents the production of turbulent energy by mechanical shear, while the second represents production by buoyancy forces. Note that insofar as it affects the rate of production of turbulent kinetic energy through work done by buoyancy forces, the flux of density defect associated with a flux of latent heat is only about 7 percent as effective as that contributed by sensible heat.

The third term on the right, entered here simply as -D, represents the sum of vertical divergence terms of unknown magnitude. To a first approximation they are often neglected, this constituting the so-called "local dissipation assumption." In the present treatment it is still necessary to follow this course. However, these terms, especially to the extent that their contributions may differ over water surfaces from what they are over rigid land, remain a subject of continuing study within the Lake Michigan micrometeorological project.

For conditions typical of the present experiments, the relative importance of the buoyancy production term can be estimated from the observations of the diurnal energy balance summarized elsewhere (Ref. 2, Fig. 1), where the maximum values of H and LE observed were 2 and

10 mW cm^{-2}, respectively. This corresponds to a total flux of density defect (H + 0.07 LE) less than 3 mW cm^{-2}. Inserting appropriate values for the remaining factors in the buoyancy term, one finds this corresponds to a kinetic energy production rate of about 7 ergs $g^{-1}sec^{-1}$. This compares to mechanical production rates approaching 70 ergs $g^{-1}sec^{-1}$ in winds of 6 or 7 m sec^{-1} at a height of 5 m over open water. It follows that in winds of 5 m sec^{-1} or less, or at elevations of, say, 8 m or more, consideration should be given to contributions by buoyancy to the kinetic energy budget. Corrections of this kind were made where required in computing the results presented in Figure 1. As expected, the adjustments were generally quite small.

In stable stratifications it is not immediately clear just how the energy budget adjusts. During the present series of observations, some small negative heat fluxes were observed on those occasions when air-sea temperature differences indicated that thermally stable conditions prevailed. However, the upward flux of density defect due to evaporation continued at a comparatively high rate; consequently, the sum (H + 0.07 LE) tended to converge upon zero, without actually reversing the sign. During extreme conditions of very cold surface water, the latent heat flux could be expected to reverse as well; that is, downward vapor transfer and surface condensation could occur. Such conditions do obtain over Lake Michigan, notably in the early spring. Hence these phenomena will be available for future study in the continuing investigation.

From the foregoing, it follows that in the prevailing, near-neutral conditions over open water, the energy equation reduces to

$$\epsilon \simeq \frac{\tau}{\rho}\frac{d\overline{U}}{dz} = \frac{u_*^3}{kz}; \qquad \text{hence } u_* = (\epsilon\, kz)^{1/3},$$

where u_* is introduced by substituting the log profile relation for the shear. This relation is the basis of the "single-dissipation method" used to compute the stress estimates summarized in Figure 1.

Experimental Procedure

Observations were made from the Lake Michigan tower described in the introductory article to this section (Ref. 3, Fig. 1). The six-cup, low inertia anemometers described previously[4] were used. These instruments were mounted at several levels between 3 and 8 m above the surface, but with few exceptions the present results derive data recorded by the sensor located at an intermediate level near 5 m. Only when this unit was out of service were the winds recorded at higher or lower elevations utilized.

After being relayed to shore by underwater cable or radiotelemetry, the fluctuating, audiofrequency signals of the anemometers were recorded on magnetic tape for subsequent integration and computer processing at ANL. In addition, two data channels were analyzed in real time by a small, special-purpose digital computer, the variance reduction computer or Varcomp. All results shown in Figure 1 were obtained with this device, the data having been either processed in real time during the field experiment, or recomputed during later reruns of the magnetic tape at ANL. These reruns were designed to improve the choice of the digital filter (i.e., averaging interval) used.

From one point of view, the Varcomp uses the method of variance reduction analysis (Varedan);[5] from another, this portable computer evaluates a single estimate of a smoothed structure function. In either case, the operation consists of recording that fraction of the signal variance transmitted through a numerical band-pass filter defined by two averaging processes. Writing the variance of the wind signal smoothed over a particular time interval ΔT_j as $\overline{u_j^2}$, the Varedan relation takes the form:

$$\epsilon = \frac{A}{U} \left[\frac{\overline{u_j^2} - \overline{u_k^2}}{\Delta T_k^{2/3} - \Delta T_j^{2/3}} \right]^{3/2}$$

in which the numerical constant $A = 3.39$ is related to the value $\alpha = 0.49$ given earlier for the Kolmogorov constant. The numerator of the term in

brackets will be seen to constitute the net signal variance passed by the filter since this quantity represents the additional reduction in signal variance effected by increasing the average interval from ΔT_j to ΔT_k. The arithmetic program of the Varcomp circuit differs from this general Varedan approach only in that choice of averaging times is limited to $(\Delta T_j, \Delta T_k)$ pairs in which one smoothing interval is twice the other. Although this defines a usefully narrow numerical filter, only about 50 percent of the available signal energy is transmitted to the central frequency (see Ref. 6, Fig. 2, p. 387).

In addition to collecting a long-term sum of the anemometer signals for a measure of $\overline{U}$, the small computer accumulates the statistic

$$\Delta\sigma^2 \equiv \sum_{i=1}^{N} (x_{2i-1} - x_{2i})^2,$$

which can be shown to be a measure of the reduced variance term in the numerator of the Varedan relation. Quantities denoted x in the above represent samples of anemometer pulses collected during successive, constant sampling intervals ΔT, each interval typically a few tenths of a second in duration. It follows that terms within the parentheses represent a series of N successive short period wind speed changes evaluated between the central times of equally short period average wind speeds. Squaring and summing this difference over N consecutive pairs gives the Varcomp statistic. The close relation between this expression and the structure function is evident in the similar form of the latter:

$$D(t) \equiv \overline{[u(T) - u(T + t)]^2},$$

where the overbar denotes an average over elapsed time T. The two expressions will be seen to differ only in that, whereas the structure function represents a <u>set</u> of average changes in <u>instantaneous</u> wind speed evaluated over a <u>range of lag times</u> t as an independent variable, the

Varcomp statistic represents a single averaged change of average wind speeds characteristic of a single choice of lag time ΔT.

Smoothing time series data over a running, averaging interval ΔT selectively attenuates variance spectra in accordance with the (low-pass) filter function

$$\mathrm{sinc}^2 (f\,\Delta T) \equiv \frac{\sin^2 (\pi f \Delta T)}{(\pi f \Delta T)^2} .$$

(For example, see Ref. 7.) By successively smoothing such data over two averaging intervals, ΔT and $2\,\Delta T$, as in effect the Varcomp does, the net signal variance recorded is limited to that transmitted by the equivalent band-pass filter:

$$\Delta\mathrm{sinc}^2 (f, \Delta T, 2\,\Delta T) \equiv \frac{\sin^2 (\pi f \Delta T)}{(\pi f \Delta T)^2} - \frac{\sin^2 (\pi f\, 2\,\Delta T)}{(\pi f\, 2\,\Delta T)^2} .$$

This function has a maximum value ($\sim$0.52) at $f\,\Delta T = 0.37$; accordingly, the central frequency of the Varcomp band-pass filter is located at

$$f_c = (0.37/\Delta T)\ \mathrm{Hz}.$$

In the predominantly neutral and weakly unstable conditions of these measurements over open water, the psuedo-inertial, -5/3 range of downwind atmospheric speed spectra is commonly found to extend to frequencies as low or lower than $\overline{U}/z$ Hz. A Varcomp ΔT setting such that $f_c = 2(\overline{U}/z)$ is, therefore, normally used in order to insure that the filter is located well within the -5/3 region. However, initial spectral analyses of the records of this experiment indicate the presence of excessive high frequency noise, evidently as a result of deformation of the upper shaft of the anemometer cup assembly in the sustained high winds to which the instruments were exposed. Real-time Varcomp analyses using $\Delta T = 0.18\ (z/\overline{U})$, which corresponds to $f_c = 2(\overline{U}/z)$ as above, admitted a significant fraction of this spurious signal variance; consequently dissipation rates, and hence the stresses, were overestimated. To reduce

these errors, all tapes were rerun through the Varcomp with $\Delta T = 0.24$ $(z/\overline{U})$, this shifting the filter toward slightly lower frequencies $[f_c = 1.5\ (\overline{U}/z)]$ and away from the region of noise. The results obtained and plotted in Figure 1 may still be slightly high. The point will be better understood when analyses of power spectra for all runs are completed.

It will be noted that the definition of the averaging interval ΔT in terms of the ratio $z/\overline{U}$ effectively limits Varcomp analyses to consideration of normalized turbulence spectra; systematic variations in turbulence intensity (and hence ϵ, and ultimately the apparent stress) due to variations in the height of measurement, and the variation of wind with that height, are eliminated.

Discussion

Figure 1 plots results of the wind stress measurements over Lake Michigan obtained by the single-dissipation, Varedan method. These are presented in the more or less standard form of equivalent drag coefficient $C_{d_{10}}$ vs. $\overline{U}_{10}$, the average wind speed at the 10-m level. Also shown are two empirical relations given by Deacon[8] and Wu,[9] respectively, each of these having been derived by fitting results obtained by many investigators, who used many different experimental procedures. The third and nearly horizontal line on the diagram represents an average of more than one hundred stress determinations computed from wind profile measurements made by the Hamburg group, using a semistabilized mast mounted on a buoy in the open sea.[10]

Since final power spectra from records of these preliminary trials over Lake Michigan are yet to be completed, it would be premature to discuss these results in detail. Moreover, preparations are now being made to return to the field for additional measurements during 1971 with improved equipment (notably with a new version of the low-inertia anemometer featuring faster response and reduced upper shaft runout). But the close correspondence to Deacon's relation (and to a lesser extent, to Wu's) is worth noting, especially in the matter of the slope, since the amplitude of the present,

single-dissipation estimates of $C_{d_{10}}$ may still be slightly too large due to instrumental noise.

The systematically and markedly different results obtained by the Hamburg group are intriguing. Since simultaneous covariance measurements by Hicks[1] more nearly follow Wu's curve, the nearly constant drag coefficients obtained from the Hamburg stailized mast profiles are all the more difficult to accept. The point is an important one since the behavior of the drag coefficient at wind speeds greater than 12 or 15 m sec^{-1} is a matter of both theoretical interest and practical value. There are reasons to believe and some data to support the position that $C_{d_{10}}$ does tend to become constant at higher wind speeds; but the ultimate maximum value is generally expected to be considerably greater than that suggested by the flat Hamburg curve.

To the overall air-sea interaction problem, wind stress at speeds greater than 15 m sec^{-1} is important not only because most momentum transfer occurs during such conditions, but also because these apparent extremes frequently characterize average conditions for long periods over large expanses of open ocean. In the Great Lakes, periods of maximum wind stress are associated with the greatest horizontal mixing by larger scale circulations; in Lake Michigan in particular, such conditions probably account for periods of maximum water transfer between the southern and northern basins, and between the northern basin and Lake Huron as well.

Below 5 m sec^{-1} stresses over water become very small and difficult to measure by any means. Even the probably excessive value $C_{d_{10}} \simeq 2 \times 10^{-3}$ at 3 m sec^{-1} shown in the figure corresponds to a surface stress of only 0.2 dyne cm^{-2}. The several high drag coefficients at low wind speed obtained by the present experiments are partially accounted for by the fact that the data were recorded in unstable conditions. But supporting temperature data available during these trials are not considered sufficiently reliable to make more than this qualitative observation. Accurate resolution of the variation of drag coefficients as a function of stability awaits more accurate measurements over a wider range of known stability conditions.

References

1. Hicks, B. B. This report.
2. Hicks, B. B., H. C. Martin, and R. L. Hart. This report.
3. Frenzen, P. This report.
4. Frenzen, P. Argonne National Laboratory Radiological Physics Division Annual Report, July 1966-June 1967. ANL-7360, p. 160.
5. Frenzen, P. Quart. J. Roy. Meteorol. Soc. 91, 28 (1965).
6. Frenzen, P. Proc. USAEC Meteorol. Inf. Mtg., 11-14 Sept., 1967, Chalk River, Ontario. Report AECL-2787, p. 381.
7. Bracewell, R. M. The Fourier Transform and Its Applications (McGraw-Hill, New York, 1965).
8. Deacon, E. L. and E. K. Webb. Small scale interactions, The Sea (Interscience, New York, 1962), p. 43.
9. Wu, J. J. Geophy. Res. 74, 44 (1969).
10. Brocks, K. and L. Krügermeyer. Berichte Inst. Radiomet. and Mar. Meteorol. Hamburg, No. 14 (1970), as discussed by H. U. Roll during NATO Advanced Study Institute, Isle of Man, Sept. 1970.

THE DETERMINATION OF CHIMNEY PLUME RISE THEORY AND PRACTICE*

Harry Moses

Information on plume rise is important in determining resulting concentrations of a pollutant on the ground. Practical use of plume rise values may be made in connection with stack design, the use of urban air pollution models, and in evaluating the hazards to a population complex.

The first work on plume rise was performed in England by C. H. Bosanquet in 1935, but a few years later, in 1941, R. H. Sherlock and E. A. Stalker at the University of Michigan carried out the first important work in this country. They performed their experiments in a wind tunnel. The work was performed at the request of the Commonwealth Edison Company of Chicago, Illinois to alleviate a serious downwash problem in one of its plants. During the 1950's the theoretical foundation of plume rise was established and during the 1950's and 1960's many field experiments to measure plume rise were performed. The most important of these were made by H. Rauch in Germany; by D. H. Lucas, D. J. Moore, and G. Spurr in England; by B. Bringfelt in Sweden; by P. R. Slawson in Canada; and by the Tennessee Valley Authority in the United States. A useful set of measurements was also obtained by the author and his collaborators J. E. Carson and G. H. Strom at the Argonne National Laboratory.

Many different measuring techniques were used. These involved photography using both stereo and single cameras, aircraft, Geiger-Mueller detectors for radioactive plumes and lidar. A mathematical derivation is presented for converting points on the film to points in space for a given coordinate system based on the Argonne stereo techniques. Data from 10 sets of experiments involving 615 observations and 26 different stacks were used to study the relation between plume rise and related meteorological and stack parameters.

---

*Abstract of thesis submitted to the Department of Meteorology and Oceanography of the University of Michigan in partial fulfillment of the requirements for the Doctor of Philosophy degree.

The data were subdivided into three classes depending on stack size: 1) data from small stacks - those taken in the Argonne experiments; 2) data from intermediate stacks - those of Duisberg, Gernsheim and Harwell; and 3) data from large stacks - those of TVA - Paradise, Gallatin and Widows Creek, and those of Lakeview in Ontario, Canada. The data obtained by Bringfelt in Sweden were used as an independent data set and contained measurements from stacks smaller than that at the Argonne National Laboratory to those approaching the TVA stacks.

The second portion of this study deals with the development of techniques for determining plume rise. First, seventeen commonly used formulas were tested for goodness of fit. The criteria used were: 1) the ratio of observed to calculated plume rise; 2) the root mean square of the differences between observed and calculated plume rise values; and 3) the correlation coefficient. Additional information concerning each of the seventeen formulas are presented such as the mean calculated plume rise and the standard deviation of the calculated plume rise values.

In an attempt to improve upon the formulas appearing in the literature, least squares fitting procedures were used to obtain formulas which would provide a better fit. The three criteria of merit given above were used. The selected functional forms involved those factors which, on physical grounds, markedly influence the rise of a smoke plume, viz., buoyancy, momentum, wind speed, and stability. The results indicated some improvement over those obtained from the formulas in the literature but left much to be desired.

In working with the data the writer developed what he has called the Tabulation Prediction Scheme. This technique is a method whereby an estimate of the value of a dependent variable may be obtained from information on the independent variables. Combinations of the independent variables - wind speed, heat emission rate, momentum rate and stability - are arranged in an ordered sequence. For each combination of independent variables, the cumulative percentile frequency distribution of the dependent variable based on past measurements is given along with other statistics such as the mean, standard deviation, and interquartile range, i.e., the difference in plume rise between the 75th and 25th percentile values. Thus, one may look up the combination of the independent variables just as one looks up words in a dictionary to obtain the percentile frequency distribution of the dependent variable. The mean given may be considered as the best estimate for the given conditions. This system appears to offer a significant improvement over any of the previously developed formulas and is much easier to use. Further, it provides not only a point estimate, but the entire frequency distribution of past occurrences, for the conditions of interest. The Tabulation Scheme is recommended as the method to be used in calculating plume rise.

MIXING HEIGHTS, VENTILATION RATES AND OBSERVED GROUND SO_2 CONCENTRATIONS

Harry Moses, Donald F. Gatz, Arthur C. Strong* and Gunther A. Zerbe.

A program of low-level atmospheric soundings from Chicago Midway Airport began in April 1969 to determine urban mixing heights and ventilation rates. Simultaneously, the City of Chicago Department of Environmental Control measured SO_2 concentrations continuously at eight stations. This paper presents a brief climatology of mixing height and ventilation rate and explores the relationships between air quality and mixing height data for the first year of soundings.

Analysis of the data shows a weak relationship between SO_2 concentrations and mixing height and ventilation rate.

Introduction

The concept of atmospheric mixing height assumes the existence of a layer near the ground in which atmospheric aerosols or contaminants have accumulated but are well stirred. The pall of atmospheric "dirt" one observes when flying into a large city or even approaching it by a ground-based vehicle, no doubt, delineates the aerosol mixing layer. This layer is appreciably more turbulent than the layer above.[1] It is also a common belief that this layer is capped by an inversion so that its thickness may be determined from the temperature-height or temperature-pressure curve.

Whether the mixing layers indicated by the aerosol, turbulence, or stability are one and the same during all hours of the day is questionable. McCaldin and Sholtes[1] presented a few aircraft measurements showing a correspondence among all three. With complete mixing in the mixed layer, and the same input from the surface, aerosol concentrations should vary inversely with the depth of the mixed layer.

One objective of this study is to determine the relation between mixing height and pollutant concentrations. To provide information on the mixing layer and other meteorological parameters necessary for use in air

* Air Pollution Meteorologist, National Oceanic and Atmospheric Administration, Environmental Meteorological Support Unit, National Weather Service.

pollution abatement procedures the Weather Bureau (now the National Weather Service) in collaboration with the National Air Pollution Control Administration (now the Air Pollution Control Office) established Environmental Meteorological Support Units (EMSU) in five cities, including Chicago, in 1969. The second objective is to summarize the first year of mixing height and ventilation rate measurements at the Chicago Midway Airport.

EMSU units release two 403-MHz radiosondes per day, Monday through Friday; one within 30 minutes of sunrise, and the other around 1000 LST. The radiosondes carried aloft on a 100-gram balloon provide data on temperature, pressure and relative humidity and ascend at about 200 meters per minute. Single-theodolite readings made every 30 seconds are used to determine wind speed and direction.

Definitions of Mixing Height and Ventilation Rate

We have used the definitions of mixing height and ventilation rate given by the U.S. Weather Bureau[2] and by Holzworth.[3] The following paragraphs briefly review these definitions.

Mixing Height Definitions

Morning Mixing Height - 5°C. Because of the thermal properties of city buildings and streets, an urban area cools more slowly than the surrounding rural area after sundown. Further, cooling of the surface layers often leads to the formation of inversions in the country; stability also increases in the city, but to a lesser degree, and inversions are less frequent.

When soundings are made in rural areas the urban surface temperatures are approximated by adding 5°C to the rural surface temperature. The 5°C morning mixing heights are probably an overestimate of the maximum urban heat island relative to Midway Airport and are not presented in this report.

Morning Mixing Height - 3°C. Midway Airport is definitely within the urban area, but probably not in the area of maximum heat island effect. Mixing heights based on a surface temperature of 3°C greater than

that measured at Midway Airport are presented in this report as a reasonable index of the Chicago mixing depth.

Observed Morning Mixing Height. The "observed" mixing height is defined as the height above ground where the observed lapse rate first becomes greater than pseudoadiabatic or approximately 6°C per kilometer.

Afternoon Maximum Mixing Height. This version of the mixing height is determined "after the fact." It represents the height above ground where the dry adiabat through the observed afternoon maximum temperature intersects the temperature profile measured at 1000 LST.

The Ventilation Rate. The ventilation rate is defined as the product of the mixing height and the mean wind speed in the mixed layer. One would expect that for a constant emission rate of pollutants, concentrations in the mixed layer would be high if the ventilation rate were low, and vice versa. With light winds and a low mixing height, high pollution conditions are expected.

The mean wind needed for calculating the ventilation rate was computed in two ways.

Arithmetic Mean Wind. In this method the wind directions at all the standard reporting heights (every 100 m up to 1000 m, every 200 m from 1000 to 1400 m, and every 400 m above 1400 m) within the mixing layer are averaged arithmetically. The arithmetic mean wind speed is computed from wind speeds at the same levels.

The Vector Mean Wind. In this method displacement vectors of the 30-sec wind measurements in the mixing layer are plotted and added vectorially to determine the actual position at the top of the layer. The resultant vector is then projected on a horizontal plane. The azimuth direction of this vector is the vector mean direction, and its magnitude divided by the duration of the flight to that point is the vector mean wind speed.

The ventilation rate may be calculated from either mean wind speed, but the ventilation rates reported in this paper were computed from the vector wind.

TABLE 1. Annual Means and Ranges of Mixing Heights and Ventilation Rates, 15 April, 1969-14 April, 1970. Chicago Midway Airport.

	Mean	Maximum value	Minimum value
3°C morning mixing height, m	428	1900	30
Afternoon maximum mixing height, m	1127	2800	200
Afternoon ventilation rate, m^2 sec^{-1}	8889	36,480	408

The Climatology of Mixing Heights and Ventilation Rate

Means and Ranges

Annual average values of the 3°C morning mixing height, the afternoon maximum mixing height, and the afternoon ventilation rate are presented in Table 1. Also shown are the annual ranges of these variables. These data are based on the measurements obtained during the first year of operation of the Chicago EMSU unit.

Monthly means, maxima, and minima of the mixing heights and ventilation rate are presented in Figure 1. Figure 1 shows that the mean morning mixing height reaches a minimum during the summer and rises in the winter. This is also true of the monthly maximum curve. The summer minima probably result from the frequent nocturnal inversions that occur during the summer. The curve showing the mean afternoon mixing height reaches a maximum during the summer and falls off during the colder season. This is due to the greater heating of the ground on summer days to produce a deeper convective layer.

The mean afternoon ventilation rate (Figure 1d) also shows a maximum during the summer, but its amplitude is less than the afternoon mixing depth. The ventilation rate is the product of mixing height and wind speed. Although the summer mixing height is greater, the summer wind speeds are

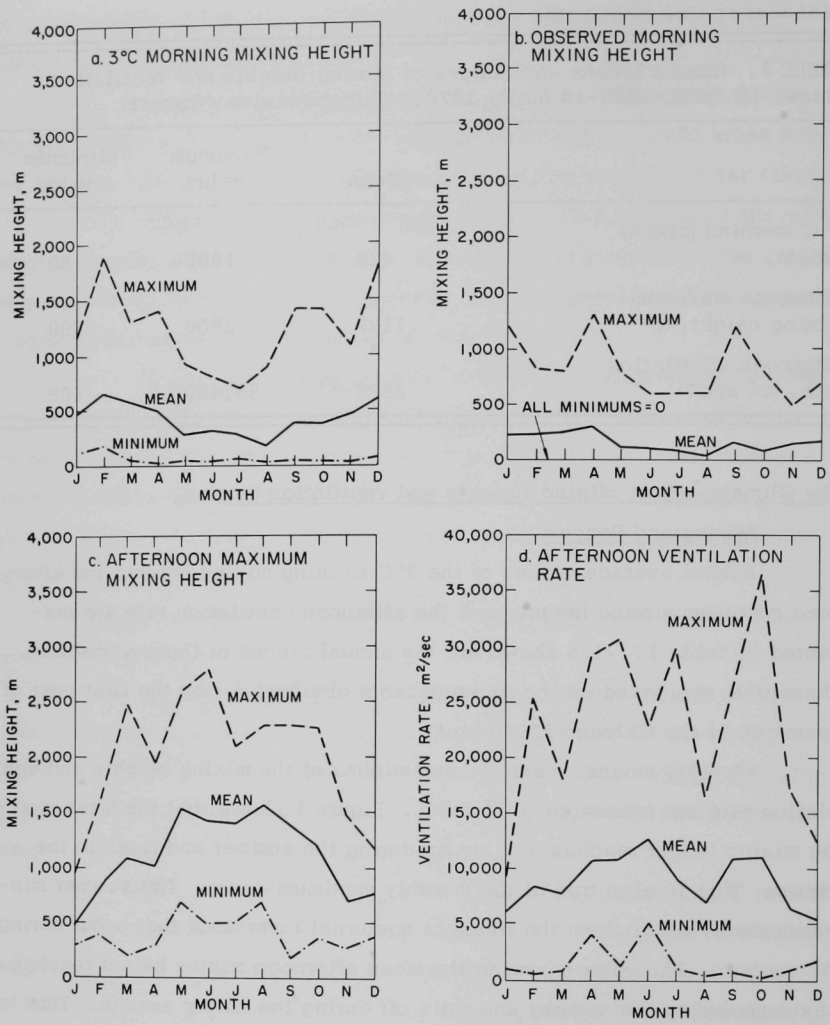

FIG. 1--Annual variation of monthly maximum, mean, and minimum mixing heights and ventilation rates, 15 April, 1969-14 April, 1970, Chicago.

less than those of the winter. Thus we see two opposing factors, light winds but large mixing heights in the summer, and the opposite in winter. As a result the amplitude of the average ventilation rate is smaller than the amplitude of the afternoon mixing height curve.

Relation to Wind Direction

Mixing heights, and therefore also ventilation rates, are determined by the temperature structure of the lower atmosphere. This structure is, in turn, dependent on the energy exchange properties of the surface. Because water and land differ markedly in these respects, Chicago mixing heights and ventilation rates should differ for onshore winds from Lake Michigan, which is east of the city, and for winds with a trajectory over land.

Figure 2 gives polar diagrams of mixing height and ventilation rate. The total length of each spoke represents the percent of observations with the wind blowing from that direction. The frequencies of occurrence of mixing height or ventilation factor in three group intervals are presented on each spoke as indicated in the figure keys. Thus, one may obtain a percentage frequency distribution, although a crude one, of the mixing height and ventilation factor for 8 points of the compass. Note that the data are stratified by heating season. The heating season is considered as the period from November 1 to April 30. The nonheating season is the remainder of the year--May 1 to October 31.

Figure 3 shows similar information in somewhat different form. In this figure the radius of the circle is graduated in terms of mixing height or ventilation factor. The isopleths drawn are lines of equal percentile values. For example, the 50th-percentile isopleth shows the median value of mixing height or ventilation factor at each of the directions.

Together, Figures 3a-f show the directions where the highest and lowest mixing heights and ventilation rates occur. They also show the most frequent combinations of wind directions, mixing heights and ventilation rates.

3°C Morning Mixing Height. Mean values of this parameter are higher in winter than in summer as brought out in Figure 1a. Figure 2a

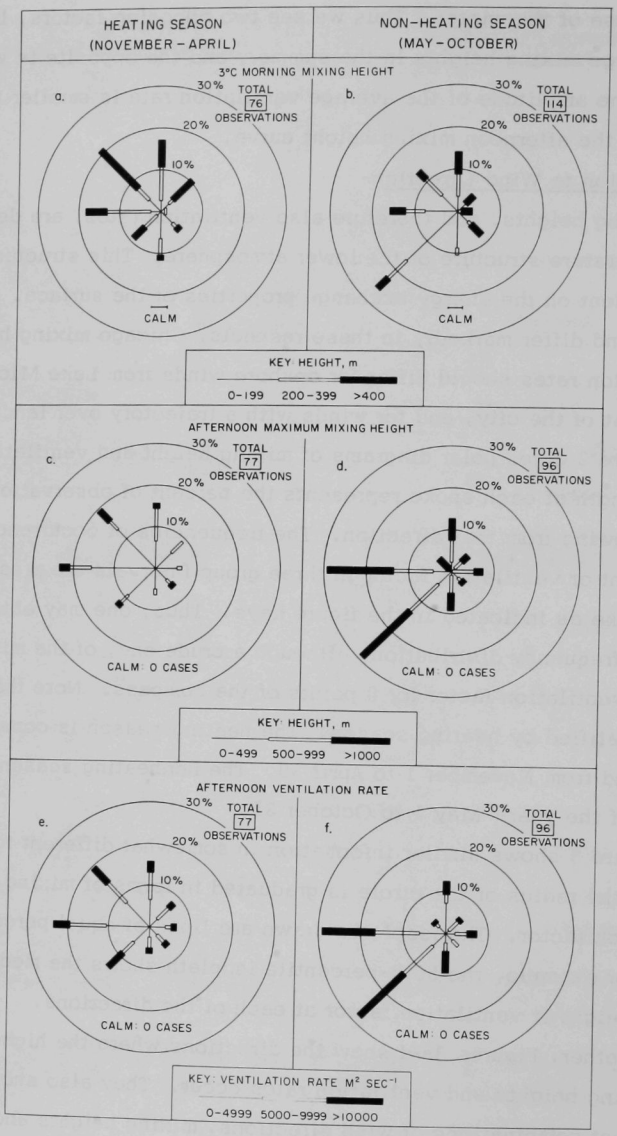

FIG. 2--Mixing height and ventilation rate roses for heating and nonheating season, 15 April, 1969-14 April, 1970, Chicago.

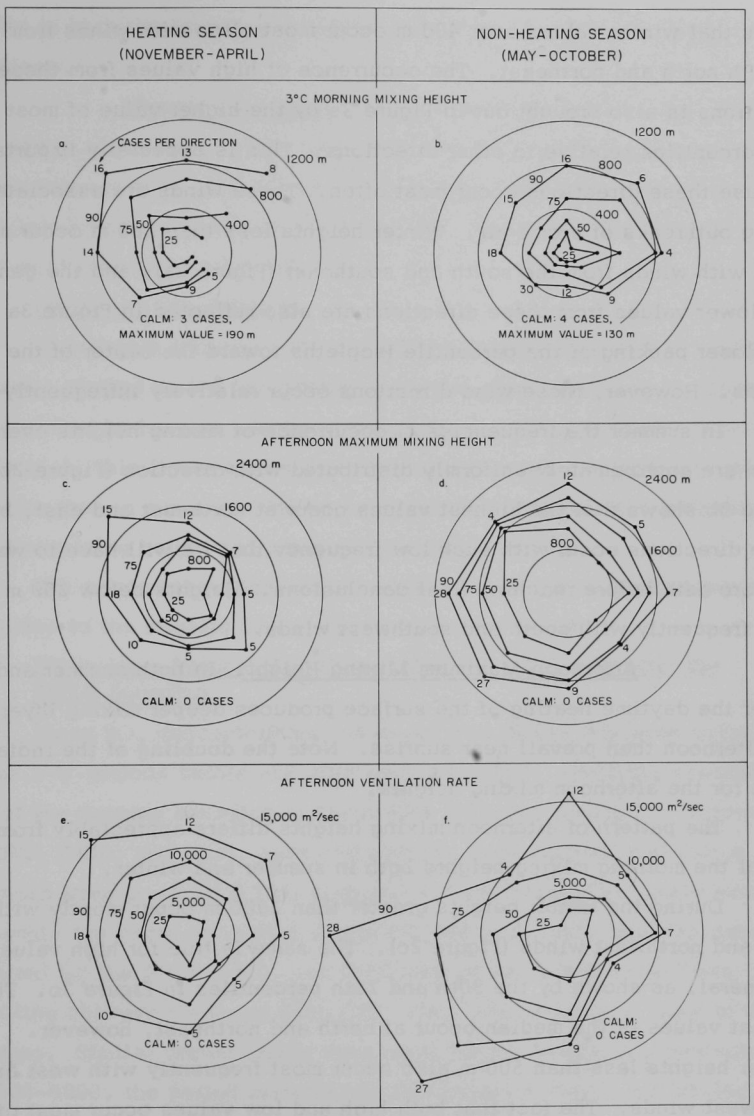

FIG. 3--Mixing height and ventilation rate percentile roses for heating and nonheating seasons 15 April, 1969-14 April, 1970, Chicago. Percentiles shown are the 25th, 50th, 75th, and 90th.

shows that winter values over 400 m occur most often with winds from west through north and northeast. The occurrence of high values from these directions is also brought out in Figure 3a by the higher value of most of the percentiles relative to other directions. This is especially important because these directions occur most often. These winds are associated with strong outbreaks of arctic air. Winter heights less than 200 m occur most often with winds from the south and southeast (Figure 2a), and the generally lower values from these directions are also reflected in Figure 3a by the closer packing of the percentile isopleths toward the center of the circles. However, these wind directions occur relatively infrequently.

In summer the frequencies of occurrence of mixing heights over 400 m are approximately uniformly distributed with direction (Figure 2b). Figure 3b shows that the highest values occur at northeast and east, but these directions occur with such low frequency that we will have to wait for more data before reaching final conclusions. Heights below 200 m occur most frequently with south and southwest winds.

Afternoon Maximum Mixing Height. In both summer and winter the daytime heating of the surface produces deeper mixing layers in the afternoon than prevail near sunrise. Note the doubling of the radial scale for the afternoon mixing heights.

The pattern of afternoon mixing heights differs appreciably from that of the morning mixing heights both in summer and winter.

During the winter heights greater than 1000 m occur mostly with west and northwest winds (Figure 2c). The same is true for high values in general, as shown by the 90th and 75th percentiles in Figure 3c. The highest values of the median occur at north and northeast, however. Winter heights less than 500 m also occur most frequently with west and northwest winds. The fact that both high and low values occur most often with the same wind directions is possible because these directions occur much more frequently than any of the others. When the other directions occur, however, the mixing height is more likely to be low than high.

Summer is again dominated by west and southwest winds, and

heights in both the lowest and highest categories are greatest from these directions.

Afternoon Ventilation Rate. In winter the west and northwest winds and in summer the southwest and west winds dominate. Ventilation rates over 10,000 m^2 sec^{-1} occur most frequently with winds from the latter directions (see Figures 2f and 3f). Rates less than 500 m^2 sec^1 occur most often with north winds.

Frequency Distributions

Cumulative frequency distributions of mixing heights and ventilation rates plotted on log-probability paper are given in Figure 4. These are stratified by heating and nonheating season. As also shown previously by Figure 1, this figure shows that 3°C morning mixing heights are greater in winter than in summer. The opposite is shown for both the afternoon maximum mixing height and afternoon ventilation rate.

The most striking feature of Figure 4 is the close approximation of all curves to the straight line or log-normal distribution.

Three-Hour Average SO_2 Concentrations before and after the EMSU Sounding

Mean SO_2 concentrations representative of the city were calculated for the 3-hr periods before and after each sounding. Since the average time of the morning sounding is about 0500 CST, the hourly SO_2 values for 0300, 0400, and 0500, were averaged for each station, and then a city-wide average of all 8 TAM stations was computed. An hourly average represents the value prevailing during the previous hour, thus the mean computed for the 0300, 0400, and 0500 data represents the condition prevailing between 0200 and 0500 CST, i.e., the period just prior to the sounding. Similar computations were made for the hourly SO_2 averages for 0600-0800, the period immediately following the morning sounding. Similar averages were obtained for the periods 0900-1100 and 1200-1400, i.e., just before and just after the afternoon sounding.

Cumulative frequency distributions for SO_2 concentrations in the four 3-hr periods are shown in Figure 5, stratified by season. In each

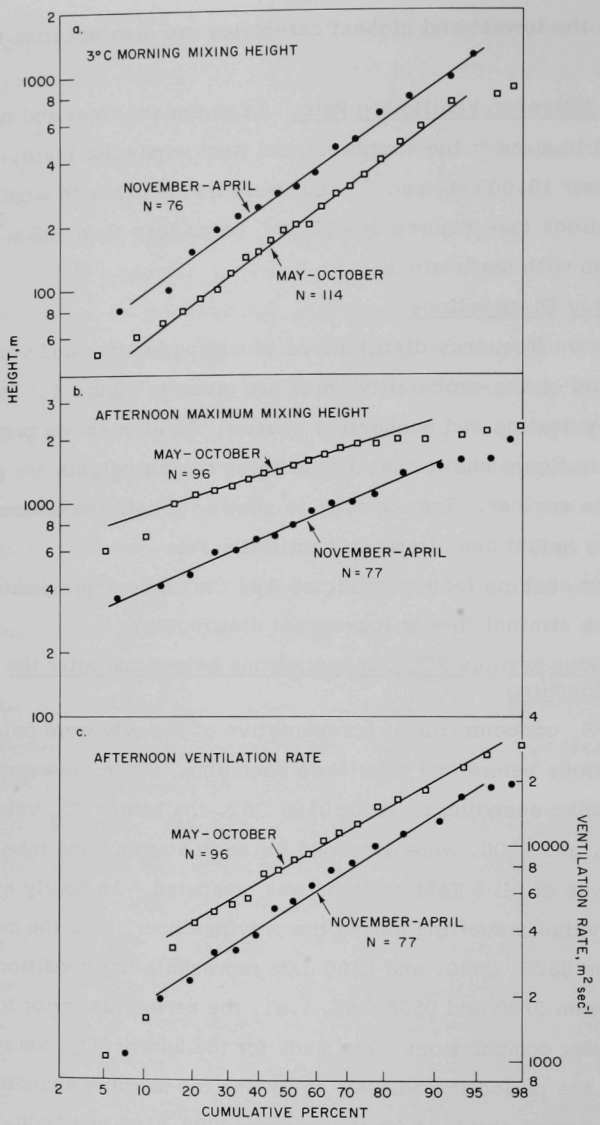

FIG. 4.--Mixing heights and ventilation rates--cumulative frequency distribution, heating and nonheating seasons, 15 April, 1969-14 April, 1970, Chicago. N = number of cases.

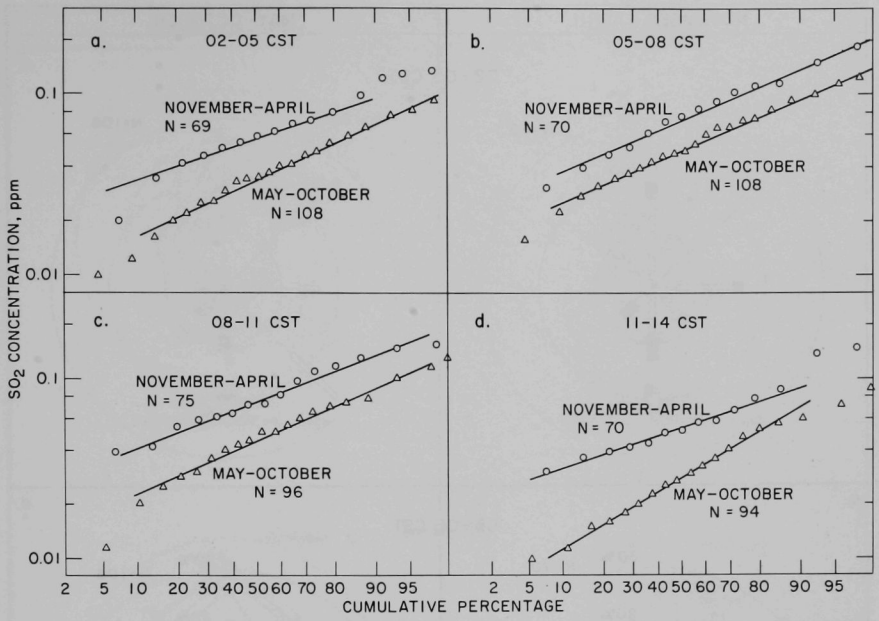

FIG. 5.--Cumulative frequency distributions of 3-hr city-wide SO_2 average concentrations, heating and nonheating seasons, 15 April, 1969-14 April, 1970, Chicago. N = number of cases.

case, winter concentrations are higher. A comparison of median SO_2 concentrations reveals the usual morning concentration peak in both seasons. Again, there is a strikingly good approximation to log-normal distributions.

<u>SO_2 Pollution Roses: SO_2 Concentration--Wind Direction Relationships.</u>

Figure 6 gives polar diagrams showing a 3-class distribution of winter and summer SO_2 concentrations for 8 wind directions for the 3-hr periods 02-05 and 05-08 CST. Figure 7 is similar, but gives the distribution of SO_2 concentration percentiles for the same periods and seasons.

As before, we see that the prevailing winds are northwest in winter and southwest in summer. Again, as we have seen, SO_2 concentrations are generally higher in winter.

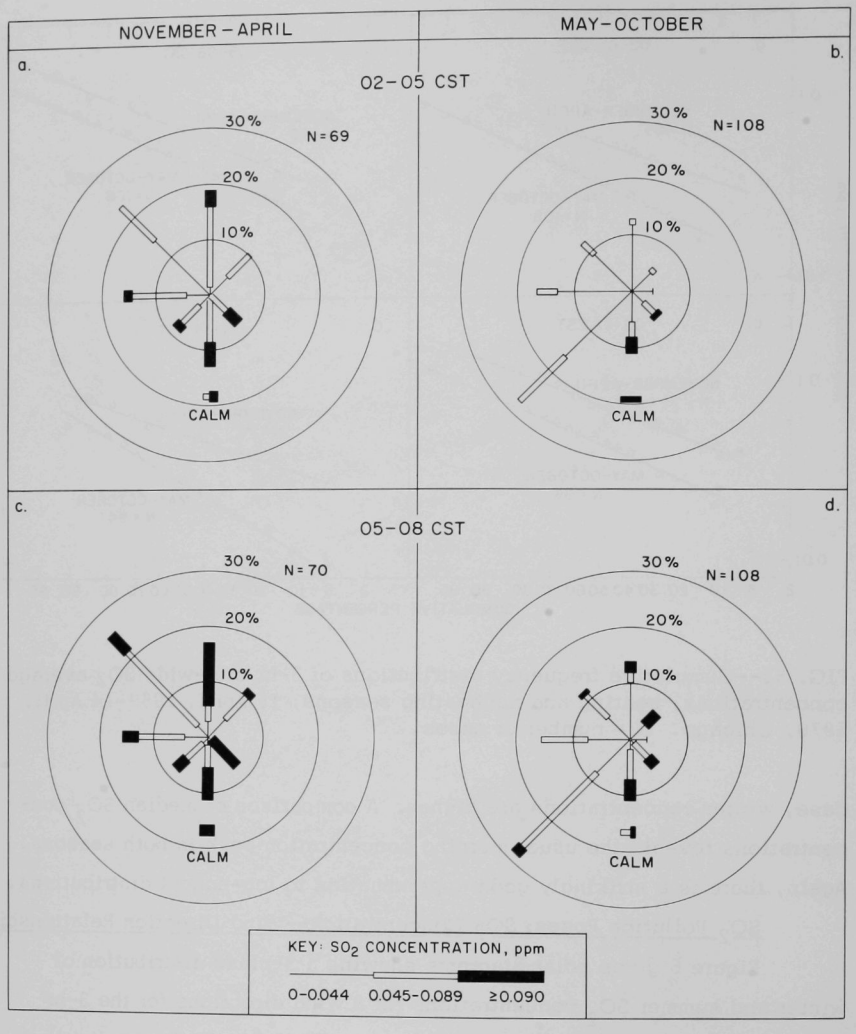

FIG. 6.--City-wide SO_2 concentration roses for 02-05 and 05-08 CST, heating and nonheating seasons, 15 April, 1969-14 April, 1970, Chicago. N = number of cases.

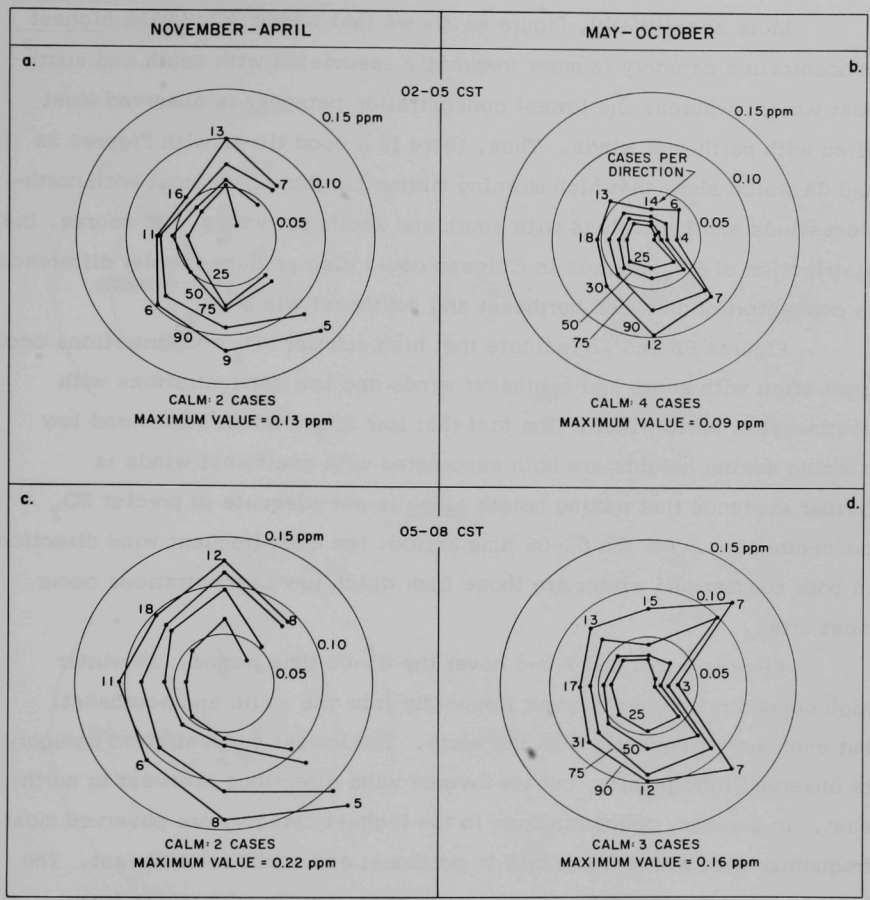

FIG. 7.--City-wide SO_2 concentration percentile roses for 02-05 and 05-08 CST, heating and nonheating seasons, 15 April, 1969-14 April, 1970, Chicago. Percentiles shown are the 25th, 50th, 75th, and 90th.

More specifically, Figure 6a shows that winter SO_2 in the highest concentration category is most frequently associated with south and southeast winds, whereas the lowest concentration category is observed most often with northwest winds. Thus, there is a good tie-in with Figures 2a and 3a which show that high morning mixing heights occur most with northwest winds and low values with south and southeast winds. Of course, the distribution of SO_2 sources in Chicago could also produce similar differences in concentration between northeast and southeast winds.

Figures 6b and 7b indicate that high summer SO_2 concentrations occur most often with south and southeast winds and low concentrations with southwest to north winds. The fact that low SO_2 concentrations and low morning mixing heights are both associated with southwest winds is further evidence that mixing height alone is not adequate to predict SO_2 concentrations. For the 02-05 time period, the most frequent wind directions in both summer and winter are those from which low concentrations occur most often.

Figures 6 c-d and 7 c-d cover the 05-08 time period. In winter high concentrations still occur frequently from the south and southeast, but even more frequently from the north. The lowest concentration category is observed infrequently, but its favored wind directions are west to northeast. In summer, concentrations in the highest category are observed most frequently with winds from north to northeast and south to southeast. The lowest concentration category occurs most frequently with winds from southwest through north. Again in this time period, high winter concentrations tend to occur with the same wind directions as low morning mixing heights. The directions of low concentrations and high mixing heights also agree quite well. However, the relation is again poor in summer. For both summer and winter, the direction of most frequent winds is one where SO_2 concentrations are likely to be in the middle and low categories.

Figures 8 and 9 cover the 08-11 time period. The directional pollution characteristics of this period and the final (11-14) period will be compared with afternoon mixing heights.

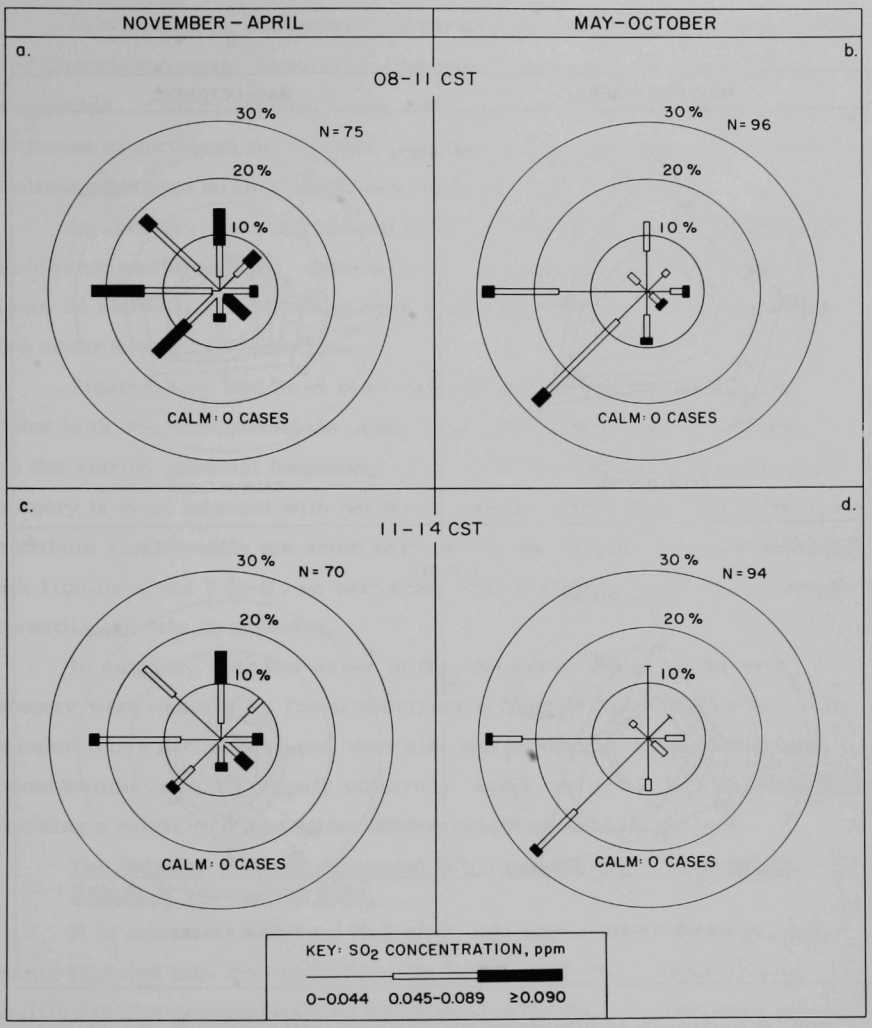

FIG. 8.--City-wide SO_2 concentration roses for 08-11 and 11-14 CST, heating and nonheating seasons, 15 April 1969-14 April, 1970, Chicago. N = number of cases.

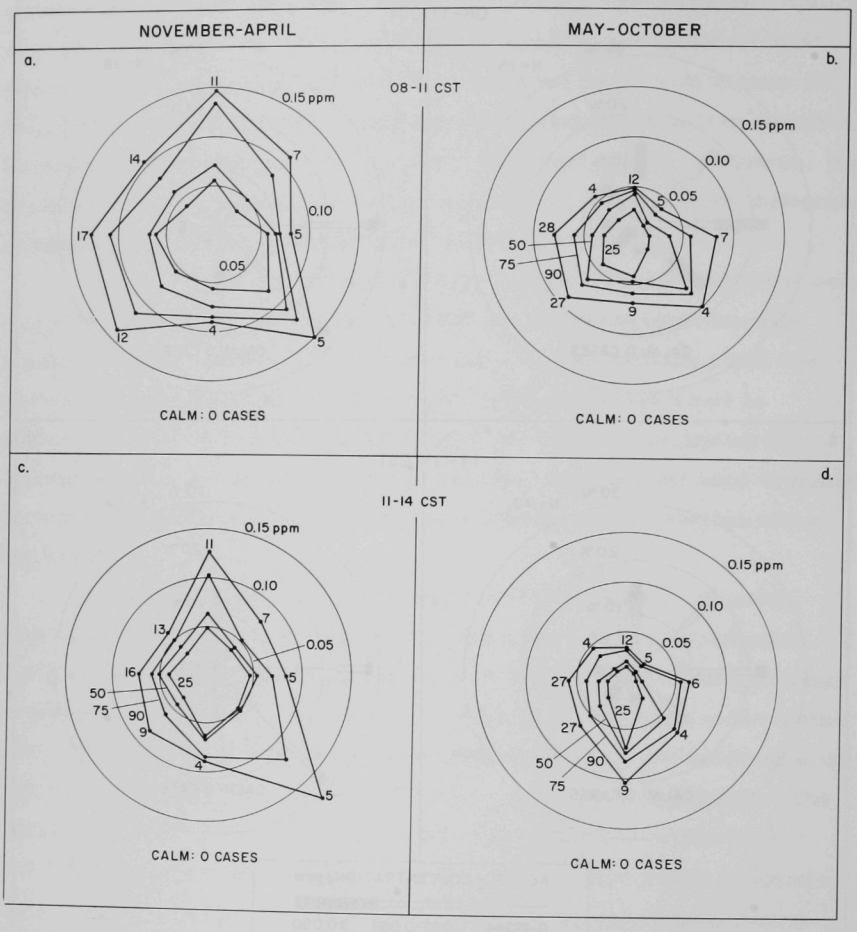

FIG. 9.--City-wide SO_2 concentration percentile roses for 08-11 and 11-14 CST, heating and nonheating seasons, 15 April, 1969-14 April, 1970, Chicago. Percentiles shown are the 25th, 50th, 75th, and 90th.

In winter, SO_2 concentrations in the highest category occur with all wind directions; north, southeast, southwest, and west have the highest frequencies. Concentrations in the low category occur infrequently, with northwest to northeast the favored directions. No particular relationship to either afternoon mixing height or ventilation rate is apparent.

In summer, west and southwest winds are so predominant that both the highest and lowest SO_2 categories occur most frequently with them. Figure 2d shows that both the highest and lowest mixing height categories also occur from these directions.

Figures 8c-d and 9c-d show data for the 11-14 CST period. In winter high SO_2 concentrations occur most with north winds; southeast has the second greatest frequency. SO_2 in the lowest concentration category is most frequent with northwest winds. Other directions that contribute significantly are southwest, west, and northeast. By comparison with Figures 2 and 3 (c-f), no particular relationship to either mixing height or ventilation rate is apparent.

In summer, very few cases of SO_2 concentration in the highest category were observed. The predominant southwest and west winds included those few cases, and were also the directions where the lowest concentration category usually occurred. Again, no conclusions are apparent regarding a relationship to either mixing height or ventilation rate.

The Relation between Observed SO_2 Concentrations and Mixing Height or Ventilation Rate

It is commonly believed that when the mixing height is large, pollutants injected into the atmosphere are distributed over a large volume resulting in low concentrations. Small mixing heights, by the same reasoning, result in high concentrations. Similarly, large ventilation rates should occur with low pollutant concentrations and vice versa.

With the availability of the urban EMSU soundings to provide data on mixing heights and ventilation rates, and, with access to the SO_2 concentrations provided by the Telemetered Automatic Monitoring (TAM) Network of the Department of Environmental Control of the City of Chicago,

(see Figure 10) it has become possible to test the relation between mixing height or ventilation rate and SO_2 ground concentration.

Direct Comparisons: SO_2 Versus Mixing Heights and Ventilation Rate

The data were stratified by heating and nonheating seasons as before. Scatter diagrams relating the 3°C morning mixing height with city-wide average SO_2 concentrations for the 3-hour period between 0500 and 0800 CST are shown in Figure 11a and b. A general inverse relationship is indicated by the fact that the highest SO_2 concentrations occurred with relatively low mixing heights and the highest mixing heights were accompanied by low concentrations. However, there is considerable scatter in the points. With a little imagination one may see the plausibility of fitting a hyperbola to the data. A hyperbolic fit is expected since the concentration varies inversely as H, the mixing height in conventional diffusion equations which take the mixing layer into account.[4]

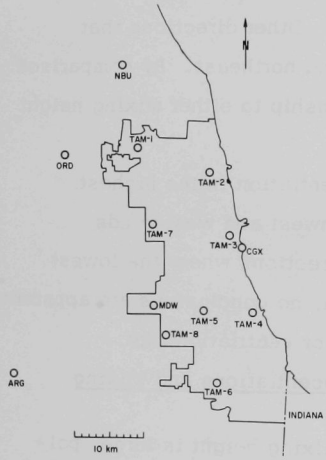

FIG. 10.--Map showing locations of Telemetered Air Monitoring (TAM) Stations in City of Chicago and Meteorological observing stations at Meigs Field (CGX), Midway Airport (MDW), Glenview Naval Air Station (NBU), O'Hare Airport (ORD), and Argonne (ARG).

A set of charts drawn for the 02-05 CST time period (not shown) indicated similar results.

The relationship between the afternoon maximum mixing depth and SO_2 concentrations in the 11-14 CST time period is shown in Figure 11 c and d. No direct relationships are apparent. Neither was any found for the 08-11 period (not shown).

Scatter diagrams relating afternoon ventilation rate to SO_2 concentrations in the 11-14 CST time

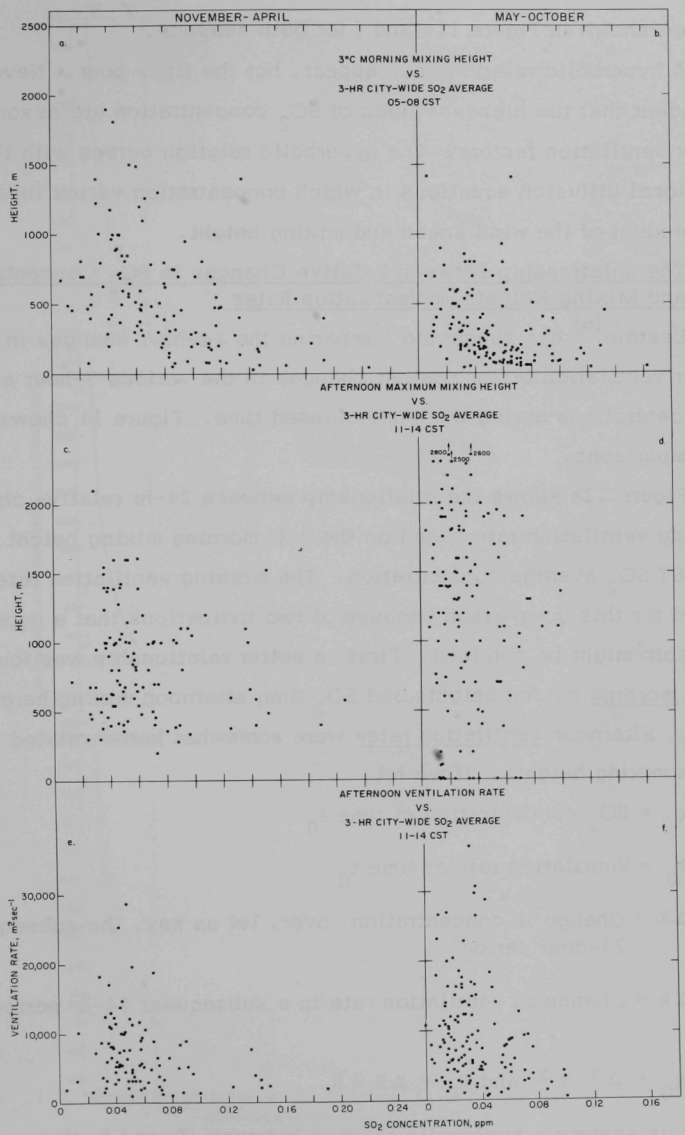

FIG. 11.--Scatter diagrams relating mixing height or ventilation and 3-hour city-wide SO_2 concentrations, 15 April, 1969-14 April, 1970, Chicago.

period are shown in Figure 11e and f for both seasons.

A hyperbolic relation does appear, but the fit is poor. Nevertheless, it is evident that the highest values of SO_2 concentration are associated with low ventilation factors. The hyperbolic relation agrees with the conventional diffusion equations in which concentration varies inversely as the product of the wind speed and mixing height.

The Relationship Between Relative Changes in SO_2 Concentrations and Mixing Heights or Ventilation Rates

Epstein[5] has suggested comparing the 24-hour changes in mixing height or ventilation factor against changes in the various 3-hour average SO_2 concentrations during the same elapsed time. Figure 11 shows three such comparisons.

Figure 12a shows the relationship between 24-hr relative changes in morning ventilation rate based on the 3°C morning mixing height and the 05-08 CST SO_2 average concentration. The morning ventilation rates were computed for this comparison because of two indications that a good relationship might be obtained. First, a better relationship was found between morning mixing heights and SO_2 than afternoon mixing heights. Secondly, afternoon ventilation rates were somewhat better related to SO_2 than mixing heights. If we let

X_0 = SO_2 concentration at time t_0

R_0 = Ventilation rate at time t_0

ΔX = Change in concentration, over, let us say, the subsequent 24-hour period

ΔR = Change in ventilation rate in a subsequent 24-hr period,

then let

$$X_0 + \Delta X = X \text{ and } R_0 + \Delta R = R.$$

Also, let us assume a hyperbolic relation between X and R; then

$$XR = X_0 R_0 = K = \text{constant} \qquad (1)$$

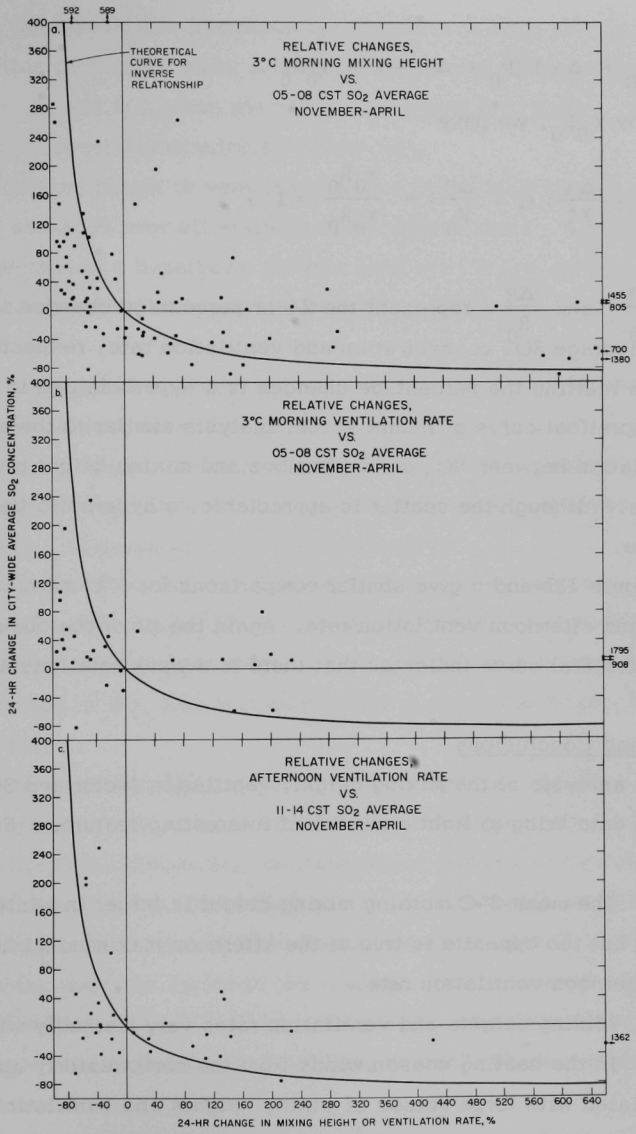

FIG. 12.--Scatter diagrams relating relative day-to-day changes in SO_2 concentrations and mixing heights or ventilation rates, 15 April, 1969-14 April, 1970, Chicago. The solid curve is the theoretical inverse relationship.

and

$$(X_0 + \Delta X)(R_0 + \Delta R) = K = X_0 R_0 \cdot \tag{2}$$

Dividing by $X_0 R_0$, we have

$$(1 + \frac{\Delta X}{X_0})(1 + \frac{\Delta R}{R_0}) = \frac{X_0 R_0}{X_0 R_0} = 1 \ , \tag{3}$$

where $\frac{\Delta X}{X_0}$ and $\frac{\Delta R}{R_0}$ represent the 24-hr percentage changes in the 3-hourly average SO_2 concentration and ventilation rate, respectively. Equation 3 relating the percentage changes is a hyperbola and is indicated as the theoretical curve of Figure 2. An analysis similar to the above holds for the relation between SO_2 concentrations and mixing height given in Figure 12a. Although the scatter is appreciable, a hyperbolic fit appears reasonable.

Figure 12b and c give similar comparisons for 3°C morning ventilation rate and afternoon ventilation rate. Again the fit of the observations to the theoretical curve indicates that there is a weak relationship.

Summary and Conclusions

An analysis of the mixing height, ventilation factor, and SO_2 concentration data bring to light a number of interesting features. Some of these are:

1. The mean 3°C morning mixing height is larger in winter than in summer, but the opposite is true of the afternoon maximum mixing height and the afternoon ventilation rate.

2. Mixing heights and ventilation rates vary markedly with wind direction. In the heating season winds from the northwesterly quadrant are associated with large values of mixing heights and ventilation rate. In the warm season large mixing heights are quite uniformly distributed with direction in the morning; in the afternoon southwesterly and westerly winds are preferred. There is a striking maximum in the summer ventilation rate with winds blowing from the southwesterly quadrant.

3. The cumulative frequency distributions of SO_2, mixing heights, and ventilation factors all show a rather close approximation to a straight line between 10 and 90% when plotted on log-probability paper. This indicates a log-normal distribution for these data.

4. Mixing height or ventilation factor and 3-hour mean SO_2 concentrations averaged over all stations show little relation. There is a slight suggestion of a hyperbolic relation between the 3°C mixing height and SO_2 concentrations and also between SO_2 and the afternoon ventilation rate.

5. A comparison of SO_2 pollution roses with mixing height and ventilation rate roses shows the anticipated inverse relationship in some cases but not in others. The distribution of sources is probably more important than mixing height or ventilation rate in determining the variation of SO_2 concentration with wind direction.

6. Twenty-four hour relative changes in mixing height or ventilation factor and in the 3-hour SO_2 concentrations soundings do indicate, although poorly, the expected relation, i.e., an inverse relationship between changes in SO_2 concentration and changes in the mixing height or ventilation factor.

It is well known that a number of meteorological variables influence pollutant concentrations. Thus, we should not be surprised to find only a weak relationship between SO_2 concentrations and one or two of the meteorological variables. Nevertheless, a number of fundamental questions remain: 1) Is the technique for determining the mixing height a valid one; in other words, does the height of the mixing layer, so determined, correspond to the aerosol layer? 2) Is there a better technique for analyzing the radiosonde data to determine the mixing height? These questions warrant further examination.

This analysis shows that mixing heights and ventilation rates are important, if not exclusive, parameters in determining pollutant concentrations and indicates strongly that such measurements should be continued and expanded to more locations.

We thank Edward W. Klappenbach and the City of Chicago Department of Environmental Control for providing SO_2 concentrations measured at the eight Telemetered Air Monitoring Stations. Thanks are also due to Mr. Paul E. Hess for assistance with a number of the figures.

References

1. McCaldin, R. O. and R. S. Sholtes. Mixing height determinations by means of an instrumented aircraft. Paper presented at the Second International Clean Air Congress, Washington, D. C., December 6-11, 1970.
2. U.S. Weather Bureau, ESSA, Department of Commerce. Provisional instructions, low-level radiosonde soundings. Unpublished (1970).
3. Holzworth, G. G. Mixing depths, wind speed, and air pollution potential for selected locations in the United States. J. Appl. Meteorol. 6 (6), 1039-1044 (1967).
4. Gifford, Franklin A., Sr. An outline of theories of diffusion in the lower layers of the atmosphere. Chapter 3 of Meteorology and Atomic Energy, Ed. David H. Slade, U.S. Atomic Energy Commision, Division of Technical Information, Oak Ridge, Tennessee (1968).
5. Epstein, E. S. Professor of Meteorology, University of Michigan, Ann Arbor, Michigan. Personal communication (1970).

AIR POLLUTION ABATEMENT BY SELECTIVE FUEL SWITCHING*

J. E. Carson, E. W. Klappenbach,† and J.-W. Lin†

One method for reducing air pollution concentrations during periods of poor diffusion conditions without turning off industry is to convert as many as possible of the large sources to alternate fuels. Sulfur dioxide is a major pollutant in Chicago; unfortunately, sufficient supplies of low-sulfur fuels are not available to replace the usual fuels at all times. Thus, an optimal SO_2 abatement program consists in part of using the available low-sulfur fuel resources for maximum effect on air quality.

The development of control strategies to reduce emissions during periods of poor air quality has been an integral part of Argonne's effort to construct and test an urban atmospheric dispersion model. These control actions have been tested three times in a full-scale experimental laboratory, the City of Chicago.

The third test in this series was conducted between May 18 and 30, 1969. Industry and the power generating plants cooperated with the City's Department of Environmental Control in conducting this unique and valuable exercise in air quality control during a "simulated air pollution incident." The components of the abatement strategy used during this test consisted of the actual and forecast weather conditions, observed and forecast SO_2 levels, location of dual-fuel plants with respect to areas of high SO_2 levels, diffusion calculations, and the availability of low-sulfur fuels. Direct contact between air pollution control officials and the utilities and major SO_2 producers was maintained during the exercise, and patrol cars were dispatched to look for possible violators. Seventy-two major SO_2 sources were requested to convert to alternate fuels.

This city-wide pollution experiment had three primary objectives: 1) to act as a trial run for establishing procedures for implementing effective SO_2 abatement procedures during a forecast period of air pollution buildup, 2) to observe changes in air quality due to fuel changes and to compare these changes with those computed from the diffusion equations,

---

*Abstract of a paper presented at the American Meteorological Society Meeting in San Francisco on January 11, 1971. Full text to be published in the Final Report for the Chicago Air Pollution Systems Analysis Program.

This work was supported in part by the Chicago Department of Environmental Control, and the National Air Pollution Control Administration of the Department of Health, Education and Welfare.

†Department of Environmental Control, City of Chicago.

and 3) to provide Argonne scientists with detailed air quality, meteorological, and SO_2 emission data during a short period to aid in the development of better methods for predicting air pollution levels.

This outdoor experiment did bring into sharper focus the practical actions that industry can and cannot realistically take to reduce or curtail SO_2 output during pollution episodes. Any air pollution abatement strategy must, of course, be based on accurate assessments of the availability of low-sulfur fuels and industrial-commercial operating procedures, so that no impossible burden will be placed on industry by air pollution control operations.

This paper discusses the results of this outdoor experiment, including changes of air quality due to fuel switching.

SULFUR HEXAFLUORIDE: ATMOSPHERIC BACKGROUND CONCENTRATIONS. PRELIMINARY RESULTS

Donald F. Gatz and James E. Carson

Over 100 air samples have been collected in Chicago urban and suburban areas and at Argonne National Laboratory and analyzed for atmospheric SF_6 backgrounds. Sampling times ranged from about 5 seconds for samples collected in evacuated 1-liter cylinders to 1 and 24 hours for samples collected in 12-liter Saran bags using a small battery powered air pump. Samples were analyzed using a gas chromatograph and a ^{63}Ni electron capture detector. SF_6 concentrations in the samples ranged from less than detectable (30 picoliters/liter in earlier samples and 2 picoliters/liter in later samples) to greater than 500 picoliters/liter. The highest values were found in 5-sec samples collected at Argonne, which has several known sources of SF_6. However, a number of the Chicago samples also showed detectable SF_6 concentrations.

Introduction

Sulfur hexafluoride is an extremely stable and inert gas that is detectable at very low concentrations in air. These properties make it very useful as an atmospheric tracer. The technology associated with its use as an air pollution tracer has been developed primarily by the National Air Pollution Control Administration.[1]

Besides the properties listed earlier, sulfur hexafluoride has a higher dielectric constant than dry air and is used in industry as an insulator in high-voltage devices. Losses, both intended and unintended, from this equipment add SF_6 to the atmosphere, where natural removal processes appear to be minimal. Thus, there have been recommendations that atmospheric SF_6 concentrations should be regularly monitored to detect any buildup.[2]

As a prelude to the use of SF_6 in a tracer experiment, it is necessary to establish a baseline atmospheric background for the location and to determine whether there are any local sources that could interfere with the interpretation of experiments.

The objective of this study was to monitor atmospheric background

concentrations of SF_6 at the Argonne National Laboratory, the site of several known sources, and in the Chicago area, where SF_6 tracer studies were planned. A limited number of samples have been analyzed previously for urban background concentrations in New York City[3] and Cincinnati.[4]

Sampling and Analysis Procedures

Air was collected in two different types of samplers. Evacuated steel cylinders were used to collect nearly "instantaneous" samples of approximately 5-sec duration. Samples of 1 hour and longer were pumped into 12-liter Saran bags using small Teflon pumps.

Samples were analyzed using a gas chromatograph to separate SF_6 from other components of the air mixture and detected with an electron capture detector. The Argonne system is patterned after one developed at the National Air Pollution Control Administration, which is a modified version of the system described by Saltzman et al.[1] The recent changes were developed by R. K. Stevens and others in the NAPCA chemistry group and include 1) use of ^{63}Ni rather than tritium in the electron capture detector, 2) operation at 220°C rather than room temperature, 3) use of a pulsed power supply, 4) a larger (2-ml) sample volume, and 5) use of ultrapure (99.999%) nitrogen as the carrier gas.

The detector system was calibrated against SF_6 standards prepared by successive dilutions of SF_6 obtained commercially. Several independent standard preparations checked to within 25%. Nevertheless, because of the inherent difficulties and uncertainties in preparing standards in the parts per billion range, results in this preliminary report are considered accurate to only ± 50%. Efforts to obtain an improved calibration are continuing.

Sample analysis is performed on 2-ml aliquots of the original unconcentrated air sample. At least 2 aliquots of each sample were analyzed. Reproducibility was ordinarily within 25%, except for values < 5 picoliters/liter, where it might reach 100%. The detector system now has a limit of detection of less than 2 picoliters SF_6 per liter of air (pl/l). For

some of the earlier results, the detection limit was between 20 and 30 pl/l. those samples containing undetectable SF_6 at the higher detection limit are reported as < 30 pl/l.

Sample Analysis

The locations and sampling times of all samples analyzed are given in Table 1.

TABLE 1. Summary of samples collected.

Location	Sampler type	Approximate sampling time	No. of samples
Argonne	bag	24 hr	38
	bag	1 hr	9
	cylinder	5 sec	40
Chicago	bag	1 hr	12
	cylinder	5 sec	34
Chicago western suburbs	cylinder	5 sec	33
Total			166

A summary of all samples collected in bags is given in Table 2. The table shows number of samples with less than detectable SF_6 as well as number of samples with detectable SF_6 in three concentration ranges. Out of 59 air samples, 38 had less than detectable SF_6 concentrations and most of these had concentrations less than 2 pl/l. Seventeen had SF_6 concentrations between 10 and 99 pl/l.

A summary of all cylinder sample results is given in Table 3. Most of these were collected when the level of detection was 20 to 30 pl/l. A number of these samples contained SF_6 well above the detection limits. Six samples had concentrations of at least 100 pl/l, and another 9 were

TABLE 2. SF_6 in bag samples

Location	Approximate sampling time, hr	No. of samples	No. of samples with less than detectable SF_6		No. of samples with detectable SF_6	
			<2pl/l[a]	<30pl/l[a]	2.0-9.9 pl/l[a]	10-99 pl/l[a]
Argonne	24	38	31		4	3
Argonne	1	9		2		7
Chicago	1	12		5		7
Total		59	31	7	4	17

[a] ± 50%.

TABLE 3. SF_6 in cylinder samples

Location	No. of samples	No. of samples with less than detectable SF_6		No. of samples with detectable SF_6		
		<2pl/l[a]	<30pl/l[a]	2.0-9.9 pl/l[a]	10-99 pl/l[a]	>100 pl/l[a]
Argonne	40	11	15	2	7	5
Chicago	34		33		1	
Chicago western suburbs	33		31		1	1
Total	107	11	79	2	9	6

[a] ± 50%.

in the 10-99 pl/l range. Tables 4 and 5 are summaries of samples containing detectable SF_6 that were collected at the Argonne site, and offsite, respectively.

TABLE 4. Summary of cylinder and 1-hr bag samples with detectable SF_6 at Argonne

Date	Bag or cylinder No.	SF_6, pl/l	Detection limit, pl/l	Wind direction, degrees[a]	Remarks
	cylinder				
21 Oct 69	2	168	30	210	Downwind of
	39	568	30	210	Zero Gradient
	44	104	30	240	Synchrotron
	8	64	30	240	(ZGS) source
	41	128	30	240	
20 Nov 69	24	60	20	270	Downwind of Tandem
	47	48	20	270	Van de Graaff source
8 Jan 70	25	3	2	260	Upwind (west) of
	21	2	2	260	ANL sources.
	2	40	2	270	Downwind of ZGS.
	41	160	2	270	Downwind of Tandem Van de Graaff
28 Jan 70	31	20	2	210	
	47	48	2	210	Downwind of ZGS
	36	98	2	210	
	bag				
30 Oct 69	1	20	20	120-240	
	3	25	20	90	
	4	25	20	120	Upwind of ANL
	5A	20	20	110	sources
	5B	28	20	120	
	7	28	20	110	
	9	35	20	90	Probably upwind of ANL source

(a) Measured at Argonne, 19 ft above ground level.

TABLE 5. Summary of Chicago and Suburban Samples with Detectable SF_6

Date	Bag or cylinder No.	SF_6, pl/l	Detection limit, pl/l	Wind direction, degrees	Remarks
	cylinder	Chicago samples			
30 Oct 69	19	24	24	90-110	Argonne not upwind
	bag				
28 May 69	1	22	20		
	2	64	20		
	3	80	20	320-70	Argonne not upwind
	5	26	20		
	6	48	20		
	7	33	20		
	11	48	20		
	cylinder	Suburban samples			
30 Oct 69	8	30	24	80-140	At Naperville; Argonne is possible source.
7 Nov 69	51	141	24	60	At I-55 and U.S. 45; source east of Argonne

Discussion

Clearly the best set of samples, out of those reported here, is the set of 24-hr bag samples collected at two Argonne sites between 11 February and 4 May 1970 (Table 2). These are best primarily because they were analyzed at the greatest sensitivity. In addition, they were collected in the same place on a regular schedule, over a period of about three months.

These samples were collected at two sites, both near the perimeter of the Argonne site. Location A-1 was the Meteorology Building, southwest to west of the four known sources of SF_6 on the Argonne site. Location A-2 was north to northeast of the known sources. The 24-hr samples collected at these locations should give a rough approximation of the SF_6

concentrations leaving Argonne site on a regular basis. Samples A-2 should detect any SF_6 arriving at Argonne from Chicago industrial areas to the east and northeast, and both samplers should detect "ambient" background concentrations in air arriving from the west or north.

Table 6 is a summary of the Argonne 24-hr samples. Only 7 of 38 had detectable concentrations, and in each of these cases the wind was blowing from Argonne sources to the sampler for at least part of the sampling period, based on wind measurements made at the meteorology site. There are four pairs of simultaneous samples at the two sites when only one site was downwind of Argonne sources. In all four cases, the downwind sampler had detectable SF_6, and the upwind sampler did not.

TABLE 6. Frequency Distribution of SF_6 Concentrations Measured at Argonne in 24-hr Samples February-April, 1970.

Concentration Range, pl/l[a]	Number of samples	Wind at least partially from ANL sources	
		Yes	No
< 2.0	31	10	21
2.0-919	4	4	
>10.0	3	3	
Total	38		

[a] ± 50%

Thus, in the Argonne 24-hr samples, only the SF_6 sources at Argonne were detectable; all samples of air from off-site contained less than 2 pl/l.

It is also useful to consider the results of shorter-duration samples. For example, in considering the feasibility of a tracer experiment in Chicago, with 1- to 2-hr sampling times, backgrounds over similar time periods would establish what baseline level the released gas must exceed. The following discussion is based on Tables 4 and 5, which list the detectable samples

collected over periods of 5 sec to 1 hr at Argonne (Table 4) and in Chicago and suburban areas (Table 5).

As might be expected, shorter sampling periods yield higher SF_6 concentrations than found in the 24-hr samples. Of the 21 Argonne samples with detectable SF_6 collected on 5 different days, 9 samples were associated with wind directions such that the sources could not have been at Argonne. Concentrations of 2 and 3 pl/l, barely above detection limits, were detected in 5-sec samples in westerly winds at the western boundary of the Argonne site on 8 January 1970. On 30 October 1969 seven 1-hr bag samples detected SF_6 in easterly-southeasterly winds. Again, Argonne could not have been the source. The SF_6 concentrations in these samples were only slightly above the detection limit of 20 pl/l prevailing when the samples were analyzed. Nevertheless, it appears likely that non-Argonne sources of SF_6 may be present to the east or southeast of Argonne.

The Chicago and suburban samples with detectable SF_6 are summarized in Table 5. Cylinder 19 may be disregarded as being too close to its detection limit to be absolutely certain that SF_6 was detected. However, the set of bag samples collected on 28 May 1969 provides stronger evidence. Samples 1 and 5 were collected sequentially at South Lake Shore Drive and 31st St.; samples 2 and 6 were collected sequentially at Lake Shore Drive and Ohio Street. A fourth pair of samples, collected sequentially in Lincoln Park showed less than detectable SF_6. The consistency of SF_6 concentrations in consecutive 1-hr samples at these four locations is evidence that SF_6 was actually present. The associated wind directions (near north) indicate that Argonne (southwest of the sampling points) could not have been the source of the SF_6 on this occasion.

Table 5 incidates that two suburban cylinder samples also contained detectable SF_6. The 30 October 69 sample could have detected the sources at Argonne, but recall that also on this day, SF_6 was detected in southeast winds at Argonne from non-Argonne sources. The 7 November 69 sample was collected between Argonne and Chicago in easterly winds and indicates a source somewhere in the Chicago industrial region.

Our results for Chicago and urban and suburban areas are compared with previous results in other cities in Table 7. Our measured concentrations agree with the measurements of Turk et al.[3] in the vicinity of Manhattan power plants, and are considerably greater than those found in Cincinnati.

TABLE 7. Background Concentrations of SF_6 in Urban Areas

City	Investigator	SF_6 concentrations, pl/l[a]	
New York	Turk et al.[3]	Near power plants	10-400[b]
		Not near power plants	0-10[b]
Cincinnati	Clemons et al.[4]		0.04-0.20
Chicago	This study		22-140

(a) ± 50%

(b) It is not clear whether these numbers also include container backgrounds of up to 10 pl/l.

Conclusions

Several preliminary conclusions may be made. First, only Argonne sources have been detected in 24-hr samples at Argonne, Second, there is a strong likelihood that additional sources of SF_6 exist within the Chicago industrial region. Third, ambient concentrations upwind of these sources are less than 2 pl/l.

Finally, additional measurements should be made to verify these preliminary results.

We thank Tom Duffy and Dick Kasper of the Argonne Industrial Hygiene and Safety Division for their considerable efforts in setting up the analytical system and analyzing the samples, and for helpful discussions.

References

1. Saltzman, B. E., A. I. Coleman, and C. A. Clemons. Halogenated compounds as meteorological tracers; stability and ultrasensitive analysis by gas chromatography. Anal. Chem. 38 (6), 753-758 (1966).
2. American Chemical Society. Cleaning our environment: the chemical basis for action, report by the Subcommittee on Environmental Improvement, Committee on Chemistry and Public Affairs. American Chemical Society, Washington, D. C. (1969) p. 45.
3. Turk, A., S. M. Edmonds, H. L. Mark, and G. F. Collins. Sulfur hexafluoride as a gas-air tracer. Environ. Sci. Technol 2 (1), 44-48 (1968).
4. Clemons, C. A., A. I. Coleman, and B. E. Saltzman. Concentration and ultrasensitive chromatographic determination of sulfur hexafluoride for application to meteorological tracing. Environ. Sci. Technol. 2 (7) 551-555 (1968).

SULFUR DIOXIDE POLLUTION CHARACTERISTICS OF CHICAGO LAKE BREEZE CIRCULATIONS

Donald F. Gatz

Pollution patterns of SO_2 hourly average concentrations during 1966 and 1967 Chicago lake breezes were examined to determine: 1) The incidence of SO_2 concentrations greater than 0.15 ppm in lake breeze situations, 2) the relative pollution levels at the eight observing stations before and after the passage of the lake breeze front, and 3) the relative pollution characteristics of "classic" and "nonclassic" lake breezes.

In classic lake breezes, $SO_2 > 0.15$ ppm occurred in about 6% of the station hours of lake air during both years of study. For the nonclassic type, the percentages were 14.5 and 5.9 in 1966 and 1967, respectively. These figures are to be compared with the observed city-wide annual averages of 14.9 and 14.4% for the two years.

For both lake breeze types, relative frequencies of $SO_2 > 0.15$ ppm varied markedly with station location and season, being highest near sources and in winter. At stations near both SO_2 sources and the lake shore, an intrusion of lake air usually resulted in a drop in the hourly average concentration of SO_2, except in those cases where the station felt the effects of a lake breeze fumigation of strong local sources. Further inland, most often there was no change in SO_2 concentration as the lake breeze front passed. At the farthest inland stations, if any change in the hourly average occurred at the front, it was likely to be a slight increase in concentration.

Introduction

An important part of the meteorological studies in support of Argonne's Chicago Air Pollution System Analysis Program has been the identification and characterization of weather phenomena associated with incidents of severe pollution.

A number of different types of weather events have been observed to occur in association with high SO_2 concentrations. The SO_2 pollution characteristics of one of these--the lake breeze--have been studied in detail and are the subject of this paper. The study period was 1 January, 1966 through 31 December, 1967.

The main objective of this study was to investigate the incidence of high SO_2 concentrations in lake breeze situations. Specifically, the following questions were posed:

1. How do frequencies of $SO_2 > 0.15$ ppm in lake air (i.e., in east winds off Lake Michigan during lake breezes) compare with average conditions?
2. How do these frequencies vary with season?
3. How do they vary with station location?

A second objective was to compare for all lake breeze events, regardless of pollution level, the SO_2 concentrations in the lake air with those in the air displaced at each station the lake air passed. The questions asked were:

1. Do SO_2 concentrations increase or decrease as the lake breeze passes a sensor?
2. Does the location of the sensor determine whether the SO_2 concentration increases or decreases as the lake breeze front passes?

The remaining objective was developed during the course of the study when it was discovered that certain lake breeze events not of the conventional kind occur in Chicago. Because transport of pollutants is such an important part of the pollution picture, and because the circulations of these "other" lake breezes, at least at the surface, appear to be identical to those of conventional lake breezes, all occurrences of both types of events were identified for 1966 and 1967. The final objective of this work was thus to compare "classical" and "other" lake breezes (from now on called Type I and Type II, respectively) with respect to the questions listed earlier.

Definitions, Data, and Procedures

Choosing the criteria for identifying lake breeze cases and their beginnings and endings was a difficult task. Those finally chosen are based mostly on characteristics of lake breezes described in the literature. The choice was also influenced by experience gained in this study through the examination of almost 100 lake breezes of both types. The criteria involve certain limits on three parameters: circulation, cloudiness, and

wind speed.

Circulation

The circulation requirement is as follows: a wind shift from a "westerly" sector to an "easterly" sector must occur. This wind shift must occur first along the lake shore, creating a convergence zone some distance inland, with easterly winds to the east and westerly winds to the west. Usually the convergence zone moves inland with time, sometimes as a series of advances and retreats. However, only the existence of an inland convergence zone is required--not its movement.

The "westerly" sector was chosen as 190° to 350°, inclusive. The "easterly" sector chosen was 1° to 135°, inclusive. The following considerations contributed to their selection. The "westerly" sector was defined only for use in the first step of data screening to select cases. This step was done by computer and consisted of listing all hours in the two years of data during which westerly winds were observed inland (at Midway Airport) at the same time that easterly winds were observed on the lakefront (at Meigs Field). The actual limits chosen were not crucial to the eventual identification of cases, as long as they were sufficiently broad that at least two consecutive hours of every valid case were found by the computer. Final selection of cases was made by the author, using hourly plots of winds and other weather data from the eight Chicago Telemetered Air Monitoring (TAM) stations,[1] four Chicago-area airport weather stations, and Argonne. Station locations are shown in Figure 1.

Two different definitions of the "easterly" wind sector were employed during different stages of the identification procedure. For the initial computer screening, a 1 to 170° sector was used. A more important choice of easterly sector was that used to determine the duration of the lake breeze. At each TAM station, duration was taken as the number of consecutive hours the wind direction was between 1° and 135°. The northerly limit is most justified physically for the lakefront TAM stations, where it separates land trajectories from lake trajectories. It could be argued that a more easterly direction should be required for stations

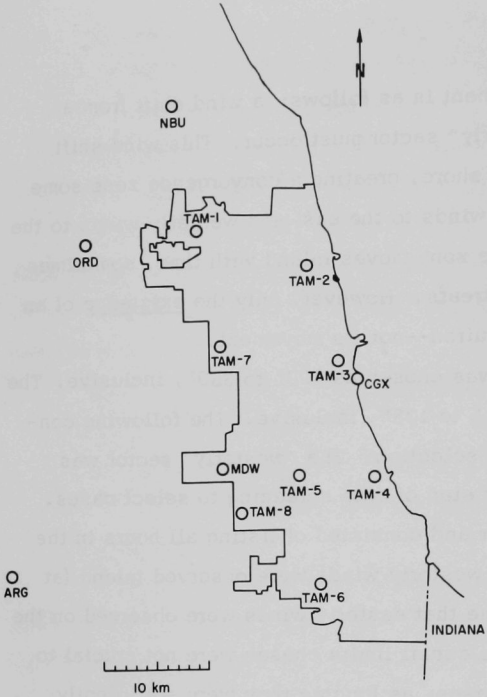

FIG. 1.--Map of the Chicago Area, showing the TAM Network, Midway Airport (MDW), O'Hare Field (ORD), Glenview Naval Air Station (NBU), Meigs Field (CGX), and Argonne (ARG).

farther inland. However, that seemed to be an unnecessary complication of the procedure. As a practical matter, when lake air arrives at a station, a large wind shift occurs, and the final direction is well east of 1°. The choice of 1° seldom affected the duration by more than a few station hours.

The choice of the limiting wind direction toward southeast was more difficult. In contrast to the sudden, large wind shift through north at the onset, most Chicago lake breezes end in a gradual wind shift from northeast or east to southeast, then to south-southeast, and eventually to south or southwest. Moreover, the choice affects the incidence of high SO_2 concentrations in lake air because of the concentration of large sources in the southeastern and southern sections of the city. There were two basic reasons for choosing 135°:

1. It is approximately the southern limit of an over-lake trajectory

for most TAM stations, and

2. A wind shift through 135° at the end of the lake breeze is usually irreversible. That is, once past 135°, the wind usually continues to shift toward south and does not return. The wind shift through 135° is thus a clear indication that the lake breeze is over.

There is one qualification to the rules for fixing the duration of the lake breeze: The latest hour allowed for the end of an event was midnight of the day it began. This measure was necessary to provide a reasonable end point for certain Type II lake breezes in which easterly winds continue on for many hours or even days.

Cloudiness

If the convergence line (also called the wind shift line, or lake breeze front) passed Midway, the average cloudiness (not including the winds between 1° and 135° at any TAM station was required to be less than 0.6 (see Hall[2]) for the event to be classed as a Type I lake breeze. There was no maximum cloudiness limit if the lake breeze front did not reach Midway.

Wind Speed

We also know from the work of Hall[2] that lake breezes are unlikely when the 2000-ft wind speeds measured at 1000 CST at Joliet are over 13 kt from the north or 10 kt from the south or southwest. However, soundings are no longer taken at Joliet and it is difficult to translate these limits to surface wind speeds at one of our ground-level stations. Examination of many lake breezes in this study showed that surface wind speeds at Midway were consistently less than 10 kt before lake breeze onset. Therefore, 10 kt was selected as the maximum pre-onset wind speed allowable (at Midway Airport) for a Type I lake breeze. In practice it was found that whenever wind speeds over 10 kt occurred prior to an intrusion of the lake air, the event was clearly Type II because of the presence of heavy cloudiness.

There is one feature of most textbook descriptions of lake breezes that is absent from the definition used here, namely, the horizontal tempera-

ture gradient across the shoreline. This temperature difference is usually considered to be the driving force of the lake breeze circulation. However, a number of the lake breezes examined in this study occurred even though air over the land was cooler than air over the lake (i.e., Meigs Airport temperature during the first hour of onshore winds). These events were similar in all other ways to the lake breezes that occurred with warmer air over the land. It seems reasonable that they were indeed lake breezes. Therefore, in this study warmer air over the land was not required for an event to be listed as a lake breeze.

Type I lake breezes are defined as events that meet the circulation, cloudiness, and wind speed criteria; Type II lake breezes meet the circulation criteria, but fail one or both of the others.

Results and Discussion

Table 1 is a summary of both types of lake breezes identified in Chicago in 1966 and 1967. Sixty Type I and 35 Type II lake breeze days were found. The numbers of events in both categories were slightly higher in 1966 than in 1967.

TABLE 1. Summary of Type I and Type II Lake Breezes in Chicago, 1966-1967

	1966		1967		Total	
Month	I	II	I	II	I	II
Jan	1	3		1	1	4
Feb	1	2	1		2	2
Mar	2	3		2	2	5
Apr	1	4		1	1	5
May	3	2	4		7	2
Jun	6		3	3	9	3
Jul	4	2	6	3	10	5
Aug	7	1	5	3	12	4
Sep	4	1	2	1	6	2
Oct	5		3		8	
Nov			2		2	
Dec		2		1		3
Total	34	20	26	15	60	35

Both types were found throughout the year except for an absence of Type I in December and Type II in October and November. The frequency of Type I lake breezes varies strongly with seasons; the largest numbers occur from May through October. Type II lake breezes are rather uniformly distributed throughout the year.

Many of the Type II lake breezes were associated

with precipitation; some of these appear to be similar to the "lake snow" case documented by Williams.[3] The cases with precipitation, and some other cases as well, were accompanied by heavy cloud cover.

One other subtype of Type II occurred frequently and was sometimes accompanied by 0.8 to 0.9 cloud cover. This type occurs in response to changing wind directions associated with shifting pressure patterns or frontal passages. In cases where the gradient wind shifts from offshore to onshore, a convergence zone sometimes forms near the shore and moves inland with time, just as the lake breeze front does. In contrast to the lake breeze, however, circulation does not die out in the late evening. On the contrary, easterly winds may continue for many hours or even days.

TABLE 2. Severity of SO_2 Pollution in Lake Air

Type	Year	Total station hours of lake air	SO_2 > 0.15 ppm in lake air: Station hours	Percent of total
I	1966	1440	87	6.0
	1967	991	57	5.8
II	1966	997	145	14.5
	1967	953	56	5.9
City-wide annual percentage of hours with SO_2 > 0.15 ppm			1966	14.9
			1967	14.4

The main concern in this study was to determine the incidence of high SO_2 concentrations in lake air. SO_2 concentrations above 0.15 ppm occurred often enough to provide reasonable statistics for comparison with average conditions. Hence, this value was chosen as the reference. It corresponds roughly to the 24-hour average limits of SO_2 concentrations now being set by various states.

Table 2 shows, for each year of the study, and for both lake breeze types, the number of station hours of lake air observed and the number and

percentage of hours with $SO_2 > 0.15$ ppm. For each year, the city-wide average percentage of hours of $SO_2 > 0.15$ ppm is also given in comparison.

For both years the annual percentage of hours with $SO_2 > 0.15$ ppm during Type I lake breezes was about half the city-wide average for that whole year. This is perhaps inconclusive because most of the Type I lake breezes occur during the summer, when average pollution conditions are also lower than the yearly average. A more conclusive comparison, on a monthly basis, is planned.

The percentage of station hours with $SO_2 > 0.15$ ppm in Type II lake breezes was almost equal to the annual city-wide average in 1966, but about half that average for 1967. Type II lake breezes are quite uniformly distributed over the year, so the comparison is a valid one in this case.

The annual variation of lake breeze station hours per month and the percentage of those hours with SO_2 over 0.15 are shown in Figure 2. For Type I lake breezes, the station hours per month peak during the summer, but SO_2 in lake air is very seldom above 0.15 ppm then. Winter has relatively few hours of Type I lake breezes, but when they occur they are quite likely to be high in SO_2. Figure 2 shows that a significant number of Type II lake breeze hours occurs in winter and that 20 to 50% of these hours have SO_2 over 0.15 ppm.

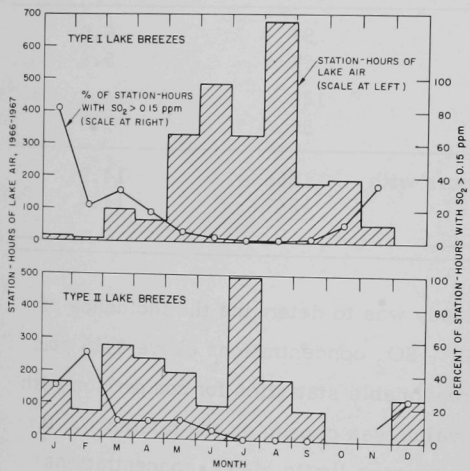

FIG. 2.--Annual variations of Type I and Type II lake breeze station hours per month and the percents of those hours with $SO_2 > 0.15$ ppm

The stations receiving the most hours of high SO_2 concentrations in lake air are revealed in Table 3. Type I lake breezes give high SO_2 values to TAM-6

TABLE 3. Hours of SO_2 > 0.15 ppm in Lake Air at TAM Stations, 1966-1967.

TAM station	1	2	3	4	5	6	7	8	Total
Type I	3	5	28	14	20	35	23	16	144
Type II	1	2	73	21	42	32	19	11	201
Total	4	7	101	35	62	67	42	27	345

most often, while Type II lake breezes pollute TAM-3 most, and to an even greater extent. These results probably reflect the greater role of Type II lake breezes during winter in an area with strong sources nearby.

The second major concern of this study was the change in SO_2 concentration that occurs as the lake air front passes a station. Visual observations indicate that lake air is frequently very smoky, especially the first few hundred feet behind the front.[2] Hourly averages of SO_2 concentrations at the TAM stations were examined to see whether SO_2 behaves like the smoke in lake breezes. The investigation involved listing the SO_2 average for the last hour when the vector average wind direction was westerly and the first hour when it was easterly for every passage of a lake air front over a TAM station. The difference between these two figures was taken as the change in SO_2 at the wind shift line. Figures 3-5 show the distribution of these changes in SO_2 during both types of lake breezes at each TAM station.

Figure 3 shows results for TAM-3 and -4. There is a clear trend, especially at TAM-4, for SO_2 to <u>decrease</u> when the lake air passes. Thus at these lakefront stations the lake air is cleaner than the air present there before the lake air moved in. This is true for both types. There is an apparent paradox here. SO_2 concentrations usually decrease at TAM-3 as the lake air comes in. Yet TAM-3 had the highest number of hours with SO_2 > 0.15 ppm in Type II lake breeze air (Table 3). The explanation is that SO_2 concentrations in the original air are frequently high enough that the decreases that occur with a shift to lake air can still leave SO_2 concentrations above 0.15 ppm.

Figure 4 shows results for TAM-2, -6, and -8. At these stations

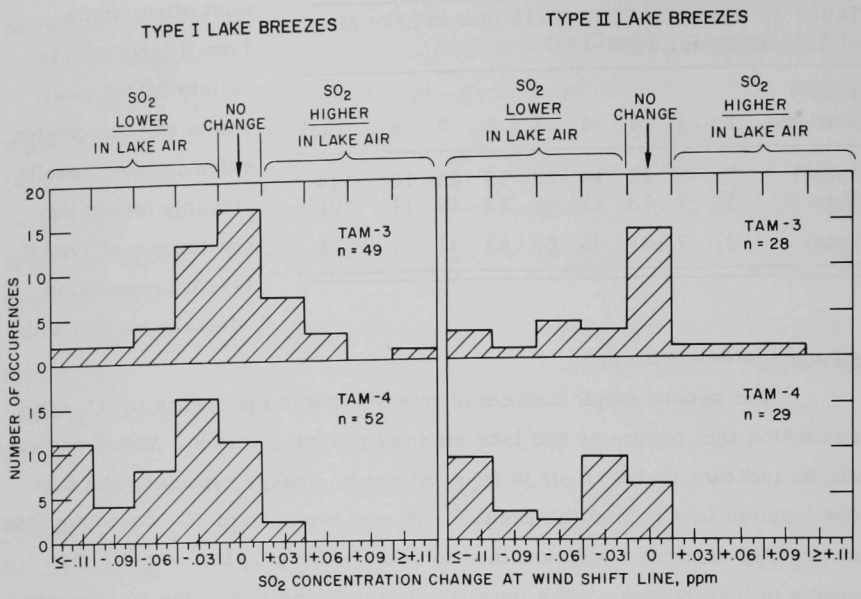

FIG. 3.--Frequency distribution of SO_2 concentration change at Type I and Type II lake breeze fronts for TAM-3 and TAM-4.

there is usually no change at all in SO_2 concentrations as the lake air moves in. For the small number of cases where some change was noticed, increases and decreases, sometimes quite large, were about equally likely. The one exception to this pattern was TAM-6 Type I lake breezes, which were more likely to produce increases than decreases. Figure 5 shows the results for TAM-1, -5, and -7. Here again there was a strong tendency for no change, but when changes occurred, they were quite likely to be increases, sometimes large ones.

The general picture that appears from these figures is one in which pollution at stations near the lake shore, like TAM-3 and -4, decreases in air fresh off the lake. At intermediate distances (TAM-5 and -8), SO_2 might increase or decrease as the front passes. What happens in an individual

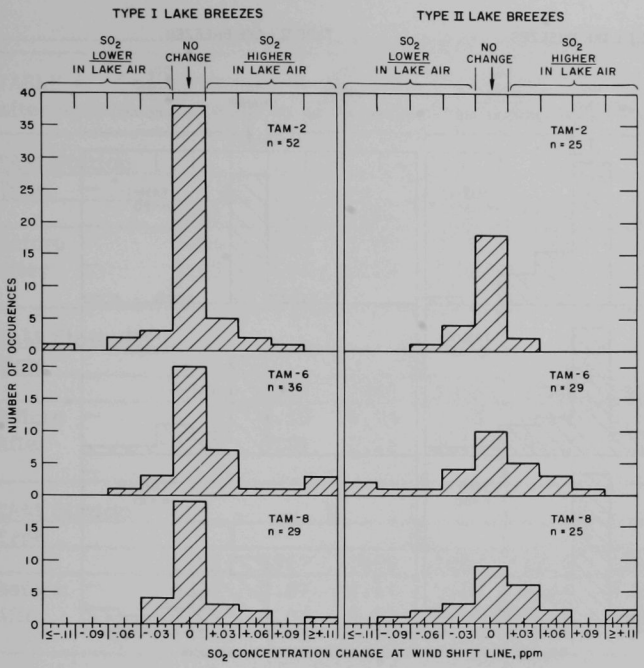

FIG. 4.--Frequency distribution of SO_2 concentration change at Type I and Type II lake breeze fronts for TAM-2, TAM-6, and TAM-8.

case probably depends on the particular combination of the general pollution level that day and the exact direction of the wind with respect to upwind sources. The farthest inland stations (TAM-1 and -7) occasionally show SO_2 increases. The frequency distributions of changes in SO_2 at individual stations tell only part of the story, however. It is also helpful to consider the value of SO_2 concentration during the last hour of westerly winds and the first hour of easterly winds averaged over all events of each type. These averages are presented in Table 4 for both lake breeze types and for both years of data at each station.

The table reveals several important points. First, at all stations the direction of change found for 1966 is remarkably consistent with that found for 1967 and, of course, these directions agree with the trends indicated for the various stations in Figures 3-5. Secondly, Table 4 shows that stations 3 and 4 had the highest SO_2 concentrations in the air that the lake air replaced. This is true for both types of lake breezes. Hence,

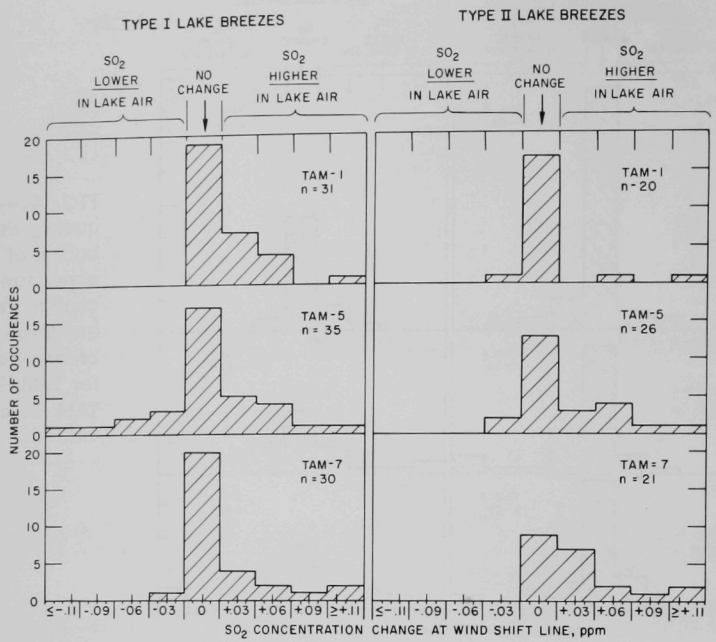

FIG. 5.--Frequency distribution of SO_2 concentration change at Type I and Type II lake breeze fronts for TAM-1, TAM-5, and TAM-7.

the beneficial effects of the clean lake air occur where they are needed most. Moreover, the stations that experience increases in SO_2 as the lake air comes in usually have rather low SO_2 to start with, so the increases are not a serious matter.

We have seen that the picture painted by city-wide data on pollution in lake air is rather bright. It is also useful to consider conditions in local areas.

High SO_2 concentrations (approaching 1 ppm) have been observed at Chicago TAM stations during lake breezes. These occurrences are few in number, but they show that lake breezes can lead to high pollution levels in local areas near large sources. Most of these cases probably are not

TABLE 4. Comparison of Average SO_2 Concentrations for Hours before and after Arrival of Lake Air at TAM stations. Concentrations in ppm.

TAM Station	1				2			
Type	I		II		I		II	
	1966	1967	1966	1967	1966	1967	1966	1967
Before	0.01	0.02	0.03	0.02	0.04	0.04	0.05	0.06
After	0.03	0.04	0.04	0.03	0.04	0.04	0.05	0.05
TAM Station	3				4			
Type	I		II		I		II	
	1966	1967	1966	1967	1966	1967	1966	1967
Before	0.10	0.10	0.24	0.16	0.14	0.13	0.30	0.10
After	0.09	0.07	0.21	0.11	0.07	0.07	0.17	0.06
TAM Station	5				6			
Type	I		II		I		II	
	1966	1967	1966	1967	1966	1967	1966	1967
Before	0.07	0.07	0.12	0.09	0.04	0.04	0.10	0.04
After	0.07	0.04	0.13	0.07	0.07	0.05	0.10	0.05
TAM Station	7				8			
Type	I		II		I		II	
	1966	1967	1966	1967	1966	1967	1966	1967
Before	0.02	0.02	0.08	0.05	0.03	0.04	0.09	0.07
After	0.03	0.06	0.11	0.08	0.03	0.07	0.12	0.07

detected by the existing TAM network.

Visual observations of industrial plumes along the lake shore by the author and by Lyons[4] indicate that dense concentrations of smoke can reach the surface within a few stack-heights of their source. This occurs through the fumigation mechanism. The unstable boundary layer that forms in the lake air as it moves inland quickly grows upward and reaches plume height, and pollutants are rapidly mixed downward to the surface. Observations indicate that the problem is most severe along Chicago's south lake shore, where a number of large industries are located.

Conclusions

1. In Type I lake breeze air, percentages of hours with $SO_2 > 0.15$ ppm are about half the annual city-wide percentages. This comparison is not conclusive because most lake breezes occur in summer when average pollution levels are also lower than the annual average. A more valid comparison will be made using monthly city-wide percentages.

In 1966 the percentage of hours with $SO_2 > 0.15$ ppm in Type II lake breezes was very close to the city-wide annual percentage. In 1967 the percentage in Type II lake breezes was only about half of the city-wide value. These comparisons are probably valid because this type occurs quite uniformly throughout the year.

2. Frequencies of $SO_2 > 0.15$ ppm vary markedly with season for both lake breeze types, being highest in winter.

3. These frequencies also vary markedly with station location. In Type I lake breezes, the highest frequency occurred at TAM-6, while in Type II the highest frequency was at TAM-3.

Although high SO_2 concentrations sometimes occur locally during lake breezes, city-wide average pollution levels are generally low. In particular, at lake shore stations TAM-3 and TAM-4 a lake air intrusion means cleaner air. Farther inland, most often there is no change in SO_2 concentration. At the farthest inland stations the changes that do occur are likely to be increases in concentration. However, those stations usually start with low SO_2 values, so the increases that occur aren't serious. This applies to both types of lake breezes.

Chicago Lake Breeze Structure: Review of Present Knowledge

We have seen that lake breezes can affect the concentrations of SO_2 in Chicago. In order to use an urban air pollution model to compute SO_2 concentrations for lake breeze regimes, we need to know the structure of the lake breeze. This section reviews present knowledge of the physical structure of Chicago Type I lake breezes, the only type that has been studied to any extent. This review is based heavily on the recent work and

literature reviews of Olsson[5] and Olsson and Lyons.[6]

The lake breeze circulation at Chicago consists of the lake breeze itself, an onshore-flowing layer 300 to 700 m thick, and above this a return flow layer that may be more than 1000 m thick. The lower portion of the lake breeze is very stable over the lake.

The stable layer may be up to 300 m thick. As it moves ashore, a superadiabatic layer grows upward into it from the effects of the warm land and the rough city surface. The stable layer is completely destroyed by the superadiabatic layer within a few (< 5) km of the shoreline.

The lake breeze front moves inland at a rate of about 1 m/sec. Winds within the lake breeze layer are ordinarily less than about 5 m/sec, with the maximum speed within 100 to 300 m of the surface. Ordinarily winds behind the front exceed the speed of the front itself. Continuity principles indicate, and observations confirm, the existence of a convergence zone at the lake breeze front. This zone may be less than 500 m across and contain updrafts averaging 0.5 to 1.0 m/sec. Updrafts may reach 5 m/sec in extreme cases.

In the return flow, wind speeds are usually less than 5 m/sec but may exceed that strength occasionally. The circulation is completed by subsidence over the lake where downdraft speeds may reach 0.6 m/sec.

References

1. Booras, S. G. and C. E. Zimmer. A comparison of conductivity and West-Gaeke analyses for sulfur dioxide. J. Air Poll. Control Assoc. 18 (9), 612-615 (1968).
2. Hall, C.C. Forecasting the lake breeze and its effects on visibility at Chicago Midway Airport. Bull. Am. Meteorol. Soc. 35, 105-111 (1954).
3. Williams, G. C. An occurrence of lake snow: One of the direct effects of Lake Michigan on the climate of the Chicago Area. Monthly Weather Rev. 91, 465-467 (1963).
4. Lyons, W. A. Personal communication (1969).
5. Olsson, L. E. Lake effects on air pollution dispersion. The University of Michigan, Office of Research Administration, Ann Arbor, Technical Report 02621-1-T (1969).

6. Olsson, L. E. and W. A. Lyons. Air pollution dispersion in a lake breeze regime: Trajectory study using tetroons, smoke photography, and aircraft measurement of aerosols. Paper 69-29 presented at the 62nd Annual Meeting of the Air Pollution Control Association, New York City, June 1969.

URBAN-RURAL DIFFERENCES IN TEMPERATURE AND DEW POINT IN THE CHICAGO AREA

Bernice Ackerman

Observations from Chicago Midway Airport and Argonne National Laboratory have been used to study urban-rural differences in temperature and dew point. A definite urban heat island exists and tends to be more pronounced at night than during the day. No well-defined city effect was found in atmospheric moisture but urban-rural dew-point differences of 2° F or more of either sign are not uncommon. A diurnal cycle occurs in both the difference in temperature and in dew point. The chief seasonal effect seems to be a modification of this cycle.

Introduction

It long has been recognized that cities can modify the local climate. The increasing concern over the impact of human activity on the environment has brought with it a need for information on the effect of human settlements on the atmosphere. Evidence now accumulating suggests more subtle and far-reaching effects on the weather than the local ones which we all recognize.

The ultimate source of the energy which drives the atmospheric circulations is, of course, the sun. However, the atmosphere is practically transparent to solar radiation and can derive the needed energy only through the intermediary of the terrestrial surface — through terrestrial radiation and turbulent flux of sensible and latent heat. Changes in surface characteristics, such as occur when structures are erected and roads are paved, result in modification of the local transfer of energy from the earth to the atmosphere. Urbanization can also modify the atmospheric energy balance in other ways, e.g., through the direct production of heat in combustion and by introduction into the atmosphere of solids, gases, and chemicals which affect the scattering and absorption of radiation.

As one phase in a study to examine the impact of an urban complex on atmospheric processes, this report considers climatological differences between the temperature and humidity in a city and those in a nearby rural

location. The basic data are 20 years of recorded hourly observations made at Argonne National Laboratory and at Midway Airport, the official Weather Bureau station in Chicago. The basic parameters considered are the differences in Midway and Argonne temperatures and dew points for each hour. Throughout this report the differences refer to Midway values minus Argonne values.

Site Characteristics

Argonne National Laboratory is located on 3700 acres of gently rolling terrain southwest of Chicago. The surrounding area is largely rural, but there has been an increasing conversion of farmland to suburban type housing developments over the last few years. The meteorological measurements are made in an open field at the southwest corner of the Laboratory. Aside from a nearby small, one-story building, the closest Laboratory structures are about a mile away, and the nearest settlement is a town of about 4000 population 1-1/2 miles to the southwest.

Chicago Midway Airport is 9 miles southwest of the center of the city and about 14 miles northeast of the Argonne Meteorological Tower. It is a small airport, roughly one mile on a side, crisscrossed with runways. The surrounding area has typically urban land usage with industrial and commercial, as well as residential, structures. There are no towering buildings, but the areal density of one- to four-story structures is high. When winds are from NW through E to SSW, air arriving at Midway has a long fetch over the city. The area to the southwest is urban for the first 3 or 4 miles, opening to suburban interspersed with forest preserves beyond. The topography in the vicinity of Midway is quite flat.

Instruments

The period of record available for the study was from January 1950 to April 1970. Unfortunately changes in instrumentation occurred at both Argonne and Midway during these years. The instruments, sites, and dates

of operation, are shown in Table 1.

TABLE 1. Argonne and Midway Instrumentation, 1950-1970.

Location	Variable	Instrument	Elevation above ground, ft.	Dates
Midway, near Terminal Bldg.	Temperature	Mercury in glass	5	1/1/50-7/31/63
	Dewpoint	Dry and wet bulb, mercury in glass	5	1/1/50-7/31/63
Midway, NW quadrant	Temperature	Liquid in capillary (hygrothermometer)	4	8/1/63-present
	Dewpoint	Dewcel	4	8/1/63-present
Argonne, SW corner	Temperature	Bourdon tube (hygrothermograph)	5	1/1/50-6/30/51
		Copper-constantan thermopile	3.5	7/1/51-8/5/52
			5.5	8/5/52-present
	Dewpoint	Relative humidity and temperature (hygrothermograph)	5	1/1/50-3/31/58
		Dewcel	5.5	4/1/58-12/1/60
			4.7	12/1/60-present

At Argonne, the recorded dew-point temperature and relative humidity are with respect to ice at temperatures below freezing. These have been corrected to give values relative to water at all temperatures in order to make them compatible with the international conventions practiced by the Weather Bureau at Midway.

The Argonne measurements are continuously recorded. When the hygrothermograph was used, the value on the hour was read from the chart, but because of instrument response it represents an average over several minutes. Measurements by the thermopile and dewcel are automatically averaged over a 10-minute interval centered on the hour. The measurements at Midway were made about 20 minutes after the hour through April of 1957, and a few minutes before the hour since then. The instruments are read at the observation time but again, because of instrument response, represent averaged values over a few minutes. More complete descriptions of the techniques of the measurements can be found in Weather Bureau Manual, Circular N[1] for Midway and in the Argonne 15-year Climatological Summary for Argonne.[2]

Because of the changes in instrumentation, two sample periods have

been used for the temperature study and three for the humidity study. These were as follows.

Temperature

I. April 1950 through March 1963: Mercury thermometer at Midway Terminal; thermopile at Argonne (hygrothermograph to July 1, 1951).

II. April 1963 through March 1970: Hygrothermometer mid-field at Midway (mercury thermometer at terminal to August 1, 1963); thermopile at Argonne.

Dew Point

I. April 1950 through March 1958: Dry and wet bulb at Midway Terminal; hygrothermograph at Argonne.

II. April 1958 through March 1963: Dry and wet bulb at Midway Terminal; dewcel at Argonne.

III. April 1963 through March 1970: Dewcel mid-field at Midway (dry-wet bulb at terminal to August 1, 1963); dewcel at Argonne.

Temperature

The existence of an urban "heat island" (higher temperatures in a city than in the surrounding rural area) has been documented for cities of all sizes all over the world. In their climatological study for Argonne, Moses and Bogner[2] compared the Midway and Argonne temperatures for the 15-year period from 1950 through 1964. The work reported here is an extension and reworking of their study, using an additional 5 years of data.

The cumulative frequency distributions of the hourly difference, Midway temperature minus Argonne temperature, are shown in Figure 1 for the periods 1950-1963 and 1963-1970. There is no significant difference between the distributions, and either of the two periods may be considered representative of the full 20 years. The frequency distribution shown in the lower part of Figure 1 is for the whole 20-year period.

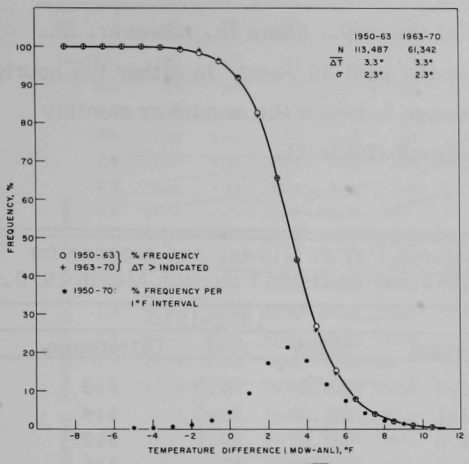

FIG. 1.--Ogives of the hourly difference, Midway temperature minus Argonne temperature, for the periods April 1950 through March 1963 and April 1963 through March 1970. Frequencies are given as the percentage of total hours in each period in which the temperature difference was equal to or greater than value given on the abscissa. Also shown are the percentage frequencies of the hourly temperature differences, in 1°F intervals, for the whole 20 years.

It is obvious from Figure 1 that at any given hour the city temperature is likely to be higher than the rural one; this was true in 94% of the hours from 1950 to 1970. The average value of the temperature difference between the two stations was +3.3°F. Although they represent only 6% of the observations, negative temperature differences did occur on nearly 10,000 hours. The frequency distribution of temperature difference is not perfectly symmetric but is very close to it, with the upper and lower deciles lying at +6.2°F and +0.7°F.

Although one may argue about the representativeness of airport measurements in studies of urban effects, it is difficult to explain the large positive airport-rural temperature difference except by city influence. Although the elevation at Argonne is 140 ft higher than that at Midway it is doubtful that this could account for even a few tenths of a degree of the observed temperature difference.

Landsberg[3] gives an average city anomaly of only 1°F for Chicago, considerably less than the 3° found in the last 20 years. He does not give the source of his numbers but states that the anomaly is relative to a "regional normal." This base may not be unaffected by human settlements. Also, Landsberg's value may be derived from much earlier data, so that the dis-

agreement could reflect the growth of the city. There is, however, no evidence of an increasing trend over the past 20 years, in either the hourly difference (Figure 1) or in the difference between the annual or monthly average temperatures at the two stations (Table 2).

TABLE 2. Monthly Average Temperatures (°F) at Midway and Argonne for Periods April 1950 through March 1963 and April 1963 through March 1970.

	1950-1963			1963-1970		
Month	MDW	ANL	Difference	MDW	ANL	Difference
January	23.8	20.5	3.3	23.6	20.3	3.3
February	28.7	25.6	3.1	26.9	23.5	3.4
March	36.1	33.1	3.0	36.6	33.6	3.0
April	49.1	46.8	2.3	50.0	47.4	2.6
May	60.9	57.9	3.0	59.6	56.8	2.8
June	70.7	67.3	3.4	70.5	67.4	3.1
July	74.7	71.0	3.7	74.2	71.0	3.2
August	73.8	70.1	3.7	71.9	68.2	3.7
September	66.3	62.8	3.5	65.5	61.8	3.7
October	55.4	52.2	3.2	54.7	51.6	3.1
November	39.7	36.6	3.1	41.6	38.6	3.0
December	28.5	25.3	3.2	28.5	25.1	3.4
Year	50.7	47.5	3.2	50.4	47.2	3.2

The influence of the city on the temperature may vary with season since there are seasonal changes in the state of the atmosphere and in the nature of the ground surfaces as well as in the activity of the city. Cumulative frequency distributions and other statistics of Midway-Argonne temperature differences for each of the 12 months are given in Figure 2. The average temperature difference was smallest in spring and largest in late summer, but the chief seasonal effect seems to be a broadening of the frequency distribution during the summer months. Large positive temperature differences occurred most often from June through September. Thus, the heat island is likely to be most pronounced during the summer, particularly in August when temperature differences of 5° or more occurred 25% of the time. At the other extreme, Midway temperatures were below

TEMP DIF DEG F	JAN	FEB	MAR	APR	MAY	JUN	JUL	AUG	SEP	OCT	NOV	DEC	TOTAL HOURS
MAXIMUM	539	181	119	248	182	209	162	163	152	120	376	176	
10.5	.26	.61	.17	.13	.48	.95	.80	1.26	1.24	.21	.07	.38	338
9.5	.67	.98	.42	.33	.88	1.70	1.55	2.13	1.92	.49	.15	.69	274
8.5	1.53	1.91	1.13	1.05	1.67	3.35	3.26	3.59	3.27	1.11	.37	1.63	611
7.5	3.09	3.72	2.59	2.00	3.76	5.83	6.00	6.75	6.07	2.47	1.11	3.43	1176
6.5	6.41	7.80	5.52	4.80	7.54	10.36	9.96	12.30	11.88	5.66	3.41	6.33	2292
5.5	13.36	16.27	11.54	10.20	13.82	17.22	17.43	21.35	20.21	12.13	8.25	12.44	4217
4.5	26.61	29.32	22.12	20.24	22.85	27.64	28.30	35.54	33.23	23.80	19.67	23.97	7102
3.5	46.93	48.17	39.00	37.33	38.97	42.51	44.64	53.59	51.40	41.79	39.38	45.25	11025
2.5	69.44	68.40	60.82	57.02	57.94	60.42	62.48	71.63	71.19	63.64	64.56	73.35	12883
1.5	85.53	86.06	79.68	73.26	74.42	76.11	78.14	86.92	86.80	81.99	84.01	91.12	10412
0.5	94.94	94.80	90.66	84.47	85.98	87.21	88.45	94.89	95.03	92.31	94.87	97.48	5955
-0.5	98.25	98.40	95.90	91.12	92.37	93.62	93.56	98.00	98.31	96.82	98.29	99.09	2690
-1.5	99.55	99.53	98.46	95.55	96.25	96.68	96.86	99.40	99.58	98.61	99.54	99.74	1333
-2.5	99.74	99.85	99.53	97.57	97.88	98.27	98.50	99.84	99.92	99.53	99.76	99.90	540
-3.5	99.86	99.95	99.76	98.78	98.84	99.10	99.25	99.96	99.95	99.84	99.95	99.94	251
-4.5	99.88	99.97	99.90	99.36	99.21	99.44	99.57	99.98	99.97	99.92	100.00	99.98	101
-5.5	99.92	99.97	100.00	99.72	99.36	99.56	99.84	99.98	100.00	99.98	100.00	99.98	57
-6.5	99.94	99.97	100.00	99.86	99.50	99.66	99.92	100.00	100.00	100.00	100.00	99.98	26
-7.5	99.98	99.97	100.00	99.93	99.61	99.72	99.94	100.00	100.00	100.00	100.00	100.00	17
-8.5	99.97	99.97	100.00	99.95	99.67	99.82	99.94	100.00	100.00	100.00	100.00	100.00	9
-9.5	99.97	99.97	100.00	99.97	99.69	99.86	99.94	100.00	100.00	100.00	100.00	100.00	4
-10.5	99.97	99.97	100.00	99.97	99.74	99.87	99.97	100.00	100.00	100.00	100.00	100.00	6
MIN	99.99	99.99	100.00	99.99	100.00	99.99	100.00	100.00	100.00	100.00	100.00	100.00	23
MINIMUM	-121	-119	-54	-105	-214	-176	-174	-56	-46	-56	-43	-69	
MEAN	341	350	301	269	286	315	324	383	376	316	308	350	
DEVIATION	209	208	207	238	263	271	260	235	228	202	178	180	
TOTAL HOURS	5207	4751	5197	5038	5208	5038	5208	5208	5040	5204	5037	5206	61342

TEMPERATURE DIFFERENCE GREATER THAN

FIG. 2.--Ogives of the hourly difference, Midway temperature minus Argonne temperature, for each month (April 1963 through March 1970). Frequencies are given as percentage of the total observations for each month. The isolines show the percentiles of the distributions. The means and standard deviations at the bottom of the table are given to hundredths of a degree but are significant to no more than one tenth of a degree. Maxima and minima are given to tenths of a degree.

those at Argonne most often in the spring and early summer. This occurred in about 10% of the hours in April through July as compared to 3 to 4% of the hours in winter months.

There is a well-defined diurnal cycle in the urban-rural temperature differences. In fact, the seasonal effect is seen most clearly in the day to night variation. The frequency distributions of temperature differences were

determined for 2-hour periods throughout the day for two seasons, a warm season from April through September and a cold season from October through March. The averages (Table 3) and percentile values of these distributions (Figure 3) indicate a shift in the distributions of 1.5° to 2° F toward lower values after sunrise, with a reverse shift at sundown. The frequency of large positive temperature differences was greater at night than during the day, whereas most of the negative differences occurred during the day.

TABLE 3. Averages of the hourly temperature difference (Midway minus Argonne) for 2-hour periods in the warm season (April-Sept.) and cold season (Oct.-Mar.). Data, April 1963 through March 1970.

Average temperature difference, °F		
Hour	Warm season	Cold season
00-01	4.6	4.0
02-03	4.2	3.9
04-05	4.0	3.8
06-07	2.6	3.4
08-09	2.1	2.5
10-11	1.9	2.1
12-13	1.9	2.1
14-15	2.0	2.4
16-17	2.2	3.2
18-19	3.8	3.8
20-21	4.8	3.9
22-23	4.9	4.1
All	+3.3	+3.3

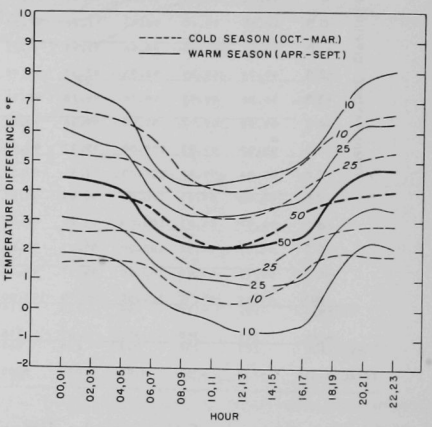

FIG. 3.--The medians and upper and lower quartiles and deciles of the frequency distributions of the hourly difference, Midway temperature minus Argonne temperature, for two-hour periods during the day. The data (April 1963 through March 1970) were divided into two seasons, a warm season from April through September and a cold season from October through March.

The amplitude of the diurnal cycle is smaller in the cold season than in the warm season, the major seasonal change occurring in nighttime conditions. The average nighttime temperature difference is greater during the

warm than the cold season, while the reverse is true for the average daytime difference (Table 3). Although during both seasons large positive temperature differences are more likely to occur at night than during the day, the nighttime values are greater during the warm season than during the cold season. During the period 1963-1970, differences between Midway and Argonne temperatures of 5°F or more (Midway higher) occurred in about 40% of the dark hours during the warm season but in roughly 25% of the dark hours during the cold season. The frequencies of daytime positive temperature difference were about the same during both the cold and warm season. A negative urban-rural difference, primarily a daytime occurrence, was more frequent in the warm season than the cold.

The diurnal cycle in the strength and frequency of the heat island effect can be due to several factors. The sharp change in the temperature difference between about 0500 and 0600 during the warm season (Figure 3) suggests that the rural surface warms more rapidly in the morning, probably because of lower heat conductivity. A similarly sharp change between 1700 and 1800 suggests that the rural surface cools more rapidly after sunset, possibly because less of the daytime heat was stored and also because the flow of heat from the deeper layers to the surface is slower.

The fact that most of the negative temperatures occurred during the day and were also more frequent during the summer than during the winter suggests a lake breeze effect. Negative anomalies could occur when, at any given hour, the lake breeze has reached Midway but not Argonne. Simultaneous occurrence of easterly winds at Midway and westerly winds at Argonne are most frequent in the months April through August.[2] However, if this is the explanation, the dropoff in the frequency of negative anomalies in August is puzzling. If the thermal lag of the city surface is greater than that of the soil and air, then the city may reach its seasonal maximum temperature in August. Air which moved in from a warmer lake (than in July) may then have warmed rapidly as it crossed the 8 or 10 miles of the city to Midway.

Atmospheric Moisture

Water vapor is one of the most variable constituents of the air. As a consequence the influence of an urban complex on the moisture content of the low level atmosphere is difficult to separate from other contributing factors. Available reports indicate that the relative humidity is usually lower in the city than in the country. However, relative humidity is a sensitive function of temperature, and the few studies that have been made of urban-rural differences in atmospheric vapor content are quite contradictory. Nevertheless, there seems to be an almost general acceptance of the city as being slightly "dry" relative to the surrounding countryside, a conclusion which can be supported by scientific reasoning if not observation.

Natural surfaces are primarily vegetation-covered porous soils which tend to retain rainfall, while the city has a high coverage of materials such as concrete, asphalt, and brick which favor rapid and complete runoff. Thus, evaporation from the city surface, with its low retention of water, should be less than over the open country. Moreover, because of the higher temperature and the numerous structures, the turbulent and convective flux of moisture from the surface air to higher levels is expected to be higher over the city. Although these city effects probably do exist, it is not at all clear that they are the only ones. For instance, water vapor is a by-product of combustion, as is dramatically obvious on cold days when condensation occurs in the effluents from stacks and from automobile exhaust.

The dew point is a better measure of the water vapor content than is relative humidity. For this reason the basic parameter used in this climatological study was the difference between the hourly dew points at Midway and Argonne. The 20 years were broken into three periods, 1950-1958, 1958-1963, 1963-1970, as described in the section on instruments.

Whereas the observed temperature differences were nearly identical for the early and late parts of the 20 years, the same is not true for the dew-point differences. The frequency distributions (Figures 4 and 5) indicate smaller (algebraic) dew-point differences during the first 8 years; the median and the mean for the period 1950-1958 were about 1°F smaller than

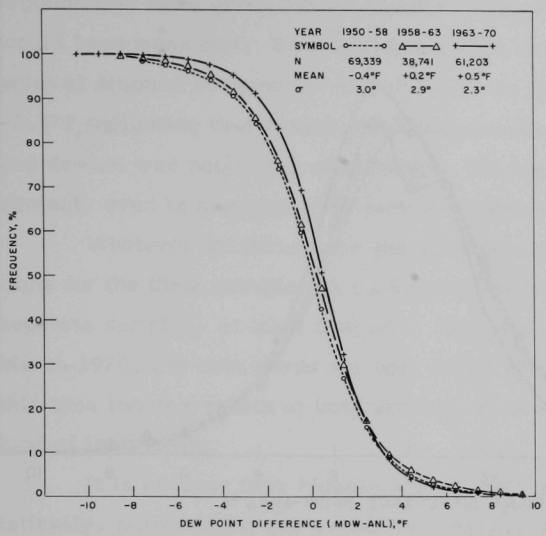

FIG. 4.--Ogives of the hourly difference, Midway dew-point temperature minus Argonne dew-point temperature for three periods: April 1950-March 1958, April 1958-March 1963, and April 1963-March 1970. The frequencies are given as the percentage of total hours in which the dew-point difference was equal to or greater than the value shown on the abscissa.

they were during 1963-1970. The frequency distributions (Figure 5) are quite smooth and nearly symmetric with slight skewness to the left. The distribution for the earlier period is broader than that for the last seven years with somewhat larger frequencies of negative dew-point differences.

The disparity between the early and late periods may be due to climatological fluctuation or to changes in instruments. The annual average dew-point difference changed by as much as 1°F or more from one year to the next (pointing out the pitfalls of short-term urban-rural comparisons) but were fairly consistent within any one period, with rather different characteristic values in the years 1950-1958 (mostly negative) and the years 1963-1970 (mostly sizable positives). This suggests instrumentation as the reason for the disparity between the three periods. If the climatological fluctuations in dew point between period I and II is estimated from the Midway data and that between period II and III from the Argonne measurements (instruments having been the same) then the monthly average dew points given in Table 4 can be used to estimate the magnitude of instrumental differences. From period I to II the annual average dew point at Midway changed by -0.8°F, while that at Argonne changed by -1.6°F, indicating that the hygrothermograph at

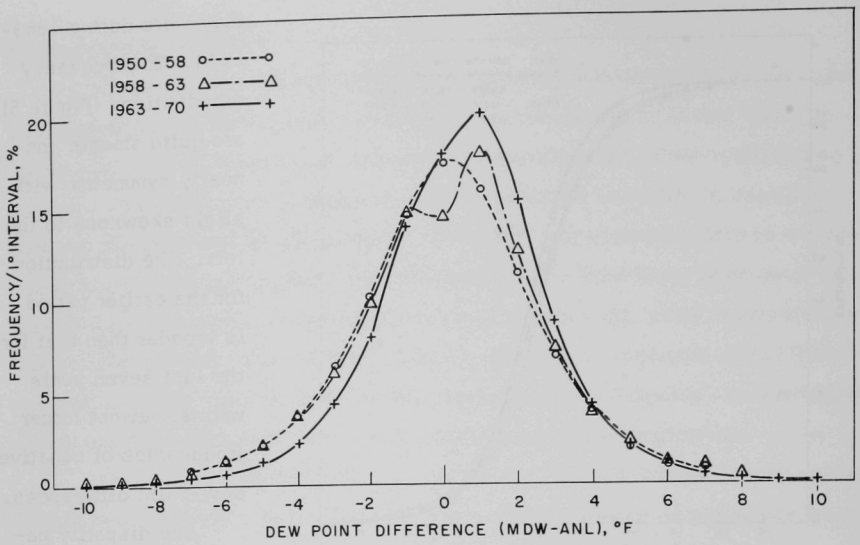

FIG. 5.--Percentage frequency distributions of the hourly difference, Midway dew point minus Argonne dew point, for three periods: April 1950-March 1958, April 1958-March 1963, and April 1963-March 1970. The frequencies are for 1° F intervals.

TABLE 4. Monthly Average Dew Point at Midway and Argonne for Three Temporal Periods (° F).

	Midway			Argonne		
Month	1950-58	1958-63	1963-70	1950-58	1958-63	1963-70
January	18.5	13.0	14.3	18.1	10.9	14.2
February	22.5	18.9	16.0	22.0	17.7	15.7
March	25.1	26.5	24.7	24.6	25.5	24.6
April	35.9	34.7	36.7	36.9	34.8	36.5
May	45.5	46.1	44.2	46.2	47.5	44.2
June	57.5	53.5	55.4	58.2	54.7	55.3
July	61.7	60.0	60.7	62.2	60.1	60.6
August	60.4	62.5	59.5	60.9	62.8	58.7
September	51.4	54.7	53.2	51.8	54.1	52.4
October	42.3	43.6	40.7	41.8	43.9	39.9
November	28.8	30.6	31.8	28.3	29.8	30.8
December	22.0	18.8	20.9	21.4	18.3	19.7
Annual	39.4	38.6	38.3	39.5	37.9	37.8

Argonne may have given systematically higher dew points than the dewcel would have measured. Similarly from period II to III the annual average dew point at Argonne changed by -0.1°F, while the Midway average changed by -0.3°F, indicating that systematic disagreement between the psychrometer and dewcel was negligible or unlikely. The large variability in moisture content, even in averages over several years, is clearly evident in Table 4.

Whatever the causes for the discrepancies, the frequency distributions for the three periods are sufficiently different to warrant using three separate samples, at least initially. The last 7 years, from April 1963-March 1970, are considered the best of the three periods, since during this time the dew points at both stations were measured using the same kind of instrument.

It is obvious from Figures 4 and 5 that the city air is, characteristically, neither drier nor wetter than country air. Although the dew points at Midway were above those at Argonne more often than the other way around, the frequency distributions are centered close to a zero dew-point difference. The medians for the three periods, in chronological order, were 0°F, +0.4°F, and +1°F. The median and average dew-point differences for the 20 years were +0.5°F and +0.1°F, respectively. During the last seven years, a positive difference of any magnitude occurred twice as often as a negative difference of the same magnitude, e.g., Midway dew points were 2°F or more above Argonne dew points 24% of the time, whereas they were 2°F or more below only 12% of the time.

It becomes clear why previous studies have been contradictory. Since sizable differences of either sign occur between city and country dew points, it is important to determine under what conditions the city moisture is higher than the country, and under what conditions it is lower. As the initial step in isolating the pertinent meteorological factors, the 1963-1970 data were examined for temporal variations.

No systematic seasonal variation appears in a comparison of the frequency distributions of dew-point difference for each month (Figure 6). The average urban-rural dew-point difference was greater than or equal to

DEW POINT DIFFERENCE GREATER THAN (DEWPT DIF DEG F)	JAN	FEB	MAR	APR	MAY	JUN	JUL	AUG	SEP	OCT	NOV	DEC	TOTAL HOURS
MINIMUM	-123	-97	-155	-218	-289	-120	-120	-114	-82	-85	-84	-89	
10.5	.03	.10	.32	.09	.19	.09	.07	.01	.03	.19	.09	.15	74
9.5	.11	.18	.44	.11	.23	.13	.11	.01	.09	.21	.15	.30	36
8.5	.24	.39	.63	.31	.38	.49	.15	.05	.17	.44	.19	.61	101
7.5	.67	.61	.92	.57	.53	.77	.44	.13	.35	.78	.39	1.05	161
6.5	1.22	1.03	1.49	.91	.96	1.27	.85	.42	.85	1.24	.81	1.80	288
5.5	2.57	2.02	2.74	1.46	1.71	2.39	1.70	1.19	1.94	2.40	1.82	3.36	636
4.5	5.05	3.97	4.32	2.77	3.21	3.89	3.14	3.22	4.59	4.68	4.06	6.53	1232
3.5	8.87	7.99	7.93	5.57	6.48	7.19	6.46	7.68	9.60	9.74	8.74	14.07	2602
2.5	16.70	16.35	15.41	11.61	13.22	13.27	14.59	17.50	20.26	19.17	18.76	27.10	5287
1.5	28.82	30.26	28.86	25.56	26.83	25.79	27.42	35.21	37.98	36.26	38.09	45.27	9202
0.5	47.60	47.73	44.85	46.18	41.65	43.45	46.29	58.16	57.91	58.01	62.33	67.05	12102
-0.5	66.21	66.84	60.37	65.02	59.15	62.21	64.02	76.64	73.66	76.01	79.57	82.98	10765
-1.5	80.23	81.75	75.73	82.55	75.22	77.09	78.22	88.08	86.03	89.23	91.14	92.91	8434
-2.5	87.28	91.26	87.16	90.76	85.58	86.49	86.92	94.34	93.09	96.09	96.60	97.02	4806
-3.5	92.29	96.24	93.77	95.31	92.22	91.97	91.94	97.33	96.67	98.75	98.74	98.69	2619
-4.5	95.87	98.37	96.50	97.30	95.84	95.31	95.43	98.62	98.44	99.46	99.56	99.38	1332
-5.5	98.38	99.24	97.67	98.59	97.72	97.61	97.16	99.30	99.38	99.76	99.82	99.76	731
-6.5	99.25	99.72	98.19	99.30	98.92	98.63	98.36	99.61	99.72	99.86	99.93	99.90	357
-7.5	99.61	99.87	98.80	99.58	99.36	99.27	99.08	99.78	99.93	99.96	99.95	99.92	191
-8.5	99.84	99.93	99.15	99.74	99.44	99.69	99.39	99.86	100.00	99.98	100.00	99.96	94
-9.5	99.92	99.97	99.44	99.84	99.65	99.83	99.55	99.96	100.00	100.00	100.00	100.00	60
-10.5	99.98	100.00	99.76	99.91	99.74	99.91	99.76	99.97	100.00	100.00	100.00	100.00	46
MIN	100.00	100.00	100.00	100.00	100.00	100.00	100.00	100.00	100.00	100.00	100.00	100.00	47
MAXIMUM	121	128	155	163	348	181	441	124	131	147	327	174	
MEAN	29	43	13	22	-3	6	10	74	79	90	99	135	
DEVIATION	252	277	270	226	263	257	261	204	221	209	198	214	
TOTAL HOURS	5207	4751	5204	5038	5195	5000	5153	5180	5028	5204	5037	5206	61203

FIG. 6.--Ogives of the hourly difference, Midway dew point minus Argonne dew point, for each month (April 1963 through March 1970). Frequencies are given as percentage of total observations for each month. The isolines show the percentiles of the distributions. The means and standard deviations at the bottom of the table are given to hundredths of a degree but are significant to no more than one tenth of a degree. Maxima and minima are given to tenths of a degree.

zero in every month but was closest to zero during the months of March through July. The sharp differences between the frequency distributions for December and January and between those for July and August are puzzling. (The measurements for 1950-1958 show a more consistent variation from winter to summer, with a higher frequency of negative differences during summer, especially early in the season.)

The diurnal cycle is stronger, and the principal seasonal effect is to

modify this cycle. The percentile values of the frequency distributions for 2-hour periods, plotted in Figure 7, indicate a 1° to 1.5°F shift to lower dew-point differences during the day, with the greatest change occurring right after sunrise. Negative dew-point differences occurred more frequently during the daylight hours, whereas large positive differences occurred more often at night. The average dew-point difference for each 2-hour period (Table 5) is above zero except for a few hours after sunrise; the largest positive values are at night. Although the average is close to zero throughout the day during the warm season, this is true only during the forenoon in the cold season.

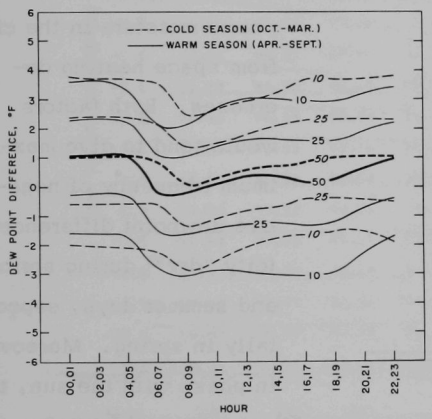

FIG. 7.--The medians and upper and lower quartiles and deciles of the frequency distributions of the hourly difference, Midway dew point minus Argonne dew point, for 2-hour periods during the day. The data (April 1963 through March 1970) were divided into two seasons, a warm season from April through September and a cold season from October through March.

The seasonal change is largest in late afternoon and early evening. Negative dew-point differences occurred almost twice as often on summer afternoons and evenings as they did during the same hours in the cold season. At the same time positive dew-point differences in excess of 1°F occurred more often during winter evenings than they did in summer.

The high relative frequency of positive dew-point differences at night is probably traceable to the more rapid cooling of the country surface (witness strong heat island at night) and consequently greater loss of water vapor to the country surface in the form of dew. Thus, the higher Midway dew points at night are probably largely due not to added source of water vapor in the city but to a sink of water vapor in the country. This moisture is returned to the

air by evaporation after the sun rises and the surface heats up, causing the difference between the moisture content at Midway and Argonne to decrease again.

TABLE 5. Averages of the Hourly Dew-point Difference (Midway minus Argonne) for 2-hour Intervals in the Warm Season (April-Sept.) and the Cold Season (Oct.-Mar.). April 1963 through March 1970.

Hour	Average dew-point difference, °F Warm season	Cold season
00-01	1.0	0.9
02-03	1.0	0.8
04-05	0.9	0.8
06-07	-0.4	0.7
08-09	-0.4	-0.2
10-11	0	0.1
12-13	0.2	0.5
14-15	0.1	0.7
16-17	0	1.0
18-19	0.1	1.0
20-21	0.6	1.0
22-23	0.8	0.9
All	+0.3	+0.7

In spring and summer the bare ground is wet, because of recent snow-melt and high rainfall. Thus, as the weather warms the evaporation rate is especially high in the country while the contribution to the atmospheric moisture in the city from space heating decreases. Both factors would tend to give maximum frequency of negative dewpoint differences (city "dry") during spring and summer days, especially in spring. Moreover, in phase with the sun, the period of typical daytime conditions is shortened during the cold season. The joint occurrence of reduced evaporation in the country and an accumulation of moisture generated by cold season space heating could explain the higher frequency of positive dew-point differences in winter afternoons. The high frequency of positive differences in the early winter evenings is probably due to the early nocturnal cooling and dew formation in the country.

The flux of moisture between surface and air is closely related to temperature. Thus, it is not surprising that urban-rural differences in temperature and dew point are correlated. The cumulative frequency distributions of urban-rural dewpoint difference for several classes of temperature difference are tabulated in Figure 8. It is clear from both the averages

DEWPT DIF DEG F	TEMPERATURE DIFFERENCE - DEGREES F >9	8-9	6-7	4-5	2-3	-1-+1	-3--2	<-3	TOTAL HOURS
MAXIMUM	327	163	181	441	348	155	112	88	
10.5	1.47	.28	.20	.08	.05	.16	.25		74
9.5	3.26	.61	.27	.09	.06	.24	.63		36
8.5	6.06	1.45	.43	.18	.12	.46	1.26	.82	101
7.5	9.31	3.36	.87	.29	.21	.75	1.90	1.23	161
6.5	14.86	6.66	1.77	.54	.40	1.19	2.28	2.05	288
5.5	21.73	11.98	4.19	1.29	.92	1.93	3.67	2.46	636
4.5	31.20	20.50	9.02	3.06	1.92	3.22	6.46	4.93	1232
3.5	41.33	29.91	17.22	8.03	4.57	6.24	8.61	8.23	2602
2.5	53.43	43.58	29.84	18.46	11.52	12.20	14.06	12.75	5285
1.5	64.21	57.31	47.17	35.65	26.33	23.37	23.82	22.22	9198
0.5	77.28	72.43	63.99	56.21	47.82	41.53	38.78	31.68	12101
-0.5	85.94	83.08	77.08	73.56	67.56	59.72	52.97	41.97	10765
-1.5	90.52	89.07	87.45	86.14	82.83	76.36	67.17	55.96	8434
-2.5	93.79	93.72	92.68	92.87	91.29	87.18	77.94	62.96	4806
-3.5	96.56	96.58	96.03	96.41	95.64	93.16	85.17	74.89	2619
-4.5	98.03	98.03	97.56	98.19	97.80	96.31	90.74	81.48	1332
-5.5	98.52	98.82	98.56	99.04	98.94	98.20	94.16	87.65	731
-6.5	99.50	99.32	99.04	99.45	99.44	99.11	96.95	91.76	357
-7.5	99.67	99.66	99.44	99.65	99.66	99.60	98.60	94.65	191
-8.5	99.67	99.77	99.69	99.77	99.79	99.76	99.23	95.47	94
-9.5	99.67	99.94	99.86	99.83	99.88	99.85	99.61	96.70	60
-10.5	99.83	99.94	99.92	99.91	99.96	99.89	99.74	98.35	46
MIN	100.00	100.00	100.00	100.00	100.00	100.00	100.00	100.00	47
MINIMUM	-114	-146	-166	-218	-126	-138	-157	-289	
MEAN	288	202	119	67	26	0	-36	-140	
DEVIATION	366	299	262	222	210	244	320	408	
TOTAL HOURS	612	1785	6480	18082	23243	9962	789	243	61196

DEW POINT DIFFERENCE GREATER THAN

FIG. 8.--Ogives of the hourly difference, Midway dew point minus Argonne des point, for several classes of temperature difference. Frequencies are given as percentage of the total hours during the period April 1963 through March 1970 for which the temperature difference fell into the categories given in headings. Other conventions are the same as in Figure 2.

and the percentiles that the Midway dew point is most likely to be higher than that at Argonne when the heat island is most pronounced. This tends to support the speculation that a large fraction of the positive urban-rural differences is due to differential rates of nighttime radiational cooling and dew formation. This does not, however, account for all positive anomalies, and city sources of moisture cannot be discounted.

In hours during which Midway was colder than Argonne, the dew-point difference was as likely to be negative as positive. It was previously speculated that the negative temperature deviations were due largely to lake breezes which had reached Midway but not Argonne. However, under these circumstances the dew-point difference should usually be positive--they would be negative only when very humid air masses were over the region.

Summary

Twenty years of measurements from Chicago Midway Airport and Argonne National Laboratory have been used to investigate some of the general features of the urban-rural differences in water vapor content and temperature. A pronounced heat island effect, averaging about 3°F , was found in Chicago, with a low but not negligible number of hours in which the city temperature was below that in the country. There is no uniform, clearly defined city effect in atmospheric moisture, but urban-rural differences of 2°F or greater (both positive and negative) were not uncommon. The dew points at Midway tended to be higher than those at Argonne slightly more frequently than they were less.

The urban heat island was most pronounced at night, and positive dew-point differences (Midway minus Argonne) were also more frequent during the dark hours. The average urban-rural differences in both variables tended to be smallest during the daytime, and negative values were also most frequent. The dominant cause for the diurnal variations is believed to be differential rates of nighttime cooling of the city and country surfaces.

Seasonal effects are relatively small. The nighttime "heat island" is as frequent in winter as summer, but very large temperature differences

are less likely to occur in winter. The city temperature is most likely to be below that in the country during warm season days, suggesting a lake breeze effect. Seasonal variations in dewpoint differences are most obvious in the afternoon; during the summer the average difference is close to zero throughout the daytime, but during the cold season this is only true in the forenoon--in the afternoon the average is close to +1°F. This may be a reflection of the accumulation of water vapor produced in daytime combustion.

There is no question that urban-rural differences exist and the large range in the size of these differences illustrate the complexity of the relationships. Further climatological studies using multivariate controls are planned in order to isolate conditions giving rise to particular urban-rural distinctions in both temperature and moisture.

References

1. U.S. Weather Bureau. WBAN Manual of Surface Observations, Circular N. U.S. Government Printing Office, Washington, D. C., 1949.
2. Moses, H. and M. A. Bogner. Fifteen-Year Climatological Summary, January 1, 1950-December 31, 1964, Argonne National Laboratory, DuPage County, Argonne, Illinois. ANL-7084 (1967).
3. Landsberg, H. Physical Climatology. 2nd Ed. Gray Publishing Co., Inc. DuBois, Pennsylvania, 1958, p. 320.

SURFACE ATMOSPHERIC LEAD AND WHAT DEPOSITS ON HUMAN ALVEOLI

S. E. Muniak

The surface atmospheric lead concentration at Argonne for 24 months has been obtained and is reported. Two units of measurement have been employed: nanogram/m^3 and microgram/100 mg particulates. The weighted mean for the season is the most meaningful value. The weighted mean for the seasons has shifted to higher values with time.

The amounts of lead entering the human circulation from breathing Argonne's air and from eating are given; and the mass distribution of lead particulates emitted and released into the atmosphere from automobile exhaust is included, as is their form.

Interest has developed in knowing the content of lead in the surface atmospheric particulates inhaled by humans. Twenty-four months ago, a method using dithizone (diphenylthiocarbazone) was worked out to give the values of lead in the surface atmospheric particulates captured by an HV-70 9-mil filter paper. The filter papers, put on an air pump, were exposed continuously for either 48 or 72 hr, and occasionally for as long as 120 hr. This pattern was continued throughout the 24 months for which data have been obtained. Smith and Surprenant have shown that the HV-70 9-mil filter paper captures 99.9% of dioctylphthalate particulates with a mean diameter of 0.30μ at a face velocity of 150 feet/min.[1] Our air pump has a face velocity of 149 feet/min. Fitzgerald and Detwiler[2] have corroborated Smith and Surprenant's[1] observations.

To provide some feeling for the particulate size range of these atmospheric particulates in which the lead particulates are embedded, a graph was constructed from the data on surface atmospheric particulates given by Reference 3 (see Figure 1). As one can see, the size range for the number distribution encompasses 0.1 to 1.0μ and for mass distribution 0.15 to 1.4μ.

The values of lead in the surface atmospheric particulates collected at Argonne are expressed in two ways. (See Figures 2 and 3.) The unit of nanograms/m^3 gives the net air concentration over a two-week period for

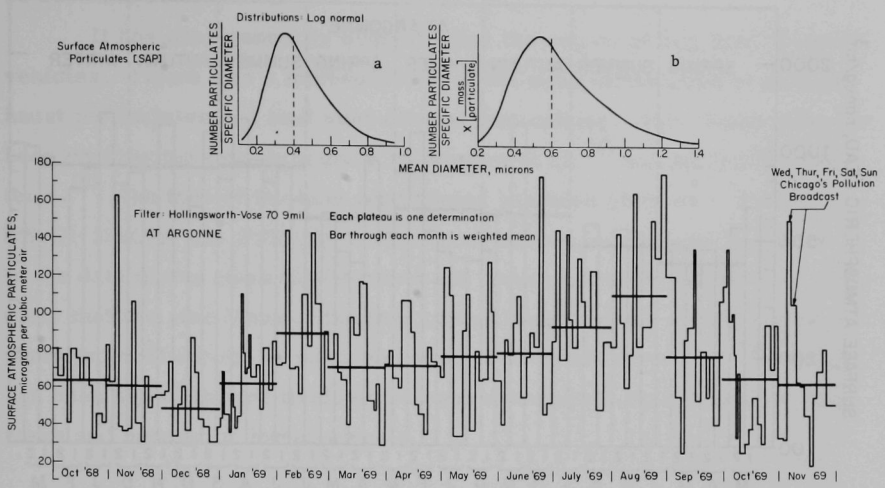

FIG. 1.--Surface atmospheric particulate (SAP) distribution. a) SAP number distribution median 0.40 μ; standard geometric deviation 1.5 ± 0.1; b) SAP mass distribution median 0.60 μ; standard geometric deviation 1.5 ± 0.1.

which a composite was made and a value of lead in these particulates was obtained. This is shown by the individual bars of the histogram. The unit of micrograms/100 mg particulates gives the net particulate concentration over a two-week period for which a composite was made and a value of lead in these particulates was obtained. This is shown by the individual bars of the histogram. The weighted mean for the six determinations comprising the entire season is shown by the horizontal line. This weighted mean is the most significant measure of the net concentration for that time period. As the graphs in Figure 2 and Figure 3 show, there can be no doubt that continued increase has occurred throughout the twenty-four months of monitoring. Comparing any two seasons twelve months apart will show that in all comparisons the most recent season has the highest net concentration. It is also of interest to note that the measures, nanograms/m^3 and micrograms/100 mg particulates, support each other in that as one increases with time

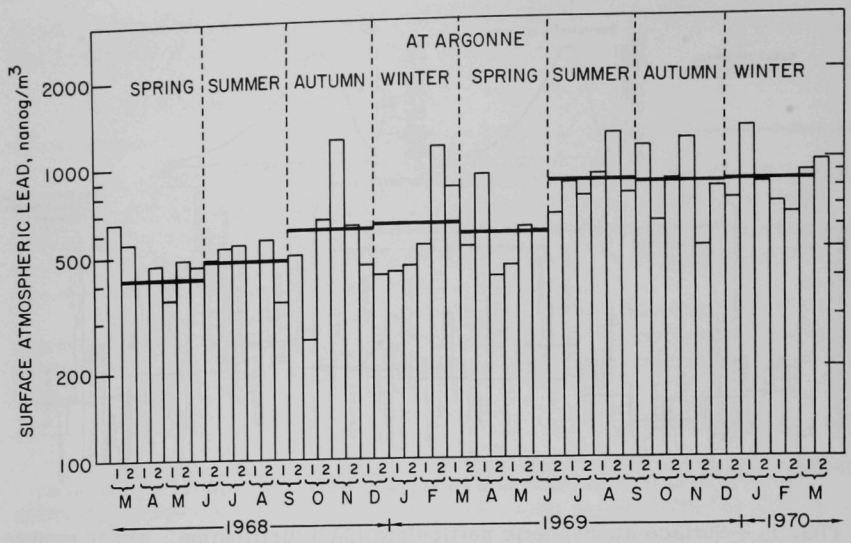

FIG. 2.--Surface atmospheric lead at Argonne, nanograms/m^3.

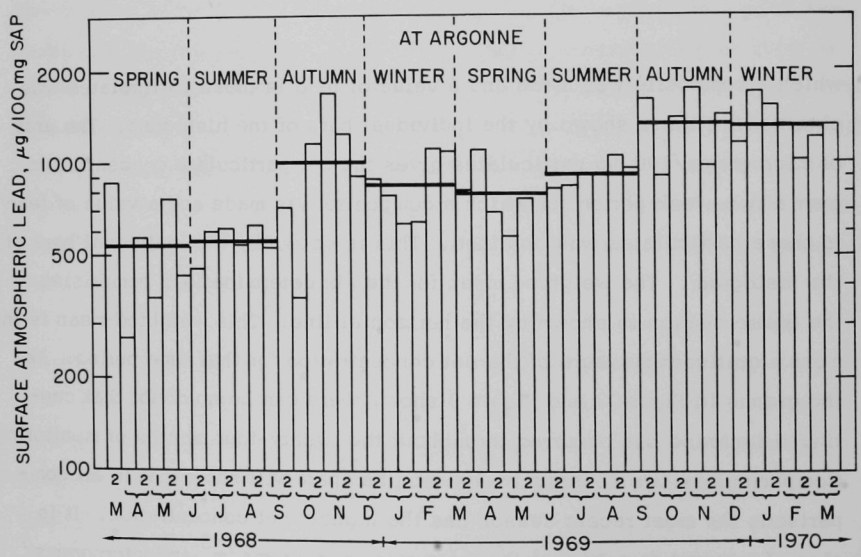

FIG. 3.--Surface atmospheric lead at Argonne, micrograms/100 mg particulates.

so does the other.

It has been generally accepted that the source of this lead is motor vehicles. Figure 4 is a representation of the mass distribution of auto exhaust particulates and lead auto exhaust particulates. This distribution has been constructed from data given by Mueller et al.[4] and Air Quality Criteria.[5] The form of the lead particulates has been given as : PbClBr, $NH_4Cl \cdot 2PbClBr$ and $2NH_4Cl \cdot PbClBr$. Both references essentially concur in the data giving mass distributions and mean particulate diameters. It is clear that the size range of the lead particulates released into the atmosphere is small enough to reach and deposit on human alveoli,[6-9] since it has been shown that particulates of mean diameters 1.0μ and smaller will reach and deposit on human alveoli.

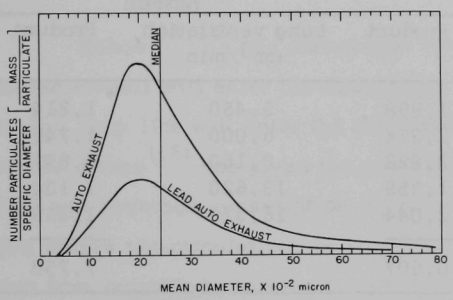

FIG. 4.--Mass distribution of lead particulates in auto exhaust compared to mass distribution of all particulates in auto exhaust. Mass median 0.24μ; standard geometric deviation 1.6 ± 0.1

Consider what a human at Argonne will be taking into his body as he breathes this surface air containing the indicated lead concentrations. (see Table 1.)

Multiplying the fraction of total day by lung ventilation and summing gives the weighted mean lung ventilation throughout a day in which all five forms of activities have occurred. (See Table 2.)

The weighted mean lung ventilations for male and female are, respectively, 10,600 cm^3/min or 0.64 m^3/hr and 7,750 cm^3/min or 0.46 m^3/hr.

TABLE 1. Lung Ventilation of Men and Women during Various Activities

Activity	Energy rate, cal/min (M)	Energy rate, cal/min (F)	Time, hr	Fraction of total day	Lung ventilation, cm^3/min (M)	Lung ventilation, cm^3/min (F)
Sleeping and lying	1.0	1.0	8	0.333	6,000	5,450
Sitting	1.5	1.1	7	0.291	8,160	6,000
Standing	2.5	1.5	5	0.208	13,620	8,160
Walking	3.0	2.5	2	0.0833	16,320	13,620
Spasmodic activities	4.5	3.0	2	0.0833	24,450	16,320

TABLE 2. Weighted Mean Lung Ventilation

Fraction of day	Men: Lung ventilation, cm^3/min	Men: Product	Women: Lung ventilation, cm^3/min	Women: Product
0.333	6,000	1,998	5,450	1,814
0.291	8,160	2,374	6,000	1,746
0.208	13,620	2,832	8,160	1,697
0.0833	16,320	1,359	13,620	1,134
0.0833	24,540	2,044	16,320	1,359
Weighted mean		10,607		7,750

Using the most recent weighted mean of the season, winter 1969-1970, one has 860 nanograms/m^3 of lead in Argonne surface atmosphere. The human male will have a lung ventilation of 0.64 m^3/hr. As only 70% of the lung ventilation will be alveolar ventilation,[11] one will have 0.45 m^3/hr ventilating the alveoli of the human male, and 0.32 m^3/hr ventilating the alveoli of the human female. Taking the product of the lead concentration and the human alveolar ventilation, one has the amount of lead in the ventilating alveolar space per hour. With the size distribution and the concentration of the surface atmospheric particulates, one can use

25% as the fraction of the total mass in the air ventilating alveoli that will deposit on the alveoli.[6-9,12]

TABLE 3. Calculation of Lead Deposition in Human Alveoli

(M)		(F)	
860 ng/m^3 x 0.45 m^3/hr	= 387 ng/hr	860 ng/m^3 x 0.32 m^3/hr	= 275 ng/hr
387 ng/hr x 0.25	= 96.7 ng/hr	275 ng/hr x 0.25	= 68.7 ng/hr

Multiplying ng/hr by 24 gives ng/day deposited on alveoli, or

(M) 2,320 ng/day deposited on alveoli, net mean for winter 1969-1970

(F) 1,649 ng/day deposited on alveoli, net mean for winter 1969-1970.

Kehoe[13,14] has shown that virtually all the lead deposited in human alveoli will enter the circulation, whereas if the lead is taken orally, only 10% will enter the circulation, the remainder going out in the stool. Kehoe[15] has given the content of lead in normal American adult food and beverage consumption per day as 190 ± 60 μg/day. Of the 190 μg/day, 10% enters the circulation, or 19 μg/day. Add what is entering the circulation from breathing, namely 2.3 μg/day, and the total is 21.3 μg/day.

Conclusions

It is clear that breathing Argonne air contributes 10% of total lead taken into the circulation; but percent of total is not a measure of a contribution to creating a toxic state in the human. The most significant measure would be the total mass withdrawn into critical tissues as it makes its initial passes through the capillaries of the critical tissues. This information has not been obtained.

It is equally clear that an increase in concentration with time for surface atmospheric lead at Argonne has taken place. This increase in concentration of a potentially toxic pollutant is sufficient to cause legislators

concern.

References

1. Smith, W. J. and N. Surprenant. Properties of Various Filtering Media for Atmospheric Dust Sampling. Am. Soc. Testing Mater. 53, 1122 (1953).
2. Fitzgerald, J. J. and C. G. Detwiler. Collection Efficiency of Air Cleaning and Air Sampling Filter Media. Am. Ind. Hyg. Quart. 16, 123 (1955).
3. Am. Soc. Testing Mater. Standards on Methods of Atmospheric Sampling and Analysis. Committee D-2, 2nd Ed., October 1962, p. 122.
4. Mueller, P. K., H. L. Helwig, A. E. Alcocer, W. K. Gong, E. E. Jones. Concentration of Fine Particles and Lead in Car Exhaust. Symposium on Air Pollution Measurement Methods. Am. Soc. Testing Mater. Spec. Tech. Publ. No. 352, October 1962, p. 60.
5. Air Quality Criteria for Particulate Matter. Nat. Air Poll. Control Admin. Publ. No. AF-49, U.S. Publ. Health Service, January 1969, pp. 1-53.
6. Brown, J. H., K. M. Cook, F. G. Ney, and T. Hatch. Influence of Particle Size upon the Retention of Particulate Matter in the Human Lung. Am. J. Publ. Health 40, 450 (1950).
7. Davis, C. N. A Comparison between Inhaled Dust and the Dust Recovered from a Human Lung. Health Phys. 10, 1029 (1964).
8. Hatch, T. F. and P. Gross. Pulmonary Deposition and Retention of Inhaled Aerosols. Academic Press, New York, 1964, p. 67.
9. Dauterbande, J. and W. Walkenhorst. Deposition of Microaerosols in Human Lungs with Special Reference to the Alveolar Spaces. Health Phys. 10, 981 (1964).
10. Nat. Acad. Sci. Recommended Dietary Allowances. Food and Nutrition Board, 7th Ed., 1968, p. 2.
11. Comroe, J. H. Physiology of Respiration. Year Book Medical Publ., Chicago, 1965, p. 218.
12. Task Group on Lung Dynamics. Deposition and Retention Models for Internal Dosimetry of the Human Respiratory Tract. Health Phys. 12, 178 (1966).
13. Kehoe, R. A. Experimental Studies on the Inhalation of Lead by Human Subjects. Pure Appl. Chem. 3, 129 (1961).
14. Kehoe, R. A. The Metabolism of Lead. Man in Health and Disease: The Haben Lectures. J. Roy.Inst. Publ. Health Hyg. 1961, 51-77 (1961).
15. Kehoe, R. A. Toxicological Appraisal of Lead in Relation to the Tolerable Concentration in the Ambient Air. J. Air Poll. Control Assoc. 19, 694 (September 1969).

WIND TUNNEL FACILITY

Erich J. Plate*

Argonne National Laboratory has constructed a small boundary layer type wind tunnel for initiating research on modeling of wind fields and of diffusion problems. The wind tunnel is of the open circuit type; the air is drawn into the wind tunnel's test section by an axial vane fan located at the outlet end. The test section is 10 ft long and has a cross-sectional area about 24" high and 30" wide. The ceiling is adjusted to control the pressure gradient in the test section. Experiments are to be performed on the surface of a polished aluminum plate which is elevated by 4" from the tunnel floor. The wind velocity is continuously variable from about 0.5 m/sec to 20 m/sec. At the inlet of the test section, a grid is provided for generating high turbulence levels in the test section. The interactions of these turbulence levels with the developing boundary layer are thought to lead to thick regions with logarithmic velocity distribution in the boundary layer along the aluminum plate.

The wind tunnel is equipped with instruments for measurements of time varying pressures and air velocities. Velocities are measured with hot wire anemometers and recorded on magnetic tape. They will be analyzed on the Argonne IBM 360 Computer after first having been converted into digital form on the Argonne A/D Conversion System. Although the present data handling capabilities are limited to signals of frequencies of less than 500 Hz, it is believed that they suffice for studying the large eddies of the turbulence in the wind tunnel. These are responsible for most of the transfer processes, and they are, therefore, of particular importance: they are the eddies that must be scaled properly if atmospheric exchange processes are to be modeled in a wind tunnel.

*Visiting Scientist, April 1969 to June 1970. Now Professor at Karlsruhe University, Germany.

Construction of the tunnel was paralleled by the preparation of a report on the aerodynamics of the atmospheric boundary layer which will be published in the AEC Critical Review Series.[1] Apart from a description of the physical processes of exchange and energy transfer near the ground, the report contains suggestions for wind tunnel studies which might aid in furthering the understanding of the lower atmosphere.

Reference

1. Plate, E. J. The Aerodynamic Modeling of the Atmospheric Boundary Layer, U. S. Atomic Energy Commission, to be published.

THE ANATOMY OF AN AIR POLLUTION EPISODE

Harry Moses, D. F. Gatz, J. E. Carson, F. G. Kulhanek and G. A. Zerbe

---

During the period November 4 through 12, 1969, an air pollution episode occurred over the Chicago area. Time series plots of the meteorological conditions associated with this episode are presented. A stagnating flat-gradient high pressure system was present with the usual inversion lid and light winds; dispersion conditions were, therefore, poor.

Maps giving isopleths of SO_2 concentrations are presented for selected times. These maps also include wind speed and direction data. Of interest are geometric configurations, as well as the movements of the high SO_2 concentration areas, shown by these charts.

A comparison is made of SO_2 values with those of the November of 1966, 1967, and 1968. In those years, at least on seven occasions city-wide 24-hour SO_2 averages exceeded those measured in this episode.

The SO_2 values obtained during the episode and also during other possible periods are compared with those of the Illinois State Standards (which values have been exceeded frequently).

Introduction

During the first and second weeks of November 1969, dispersive properties of the atmosphere over Chicago were poor. As a result, high concentrations of pollutants accumulated in the lower layers. The news media became particularly responsive to the situation--more so than on other occasions. Attention was called to the responsibility of industry and public officials for alleviating the incident. This paper examines the air quality conditions and weather associated with this episode.

Patterns of SO_2 Concentration

A picture of the distribution of SO_2 concentrations over Chicago during November 4 through 12, 1969, including the most severe part of the incident, is given by Figures 1-3. The city of Chicago has in operation a Telemetered Automatic Monitoring (TAM) network which allows a city-wide assessment of air pollution conditions. These data were plotted automatically on machine-drawn maps as shown in these figures. Figure 4 shows the

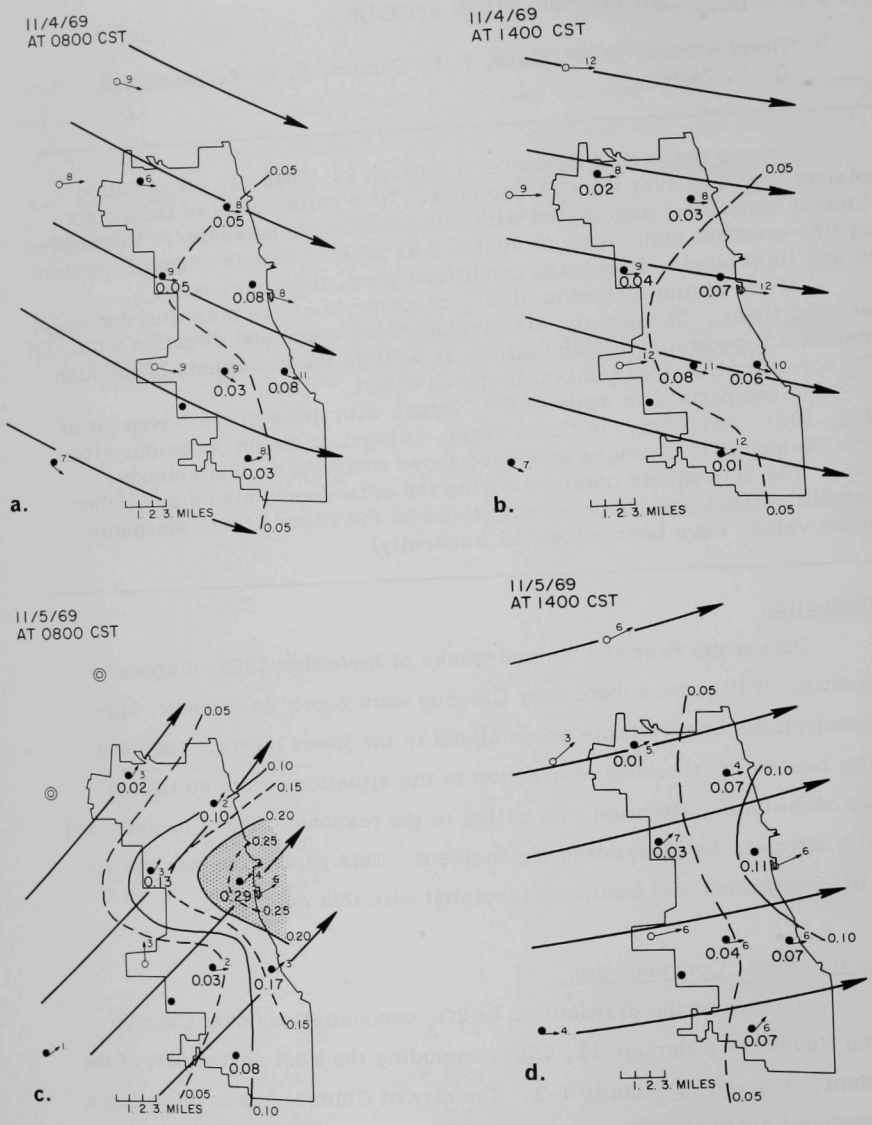

FIG. 1.--SO_2 Concentration isopleths and wind data for November 4 and 5, 1969, Telemetered Automatic Monitoring Stations, Chicago.

location of the TAM stations. Figure 1 shows the distribution of the SO_2 concentrations at 0800 and 1400 for November 4 and 5. On November 4 the winds were fairly brisk, up to 12 miles an hour in the afternoon, and the concentrations were fairly low. A buildup occurred on November 5; this was associated with lighter winds blowing from the southwest. There we see a pocket of high concentration, 0.29 ppm, at TAM Station 3. The greater mixing in the afternoon at 1400 shows a reduction in levels of SO_2.

Figure 2 shows the buildup of SO_2 concentrations on November 6. The stippled area shows the portions of the city which recorded SO_2 levels of 0.20 ppm or greater. The peak values of SO_2 concentration occurred at 1200 on November 6, when TAM Station 7 showed a value of 0.75 ppm. During this time the winds were light and a lake breeze was beginning to come in, as seen by the flow at Station 1. By 1400 an easterly wind had set in, and the concentrations were substantially reduced. Nevertheless, the western part of the city showed concentrations greater than 0.20 ppm as indicated by the stippling. Levels of pollution continued to decrease through 2200 on the 6th. We see that, although there is a pocket of high values in the west, all stations were recording values below 0.20 ppm. Figure 3 (a and b) shows the values of SO_2 at 0800 and 1400 on November 10th. A pocket of high pollution occurred at 0800 on the 10th with southwesterly winds, but by 1400 the winds had increased and the levels of SO_2 concentration had decreased. The incident was considered over on 1400 November 12. Figure 3 (c and f) shows the isopleth patterns for SO_2 concentrations at 0800 and 1400 on November 11 and 12.

These charts show the patchiness of the SO_2 distribution over the city. Even though Chicago was recognized as having an air pollution incident, some parts of the city were relatively clean; the high concentrations were confined to limited areas. It is important to realize that in a city like Chicago with diverse terrain and a heterogeneous distribution of sources, uniform conditions do not prevail. A change in the wind direction can result in a marked change of the air quality in only one part of the city.

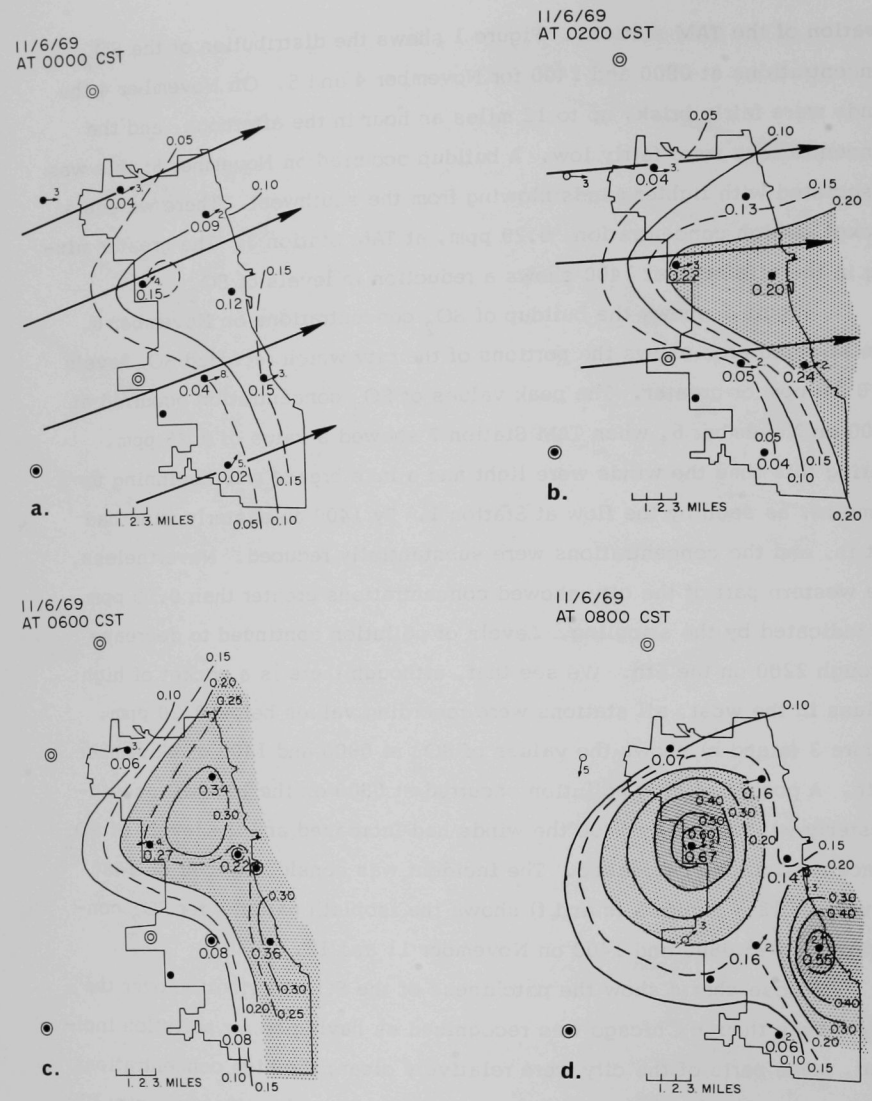

FIG. 2.--SO_2 Concentration isopleths and wind data for November 6, 1969, Telemetered Automatic Monitoring Stations, Chicago.

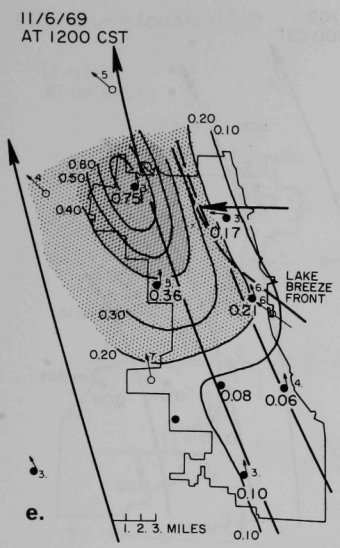
11/6/69
AT 1200 CST
0.20
0.10
0.80
0.50
0.75
0.40
0.17
0.36
0.21
LAKE
BREEZE
FRONT
0.30
0.20
0.08
0.06
0.10
0.10
1. 2. 3. MILES
e.

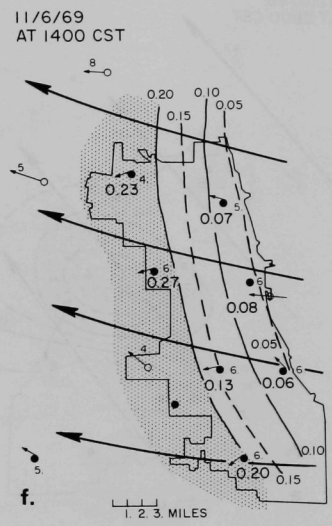
11/6/69
AT 1400 CST
0.20
0.10
0.05
0.15
0.23
0.07
0.27
0.08
0.05
0.13
0.06
0.10
0.20
0.15
1. 2. 3. MILES
f.

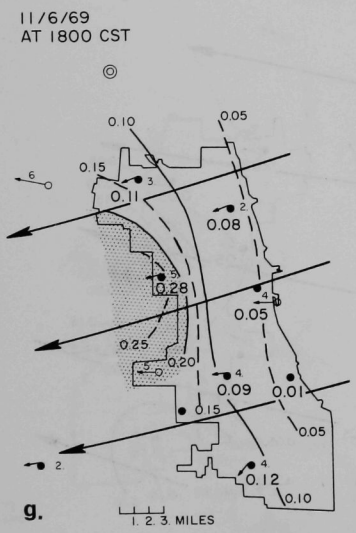
11/6/69
AT 1800 CST
0.10
0.05
0.15
0.11
0.08
0.28
0.05
0.25
0.20
0.09
0.01
0.15
0.05
0.12
0.10
1. 2. 3. MILES
g.

11/6/69
AT 2200 CST
0.05
0.10
0.12
0.05
0.17
0.03
0.15
0.09
0.01
0.05
0.10
0.05
1. 2. 3. MILES
h.

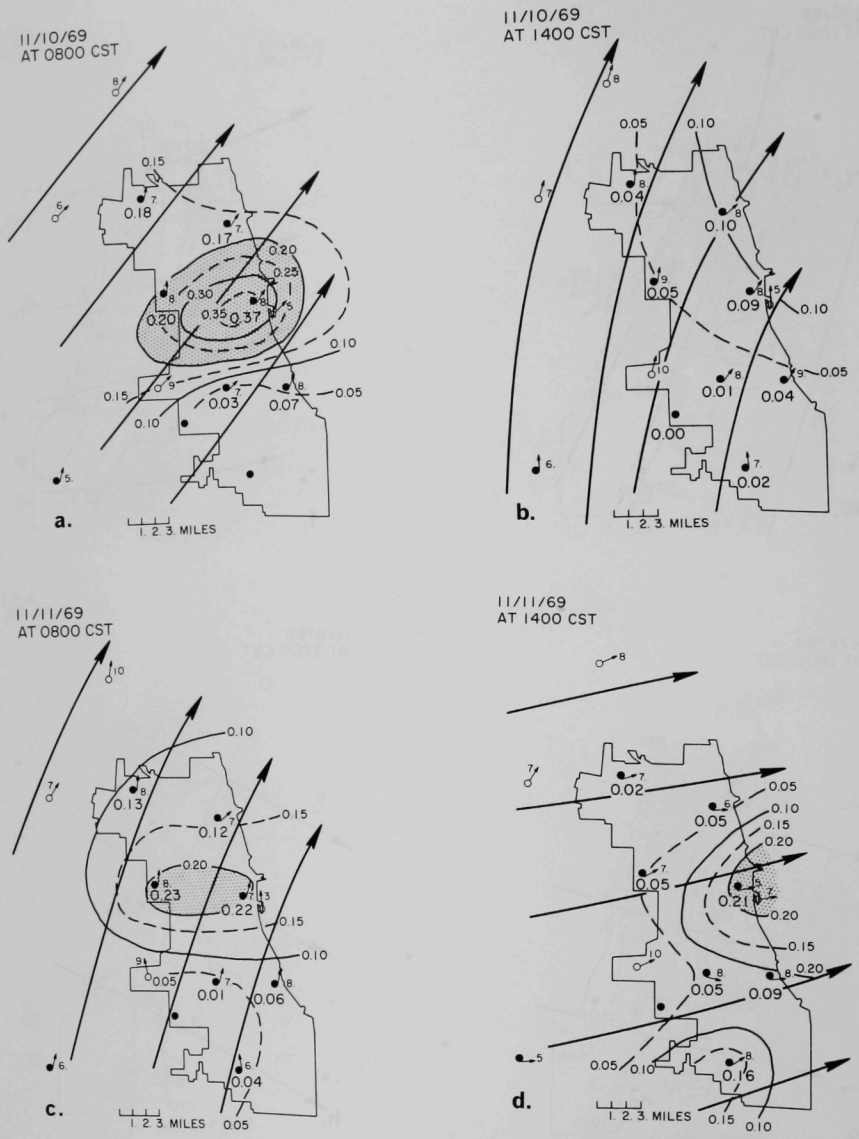

FIG. 3.--SO_2 Concentration isopleths and wind data for November 10, 11, and 12, 1969, Telemetered Automatic Monitoring Stations, Chicago.

FIG. 3.-- (continued)

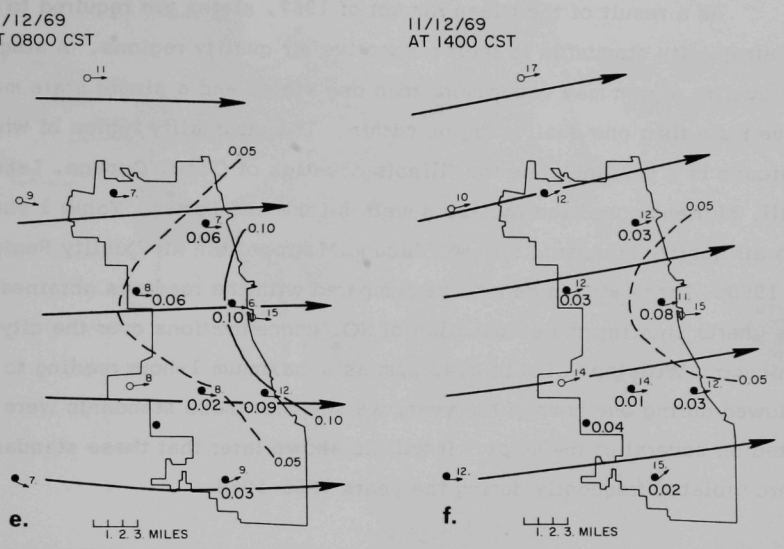

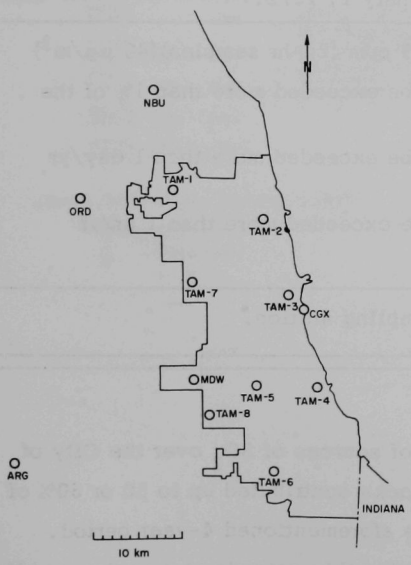

FIG. 4.--Map showing locations of Telemetered Automatic Monitoring Stations, Chicago.

Air Quality Standards

As a result of the Clean Air Act of 1967, states are required to set up air quality standards in their respective air quality regions. A single air quality region may cover more than one state, and a single state may have more than one quality region within. The air quality region of which Chicago is a part includes the Illinois counties of Cook, Dupage, Lake, Will, McHenry, and the Indiana counties Lake and Porter. Table 1 shows the air quality standards for the Chicago Metropolitan Air Quality Region in 1969. These standards may be compared with the readings obtained on the charts showing the distribution of SO_2 concentrations over the city of Chicago. With the value of 0.42 ppm as a maximum 1-hour reading to be allowed during one hour of the year, we see that these standards were violated on several of the maps. It will be shown later that these standards were violated frequently during the years 1966-1969.

TABLE 1. State of Illinois Air Pollution Standards for SO_2, 1969. Standard to be reached by January 1, 1972.[a]

Maximum annual geometric mean: 0.015 ppm (24-hr samples)(40 $\mu g/m^3$)
24-hr concentration of 0.10 ppm not to be exceeded more than 1% of the days per year (265 $\mu g/m^3$)
24-hr concentration of 0.17 ppm not to be exceeded more than 1 day/yr (450 $\mu g/m^3$)
1-hr concentration of 0.42 ppm not to be exceeded more than 1 hr/yr (1110 $\mu g/m^3$)

[a] Standards are applicable at each sampling station.

Sources of Air Pollution

Figure 5 shows the distribution of sources of SO_2 over the City of Chicago. The Commonwealth Edison stacks contributed up to 50 or 60% of the SO_2 emitted over Chicago during the aforementioned 4-year period. This utility company switched to gas during this episode at a cost exceeding

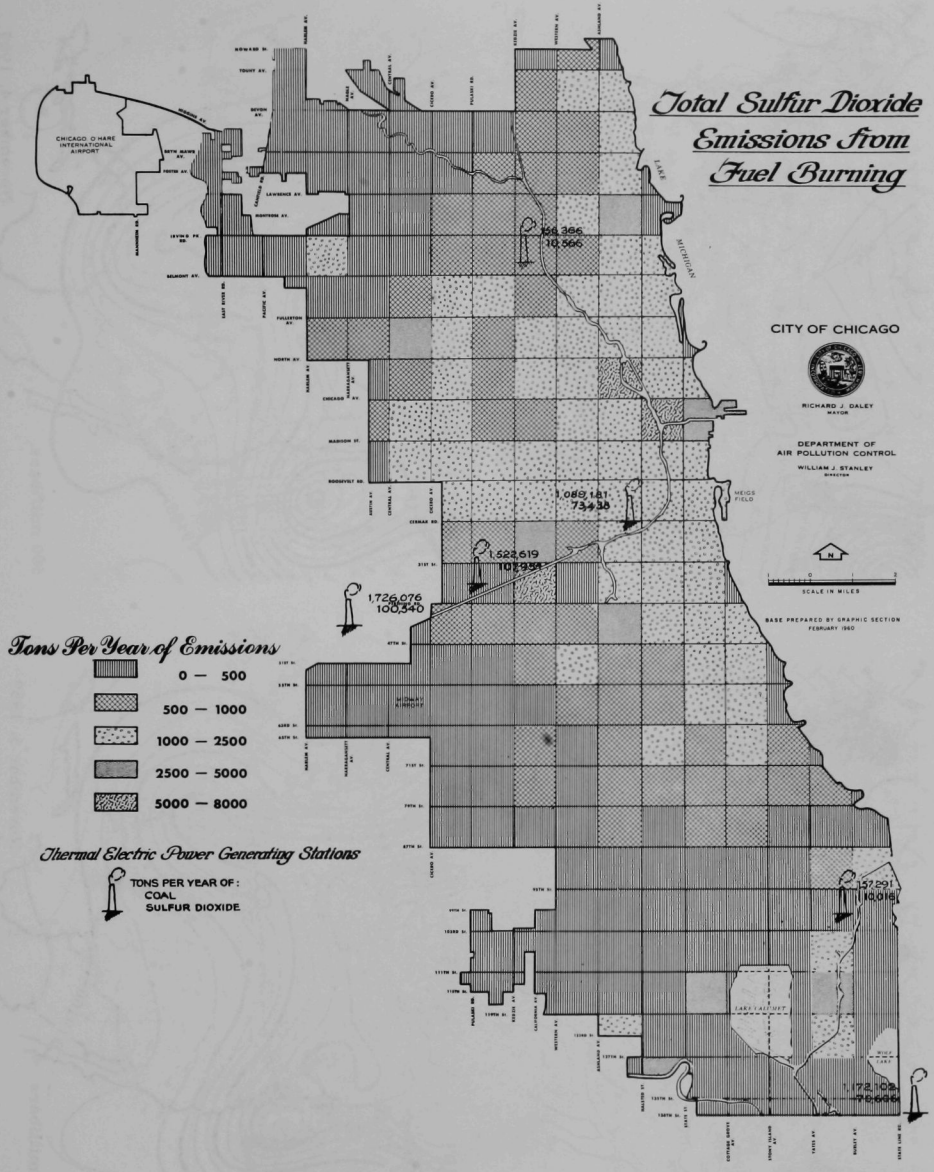

FIG. 5.--Map showing distribution of sources of SO_2 in Chicago, based on 1967 data.

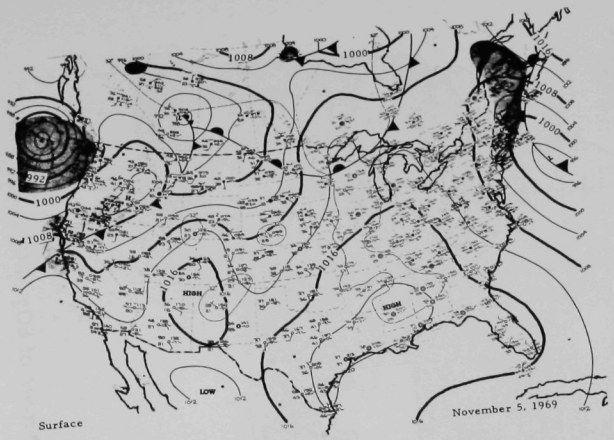
Surface
November 5, 1969
HIGH
LOW
1000
1008
1016

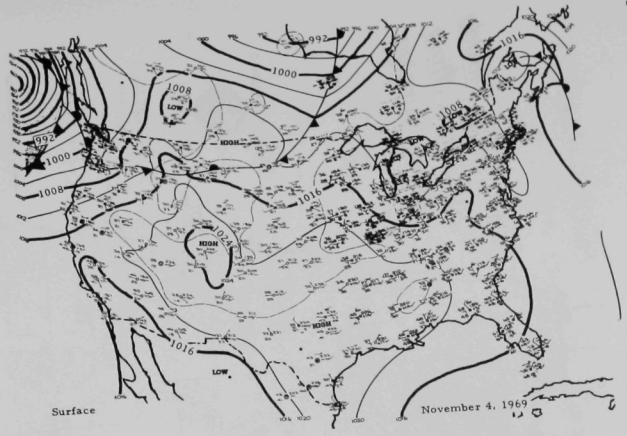
Surface
November 4, 1969
HIGH
LOW
992
1000
1008
1016

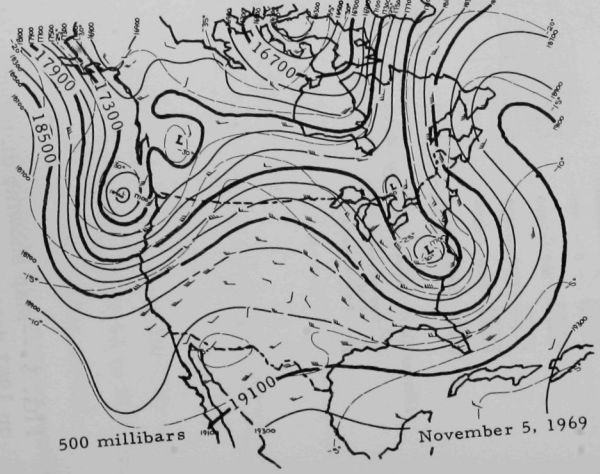
500 millibars
November 5, 1969
16700
17300
17900
18500
19100

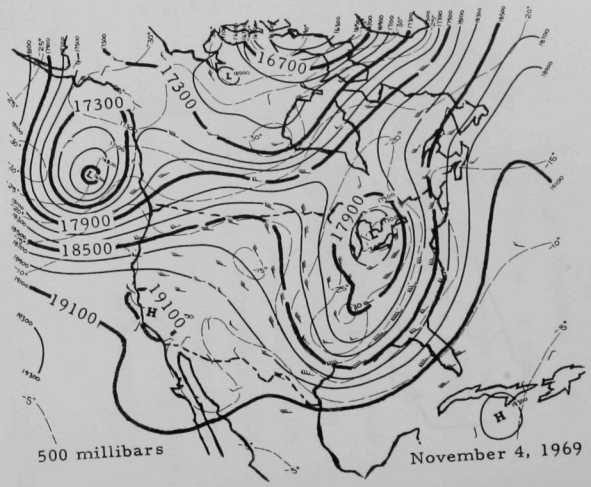
500 millibars
November 4, 1969
16700
17300
17900
18500
19100

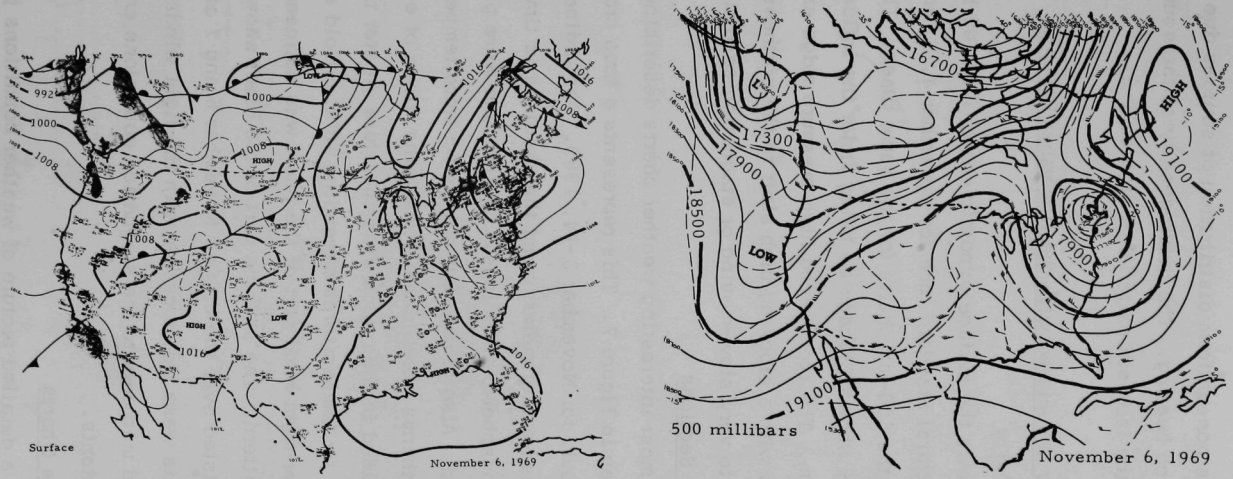

FIG. 6.--Surface and 500-millibar weather charts for November 4, 5, and 6, 1969. (Published by U.S. Dept. of Commerce, ESSA.)

$150,000. Note the non-uniform distribution of sources due to commercial and residential space heating. The heterogeneity of the sources contributes to the structure of the isopleth patterns of Figures 1-3.

Weather Conditions Associated with the November Episode

Synoptic Charts

Figure 6 shows the surface synoptic charts for 0700 Eastern Standard time or 0600 Central Standard time for November 4, 5, and 6, 1969. Also presented are the 500-mb charts for the same times. The synoptic chart of November 6 shows Chicago as being under the influence of a very flat pressure system. The pronounced high pressure ridge extended over the city of Chicago with a blocking high aloft to the northeast. This situation contributed to very slow-moving or stagnating conditions.

Time Cross Sections

One of the most interesting weather charts describing the November episode may be seen in Figure 7. This represents a time cross section of temperature and wind, for November 3-14, 1969. The ordinate is the height above ground in hundreds of meters, and the abscissa is time. The vertical lines represent atmospheric soundings. On this line were plotted the wind direction and speed. Also plotted but not shown were temperatures at each of the levels. Isotherms were drawn to show the lines of equal temperature. Stippling was included in the region of temperature greater than 8°C. Finer stippling was used for temperatures exceeding 10°C. Cold air shown on the upper left and upper right hand part of the chart was delineated with stippling of another pattern. The striking part of the chart shows the layer of warm air which existed over the city on November 6 and 7 and also on the 10th and 11th. This warm lid, together with the light winds during this period, contributed markedly to the stagnation conditions and high concentration of pollutants.

Time Series Charts

To present a detailed picture of weather conditions prevailing during the incident, time series plots of the meteorological variables and the

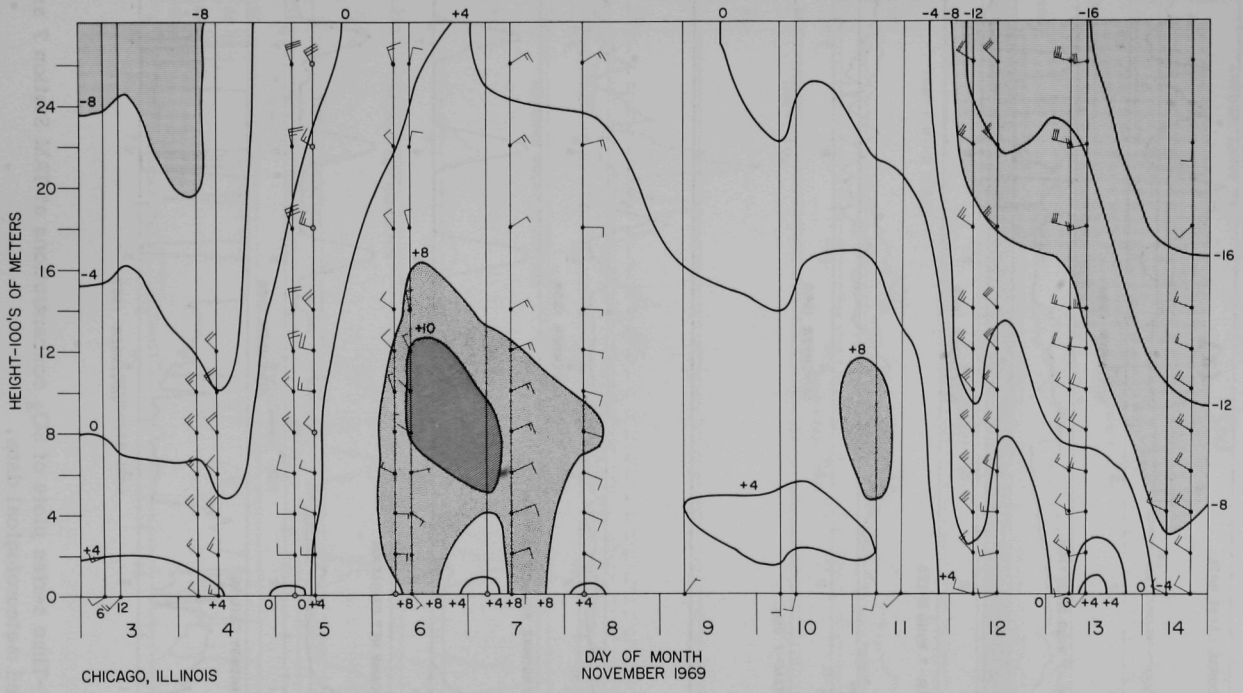

FIG. 7.--Time cross section of temperature (°C) and wind direction and speed (knots), Chicago. (Data based on U.S. Dept. of Commerce, ESSA, radiosonde data.)

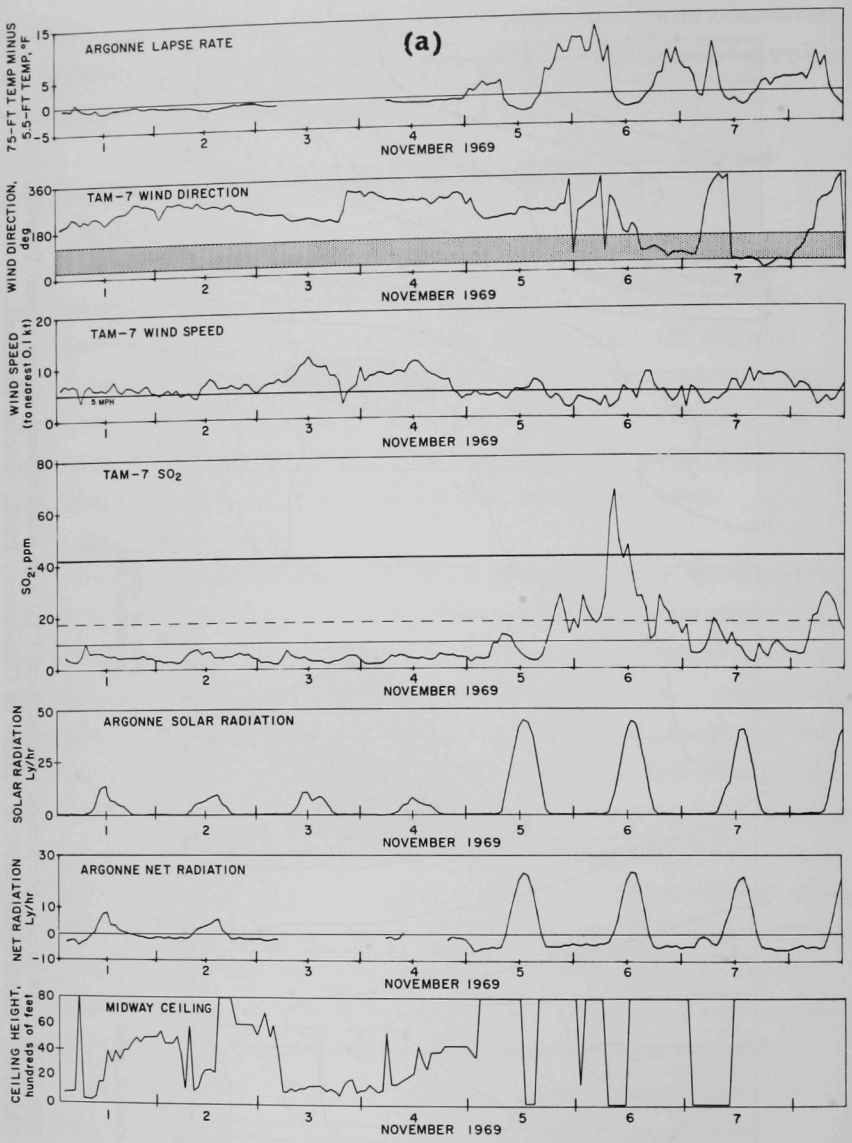

FIG. 8.--Time series plots of SO_2 concentrations at TAM Station 7 and associated meteorological data.

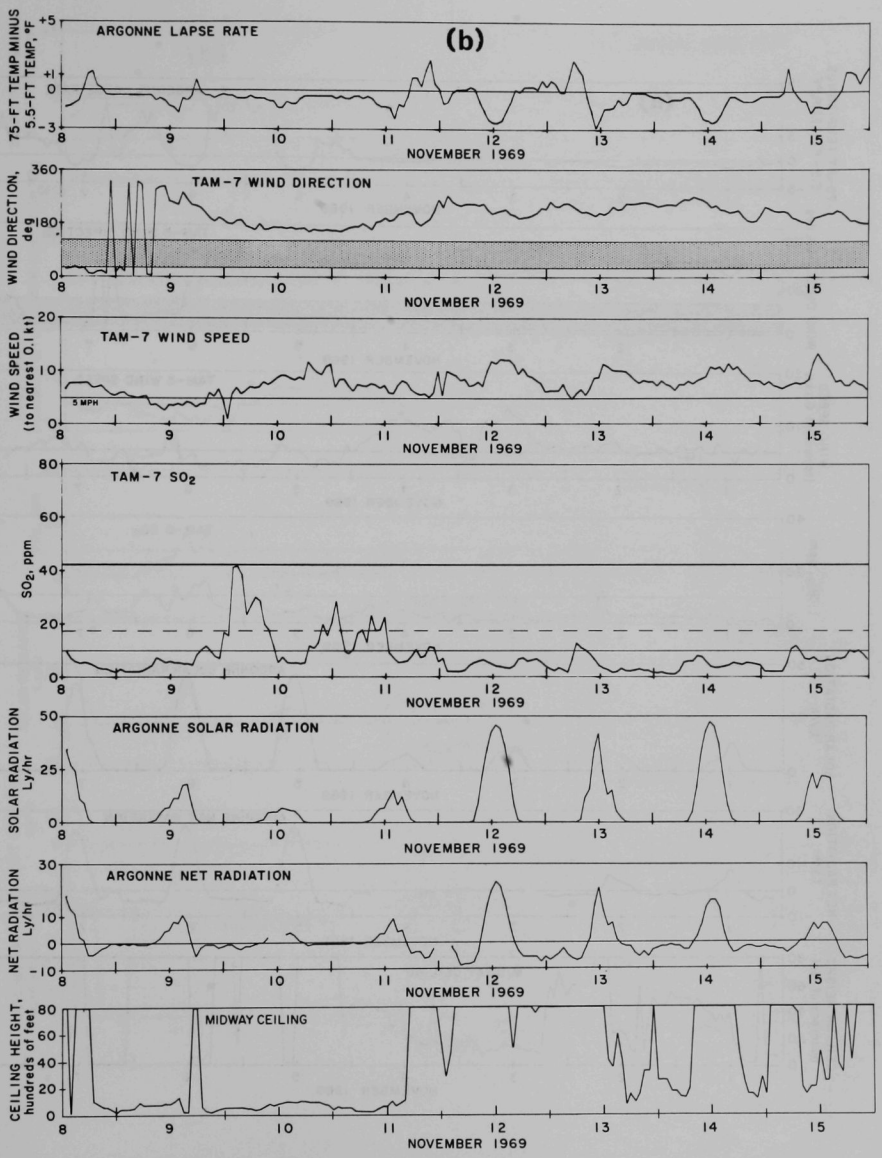
(b)
ARGONNE LAPSE RATE
75-FT TEMP MINUS 5.5-FT TEMP, °F
+5
±
0
-3
8
9
10
11
12
13
14
15
NOVEMBER 1969
TAM-7 WIND DIRECTION
WIND DIRECTION, deg
360
180
0
TAM-7 WIND SPEED
WIND SPEED (to nearest 0.1 kt)
20
10
5 MPH
0
TAM-7 SO2
SO2, ppm
80
60
40
20
0
ARGONNE SOLAR RADIATION
SOLAR RADIATION Ly/hr
50
25
0
ARGONNE NET RADIATION
NET RADIATION Ly/hr
30
10
0
-10
MIDWAY CEILING
CEILING HEIGHT, hundreds of feet
80
60
40
20
0

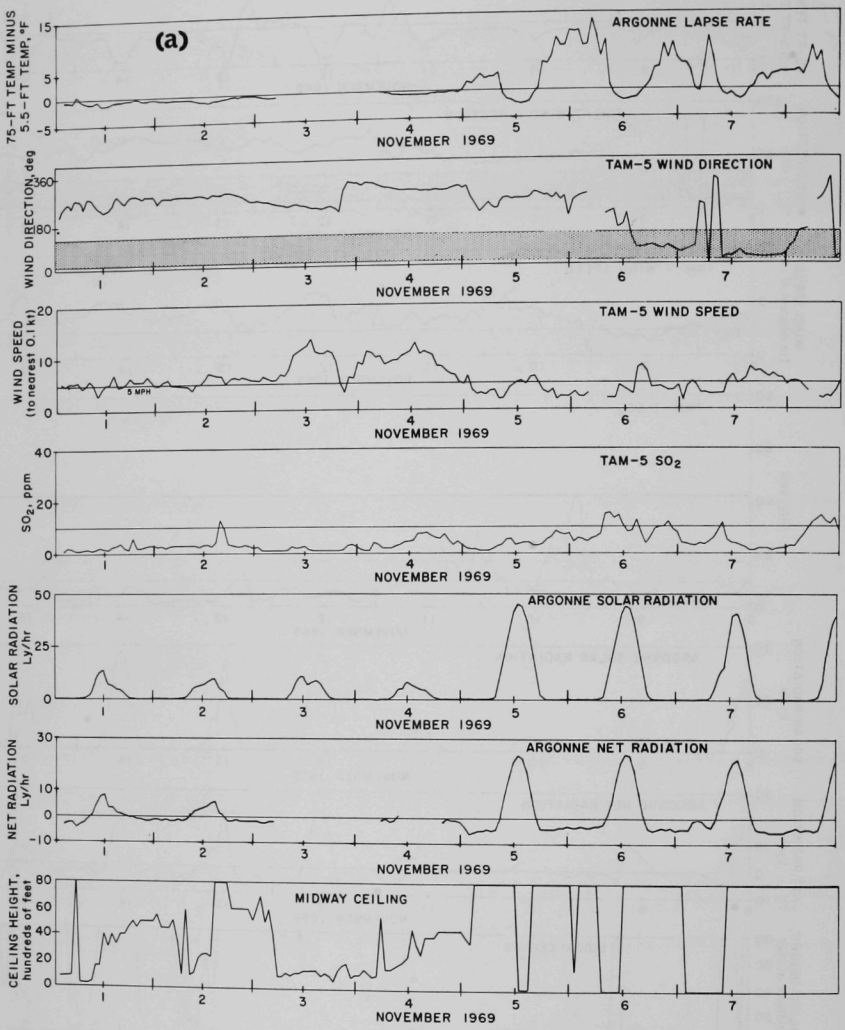

FIG. 9.--Time series plots of SO_2 concentrations at TAM Station 5 and associated meteorological data.

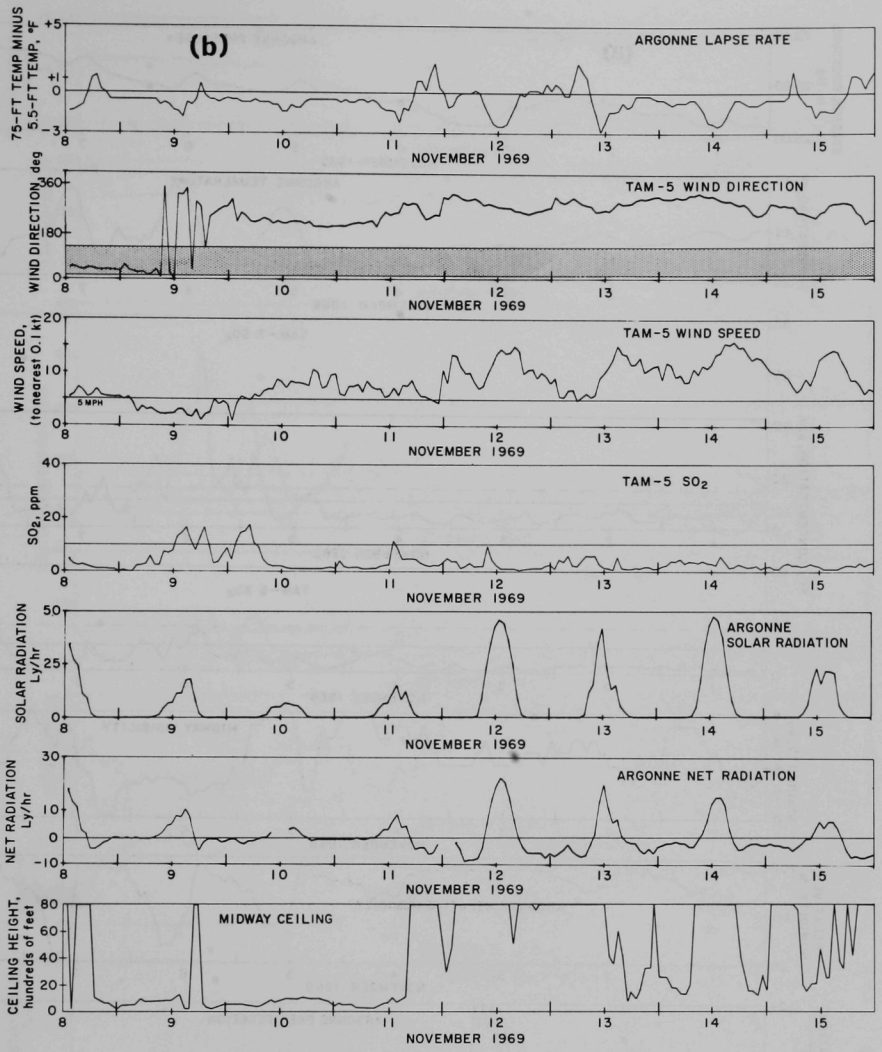
(b)
ARGONNE LAPSE RATE
75-FT TEMP MINUS 5.5-FT TEMP, °F
+5
+1
0
-3
NOVEMBER 1969
TAM-5 WIND DIRECTION
WIND DIRECTION, deg
360
180
0
NOVEMBER 1969
TAM-5 WIND SPEED
WIND SPEED, (to nearest 0.1 kt)
20
10
0
5 MPH
NOVEMBER 1969
TAM-5 SO2
SO2, ppm
40
20
0
NOVEMBER 1969
ARGONNE SOLAR RADIATION
SOLAR RADIATION Ly/hr
50
25
0
NOVEMBER 1969
ARGONNE NET RADIATION
NET RADIATION Ly/hr
30
10
0
-10
NOVEMBER 1969
MIDWAY CEILING
CEILING HEIGHT, hundreds of feet
80
60
40
20
0
8
9
10
11
12
13
14
15
NOVEMBER 1969

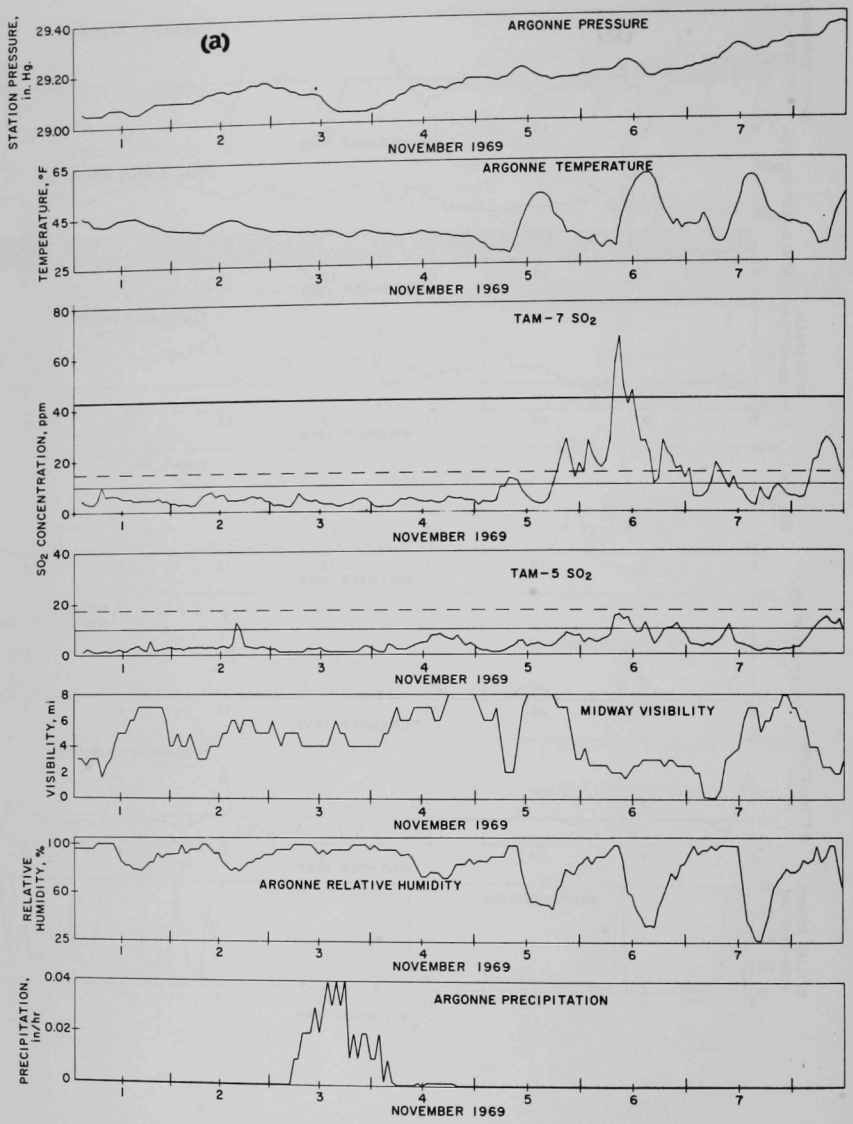

FIG. 10.--Time series plots of SO_2 concentrations at TAM Stations 5 and 7 and associated meteorological data.

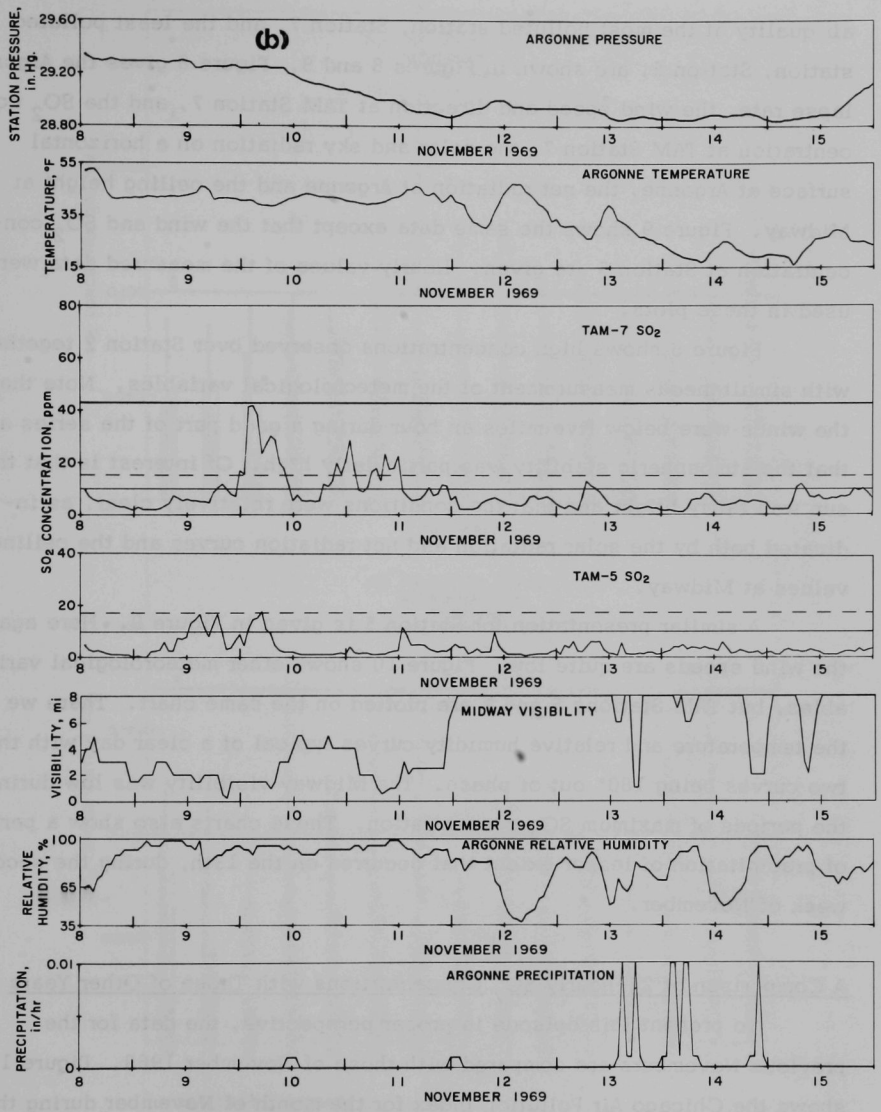
(b)
ARGONNE PRESSURE
STATION PRESSURE, in. Hg.
29.60
29.20
28.80
8 9 10 11 12 13 14 15
NOVEMBER 1969
ARGONNE TEMPERATURE
TEMPERATURE, °F
55
35
15
8 9 10 11 12 13 14 15
NOVEMBER 1969
TAM-7 SO2
SO2 CONCENTRATION, ppm
80
60
40
20
0
8 9 10 11 12 13 14 15
NOVEMBER 1969
TAM-5 SO2
40
20
0
8 9 10 11 12 13 14 15
NOVEMBER 1969
MIDWAY VISIBILITY
VISIBILITY, mi
8
6
4
2
0
8 9 10 11 12 13 14 15
NOVEMBER 1969
ARGONNE RELATIVE HUMIDITY
RELATIVE HUMIDITY, %
100
65
35
8 9 10 11 12 13 14 15
NOVEMBER 1969
ARGONNE PRECIPITATION
PRECIPITATION, in/hr
0.01
0
8 9 10 11 12 13 14 15
NOVEMBER 1969

air quality at the most polluted station, Station 7, and the least polluted station, Station 5, are shown in Figures 8 and 9. Figure 8 gives the Argonne lapse rate, the wind speed and direction at TAM Station 7, and the SO_2 concentration at TAM Station 7, the solar and sky radiation on a horizontal surface at Argonne, the net radiation at Argonne and the ceiling height at Midway. Figure 9 shows the same data except that the wind and SO_2 concentration at Station 5 are given. Hourly values of the measured data were used in these plots.

Figure 8 shows high concentrations observed over Station 7 together with simultaneous measurement of the meteorological variables. Note that the winds were below five miles an hour during a good part of the series and that the atmospheric stability was particularly high. Of interest is that the sun was fairly bright and that the conditions were relatively clear, as indicated both by the solar radiation and net radiation curves and the ceiling values at Midway.

A similar presentation for Station 5 is given in Figure 9. Here again the wind speeds are quite low. Figure 10 shows other meteorological variables, but TAM Stations 5 and 7 are plotted on the same chart. There we see the temperature and relative humidity curves typical of a clear day with the two curves being 180° out of phase. The Midway visibility was low during the periods of maximum SO_2 concentration. These charts also show a period of precipitation of lesser extent that occurred on the 13th, during the second week of November.

A Comparison of 24-hourly SO_2 Concentrations with Those of Other Years

To present this episode in proper perspective, the data for the previous Novembers are compared with those of November 1969. Figure 11 shows the Chicago Air Pollution Index for the month of November during the period 1966-1969. The Chicago Air Pollution Index (API) may be expressed as the 8-TAM Station average of the 24-hourly means. The 24-hourly mean is based on the 24 one-hourly average values taken from midnight to midnight. Albegraically it may be expressed as

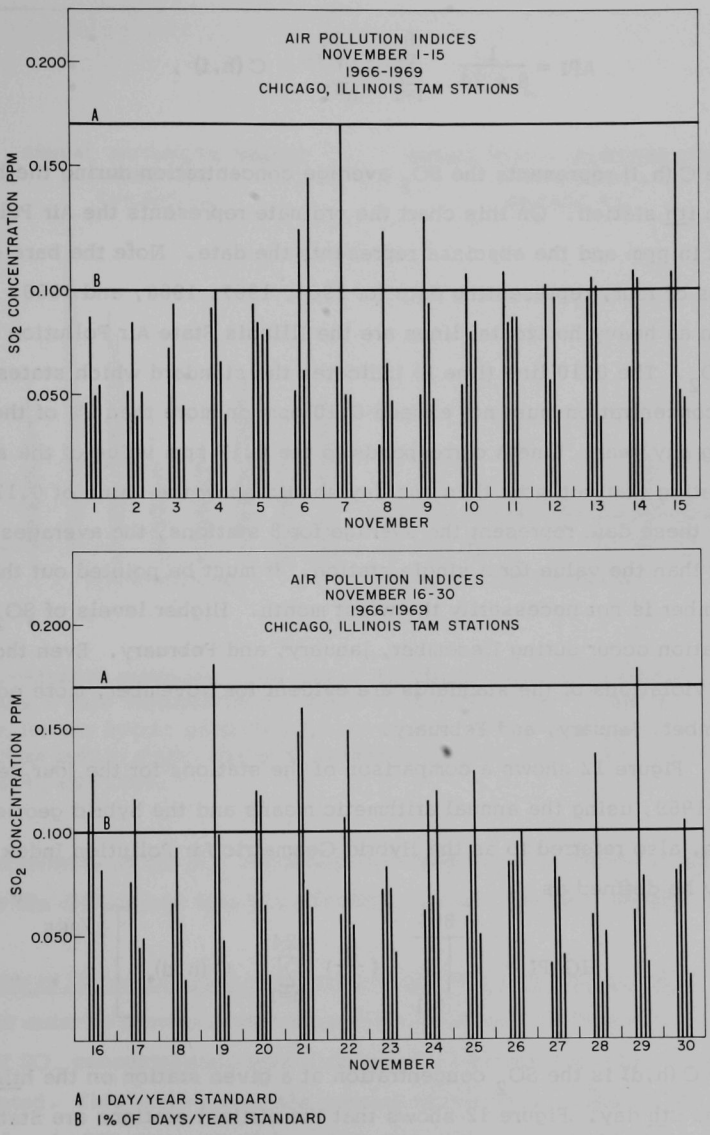

FIG. 11.--Air pollution indices, November 1966-1969, Chicago, based on TAM Station network data. In each group of four bars, reading from left to right, the bars represent the data for the years 1966, 1967, 1968, and 1969.

$$API = \frac{1}{8 \times 24} \sum_{i=1}^{8} \sum_{h=1}^{24} C(h,i) ,$$

where C (h,i) represents the SO_2 average concentration during the hth hour at the ith station. On this chart the ordinate represents the Air Pollution Index in ppm and the abscissa represents the date. Note the bars occur in groups of four, representing data for 1966, 1967, 1968, and 1969. Also shown as heavy horizontal lines are the Illinois State Air Pollution Standards for SO_2. The 0.10 line (line B) indicates the standard which states that SO_2 concentration must not exceed 0.10 ppm on more than 1% of the days during any year. Line A corresponds to the 0.17 ppm value of the standard, indicating that not more than one day should show the value of 0.17 ppm. Since these data represent the average for 8 stations, the averages may be lower than the value for a single station. It must be pointed out that November is not necessarily the worst month. Higher levels of SO_2 concentration occur during December, January, and February. Even though many violations of the standards are evident for November, more occur in December, January, and February.

Figure 12 shows a comparison of the stations for the four years, 1966-1969, using the annual arithmetic means and the hybrid geometric means, also referred to as the Hybrid Geometric Air Pollution Index (HGAPI). It may be defined as

$$HGAPI = \left[\prod_{d=1}^{365} \left(\frac{1}{24}\right) \sum_{h=1}^{24} C(h,d) \right]^{1/365} ,$$

where C (h,d) is the SO_2 concentration at a given station on the hth hour, and the dth day. Figure 12 shows that the dirtiest stations are Stations 3, 4, and 7, in that order. During the November 1969 incident, nevertheless, Station 7 had the highest concentrations. The horizontal line represents the 0.015 ppm annual standard. It is evident that this standard was violated each year by all stations but Station 1. These charts portray quite clearly

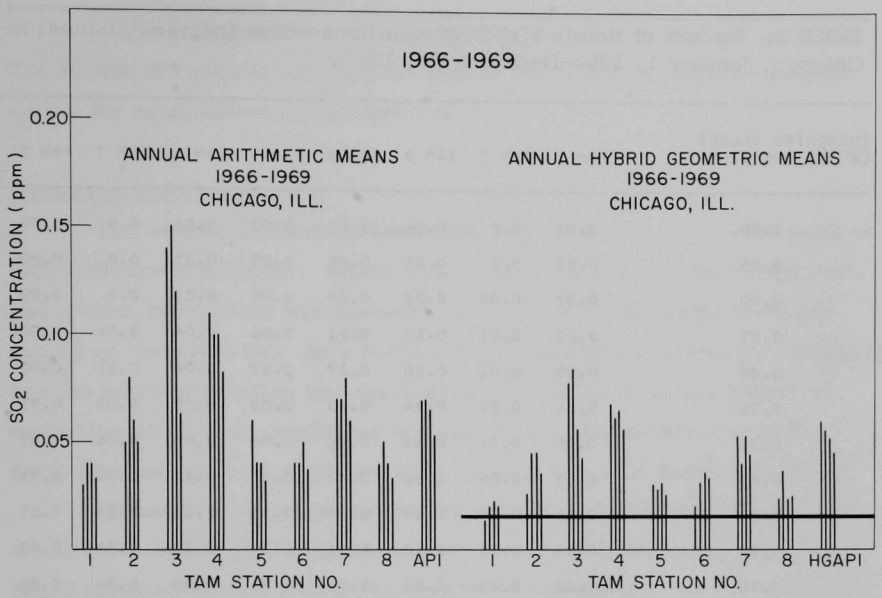

FIG. 12.--Annual averages: The annual arithmetic mean for Chicago for each of the 8 TAM Stations for the years 1966-1969 (left). A similar presentation for the hybrid geometric means (right). In each group of four bars, reading from left to right, the bars represent the data for the years 1966, 1967, 1968, and 1969.

the heterogeneity of the SO_2 concentrations over the city and point out the extent of the differences between the dirtiest parts and the cleanest.

Probability of Exceeding Hourly Values of Indicated SO_2 Concentrations

In order to provide a picture of the frequency of occurrence of hourly values of SO_2 concentrations which exceed the Illinois standards, Table 2 is presented. This table shows the percent of the total number of observations of hourly SO_2 concentrations above the values indicated in the first column. This table is based on 3 years of data beginning with January 1, 1966 through December 31, 1968. It has to be noted that a substantial part

TABLE 2. Percent of Hourly SO_2 Concentrations above Indicated Values, Chicago, January 1, 1966-December 31, 1968.

INDICATED VALUES OF SO2 CONC.(PPM)	TAM 1	TAM 2	TAM 3	TAM 4	TAM 5	TAM 6	TAM 7	TAM 8
1.00	0.02	0.0	0.04	0.03	0.02	0.01	0.0	0.00
0.95	0.02	0.0	0.06	0.05	0.03	0.01	0.0	0.00
0.90	0.02	0.00	0.08	0.09	0.05	0.02	0.0	0.00
0.85	0.02	0.01	0.13	0.11	0.06	0.04	0.01	0.00
0.80	0.03	0.01	0.20	0.17	0.07	0.04	0.01	0.00
0.75	0.04	0.01	0.34	0.23	0.08	0.05	0.02	0.01
0.70	0.05	0.01	0.55	0.36	0.09	0.08	0.06	0.01
0.65	0.07	0.04	0.82	0.48	0.10	0.11	0.09	0.01
0.60	0.11	0.07	1.37	0.66	0.11	0.14	0.18	0.01
0.55	0.14	0.11	2.12	1.01	0.14	0.22	0.31	0.03
0.50	0.22	0.25	3.53	1.52	0.21	0.30	0.56	0.04
0.45	0.30	0.39	5.34	2.29	0.27	0.41	0.92	0.08
0.40	0.48	0.63	7.69	3.41	0.44	0.50	1.41	0.11
0.35	0.71	0.93	10.33	4.76	0.67	0.63	2.02	0.19
0.30	1.01	1.73	14.25	7.05	1.05	0.98	3.14	0.39
0.25	1.59	3.24	20.56	11.24	1.88	1.56	5.53	0.92
0.20	2.53	5.63	27.39	17.20	3.08	2.80	9.00	1.94
0.15	4.76	10.57	35.96	26.05	5.94	5.42	14.74	4.12
0.10	8.04	19.01	45.17	35.52	11.22	10.24	23.73	8.46
0.05	17.47	40.43	59.94	53.00	27.32	24.39	44.41	23.95
NO.OF CASES	22290	23762	22663	24140	22723	23320	24424	23371
MAX HRLY VALUES=	1.28	0.90	1.97	1.04	1.24	1.19	0.90	1.14

of the time values greater than 0.45 ppm (the standard is 0.42 ppm) occur. The number of cases is given in the next to the last line and the maximum values for each station on the last line.

Comments and Conclusions

The weather conditions associated with this episode were typical of high pollution conditions. Winds were light to heights of about 2000 feet, and a warm layer of air was present over the city at about this level producing an inversion lid. As a result vertical mixing was markedly suppressed and the urban ventilation was small enough to allow an accumulation of contaminants. These conditions are usually associated with flat high pressure areas such as prevailed over the Chicago area during this time.

Although the episode may be considered as extending from November 4 to November 12, 1969, there were two periods of particularly high pollutant concentrations. The first occurred on November 6 and the second on November 11. On these days, the time cross section shows an enhancement of the upper warm air layers and light winds characteristic of episode conditions.

This study further points out the patchiness of the SO_2 concentration distribution over the city. Even when extremely high SO_2 levels were found, e.g., 0.75 ppm at Station 2 at 1200 on November 6, Station 4 showed only 0.06 ppm. The substantial difference in cleanliness is further brought out in Figure 12, which shows the annual arithmetic and hybrid geometric average for each of the TAM stations during the years 1966-1969 inclusive.

It is worthy of note that the first week or two in November is the time during which people burn their leaves. During light winds and stable conditions the smoke from leaf burning is dispersed slowly, thus substantially reducing the visibility. This happened on a number of days during this episode. Leaf burning was responsible in part for the general haziness and poor local visibility which prevailed during periods of this episode.

An important point brought out in this study--not recognized by the general public--is that there were many times in the 1966-1969 period during which conditions were as bad or worse. For the November conditions given in Figure 11, we see that the highest city-wide 24-hour average, which occurred on November 6, was exceeded seven times in the previous years 1966, 1967, and 1968. We know that pollution levels are appreciably higher in the winter months of December, January, and February than in November. Many more 24-hour city-wide SO_2 concentration values exceeding the worst day of this episode occurred during the period of record.

An examination of hourly values and 24-hourly values at individual stations during the episode points out that the levels indicated for the Illinois Air Pollution standards have been frequently exceeded. This is shown in Table 2 and many of the figures in this report. It must be remembered that the standards apply to an individual station. Figure 11 presents the data averaged over the entire city which includes the high as well as low concentration areas. Thus individual stations would show much higher concentrations and greater occurrence frequencies.

With the enactment and implementation of new regulations to reduce the amount of SO_2 emitted into the atmosphere, it is hoped that the concentration levels will be reduced to values below the indicated standards. The data show that a substantial reduction is necessary.

To assess properly the effect of high concentrations of harmful pollutants, one must make measurements where the people are. In the Chicago Loop area and the near north side there are many high-rise apartment buildings. An appreciable number of people live at levels 100 ft or more above ground. Further, the ventilation air intakes of such buildings are located at 100 ft or more above ground level.

Since many of the major SO_2 sources are elevated sources, i.e., the emitting stacks are several hundred feet high, it is certain that the concentration of pollutants increases with height. Therefore, measurements of ground level concentrations must not be applied to evaluating the air quality above 100 ft. From this reasoning it appears that a valid evaluation

of the impact of an episode would require measurements of pollutant concentrations at elevated levels, where a significant number of the population is found.

The authors wish to acknowledge the cooperation of several groups who have furnished data to make this study possible. These are:

1. The Chicago Department of Environmental Control, which furnished the TAM Station data, in particular Mr. Edward W. Klappenbach and Mr. Samuel Booras (present affiliation: Environmental Pollution Control System, Chicago, Illinois) and

2. The National Oceanic and Atmospheric Administration, which provided the upper air soundings, in particular, Mr. Arthur W. Strong.

Invaluable computer programming assistance was provided by the personnel of the Argonne Applied Mathematics Division: Cynthia Chamot, Janet B. Anderson, and Martin Kraimer.

METEOROLOGICAL ASPECTS OF AIR POLLUTION EPISODES

Harry Moses, John P. Bradley*, and Edward W. Klappenbach†

Introduction

The U.S. National Weather Service issues air pollution potential forecasts for regions of the United States when atmospheric diffusion is expected to be poor for a period of 36 hours or more. These forecasts provide a general picture of what may occur over a given area. Appreciable judgment is often necessary to apply these forecasts in practice.

Periods shorter than 36 hours during which pollution values are high are often of concern to persons breathing this air. Further, over a large urban complex with its multitude of sources and stacks of different heights, the concentration levels at any one time may differ considerably from one part of the city to another. A municipality or air quality region must have information on not only the locations, strengths, operating characteristics, and schedules of the sources, but also on how local weather and terrain influence the time and space variation in pollutants. A department of air pollution control must, therefore, be able to identify and act on air pollution episodes which are more restricted in duration and area than those covered by the federal air pollution potential forecasts.

An understanding of the conditions leading to air pollution episodes is essential to anticipate their occurrence and to take corrective action. For example, reliable meteorological forecasts can be used to advise public utilities and other coal users capable of switching to gas to activate an air pollution abatement strategy. Such action would prevent concentration levels from exceeding adopted standards.

Information is presented on how to identify weather conditions leading to high ground concentrations of pollutants. As will become evident, conditions which provide high pollution in the Midwest may be quite different from those on the West coast or in the Appalachian region. Nevertheless, the methods used here may be applied to any area of the country.

*Murray and Trettle, Northfield, Illinois.
†Dept. of Environmental Control, City of Chicago.

Chicago was used as an example because SO_2 concentration data, and good meteorological data were readily available, and the special features of the area are familiar to the author.

Technique for Identifying an Air Pollution Episode

The first step in providing a picture of the conditions leading to high pollution situations consisted of identifying the 20 periods in which the most serious air pollution conditions occurred over the two-year period 1966-1967. (See Table 1.) These episodes were then related to the large scale and micrometeorological conditions, including terrain effects.

TABLE 1. The Twenty Most Serious Air Pollution Episodes over Chicago, Illinois, January 1, 1966-December 31, 1967.

Episode No.	Date of beginning	First hour of episode (CST)	Duration, hr	Last hour of episode (CST)	Date of ending
		1966			
1	5 Jan	0200	41	1800	6 Jan
2	17 Jan	0400	62	1700	19 Jan
3	19 Jan	1900	23	1700	20 Jan
4	23 Jan	2300	38	1200	25 Jan
5	26 Jan	0400	32	1100	27 Jan
6	28 Jan	0000	106	0900	1 Feb
7	1 Feb	2200	52	0100	4 Feb
8	20 Feb	1700	50	1800	22 Feb
9	26 Dec	0200	39	1600	27 Dec
10	29 Dec	0600	49	0600	31 Dec
		1967			
11	2 Jan	2000	51	2200	4 Jan
12	9 Feb	0300	13	1500	9 Feb
13	12 Feb	0200	12	1300	12 Feb
14	16 Feb	1500	19	0900	17 Feb
15	24 Feb	0100	58	1000	26 Feb
16	1 Mar	0500	7	1100	1 Mar
17	9 May	2000	7	0200	10 May
18	28 Nov	1400	25	1400	29 Nov
19	20 Dec	0500	7	1100	20 Dec
20	28 Dec	0500	36	1600	29 Dec

Appropriate air quality standards may be assumed as a means for identifying an episode. For this study, a concentration of 0.3 ppm for a duration of 4 or more consecutive hours was arbitrarily used as the minimum standard for considering the existence of an air pollution episode.

The IDA Index

The severity of an air pollution episode, S, depends upon

I, the intensity of the pollutant concentration,

D, its duration, and

A, the number of people affected (for convenience represented by the average area covered).

The product of the intensity and the duration represents the dose received by an individual. The dose times the number of people or the man-dose figure may serve as an index for assessing the value of the given episode. Severity is then expressed as

$$S = I \times D \times A.$$

If air quality monitoring stations are all representative of the same number of persons, the number of stations may be a measure of the number of people involved. Where the population density varies with location, as it often does, a weighting factor should be used. In this study, the weighting factor was neglected.

Figure 1 shows the chart used to select the twenty cases. The duration is plotted on a logarithmic scale, and the number of persons affected is represented by the average area covered during the episode. The derived variable, the area coverage ratio (ACR), is given by

$$ACR = \frac{\text{No. of station hours with } SO_2 \text{ concentrations} \geq 0.3 \text{ ppm}}{\text{No. of consecutive hours in episodes}}$$

In general, the 20 points farthest from the origin were selected. It is noteworthy that these do not necessarily represent the points* having the

---

*The episodes may be denoted by points in a three dimensional space represented by a rectangular coordinate system where the axes represent intensity, duration, and area covered.

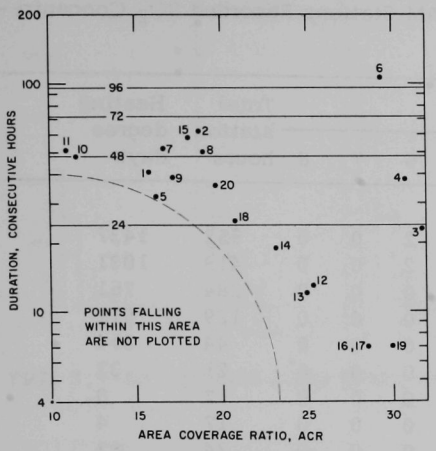

FIG. 1.--Duration vs. area coverage ratio. Episode numbers are beside points.

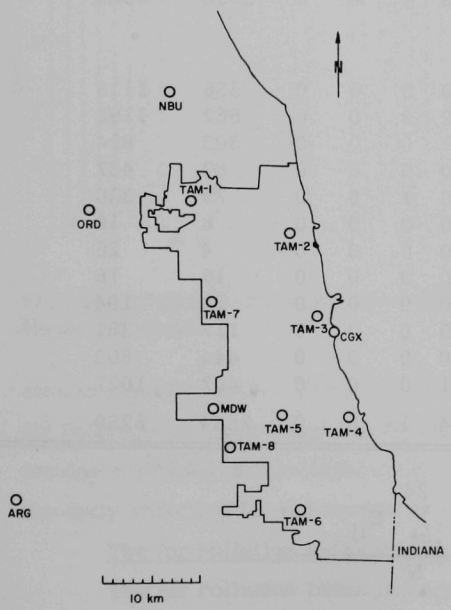

FIG. 2.--Map of Chicago area showing TAM stations

maximum man-doses--probably a sounder criteria.

The SO_2 concentrations were based on the 8 telemetered automatic monitoring (TAM) stations distributed over the city of Chicago (Figure 2). Each hourly value represents the average of 5 of the 15-minute readings centered about the hour. Table 2 gives the distribution of stations showing 0.3 ppm or greater for each month. The seasonal effect is marked: In January and February as many as 6 stations recorded 0.3 ppm or more simultaneously. In July, no more than one station was found with this value. A similar analysis showing frequency of occurrence of episodes having the indicated durations for the years 1966 and 1967 and the combination of the two years is summarized in Table 3.

The Air Pollution Index

Another technique for identifying the severity of an air pollution condition has been called the Air Pollution Index (API). This may be defined as

TABLE 2. Number of Hours in which TAM Stations Recorded SO_2 Concentrations $\geq$ 0.3 ppm.

Month	TAM station 1	2	3	4	5	6	7	8	Total station hours	Heating degree days
				1966						
Jan.	224	121	92	37	10	2	0	0	952	1437
Feb.	148	79	25	4	2	2	0	0	419	1031
Mar.	160	36	12	4	0	0	0	0	284	761
Apr.	92	17	1	0	0	0	0	0	129	511
May	38	3	0	0	0	0	0	0	44	314
Jun.	21	0	0	0	0	0	0	0	21	33
Jul.	7	0	0	0	0	0	0	0	17	0
Aug.	15	1	0	0	0	0	0	0	17	4
Sep.	18	3	0	0	0	0	0	0	24	83
Oct.	57	9	2	0	0	0	0	0	81	363
Nov.	174	38	10	2	0	0	0	0	288	653
Dec.	354	63	9	3	1	0	0	0	524	1116
TOTAL	1308	370	151	50	13	4	0	0	2790	6306
				1967						
Jan.	272	33	6	0	0	0	0	0	356	1113
Feb.	232	133	30	16	2	0	0	0	662	1198
Mar.	135	65	7	3	1	0	0	0	303	814
Apr.	44	18	1	1	0	0	0	0	87	437
May	39	9	4	1	0	1	0	0	79	330
Jun.	8	0	0	0	0	0	0	0	8	10
Jul.	4	0	0	0	0	0	0	0	4	26
Aug.	14	1	0	0	0	0	0	0	16	16
Sep.	21	0	0	0	0	0	0	0	21	104
Oct.	77	16	0	2	0	0	0	0	117	381
Nov.	194	82	22	5	0	0	0	0	444	803
Dec.	172	88	14	3	1	0	0	0	407	1027
TOTAL	1212	445	84	31	4	1	0	0	2504	6259

$$API = \frac{\sum_{j=1}^{8} \sum_{i=1}^{24} C_{ij}}{N}$$

where

C = SO_2 concentration

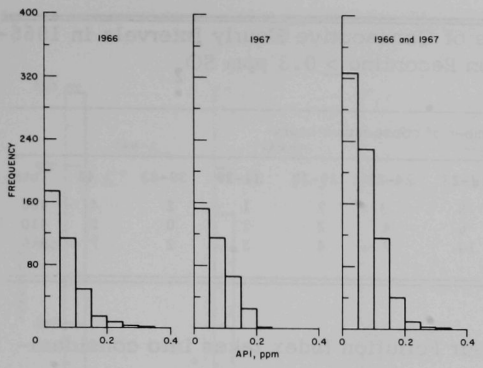

FIG. 3.--Air Pollution Index histograms.

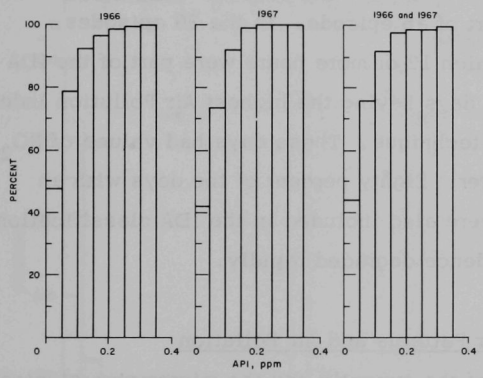

FIG. 4.--Cumulative air pollution index frequency chart.

i = hour of the day

j = station number

$N = n_i n_j$

n_i = number of hours used in computing the average

n_j = number of stations used in computing the average.

Or more simply stated, the API is calculated by averaging the 24-hour average SO_2 concentrations from all 8 stations.

Figure 3 shows the histograms and Figure 4 shows the cumulative frequency charts of the API's for 1966, 1967, and for both years. Figures 5 and 6 show the histograms and cumulative frequency bar diagrams of the average daily concentration for the TAM stations for the two years, 1966 and 1967. A marked difference in the air pollution conditions over different sections of the Chicago area is clearly shown. A picture of the day-to-day variation of the Chicago Air Pollution Index is shown in the bar diagrams of Figure 7. These figures provide a picture of the distribution of the average SO_2 concentration and the daily variation for the months of January and July, 1966.

The Air Pollution Index during the Twenty Selected Episodes

The Air Pollution Index is based upon a 24-hour period while the IDA index is based on the number of consecutive hours in which concentrations of SO_2 equalled or exceeded 0.3 ppm. The duration of IDA episodes ranged

TABLE 3. Frequency of Occurrence of Consecutive Hourly Intervals in 1966-1967 with at Least One TAM Station Recording ≥ 0.3 ppm SO_2

	Number of consecutive hours										
	< 4	4-8	9-13	14-18	19-23	24-28	29-33	34-38	39-43	≥ 44	Total
1966	280	84	12	9	8	3	2	1	2	4	406
1967	282	76	20	16	6	4	2	2	0	2	410
1966 + 1967	562	160	32	25	14	7	4	3	2	7	816

from 7 to 106 hours. Further, the Air Pollution Index takes into consideration all of the measurements, but the IDA cases include only values at or above the 0.3-ppm threshhold. Nevertheless, a comparison is possible under certain conditions. Table 4 shows a comparison based on those days in which 12 or more hours were part of an episode. In the 20 episodes, there were a total of 32 days in which 12 or more hours were part of the IDA episode. It is evident that the 16 days having the highest Air Pollution Index were also days chosen by the IDA technique. These days had values of SO_2 concentration of 0.20 ppm or greater. Eighty percent of the days with an API value of 0.18 ppm or greater were also included in the IDA classification. For smaller values, the correspondence degraded rapidly.

Relation between Synoptic Weather Patterns and Air Pollution

An examination was made of the synoptic and the micrometeorological conditions associated with the IDA episodes to identify the factors that contribute substantially to the occurrence of an air pollution incident. An objective in identifying these meteorological factors was to determine what must be forecast to anticipate an air pollution episode.

The Booz-Allen Classification

A classification system devised by Booz-Allen[1] for producing diffusion forecasts was examined. The classification system consists of 35 surface weather types and 20 patterns of the 500-millibar surface; these are listed in Tables 5 and 6. Although the identification procedure was designed to be objective, a considerable amount of subjective judgment is necessary,

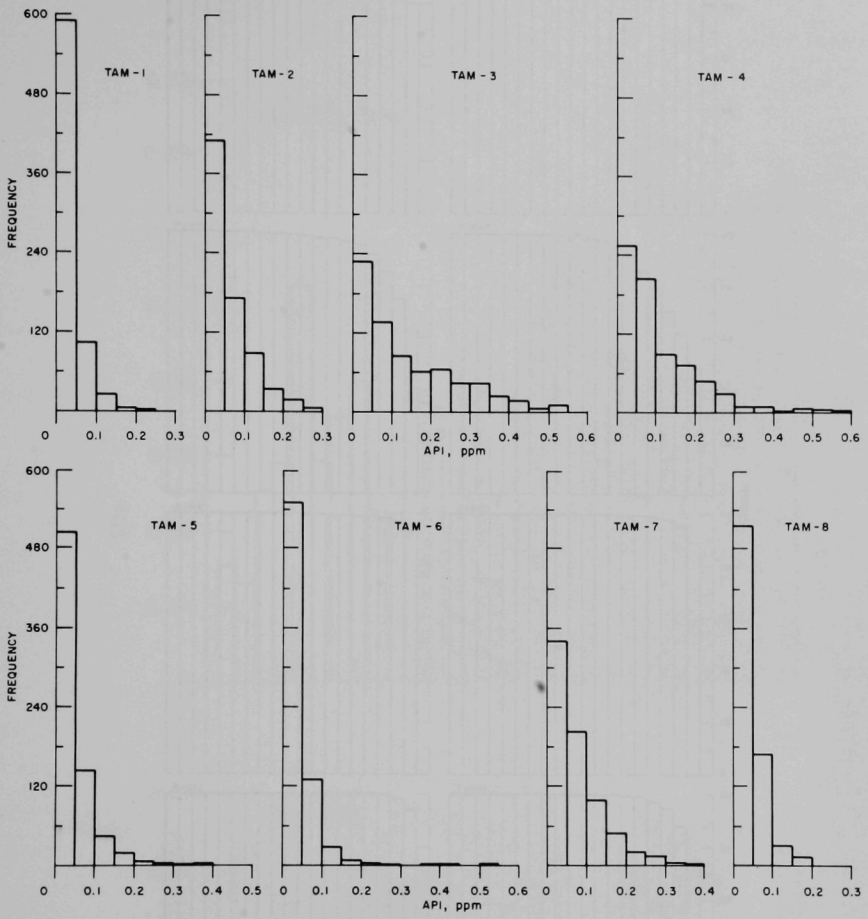

FIG. 5.--Average daily SO_2 concentration for each TAM Station, 1966 and 1967.

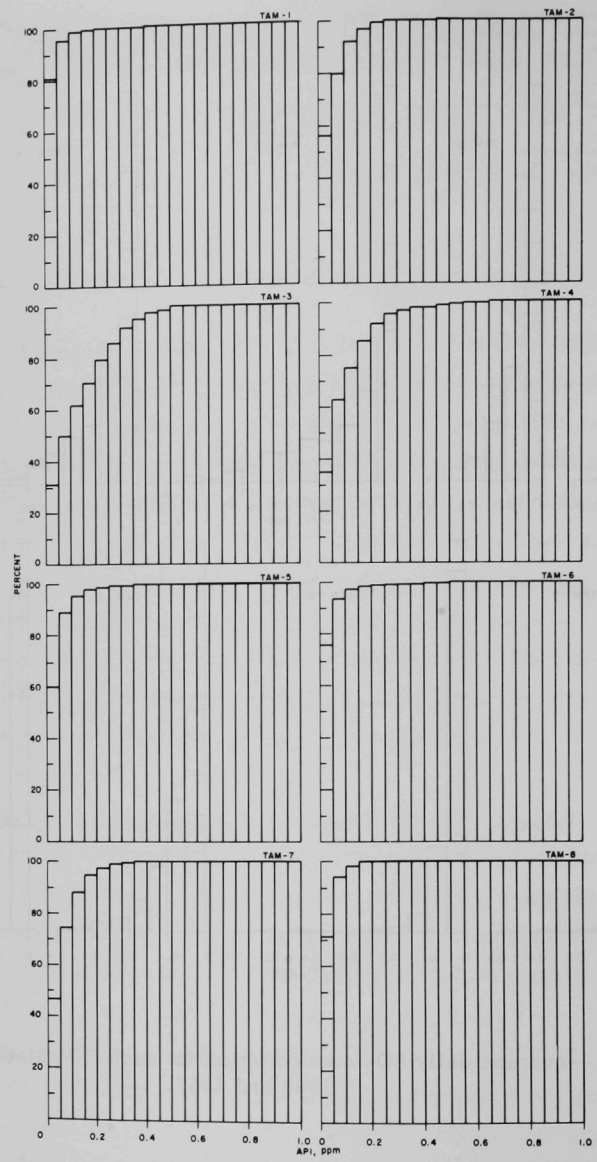

FIG. 6.--Cumulative frequency diagram of average daily SO_2 concentrations for TAM Stations.

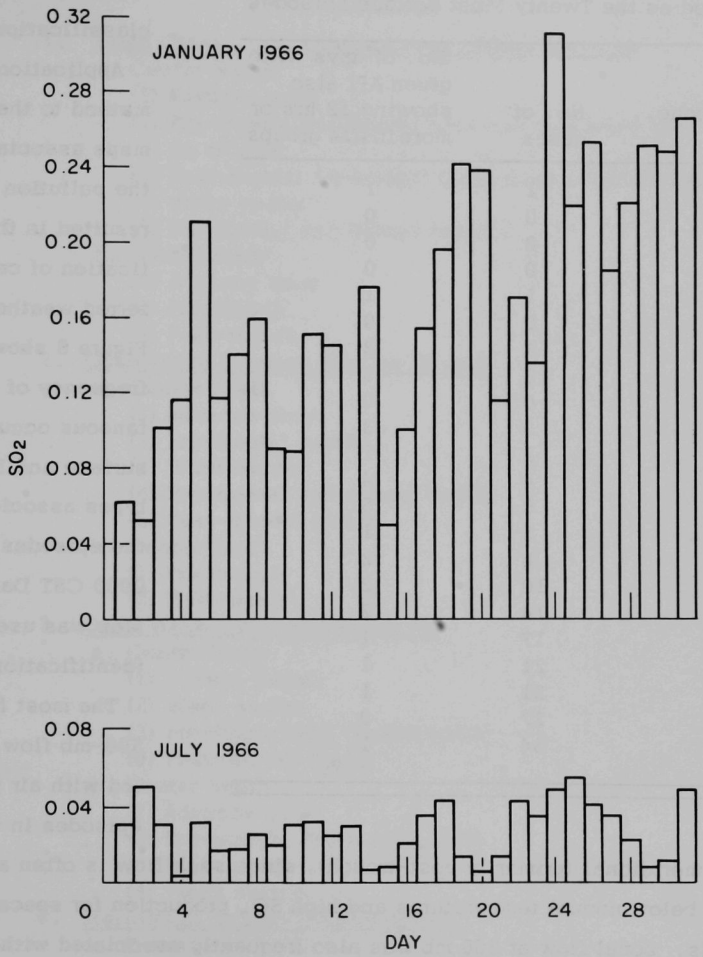

FIG. 7.--Bar diagram showing Air Pollution Index for January and July, 1966.

TABLE 4. Air Pollution Index on Days Selected by the Intensity-Duration-Area Method as the Twenty Most Serious Episodes

API SO_2 conc., ppm	No. of cases	No. of days with given API also showing 12 hrs or more in IDA groups
0.31	1	1
0.30	0	0
0.29	0	0
0.28	0	0
0.27	1	1
0.26	0	0
0.25	3	3
0.24	3	3
0.23	0	0
0.22	3	3
0.21	1	1
0.20	4	4
0.19	9	5
0.18	5	1
0.17	8	2
0.16	10	2
0.15	14	2
0.14	17	1
0.13	21	1
0.12	21	1
0.11	27	0
0.10	34	1

both in classifying the weather maps and in interpreting the classifications.

Application of the method to the weather maps associated with the pollution episodes resulted in the identification of certain preferred weather types. Figure 8 shows the frequency of simultaneous occurrence of surface and 500-mb types associated with the episodes. The 0000 CST Daily Weather Map was used in the identification procedure.

The most frequent 500-mb flow associated with air pollution episodes in Chicago was meridional (primarily post-trough), since such flow is often associated with below normal temperatures and high SO_2 production for space heating needs. Zonal flow at 500 mb was also frequently associated with air pollution episodes. This flow is usually accompanied by relatively weak, rapidly moving surface systems.

It was found that the majority of the surface types fell under the "High, Center North" and "Ridge or High, Center South" grouping. The "Deep Closed Low" category involved a deep closed low distant from

TABLE 5. Booz-Allen Surface Types

Type No.	Description
	1. Deep Closed Low (deepening or mature cyclone)
	a. Center North
1	(1) Advance zone
2	(2) Pre-frontal and frontal (occlusion or warm front) (or trough)
3	(3) Post-frontal (or trough) (cold front or occlusion)
4	(4) Warm sector
5	(5) Pre-frontal and frontal (cold)
	b. Center South
6	(1) Advance zone
7	(2) Pre-trough
8	(3) Post-trough
	2. Open Wave Cyclone Moving SE or E
	a. Center North
9	(1) Advance zone
10	(2) Pre-frontal (warm)
11	(3) Warm sector
12	(4) Pre-frontal and frontal (cold)
13	(5) Post-frontal (cold)
	b. Center South
14	(1) Pre-trough
15	(2) Post-trough
	3. Open Wave Cyclone Moving NE
	a. Center North
16	(1) Frontal (warm)
17	(2) Warm sector
18	(3) Pre-frontal and frontal (cold)
19	(4) Post-frontal (cold)
	b. Center South
20	(1) Advance zone
21	(2) Pre-trough, warm front zone
22	(3) Post-trough
23	(4) Warm sector
	4. Meridional Trough (N-S or tilted)
24	a. Pre-trough
25	b. Post-trough
26	c. Trough or frontal zone
	5. Inverted Trough
27	a. Pre-trough
28	b. Post-trough

TABLE 5. (continued)

Type No.	Description
	6. Ridge, or High, Center South
29	a. Pre-ridge
39	b. Post-ridge
	7. High, Center North (or same latitude)
31	a. Pre-inverted ridge
32	b. Center
33	c. Post-inverted ridge
34	d. E-W gradient
	8. Flat Pressure Area
35	a. Cols or other areas (except high centers) where wind is determinate

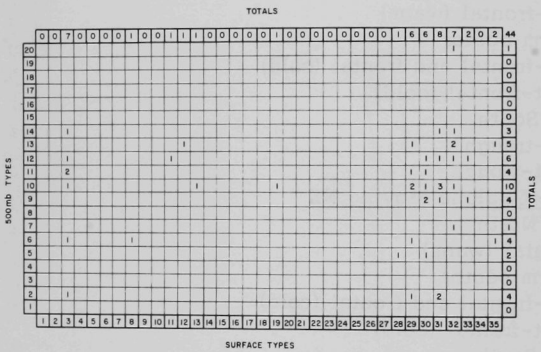

FIG. 8.--Frequency of coincident Booz-Allen surface and 500-mb types associated with the IDA Air Pollution Episodes.

Chicago, most often on the east coast. Actually, Chicago was more properly under the influence of an elongated ridge of high pressure to the west that had a "cyclonic dent" in the isobars over the Great Lakes.

In fairness to the Booz-Allen classification, it must be pointed out that it was not designed for the type of episode discussed here. Its shortcomings must, therefore, be judged accordingly.

TABLE 6. Booz-Allen 500-mb Types

1. Deep Closed Low
   a. Center North
      (1) Pre-trough
      (2) Post-trough
   b. Center South
      (1) Pre-trough
      (2) Post-trough
2. Weak Closed Low
   a. Center North
      (1) Pre-trough
      (2) Post-trough
   b. Center South
      (1) Pre-trough
      (2) Post-trough
3. Meridional Trough (N-S or tilted) (including transitional)
   a. Pre-trough
   b. Post-trough
4. Basically Zonal
   a. Westerly flow
   b. Pre-minor trough
   c. Post-minor trough
5. Meridional Ridge
   a. Pre-ridge
   b. Post-ridge
6. High, Center North (or same latitude)
   a. Pre-inverted ridge
   b. Center
   c. Post-inverted ridge
   d. E-W gradient
7. Flat Pressure Area
   a. Cols or other transitional areas (except highs) where wind is indeterminate and there is no convergence.

Similarities in Weather Patterns Associated with Episodes

An examination of the synoptic surface charts associated with the episodes showed a number of similarities. There are a) weak pressure gradients resulting in light winds, b) low surface temperature, and c) clear skies, especially at night.

Weak Pressure Gradient.--One of the outstanding features of the synoptic surface charts was that a weak pressure gradient was the rule with very few exceptions during the air pollution episodes. The two years of daily weather charts showed that levels of SO_2 concentrations invariably increased when weak pressure gradients, such as occur in a col or in an anticyclone center, passed over the city. The weak pressure gradients ordinarily mean light surface winds, but local terrain influences may act to increase air movement.

Low Temperatures.--Another striking feature was the occurrence of high pollution with cold waves. This is understandable because increased space heating results in more coal burning, and consequently more SO_2 emitted into the atmosphere.

A combination of high winds and low temperatures produce a high wind chill factor. Higher winds, therefore, are associated with two opposing factors in the production of high concentrations of SO_2. On the one hand, high winds are associated with pronounced turbulent mixing, tending to keep SO_2 concentrations low; on the other hand, high winds produce increased cooling, resulting in greater production of SO_2 and higher ground concentrations. It is the complex balance of opposing influences which results in the observed SO_2 levels.

Stability.--The presence of an inversion, either ground-based or located within the first 5000 feet, is significant in providing high levels of SO_2 concentration. An inversion aloft may produce a "lid" to keep the pollutant confined to a restricted layer. Although data on the variation of temperature with height were lacking, it is well known that during clear nights with light winds ground-based inversions are certainties in rural areas; over urban areas, an inversion may not form, but the stability increases. The increase in stability is conducive to the development of high SO_2 concentrations. Light winds and clear skies are associated with anticyclones, especially near their centers or in the ridge areas between centers in multipeaked systems.

Anticyclone Types

The conditions conducive to high levels of pollution, light winds, low temperatures and stability, occur most frequently though not always with anticyclones. Attempts have been made to classify anticyclones according to their origin, shape, and thermodynamic structure.[2] Of course, the high pressure per se has nothing to do with the occurrence of high pollution levels. Actually, the center of any type of high is conducive to high pollution conditions.

Cold Arctic Outbreaks.--The most outstanding anticyclone type which produces high pollution levels is the arctic high. Often the cold air flows over the Midwest as a series of cold "pushes." The colder the air, usually the more intense the episode. An example of this type is the 1056-mb anticyclone of January 28-31, 1966. (See Figure 9.) The temperature at the Chicago Midway Airport dropped to -20° F during this episode. Its duration, 106 hours, was the longest of the 20 episodes. The onset of such outbreaks often follows the Atlantic "northeaster," i.e., the northward movement of a deep low up the Atlantic coast and close to or over New England. A substantial fraction of the 20 episodes were associated with this pattern.

The Stagnating Bermuda High.--Frequently during the summer and fall the Bermuda high retrogrades and becomes relatively stationary over the eastern part of the United States. These situations are associated with heat waves in summer and the Indian summer in fall. Although light winds and subsidence inversions may be associated with this pattern during the day and light winds and ground-based inversions at night, high SO_2 levels are not as common, probably because of the lack of residential space heating with its associated atmospheric injection of SO_2. High particulate loading is more likely under this weather pattern.

Urban Air Pollution Case Studies

Although synoptic surface and upper air weather charts provide a picture of the large scale motion, they are frequently ineffective in

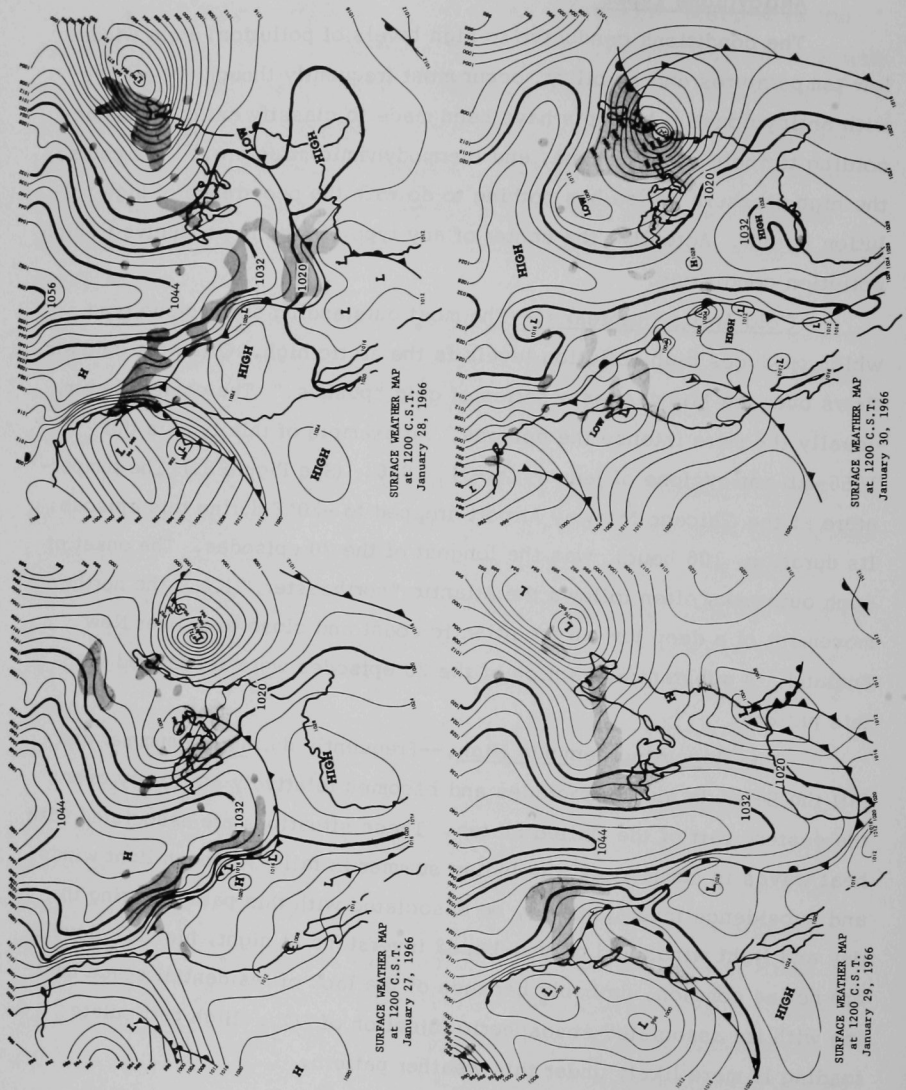

FIG. 9.--Surface and 500-mb Maps for January 27-30.

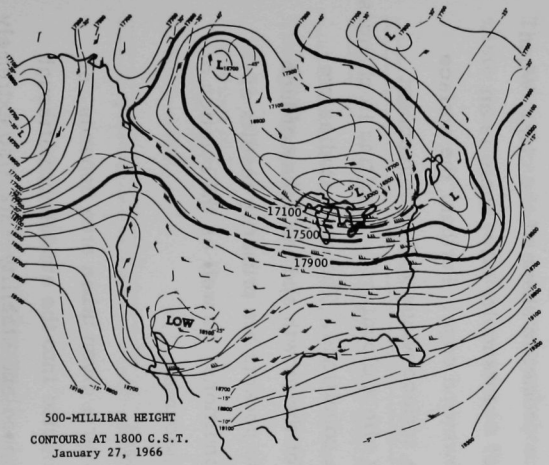

500-MILLIBAR HEIGHT
CONTOURS AT 1800 C.S.T.
January 27, 1966

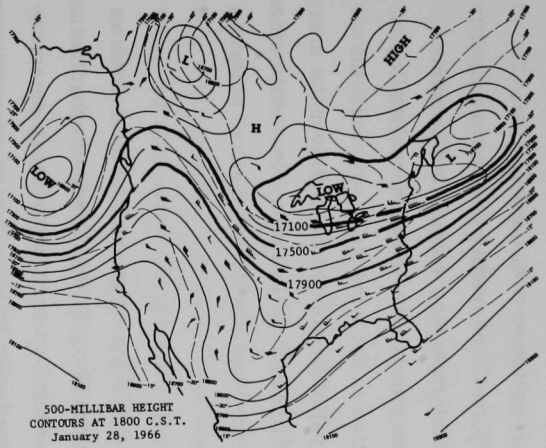

500-MILLIBAR HEIGHT
CONTOURS AT 1800 C.S.T.
January 28, 1966

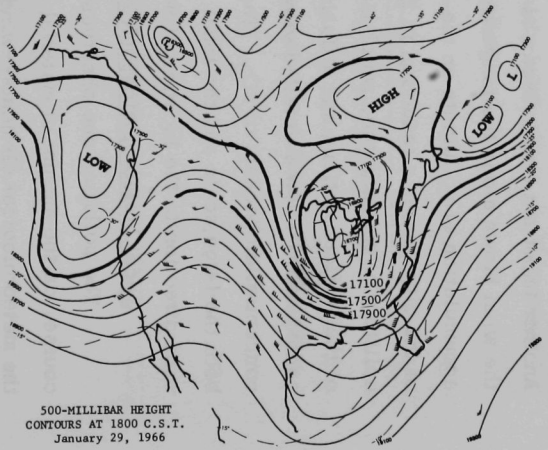

500-MILLIBAR HEIGHT
CONTOURS AT 1800 C.S.T.
January 29, 1966

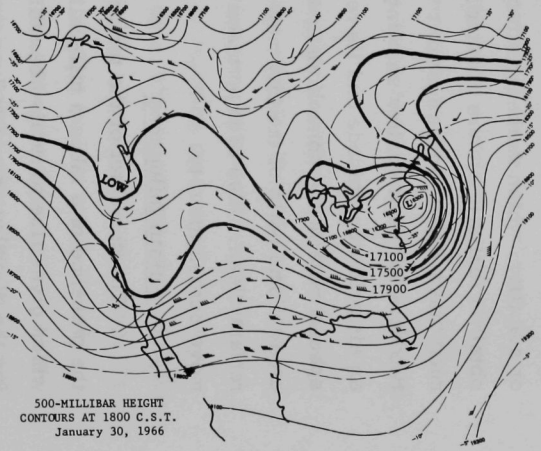

500-MILLIBAR HEIGHT
CONTOURS AT 1800 C.S.T.
January 30, 1966

determining what the local weather elements are likely to be. This is especially so for weather elements such as wind speed, wind direction, or stability, which markedly effect air pollution over a given area. To obtain a realistic picture of what is actually happening, each municipality must make a local investigation. In the following section are presented two detailed case studies showing the onset, development, and ending of an air pollution episode and its relation to the wind field patterns. Of special note is the nonuniformity of pollution concentrations over the urban area. Some parts of the city may exhibit high pollution levels, while others remain clean. Also of importance is the way in which pockets of pollution move across the city.

Terrain Influences

The character of the terrain, e.g., the orographic features such as the presence of a lake, a hill-valley complex, or the degree of urbanization which gives rise to rural-urban differences, is most important in determining the distribution and influencing the levels of air pollution concentration. Another important terrain factor is the geometric shape of the city. When the wind blows along the long axis of a rectangular city, there is an accumulation of pollutants on the downwind edge. Further, the surface of the city causes a reduction in the surface winds with a consequent uplifting or convergence, which may affect cloudiness, resulting in changes of the vertical motions and diffusion conditions. The case studies presented below show a detailed view of the growth and the decay of high concentration pockets of SO_2. These pockets are primarily results of both the large scale and the local conditions, as well as the relation of wind direction to the location of SO_2 sources.

Local Meteorological Influences

The pollution one observes over a given urban area depends, of course, on the amount of material injected into the atmosphere although the meteorological elements--wind speed and stability--are also extremely important. When the winds are light, the ventilation rate is low, and material may be injected into the city faster than it is carried away. Levels

of SO_2 concentration, therefore, rise. There are other factors operating to affect pollution levels. For example, when the winds reach a critical value, there is an increase in downwash from buildings. Thus, an increase in speed may result in higher levels of SO_2 in spite of the increased ventilation rate. Of course, the geometry and the aerodynamic effects of particular buildings, as well as the atmospheric stability, influence the concentration levels.

At night, with light winds, the presence of a strong inversion, and elevated sources (circa 100 ft), the effluent will remain high above the ground. Under these conditions, the motions are suppressed with the result that concentrations from these sources reaching the ground are low. When the sun comes up and convection starts, these sources may contribute markedly to the ground level pollution. In the extreme case, there may be a fumigation effect, i.e., the effluent is brought rapidly to the ground, giving particularly high concentrations. The pollution episode is initiated most frequently in the dark hours during stable conditions. (See Table 7.) The episode appears to terminate when fairly brisk winds set in to ventilate the city. This often occurs in the afternoon.

TABLE 7. Times of Beginning and Ending of the 20 IDA Episodes

Time interval (CST)	Frequency of onset	Frequency of ending
0100-0600	11	3
0700-1200	0	7
1300-1800	3	9
1900-2400	6	1

Case Studies

The Incident of February 12, 1967 *Background.*--

The pollution episode of February 12, 1967, was relatively short-lived. SO_2 concentrations in excess of 0.29 ppm were first recorded at

0200 CST in the Loop (TAM 3) and in Hyde Park (TAM 4) and subsequently at one or more of the 8 TAM stations through 1300 CST. During these 12 consecutive hours, there were at least 30 station hours with SO_2 concentrations of at least 0.3 ppm. At 0800 CST, 4 TAM stations recorded high SO_2 levels simultaneously.

The area coverage ratio (the number of consecutive station hours of $SO_2 > 0.29$ ppm divided by the number of consecutive hours in the pollution episode) provides a measure of the geographical area over which the pollution pall existed. For this example, the area coverage ratio was 2.50, indicating that on the average between 2 and 3 TAM stations simultaneously recorded high SO_2 levels.

During the predawn hours of February 12, the Midway Airport reported temperatures of zero or below, e.g., 0° at 0300, and -3° at 0600, 0700, and 0800 CST. Northwest of the city, the air was much colder; O'Hare Airport recorded a minimum of -16°F between 0400 and 0600 CST.

Light winds, about 4 knots, prevailed over the city, backing slowly from near north at midnight to west-northwest just prior to sunrise. By mid-morning, under brilliant sunshine and continuing light winds, temperatures rose markedly. At 1000 CST, O'Hare recorded a value above zero; the afternoon high was 17°F. The Midway temperature picture was similar.

By mid-afternoon, snow began to fall and continued for several hours. An inch of new snow had fallen at O'Hare by 1800 CST, bringing the total on the ground to 18 inches. During the same period, 2 inches of snow were deposited at Midway, bringing the total there to 19 inches. By late evening both the snow and the air pollution incident had ended.

Synoptic Conditions.--The 500-mb and surface charts are shown in Figure 10. The upper air charts show the pronounced northwesterly flow over Chicago, characteristic of cold outbreaks. The fast moving air steered the surface patterns so that the weather systems at the ground moved up quite rapidly.

The surface chart shows a 1032-mb arctic high centered over western Wisconsin. It was part of a larger system which extended far

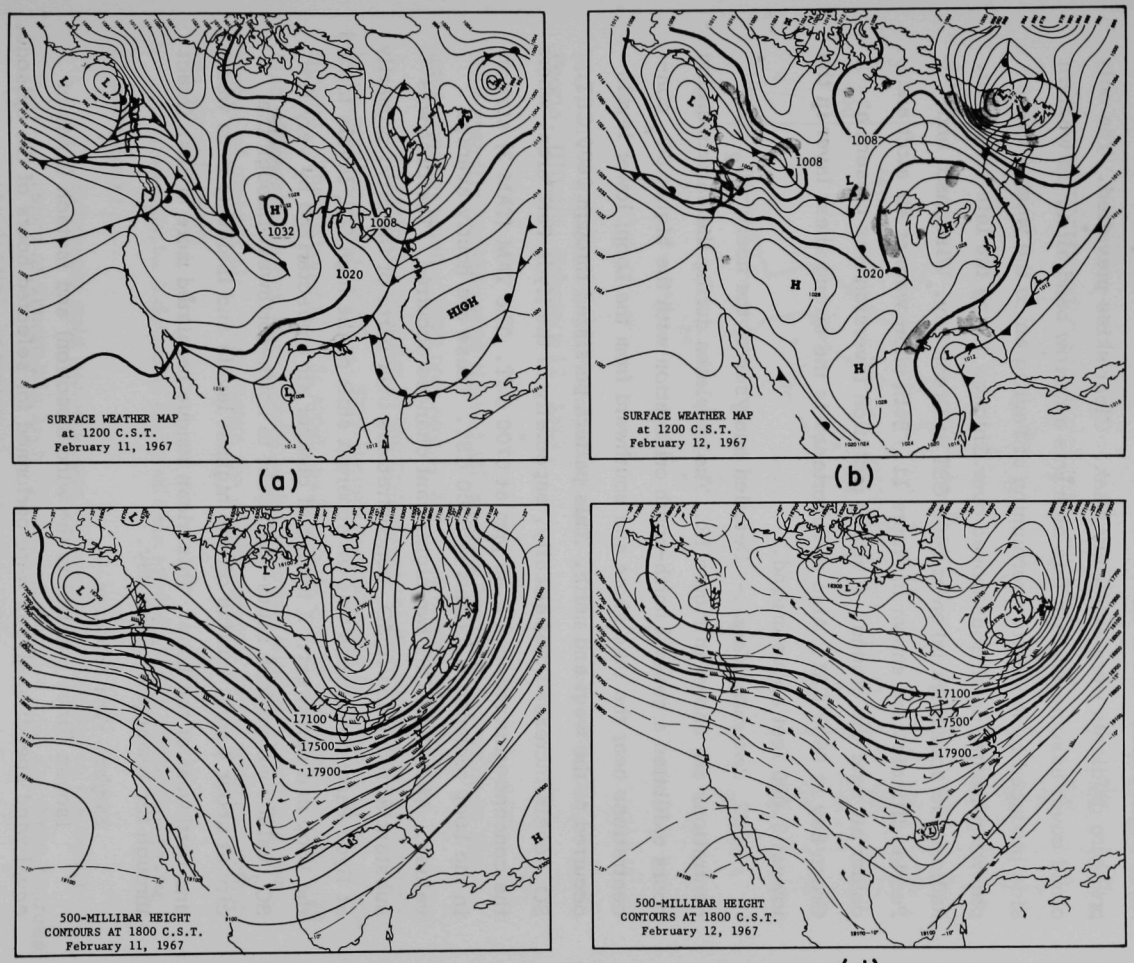

FIG. 10.--Surface and 500-mb charts for February 11 and 12, 1967.

north into Canada. As it moved over the Great Lakes region, the horizontal pressure gradients were extremely weak. Clear skies prevailed. The only cloud cover associated with this high was a narrow band along its western side produced by moderate overrunning of Pacific air to the west. These pre-warm frontal conditions moved over Chicago during the late afternoon. Radiosonde soundings taken at 0600 CST at Green Bay, Wisconsin and Peoria, Illinois, are shown in Figure 11. Both show warmer air aloft and colder air near the ground. A strong radiation inversion was present at Green Bay at 0600 CST. Also of importance is the strong shear layer in the lowest 3,000 feet above ground.

SO_2 Concentrations. -- Detailed analyses of the hourly SO_2 concentrations are shown in Figure 12. The isopleths during the early morning hours exhibited a general north-south orientation with the higher SO_2 concentrations near the lake shore and southward from the Loop; lower levels occurred to the west and north. This pattern persisted through 0800 CST. SO_2 levels increased dramatically, especially in the Hyde Park area, where the concentration reached 0.89 ppm at 0700 CST. The TAM (TAM 3) station in the Loop recorded 0.69 ppm at 0500 CST. These are hourly average values. After 0800 CST two significant changes occurred. The first was substantial reduction in SO_2 concentrations over parts of the city, primarily at Hyde Park; the second was an apparent shift of the high SO_2 levels toward the Loop and northwest. A tongue of cleaner air characterized by very low SO_2 values moved from south-southwest to north-northwest through the city at about 4 mph, cutting off the highest levels and isolating them west and northwest of the Loop. This clean tongue persisted more or less intact through the remainder of the day.

Surface Wind Patterns.--

Isogon (lines parallel to the wind direction) and isotach (lines of equal wind speed) analyses were performed for selected hours of the episode, using the TAM wind data as well as the O'Hare and Midway winds. These turned out to be particularly enlightening when superimposed upon the corresponding SO_2 isopleth figures. Note that Figure 12 clearly shows the

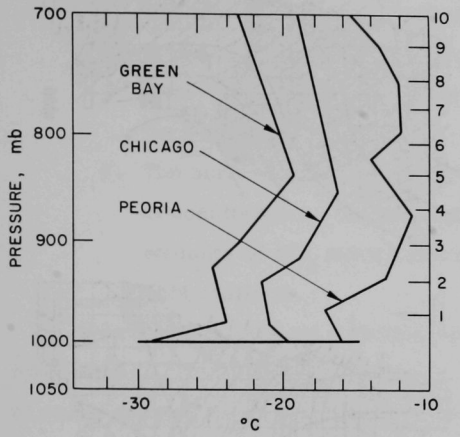

WIND DIRECTION, deg	WIND SPEED, kt	WIND DIRECTION, deg	WIND SPEED, kt
290	33	300	41
290	30	300	52
280	25	310	52
280	23	300	43
280	20	300	36
280	17	300	26
280	15	300	21
280	11	290	11
320	03	290	04
290	01	060	03
GREEN BAY		PEORIA	

FIG. 11.--Radiosonde and winds aloft data for Green Bay, Wisconsin, and Peoria, Illinois, February 12, 1967.

flow steadily backing with time at all stations instead of veering in the usual manner when a high pressure to the north moves eastward.

Of particular interest is the orthogonal relationship between streamlines and isopleths of SO_2. This feature persists and is evident in all of the figures. The orthogonality is most evident near and to the south of the Loop. Also of interest is the correspondence between the wind maximum and the tongue of cleaner air. This shows the effectiveness of high winds in reducing air pollution.

Comments.-- A detailed study of this episode leads to the following observations:

1. Extremely cold temperatures contributed markedly to the occurrence of abnormally high SO_2 concentrations from the three sources; residential, commercial, and industrial.
2. The general synoptic features indicate the confinement of the

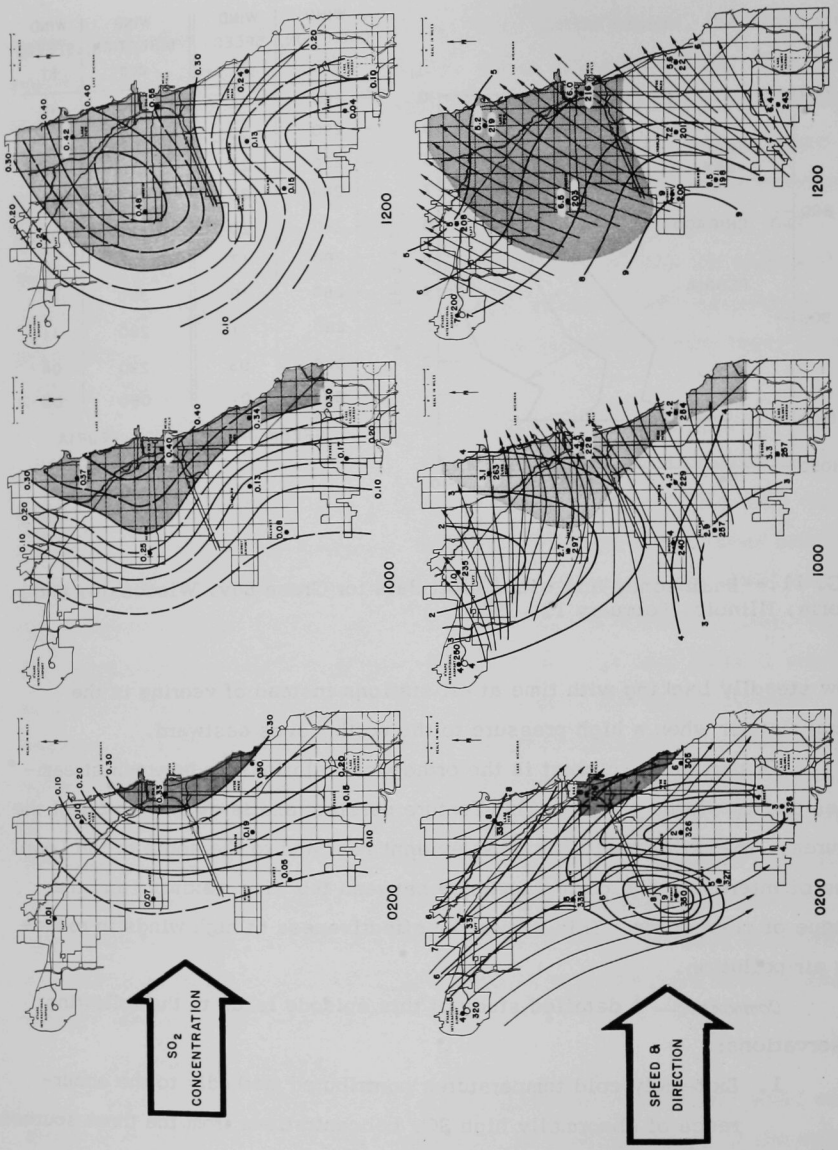

FIG. 12.--Isopleths of SO_2 concentrations over Chicago, February 12, 1967. Isopleths of wind speed (isotachs) and wind direction (isogons) over Chicago February 12, 1967.

effluent to a shallow layer close to the ground, and to the establishment of a strong horizontal temperature gradient.

3. The weak horizontal pressure gradient and strong temperature gradient across the city, as well as the changing synoptic pattern, were primarily responsible for the "abnormal" backing of the wind.

4. The surface winds appeared to transport regions of high SO_2 concentrations. As this volume containing relatively large amounts of SO_2 moved across the city, it was detected at many TAM stations.

Features of this air pollution episode may be expected to occur in other cities. This episode occurred in winter when increased combustion of sulfur bearing fuels contributed to high ground SO_2 concentrations. Since the bulk of the land east of the Rocky Mountains, excluding the deep south, is subject to cold temperatures and the effects of moving anticyclones, a similar episode is possible.

The presence of snow cover greatly enhances temperature contrasts between the inner city and surrounding rural areas, and can, under weak pressure gradient conditions, alter the "normal" behavior of air flow close to the ground. This is likely to have occurred in this case. The air flow was also affected by the size of the city with its roughness elements. Further, the temperature contrasts between Lake Michigan and the city no doubt modified the wind direction with the resulting change in the distribution of SO_2 concentrations.

The Incident of March 1, 1967. *Background.*--

The pollution episode of March 1, 1967 lasted only 7 hours, one of the briefest of the 20 cases studied. SO_2 concentrations in excess of 0.29 ppm were first recorded at 0500 CST at TAM 7 and subsequently at one or more of the 8 stations through 1100 CST. During this period, there were 20 station hours of SO_2 levels of at least 0.30 ppm. No less than 5 stations recorded high SO_2 levels simultaneously at 0800, 0900, and 1000 CST. The area coverage ratio for this episode was 2.86, a fairly high value.

The episode was brought to an end by an increase in the horizontal pressure gradient with increasing wind speeds over the city during the late morning. This case study illustrates a synoptic pattern in which an anticyclone moved fairly rapidly across the area, in contrast to that of the stagnating anticyclone. In spite of the rapid movement, there was a 7-hour period in which appreciably high values of SO_2 concentrations were recorded over a fairly large part of the city.

Synoptic Conditions.--The upper air flow, e.g., 500-mb (Figure 13), shows strong northwesterly flow (80 knot winds) at 0000 CST. The elongated north-south 1029-mb anticyclone centered over Green Bay, Wisconsin, extended southward through central Illinois to Louisiana. A warm front was located in the Great Plains. During the early morning hours, the anticyclone moved southeastward to northern Indiana and by 1200 CST was located over northern Ohio. The air pollution episode ended when the flat pressure gradient associated with the high was replaced by the stronger gradient behind the departing anticyclone. The upper air radiosonde soundings showed strong warming aloft which intensified the inversion.

SO_2 Concentrations.--A detailed analysis of the hourly SO_2 concentrations for the period of the episode are shown in Figure 14. The SO_2 levels rose sharply near sunrise reaching their highest value in the central and southern parts of the city around 0900 CST. High readings thereafter shifted to the northern parts of the city and dropped to very low values upon the termination of the episode. Lines showing the wind direction and isopleths of wind speeds, were drawn in Figure 14 for the hours corresponding to this episode. Prior to the onset of the episode, winds in the western part of the city were blowing gently from the northwest and gradually backed southerly by sunrise.

This wind pattern suggests convergence into the city prior to the episode, and to the north of the city during the episode. The lower speeds seen over the city as compared to those of Midway are probably a result of increased surface roughness over the urban complex. A comparison of the wind and SO_2 charts reveals the generally downwind increase in SO_2 con-

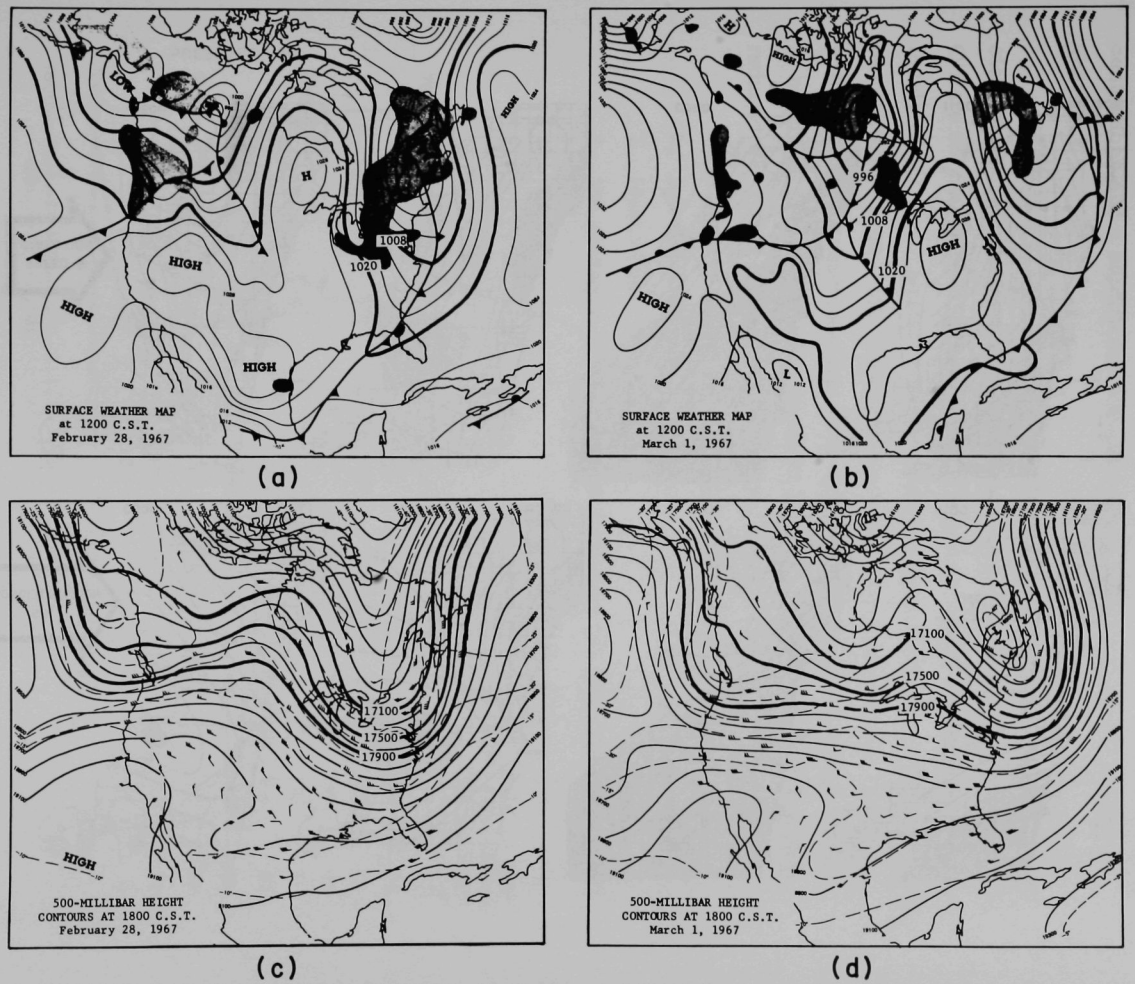

FIG. 13.--Surface and 500-mb charts for North America, February 28, 1967 and March 1, 1967.

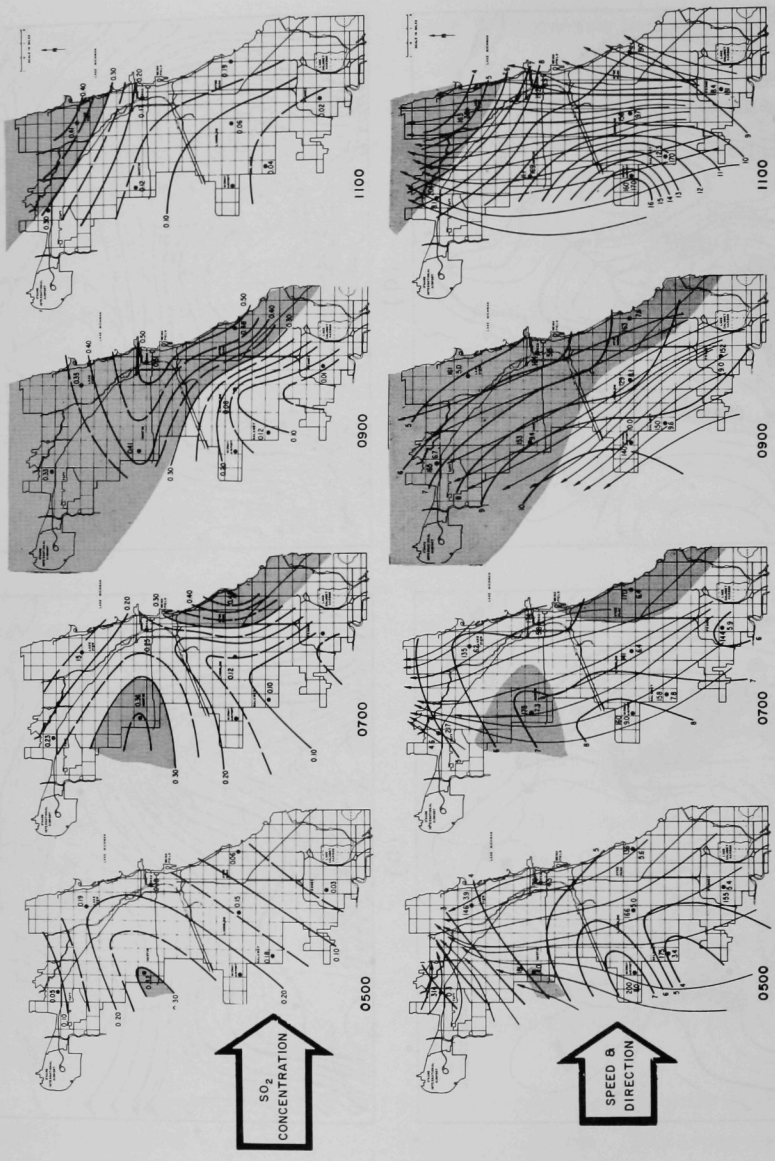

FIG. 14.--Isopleths of SO_2 concentrations over Chicago, March 1, 1967 0500 to 1100 CST. Isopleths of wind speed (isotachs) and wind direction (isogons) over Chicago March 1, 1967 0500 to 1100 CST.

centrations and a significant reduction when TAM wind speeds exceed 8 knots.

Summary and Comments. -- On the morning of March 1, 1967, under clear skies, light winds, and low temperatures (Midway minimum was 17° F, O'Hare minimum was 3° F) the Chicago area was subjected to unusually high levels of SO_2 for 7 hours. This air pollution episode began at 0500 CST and terminated at 1100 CST. When the weak pressure gradient was replaced with a strong pressure gradient wind speeds increased from nearly 5 knots to nearly 15 knots. This had occurred by noon. SO_2 levels were sharply reduced when TAM wind speeds exceeded 8 knots.

Three factors contributed to the high SO_2 measurements:

1. low temperatures,
2. light winds, and
3. the presence of an inversion aloft over the city (see Figure 15).

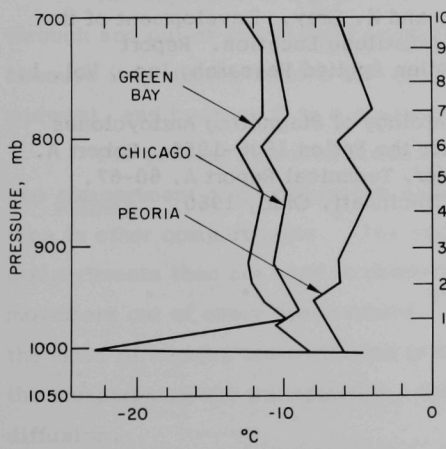

WIND DIRECTION, deg	WIND SPEED, kt	WIND DIRECTION, deg	WIND SPEED, kt
320	25	310	33
310	18	320	28
300	12	310	25
280	06	320	18
220	05	310	11
210	08	300	07
200	09	260	02
190	11	140	09
180	11	130	15
190	05	120	12
GREEN BAY		PEORIA	

FIG. 15.--Radiosonde and winds aloft data for Green Bay, Wisconsin, and Peoria, Illinois, March 1, 1967

A snow cover over the ground (5 inches at Midway and 8 at O'Hare) contributed to the low surface temperatures which contrasted with temperatures near 32°F over Lake Michigan. This strong temperature gradient, together with the urban-rural gradient, no doubt contributed to the observed behavior of the air flow, which for most locations backed for a time, although from the synoptic aspects alone, the air flow would have been expected to veer as the anticyclone centered north of Chicago moved southeastward.

With a rapidly moving anticyclone system, as was present on March 1, 1967, the duration of the air pollution episode is expected to be short. The occurrence of the high levels of SO_2 occurred because the air was cold enough to result in high space heating loads and the rapid production of SO_2. This type of synoptic situation may occur in many areas of the country.

The authors thank the Deseret Test Center, Fort Douglas, Utah, for permission to use Table 5.

References

1. Hallanger, N. L., D. A. Griffith, and K. Gray. Development of the C/B Forecast System for a Mid-Latitude Location. Report No. 9004-075-R1 (5). Booz-Allen Applied Research, Inc., Vol. 1. (January, 1968).
2. Korshover, J., Jr. Synoptic Climatology of Stagnating Anticyclones East of the Rocky Mountains for the Period 1936-1956. Robert A. Taft Sanitary Engineering Center, Technical Report A, 60-67. U.S. Public Health Service, Cincinnati, Ohio, 1960.

TRITIUM STUDIES QUANTIFY WATER MOVEMENT IN AN OLD FIELD ECOSYSTEM

C. F. Jordan and J. R. Kline

Water movement through ecosystems must be quantified in order to estimate rates at which pollutants move through and out of ecosystems. For example, it is not enough to know the concentration of mercury in the water leaving the root zone of the soil. The rate that water leaves the root zone must also be known, because the rate at which mercury leaves the root zone is the product of mercury concentration times the rate of water movement.

Movement of water through ecosystems is also of interest because management of water supplies requires knowledge of transpiration, runoff, and deep drainage. In addition, from a radiological health standpoint movement of water is important because tritiated water is released into the environment from nuclear reactors or plowshare activites.

The objective of the studies reported here is to quantify water flow through and out of an old field ecosystem. This ecosystem was chosen because it is similar in form and structure to ecosystems common in the midwest, and because it is a convenient and readily available place to work.

The general approach taken is to inject tritium labeled water into one compartment of an ecosystem and measure its activity as a function of time in other compartments.* The activity-time curves of the isotope in the compartments then are used to determine transfer coefficients for isotope movement out of every compartment.** The transfer coefficients times the mass of various compartments is the rate at which water moves out of the compartment via transpiration, runoff, evaporation, downward flow, and diffusion.

*A compartment is a portion of an ecosystem small enough to be considered homogeneous within the practical limitations of the experiment.

**A transfer coefficient is the probability of an individual particle moving out of the compartment along a given pathway per unit time.

Horizontal Movement through Upper Soil

The experimental area was in a field uncultivated for about 20 years and located in an area about 300 yards south of the meteorology building at Argonne National Laboratory. The terrain slopes downward toward the south at about a five degree angle in this area. On April 13, 1970, a hole 10 inches deep and 1/2 inch in diameter was bored in the soil. Twenty millicuries of tritium and one milliliter of water were pipetted into the hole, and the top of the hole was covered with soil. Soil samples were taken periodically in a gridwork pattern surrounding the injection point and down to a depth of 10 inches with a 1/2-inch diameter soil auger. Water was extracted from the soil with a vacuum-drying manifold designed to condense and collect water as it diffuses out of the sample.[1] Samples were counted by standard liquid scintillation techniques, and results were corrected for background and converted to dpm through the use of counting efficiency curves.

It was anticipated that it would be possible to calculate the rate of lateral flow of the tritium by measuring the time for the peak of activity to pass between two downslope sampling locations. However, horizontal movement was much slower than anticipated, and another sampling scheme was required. On May 21, duplicate samples were taken every 2 inches from the injection point for a distance of 2 feet in northerly (upslope), southerly (downslope), and westerly (perpendicular to slope) directions. Single samples were taken every foot from 2 to 6 feet.

Activity of tritium on May 21 as a function of distance upslope and downslope from the injection point is shown in Figure 1. The shape of the curve is a result of two processes, diffusion and mass transport, acting simultaneously on the tritiated water. There has been movement of tritium both upslope and downslope from the injection point due to diffusion.

Movement due to mass transport is in a downslope direction only. There is spreading of tritium away from the peak due to the mass transport process as the peak moves downslope. This spreading occurs because soil, a porous medium, acts as a series of small dams which block some of the tritiated water molecules as they flow downslope. Consequently, part of the distribution of activity in Figure 1 is due to mass transport alone. Shortly after injection, this distribution is highly skewed because it is possible for some molecules to move downslope ahead of the peak, but molecules can lag behind only the distance from the peak to the injection point. As the peak moves further from the injection point, the shape of the curve gradually tends toward a normal distribution.

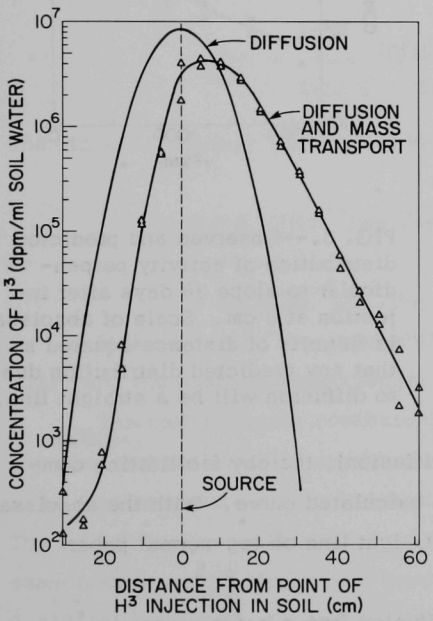

FIG. 1.--Observed distribution of activity along slope 38 days after injection at 0 cm, and predicted distribution due to diffusion process alone.

For purposes of modeling water movement through ecosystems, it is necessary to calculate the diffusion coefficient of water in the soil and the rate of water flow in a lateral direction. These calculations were made by D. Sasscer, visiting scientist from Puerto Rico Nuclear Center.

The curve of activity of tritium as a function of distance from the injection point in a direction perpendicular to the slope of the topography (Figure 2) was assumed to result only from the diffusion process. The data in Figure 2 were replotted in Figure 3 with the abscissa scale in

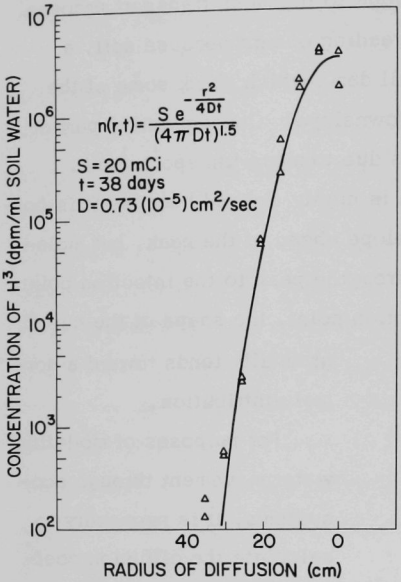

FIG. 2.--Observed distribution of activity perpendicular to slope 38 days after injection at 0 cm and predicted diffusion curve calculated from these data.

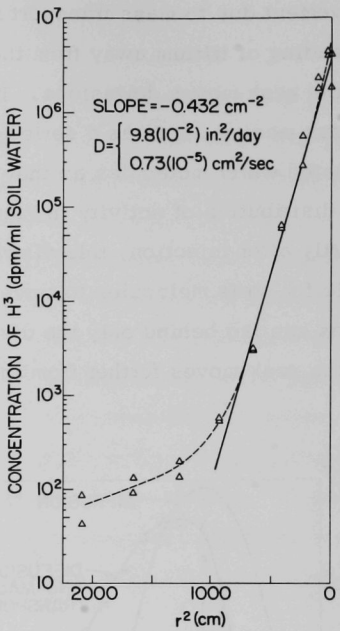

FIG. 3.--Observed and predicted distribution of activity perpendicular to slope 38 days after injection at 0 cm. Scale of abscissa is in units of distance squared so that any predicted distribution due to diffusion will be a straight line.

units of r^2 instead of r (r = radius of diffusion), thereby facilitating comparison of the observed curve with the calculated curve. With the abscissa in units of r^2, a diffusion curve is a straight line on log-normal paper (Figure 3).

The equation describing the diffusion from a point source is

$$n(r,t) = S \frac{e^{\frac{-r^2}{4Dt}}}{(4\pi Dt)^{3/2}} \qquad (1)$$

where

n = activity at distance r from the source at time t

D = diffusion coefficient

S = activity of source.

Thus, at a given time, t = T,

$$\ln\left[\frac{n(r_1 T)}{n(r_2 T)}\right] = -\frac{(r_1^2 - r_2^2)}{4Dt},$$

or $-\frac{1}{4Dt}$ equals the slope of ln [n(r,t)] when plotted as a function of r^2.

From Figure 3 we obtain

$$-\frac{1}{4Dt} = \frac{\ln(10^3)}{(122.5 - 786.9)\,cm^2}$$

and since T = 38 days (April 13 to May 21)

$$D = 0.75(10^{-5})\,cm^2/sec$$

or

$$D = 9.8(10^{-2})\,in^2/day.$$

Bulk density of the upper soil horizon in the experimental area was 1.27, and the average water content during the experiment was 32%.

The self-diffusion coefficient value of $0.73(10^{-5})\,cm^2/sec$ for the experimental soil (Morley silt loam) during April and May of 1970 appears to be similar to values obtained from other soils in laboratory experiments. The self-diffusion coefficient of a Missouri soil with approximately the same texture as the Morley silt loam is given by Brees and Graham[2] as $0.417(10^{-5})\,cm^2/sec$ at a soil temperature of 21° C. The largest value of the diffusion coefficients observed in that study was $0.833(10^{-5})\,cm^2/sec$ for Beulah loam. Nakayama and Jackson[3] report considerably higher values of the diffusion coefficient. Values for agar gel, glass beads, and various Colorado soils range from $2.40(10^{-5})\,cm^2/sec$ for agar gel to a minimum of $0.87(10^{-5})\,cm^2/sec$ for Colorado clay loam.

The calculated diffusion curve for T = 38 days is plotted in Figure 1 to give an impression of the relative contribution of diffusion towards the observed downslope distribution plotted in Figure 1.

The average distance that water molecules moved downslope due to mass transport was calculated in two ways: 1) the displacement downslope of the point at which the average number of molecules occurs is due to mass transport only because movement due to diffusion is equal in all directions. This displacement is assumed to be equal to the activity weighted average downslope movement of the tritium obtained through the use of Figures 1 and 2. It was calculated to be at a distance of 9.02 cm directly downslope from the injection point. Because it required 38 days for the average water molecule to move that distance, the rate of water flow is 0.24 cm/day. 2) If it is assumed that the molecules upslope from the peak of the activity curve in Figure 1 have moved upslope only through the process of diffusion, it is possible to calculate the displacement of the peak of the activity due to mass transport alone. The activity at the center of the curve after 38 days due to diffusion alone, would be $8.5(10^6)$ dpm/ml. We know the activity at some offset distance, r, from the source after 38 days is $3.5(10^6)$ dpm/ml (from Figure 1). Therefore, from Eq. 1, r = 8.382 cm, and the rate of water movement is 0.22 cm/day.

Vertical Movement of Soil Water

High moisture conditions

For this experiment, zero tension lysimeters[4] were used to collect water moving through saturated soil. These lysimeters are troughs one foot in length and two inches deep, and connected by tubing to collection jugs. The lysimeters are installed in narrow tunnels bored horizontally from a pit adjacent to the experimental plot. Two lysimeters were installed at each of four depths: beneath the litter, and at 5, 10, and 15 inches. Tunnels and pit were filled in after installation.

On April 13, 1970 40 mCi of tritium in 6 liters of water were sprinkled uniformly over an area 73.7 cm by 261.6 cm above the bank of lysimeters.

Collection jugs were pumped out weekly, and the water was analyzed by standard liquid scintillation techniques.

During the data analysis, it became apparent that concentrations of tritium in the lysimeters closest to the edge of the plot were lower than those towards the center, probably because of diffusion of tritium away from the plot, and for that reason only the data from the innermost lysimeters were used.

Activity as a function of depth at a series of times after tritium application is shown in Figure 4. Curves connect data points, but the shapes of the curves were adjusted so that a single exponential function could describe the amount of tritium in the soil as a function of the time since application, for the early spring period. The function is

$$Y_t = Y_0 e^{-0.693t}$$

where

Y_t = amount of tritium in the soil at a given time

Y_0 = amount of tritium initially in the soil

t = time in weeks.

The movement of the peak of tritium activity shown in Figure 4 is interpreted as follows: The peak moves downward during each storm in proportion to the amount of rainfall after the soil above the peak reaches a saturation value (about 42%). Regardless of whether it is raining, tritium continually diffuses away from the peak in an

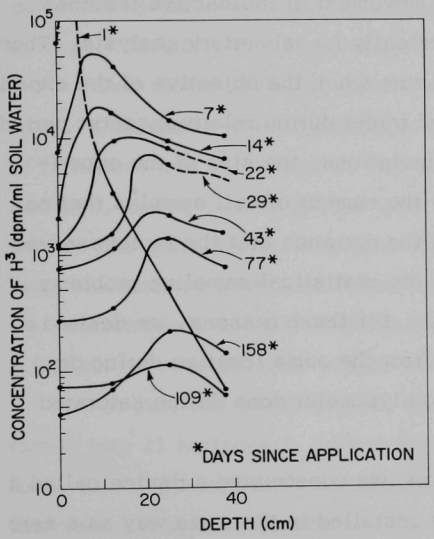

FIG. 4.--Concentration of tritium in the soil water as a function of depth at a series of times after the start of the experiment. Lines are drawn to connect data points. Where curves had to depart drastically from the data (days 1 and 29) for reasons explained in the text, or where data were missing (day 22), lines are dashed.

upward and downward direction. During rains the upper layers of soil are wet first, and that tritium which has diffused upward is washed down towards the peak before the tritium at the peak is carried further down. If the rain is relatively light, the tritium located at or near the peak may not be moved, but tritium would be moved toward the peak from above. Although tritium is continually moving out the bottom of the upper soil horizons, the peak in Figure 4 seems to be immobilized at approximately the 10-inch depth because during an average rainstorm, more tritium is carried toward the 10-inch level than is carried away from it.

Low moisture conditions

A common procedure for tracing movement of radioactive isotopes through soil is to sample the soil periodically for laboratory analysis. There are several disadvantages to this procedure when the objective of the experiment is to follow an artificially injected tracer during relatively short periods of time. Because of radiation hazard limitations, the size of the experimental plot is small, and consequently the number of soil samples that can be taken is limited. In addition, when the distance that the isotope moves is small in relation to the size of the plot, statistical sampling problems arise due to inhomogenieties of the soil. For these reasons, we desired a device that would yield water samples from the same location during dry periods in the same way the zero tension lysimeter does during saturated soil conditions.

After a season of experimentation, we constructed a device called a "cold pipe condenser" (Figure 5). It is installed in the same way as a zero tension lysimeter, that is, in horizontal tunnels at various depths extending from a pit adjacent to the experimental plot. Alcohol is pumped through coils in an alcohol-dry ice mixture in a container above ground, and then through tubing down and into the device through insulated intake tube A. The entire device is supported by tube B. The cold alcohol circulates through pipe C and out through tube D. After about 30 minutes in warm weather, or several hours in cold weather, when the absolute water content of the soil air is lower, the intake is changed to a source of warm alcohol. The ice on

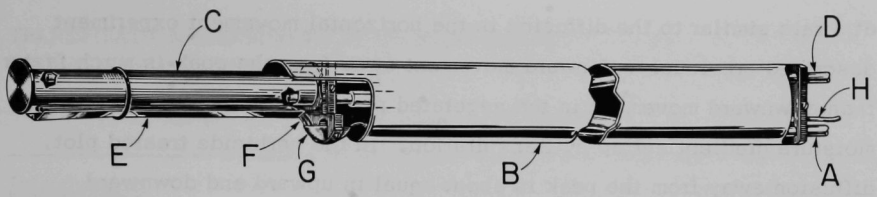

FIG. 5.--Cold pipe condenser. Overall length is 3 feet (91.44 cm), and length of the condenser, C, is one foot (30.48 cm).

pipe C melts, and the water runs down into trough E. Flow into collection cup G is aided by the capillary effect between the bars F. Water is then collected by drawing it out through capillary tube H into a hypodermic syringe. Sample volume is usually 1 to 2 ml.

Two plots, each one square meter, were designated for the experiment. Cold pipes were installed in each plot as follows: Two at a depth of 2 inches, two at 10 inches, two at 18 inches, and one at 26 inches. In addition, during each cold pipe run, water vapor above the plots was condensed and collected by additional cold pipes in transparent boxes, and vegetation samples were collected for analysis of tissue water. One plot was undisturbed, and the other was treated with herbicide to determine the influence of vegetation on tritium movement in the soil.

On July 14, 1970, in each plot, 20 mCi of tritium were injected uniformly into 21 horizontal, 1/8-in diameter holes, 5 cm apart and one meter long, at a depth of 6 inches. Cold pipe samples were collected at one-week intervals through the autumn of 1970. Data analysis is not yet complete, but a pattern is emerging. Just as in the previously described lysimeter experiment, the peak of tritium moves downward only when there has been sufficient rain to saturate the soil down to the depth of the peak. Because the herbicide treated plot suffered no transpirational loss, soil moistures are greater than in the vegetated plot, and a greater downward movement of the peak occurs in the herbicide treated plot in response to a rainstorm. Between rains in both plots, tritium diffuses downward away from the peak

at a rate similar to the diffusion in the horizontal movement experiment described previously. Upward movement away from the peak is much faster than downward movement in the vegetated plot, apparently because of the moisture gradient set up by transpiration. In the herbicide treated plot, diffusion away from the peak is about equal in upward and downward directions.

References

1. Koranda, J. J., J. R. Martin, and R. Wikkerink. Residual tritium of Sedan Crater, Part II. Soil and Ejecta Studies, U.S. Atomic Energy Commission Report UCRL-50360 (1967).
2. Brees, D. R. and E. R. Graham. The effect of soil texture and organic matter on the self-diffusion coefficient of tritiated water in Missouri soils. Soil Sci. 108, 165-169 (1969).
3. Nakayama, F. S. and R. D. Jackson. Diffusion of tritiated water in soils. Soil Sci. Soc. Am. Proc. 27, 255-258 (1963).
4. Jordan, C. F. A simple, tension-free lysimeter. Soil Sci. 105, 81-86 (1968).

TRANSPIRATION MEASUREMENT IN PINES USING TRITIATED WATER AS A TRACER

J. R. Kline, C. F. Jordan, and R. C. Rose*

Introduction

The measurement of transpiration of water by plants in the field is a problem which has not been solved, and yet this is one of the important variables needed in attempts to evaluate and quantify ecological theory, hydrological budgets, or compute plant moisture consumption in situations such as the irrigation of crops where water is a scarce resource. Approximations to transpiration or evapotranspiration have been obtained by tent methods, the cut leaf methods, heat pulse methods, or watershed balance techniques.[1,2] Recently, Taylor and Gates[3] proposed a modification of the cut leaf method which involves remote measurement of black body leaf surface temperature of both leaves which have been excised for weight loss determination and those which remain attached to the plant. Equal surface temperatures of both are taken to indicate that both are losing water at the same rate. Equations are given for correction of the loss rate from non-excised leaves when the surface temperatures are not equal. This method would require measurements on many leaves and a knowledge of the total leaf surface area of the plant for estimation of total water consumption rate by the plant.

Penman,[4] Thornthwaite,[5] and Blaney and Criddle,[6] working on evidence that transpiration is closely coupled to the regional energy budget, have proposed equations relating evapotranspiration, which is the sum of evaporation and transpiration, to such meteorological variables as temperature or, in some cases, humidity, solar radiation, wind speed, and rainfall. Pelton and Korven[7] have recently examined the approaches of these authors and found both the Thornthwaite and Blaney-Criddle methods inadequate for predictions of daily evapotranspiration but able to predict

---

*Honors student in the Radiological Physics Division during the summer semester, 1970.

weekly values with reasonable accuracy for alfalfa in a semiarid climate. The Penman method accounted for 65% of the daily variation in evapotranspiration but requires extensive modification. Total evaporation in the field is often measured in these methods by the use of lysimeters which are normally expensive and delicate instruments. With lysimeters transpiration can be determined by measuring the soil evaporation separately or by eliminating soil evaporation.

Kline, et al.[8] proposed that transpiration by plants in the field could be measured with tritiated water, using the theoretical equations for flow problems which were presented by Orr and Gillespie[9] and which have been reviewed by Bergner[10] for applications in biology and by Ljunggren[11] for applications in engineering. This method cannot be used at this time for measurement of true daily transpiration rates. It gives, instead, average daily rates for whole plants during the interval of the experiment, which may vary from 10 days in mid-summer to 4 weeks in spring and fall. The purpose of the work, reported here in part, is to extend the basic method to the measurement of water consumption by plants on a seasonal basis, to search for improved relationships between transpiration and environmental variables, and to continue development of the basic method, particularly to shorten the time interval of the measurements.

Materials and Methods

Theoretical

The method for determining transpiration rates in trees is based explicitly on the theoretical analysis of tracer dynamics in flowing biological systems which was presented by Orr and Gillespie.[9] Their equation is given by Eq. 1:

$$C = F \int_0^\infty f(t)dt, \qquad (1)$$

where C is the total capacity of the system for the flowing material, F is the flow rate of the material, and f(t) is the fraction of the total initial

tracer which is present in the system at any time subsequent to its introduction. In principle Eq. 1 should make it possible to measure transpiration in trees by injecting them with tritiated water and determining the resulting activity-time curve in some down-stream component of the tree. It is not possible, however, to obtain either the capacity, C, of a tree or the fraction of originally injected activity, f(t), because of the size of trees. Another form of Eq. 1 is given in the review by Ljunggren[11] and is shown in Eq. 2.

$$M = F \int_0^\infty f'(t)dt \qquad (2)$$

where M is the total activity originally injected, F is the flow rate through the system, and f'(t) is the specific activity of the tracer at any time subsequent to its introduction into the system. Equations 1 and 2 are analytically equivalent forms. The transformation from Eq. 1 to 2 has been demonstrated by Kline, et al.[8] The form of Eq. 2 is experimentally convenient, however, since specific activity of tissue water of plants is easily obtained and the amount of activity originally injected is under experimental control. This is the form of the expression which was used in these experiments.

Experimental

Fourteen red pine (*Pinus resinosa*) trees growing in a uniform stand in an introduced plantation on the Argonne site were injected two at a time with tritiated water in known amounts at approximately monthly intervals throughout the growing season of 1970. One milliliter of tritiated water of known specific activity (3.72×10^8 dpm/ml) was pipetted into each of four holes which had been bored at equal spaces around the base of the trees. The total injection was, therefore, 4 ml or 14.9×10^8 dpm. After injection the holes were sealed with a commercial tar-like grafting compound.

Composite needle samples were collected from each tree twice daily for the first week of the experiment and daily thereafter until tritium was no longer detectable in the tissue water. The needle samples were sealed in plastic bags and stored in a deep freeze prior to analysis. Tissue

water was extracted from the needles by a freeze dry technique described by Koranda.[12] The water was counted by standard liquid scintillation counting methods. The results were corrected for background and counting efficiency and were expressed as dpm/ml of the tissue water.

The resulting data for each tree were plotted as a function of time from the initial injection on linear coordinates. The response curves were integrated, and the value of the total integral was used to solve Eq. 2 for flow which in trees is transpiration. Details of the methods for data handling and known sources of error in the method are given in Kline et al.[8]

The trees for this experiment were selected from a closed stand of uniform age (about 18 yr) red pines. The trees varied in height from 6.4 to 7.9 meters and averaged 7.6 meters. The average diameter was 11.6 cm measured 1.9 meters above the ground, and the stand density was 2905 trees per hectare. All trees for the experiment were selected from the interior of the stand.

Results

Transpiration

Transpiration by red pines on the Argonne site for the growing season of 1970 is given in Table 1. The results show a generally increasing transpiration rate in the early part of the season, which continues through late July and then abruptly falls off during the latter part of July, August, September, and October. The increasing early season values are consistent with Penman's view[4] that transpiration is under control of external meteorological factors, such as temperature or solar radiation, when soil water is not limiting. The sharply declining values in August indicate that transpiration control shifts at that time from meteorological factors to a water limited situation in which the available soil moisture limits the rate in spite of the fact that temperature and solar radiation remain high. In the fall of the year control shifts back to meteorological factors since autumn rains tend to restore the moisture. The values at this

TABLE 1. Transpiration in Red Pines at Argonne National Laboratory as Related to Season of the Year and Meteorological Variables[a]

Tree	Time interval of estimate	Transpiration[b] ml/hr/tree	Transpiration[b] cm/day	Mean solar radiation, langleys/day	Mean daily temperature (°C)
A-B	3/30-4/24	436	0.30	410	6.7
1-2	5/5-5/26	913	0.64	498	16.7
314	6/17-6/30	1170	0.82	538	20.3
5-6	7/7-7/20	1108	0.77	512	22.5
7-8	7/21-8/6	569	0.40	526	22.6
9-10	9/1-9/25	219	0.15	320	19.2
11-12	10/8-10/23	371	0.26	237	11.1

[a] Meteorological values were provided by Dr. H. Moses from Argonne Climatological Station data. The data are not taken from the actual forest location but from an open field some 300 yards away.

[b] Values are average of two for each time interval.

time remain low because temperatures and solar radiation are at lower levels than in midsummer. For the year 1970 transpiration was limited by low availability of soil moisture only for a period of 5 to 6 weeks during the late summer.

The onset of transpiration in the spring is not controlled by either meteorological variables or available soil moisture. The primary control at this time is soil temperature. The relationship between soil temperature and the time of onset of transpiration is shown in Figure 1. In the spring frozen soils tend to thaw from the surface downward. As the soils warm a lens of frozen soil remains for a short time between the thawing front advancing downward from the surface and the region below the surface which was never frozen. The final lens of frozen soil remains at approximately 10 cm below the surface. Figure 1 shows that transpiration in red pines began within hours of the time that the final lens of frozen soil reached temperatures above the freezing point. The control of the onset of transpiration by soil temperature is consistent with the view of

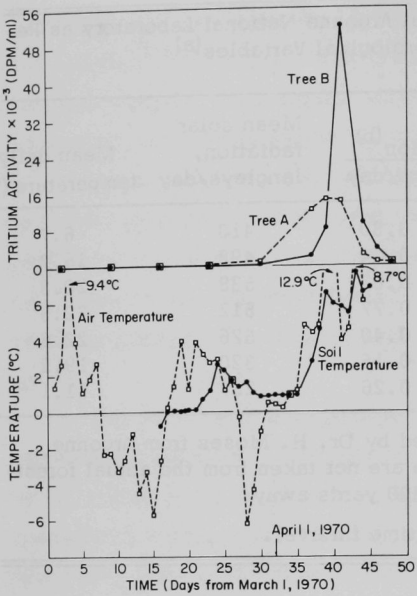

FIG. 1.--Relationship between soil and air temperatures and the onset of spring transpiration in red pines (Pinus resinosa).

transpiration as a capillary flow phenomenon since flow through a capillary cannot take place if any portion of it, regardless of how small, is plugged by ice crystals. Experiments are underway at this writing to determine what factors control the cessation of transpiration by conifers in early winter.

Confirmation of Measurements

Attempts to measure transpiration by individual plants in the field are usually subject to criticism based on the fact that the techniques required alter the quantity measured to a significant but unknown degree. Lysimeters yield the most reliable transpiration data, but these are expensive permanent installations which are restricted in their range of applicability. It is, therefore, difficult, if not impossible, to confirm the tritium method for measurement of transpiration by comparison to some other independent method. Indeed, the purpose of developing this method was that no convenient and reliable alternate method exists. Confirmation of the method by direct independent measurement on field grown plants, which would be the most desirable procedure, is therefore not feasible.

There are numerous approaches to confirmation which are individually less rigorous than direct measurement but which collectively may provide an index of reliability. These approaches can be categorized as 1) examination of the model and its assumption by theory and experiment; 2) performance of controlled but artificial experiments and comparison with data

of other investigators; and 3) indirect methods.

We have previously examined several sources of error in the first approach (Kline et al.[8]). These include theoretical and practical problems of complete mixing assumptions, the isotopic mass effect, and pathway assumptions. Details of this analysis will not be repeated. A serious source of error has recently been found, however, which has not been discussed in this context elsewhere. This is related to the assumption that tritium escapes from the tree via only one pathway, that being the transpiration stream. In reality it apparently also escapes by isotopic or molecular exchange with atmospheric water vapor. This was demonstrated by comparison of the specific activity of tritium in pine needles with that of the woody twigs on which they were growing. The expected value of A_n/A_w, the needle-to-wood activity ratio, where no isotopic exchange takes place is 1.0-1.1 because tritiated water has a lower vapor pressure than ordinary water.[13] Experimental values of the above ratio average about 0.65 during the summer months but varied from 0.9 during dry (low humidity) conditions to 0.5 during rainy conditions. The use of uncorrected specific activities from foliage would have the effect of decreasing the integral of the activity-time curve and increasing the estimate of transpiration relative to the true value. While the error is serious if neglected, it can be corrected by simple experimental methods. The data of this report are corrected for the average value of A_n/A_w, which values were collected simultaneously with the routine foliar sampling. In other situations the corrections could be avoided by simply using specific activity of water in twigs as the primary response variable since these have little contact with environmental water vapor.

One controlled experiment involving plants grown in pots has been performed, but data have not yet been analyzed. Results of this and other experiments which are being contemplated will appear in a subsequent progress report. Directly comparable results of other investigators are difficult to interpret. Penman,[4] for example, has given transpiration values in the mid-western region for a variety of vegetation types under

conditions where ground cover is complete and transpiration is at a maximum. His values range from 0.25 to 0.35 inches/day, or an average of 0.76 cm/day. Our values are 0.82 and 0.77 cm/day for June and early July, respectively, during periods when soil moisture availability was not rate limiting. Penman's data incidate that when ground cover is complete, transpiration rate is not strongly related to vegetation type. Thus, the foregoing comparisons may have validity even though the vegetative cover is different.

Rutter[14] has tabulated a large number of estimates of forest transpiration, none of which are rigorously comparable with values in this report. For a forest growing under negligible water deficit in Australia, Rutter gives total evaporation values ranging from 684 to 861 mm for the annual evaporation. The 1970 Argonne values for transpiration from April 1 to October 31 is 892 mm. The precipitation during this period was 857 mm which exceeds the 15-year average input for this period by 43.3%.[15] Rutter gives average daily transpiration of spruce and Douglas fir of 5.4 and 5.3 cm/day. The comparable figure for the Argonne red pines for a 200-day period is 4.45 mm/day. It is apparent that literature values can be used only to establish the order of magnitude of transpiration. The values obtained by the proposed method agree well with the tabulated ones, however, and establish that this method is at least as reliable as those which have been in previous use.

An indirect method of validation has recently been developed which is sufficiently important to be dealt with separately in the next section.

Measurement of Plant Biomass

In the equation of Orr and Gillespie the term C is called capacity, which in trees is simply the total water content of the tree. This is also given by the difference between the wet and dry weight of the tree. Thus, the equivalences of Eq. 3 can be stated:

$$C = (W - D) = Wm = F \int_0^\infty f(t)dt, \qquad (3)$$

where W is wet weight, D is dry weight and m is plant moisture percentage. The total integral of the activity-time curve in the above expression can be interpreted as being the mean residence time, T, of water in the plant. Under certain conditions the mean residence time can also be derived from the slope of the exponentially declining response curves of activity versus time. This is not universally true but approaches truth when the system is well mixed, when the initial time of mixing of the tracer is short with respect to the mean residence time, and when the slope of the curve is described by a single exponential function. Neither the extent to which these conditions are obtained in trees nor the sensitivity to deviations from ideal conditions is known at this time. Nevertheless there is reason to believe that the slope of the declining response curve is a limiting approximation of the mean residence time which would be given by the integral of the fractional activity time curve if it could be obtained. With these assumptions, Orr and Gillespie's equation can be transformed to give Eq. 4.

$$W = \frac{T}{m} F, \tag{4}$$

where T is the mean residence time of water in the plant, and the other variables are as defined in Eq. 3. Equation 4 is a modified version of one obtained by Zierler[16] for application to such problems as determination of blood volume in animals.

Equation 4 makes it possible in principle to measure the total weight of a tree nondestructively. This is of significance for two reasons. First, the calculated weight of the plant depends on the transpiration rate, which is given by the tritium method. Since the tree can be independently cut down and weighed, agreement between calculated and observed weight is evidence that the transpiration rate is correct. Second, the weight of a tree is itself a valuable quantity. As in almost all other areas of quantitative biology it frequently becomes necessary for an investigator to weigh the organism with which he is working. If the organism is a large tree, obtaining its weight presents some difficulty. In practice this can only be

resolved by cutting and weighing the tree although many attempts are made to obtain correlations between weights and tree dimensions so that all trees in a stand can be estimated (see Ogawa et al.[17] and Young et al.[18] for example). Correlations obtained by this method are at best valid only where they were established, and reviewers of manuscripts are justifiably critical when attempts are made to apply empirical equations from one location to plants in another, even if the same species are involved.

Eight red pines from the Argonne site which had received tritium injections were cut down and weighed in total, including roots. Tree biomass was calculated using Eq. 4. Comparisons between observed weights and calculated weights are given in Table 2. The results indicate generally good agreement, with some exceptions, between calculated and observed weights.

TABLE 2. Comparison of Directly Observed Tree Biomasses with Those Calculated by the Tritium Method

Tree	Measured dry biomass, kg	Calculated dry biomass, kg	Deviation from measured, %
1	21.3	16.9	-20.6
3	49.4	54.5	10.3
4	13.8	16.2	17.4
5	29.4	31.5	7.1
6	41.0	43.1	5.1
7	32.6	24.0	-26.4
8	13.6	13.7	0.7
10	23.6	22.5	- 4.7

It appears that the method of estimating weights by the tritium method is unbiased although at present the variability is greater than desired. When the calculated weights of trees agree repeatedly with observed weights, the assumptions required for Eq. 4 are substantiated. In particular, agreement tends to confirm the observed transpiration rate for that tree. When agreement in weights is poor, however, this does not necessarily imply equally poor estimates of transpiration since the quantities T and m could also be

in error.

Conclusions

It is concluded that the tritium method for estimating plant water consumption and plant biomass in the field is sufficiently promising to warrant further developmental work to eliminate experimental sources of error so that the method can be routinely applied. Water consumption by plants is one of the fundamental life processes. Many ecological theories relating to the distribution of plants on the earth's surface, for example, depend heavily on knowledge of the availability and use of water by plants. Quantification of theory depends in part upon the ability to measure water consumption directly with precision. Wide application of the method depends on its being simple to use, versatile, and precise. The tritium method with further development may meet these criteria well enough to make significant contributions in plant water research.

References

1. Slatyer, R. O. Plant-water Relationships. Academic Press, New York, 1967.
2. Kozlowski, T. T. Water Deficits and Plant Growth. Vol. II. Academic Press, New York, 1968.
3. Taylor, Elwynn S. and David M. Gates. Some field methods for obtaining meaningful leaf diffusion resistances and transpiration rates. Ecol. Plant. V, 103-112 (1970).
4. Penman, H. L. Vegetation and Hydrology. Tech. Comm. No. 53, Commonwealth Bureau of Soils, Harpenden (1963).
5. Thornthwaite, C. W. An approach toward a rational classification of climate. Geog. Rev. 38, 85-94 (1948).
6. Blaney, H. F. and W. D. Criddle. Determining water requirements in irrigated areas from climatological and irrigation data. USDA Soil Conserv. Serv. Tech. Pub. 96 (1950).
7. Pelton, W. L. and H. C. Korven. Evapotranspiration estimates in a semiarid climate. Can. Agricultural Eng. 11 (2), 50-53 (1969).
8. Kline, J. R., J. R. Martin, C. F. Jordan, and J. J. Koranda. Measurement of transpiration in tropical trees with tritiated water. Ecology, 51 (6), 1068-73 (1970).
9. Orr, J. S. and F. C. Gillespie. Occupancy principle for radioactive tracers in steady state biological systems. Science 162, 138-39 (1968).

10. Bergner, P.-E.E. Tracer Theory: A Review. Isotopes and Radiat. Tech. 3 (3), 245-262 (1966).
11. Ljunggren, K. A review of the use of radioisotope tracers for evaluating parameters pertaining to the flow of materials in plant and natural systems. Isotopes and Radiat. Technol. 5 (1), 3-24 (1967).
12. Koranda, J. J., J. R. Martin, and R. Wikkerink. Residual tritium of sedan crater. Part II. Soil and ejecta studies. U.S. Atomic Energy Commission Report, UCRL-50360 (1967).
13. Jacobs, D. G. Sources of tritium and its behavior upon release to the environment. U.S. Atomic Energy Commission Report, TID-24635 (1968).
14. Rutter, A. J. Water consumption by forests. Water Deficits and Plant Growth, Vol. II, Ed. T. T. Kozlowski. Academic Press, New York, 1968, pp. 23-84.
15. Moses, Harry and Mary A. Bogner. Fifteen-year climatological summary, January 1, 1950-December 31, 1964. Argonne National Laboratory Report, ANL-7084 (1967).
16. Zierler, K. L. Basic aspects of kinetic theory as applied to tracer distribution studies. Dynamic Clinical Studies with Radioisotopes. Ed. R. M. Kniseley and W. N. Tauxe, U.S. Atomic Energy Commission, Washington, D. C. 1964, pp. 55-79.
17. Ogawa, H., K. Yoda, K. Ogino, and T. Kira. Comparative ecological studies on three main types of forest vegetation in Thailand. II. Plant biomass. Nature and Life in Southeast Asia, IV, 49-81 (1965).
18. Young, Harold E., Lars Strand, and Russell Altenberger. Preliminary fresh and dry weight tables for seven tree species in Maine. Maine Agric. Expt. Sta. Tech. Bull. 12 (1964).

RECENT TRENDS IN RADIOACTIVE FALLOUT

P. F. Gustafson, D. M. Nelson, S. S. Brar,
and S. E. Muniak

Continuing measurements of gamma-emitting radionuclides in air, soil, and foodstuffs collected in the Chicago area form the basis for the study of the long-term behavior of radioactive fallout. Identification of the spring maximum in fallout deposition, assessment of the radiation dose due to short-lived gamma emitters, and the major contributors of dietary ^{137}Cs are among the outputs of this program.[1-3]

The modest, yet fairly steady, rate of nuclear testing in the atmosphere by China and France has maintained fallout rates at about 10 percent of the maximal levels seen in 1962-1964. This is illustrated in Figure 1 where the average monthly concentration of ^{137}Cs in surface

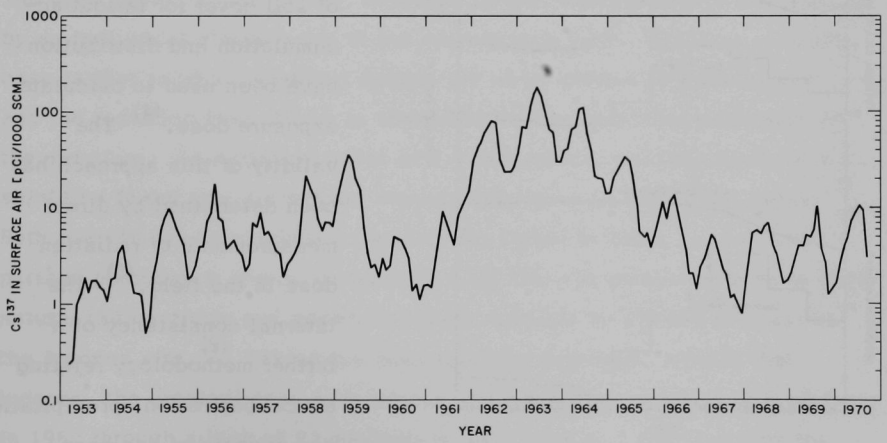

FIG. 1.--Fallout ^{137}Cs in surface air collected at Argonne National Laboratory 1953 to mid-1970.

air collected at Argonne from 1953 (the essential beginning of world-wide fallout) through mid-1970 is shown. The annual maximum clearly evident each year is termed the spring maximum, although in the early 1960's it shifted to early summer, and in 1969 the highest value in surface air occurred in August. Whether the variations in the time of the maximum are related to global meteorological conditions, or reflect more local conditions remains to be proved.

A maximum accumulation of ^{137}Cs on the ground, amounting to about 130 mCi/km^2, was reached during 1965-66 in the Chicago area (Figure 2). Since that time radioactive decay of ^{137}Cs on the ground has exceeded the input from deposition, which has ranged from 1 to 2 mCi/km^2/yr since 1966. The annual average ^{137}Cs content of the adult diet in the Chicago area, expressed in pCi/g K, and the resultant internal exposure, are also shown in Figure 2. As expected, the ^{137}Cs level in foods follows the upward trend in ^{137}Cs deposition during 1967-1970.

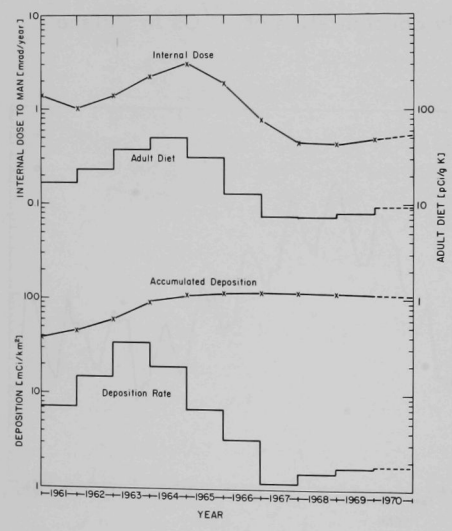

FIG. 2.--Fallout ^{137}Cs deposition rate, accumulation, dietary levels, and dose to man in the Chicago area 1961 to mid-1970.

Radioactive analyses of soil cover for fallout accumulation and distribution have been used to calculate exposure dose.[4] The validity of this approach has been determined by direct measurements of radiation dose in the field.[5] The internal consistency of a further methodology relating air concentration, precipitation, and deposition has been established, and is used to calculate deposition and exposure without the necessity

TABLE 1. External Radiation Exposure from Fallout, Argonne National Laboratory

Year	Open field dose, mR/year	Shielded (indoor) dose, mR/year
1960	8	3
1961	25	10
1962	38	15
1963	56	22
1964	26	10
1965	21	8
1966	16	6
1967	13	5
1968	12	5
1969	13	5

Note: External exposure dose from natural background (radioactivity in soil plus cosmic radiation) is 108 ± 8 mR/year at the Argonne site.

of analyzing soil samples.[6] The annual external exposure from radioactive fallout is presented in Table 1 for the years 1960 through 1969. The open field, or unshielded, exposure is that which would be experienced by an individual standing out in the open for one year. The more realistic case is that in which a person spends the major portion of time indoors, and the radiation from fallout is attenuated by the shielding properties of the structure. An empirical value of 2.5 (40 percent transmission) for the shielding factor was derived for various structures on the Argonne site.[2] Both open field and shielded exposures are listed in Table 1. For comparison purposes it should be borne in mind that the external exposure from natural radioactivity and cosmic radiation amounts to 108 ± 8 mR/year at the Argonne site.[5] Taking the more relaistic exposure, namely that indoors, the external dose from fallout has ranged from a value of 3 mR/year in 1960 through a high of 22 mR/year in 1963 back to 5 mR/year over the past decade.

References

1. Gustafson, P. F., S. S. Brar, and M. A. Korrigan. Science 133, 460 (1961).
2. Gustafson, P. F. Radiology 75, 282 (1960).
3. Brar, S. S., P. F. Gustafson, and S. E. Muniak. USAEC Health and Safety Lab. Report HASL-146 (1967), p. 225.
4. Gustafson, P. F. and S. S. Brar. Proc. Intern. Symp. on the Natural Radiation Environment, Rice Univ., Houston, Texas, April 11-13, 1963, 499-512 (1963).
5. Gustafson, P. F., J. Kastner, and J. Luetzelschwab. Science 145, 44 (1964).
6. Gustafson, P. F., S. S. Brar, and S. E. Muniak. Proc. AEC Fallout Conf., Germantown, Maryland, Nov. 1964, 497-506 (1964).

HIGH ALTITUDE RADIOACTIVITY MEASUREMENTS MADE FROM THE ARGONNE SITE

P. F. Gustafson and R. B. Keener*

In late 1968 a surplus GMD-1 (Ground Meteorological Detector) receiver and tracking system was obtained on surplus from the U.S. Air Force Logistics Command (AFLC) at Tinker Air Force Base, Oklahoma City, Oklahoma. The unit had seen use in the Far East, and although in a non-operating state, the equipment was deemed to be repairable. The GMD is used to track radiosonde balloons and receive pertinent meteorological data from such balloons. Modifications in the receiving circuit have made it possible to use the radiosonde transmitter to convey pulse data from a radiation detector carried by the balloon to the ground. The particulars of this system called GIGI have been discussed elsewhere.[1]

In the past a number of GIGI flights have been made at various points on the globe, but always away from Argonne because of the lack of GMD equipment here. Replacement parts for the equipment were hard to obtain here, but the system was given a thorough overhaul, and all repairs were made. The seven-foot dish antenna was mounted on the roof of Building 929 in the old Nike site, and the receiving equipment was located in the building itself. All the balloon inflation and launching paraphernalia (including balloons themselves) were assembled. A first test of the whole system using a conventional radiosonde was conducted during the week of October 12. This coincided, quite by accident, with the detonation on October 14, 1970, of a nuclear device in the atmosphere by the Chinese at their test site at Lop Nor.

Several GIGI flights were made from the Argonne site commencing on October 16. The equipment functioned well, and burst altitudes of between 92 and 105,000 feet were attained. A typical radiation intensity

*Electronics Division, ANL.

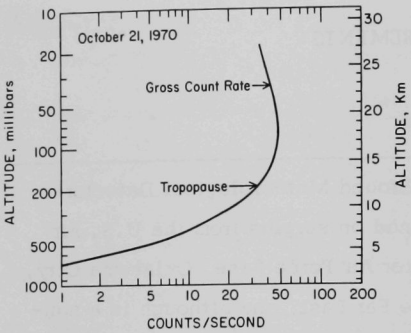

FIG. 1.--Gross count rate profile obtained from GIGI flight on October 21, 1970, from Argonne National Laboratory.

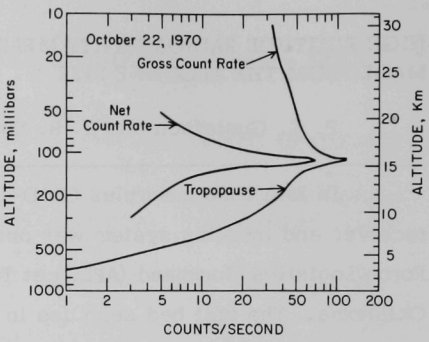

FIG. 2.--Gross count rate profile and net count rate showing fresh fission debris during GIGI flight on October 22, 1970, from Argonne National Laboratory.

versus altitude profile is shown in Figure 1. On October 22, a reasonably intense layer of radioactivity was observed at 49,000 feet as illustrated in Figure 2. Trajectory plots by NOAA (formerly ESSA) of the air mass enclosing the cloud from the nuclear test indicated that the bulk of the debris passed well north of us, and at considerably higher altitude. What is seen in Figure 2 is the southerly fringe of the main cloud. However, it points out the feasibility, indeed capability, for making high altitude measurements from our home base.

Reference

1. Gustafson, P. F. and R. B. Keener. J. Geophys. Res. 70, 5323 (1965).

A SEMIAUTOMATIC METHOD OF NEUTRON ACTIVATION ANALYSIS WITH APPLICATION TO ENVIRONMENTAL STUDIES*

D. N. Edgington and H. F. Lucas, Jr.

Introduction

Neutron activation analysis is a very important technique for the study of problems arising in environmental pollution as the sensitivity of this method allows detection limits of a nanogram or less for a large proportion of the elements in the periodic table. Sensitive methods for the analysis of trace elements are important because it appears that the recognition of a particular element as either toxic or essential in the biosphere, is not far removed from the development of improved techniques.[1]

Neutron activation analysis as a technique has undergone considerable refinement and development, especially during the last twenty years. This has been due, for the most part, to the revolution in electronics. Little more than ten years ago thallium-activated sodium iodide crystals and transistorized 400- or 512-channel pulse height analyzers were introduced so that precise techniques of gamma-ray spectrometry could be developed. More recently the introduction of large lithium-drifted germanium semiconductor detectors and 4096-channel pulse height analyzers has allowed the development of extremely high resolution gamma-ray spectrometric techniques.[2,3] With the introduction of each new development in instrumentation, there has been the claim that now the necessity for chemical separations has been eliminated, and completely instrumental activation analysis is feasible.[4] Unfortunately, for those who have to deal with environmental or biological samples, this is not the case, and more often than not extensive chemical separations are necessary, even when using the lithium-drifted

* Paper presented at IAEA symposium on the Use of Nuclear Techniques in the Measurement and Control of Environmental Pollution, Salzburg, Oct. 26-30, 1970.

germanium detector.

In the field of environmental studies it is now necessary to analyze a large number of samples for a wide range of trace constituents. In this situation the effort required in manpower, equipment, and time per analysis is critical and the choice of technique becomes paramount. Assuming (not easily defendable in many instances) that neutron activiation is the best method of analysis, several questions remain to be answered. These will include the degree of radiochemical group separation required, the type of detector, and its associated computational technique. The method of group separation may be simple or complex and depends on the number of components sought, their relative activities, half-lives and possible interferences. The choice of the detector, and with it the computational method, is more difficult. For each detector there is an optimum or best computational method which should be used. The best statistical methods of data reduction require that a computer be available.

If the activities of the components sought are great enough, the choice should go to the most sophisticated instrumental system available. However, for most environmental samples, using moderate irradiation times in conventional research reactors, the induced activities of interest are often very low. This fact, coupled with the requirement that it is necessary to analyze large numbers of samples, means that the time available for counting each sample is limited so that the detection efficiency of the counter becomes an important factor.[5] Under these conditions, it is very difficult to ignore the merits of the sodium iodide detector systems, particularly when the accuracy and precision of the analysis of the resultant gamma-ray spectra by a routine rigorous statistical technique equals that obtainable using far larger counting periods with the lithium drifter germanium system and equally sophisticated statistical methods.

The procedures described in this paper have been developed over a period of years, and analyses for twenty or more elements in one irradiated sample are made routinely on a wide range of environmental materials.

These analyses have included samples of human bone, soft tissue, and blood, marine algae, freshwater fish, sediments, and vegetation. The analytical scheme includes complete dissolution of the sample where possible, separation into groups of nuclides using automated ion-exchange techniques, and counting using a completely automatic sodium iodide gamma-ray spectrometer.

Experimental

A complete generalized diagram of the total scheme of analysis is shown in Figure 1.

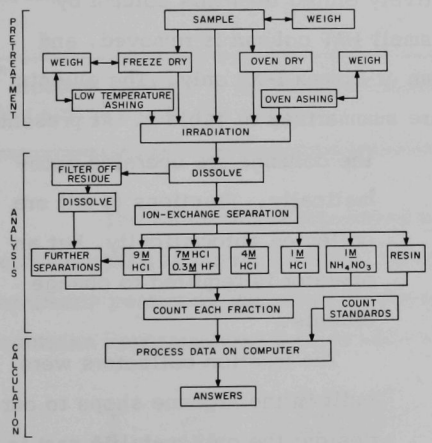

FIG. 1.--Flow diagram of the scheme of analysis.

Pretreatment of Samples

The pretreatment applied to any sample is highly dependent on the particular elements being sought and on the type of sample. In general, freeze drying of soft tissue or vegetation followed by low temperature ashing (ashing using atomic oxygen produced by an inductive discharge in which the temperature of the sample remains less than 100° C) has provided a residue which dissolves readily in concentrated hydrochloric acid after irradiation. In plant materials often a siliceous residue is observed which is filtered off and treated separately. This method is very satisfactory unless the elements sought are volatile. This is the case for mercury in fish (the mercury being present as methyl mercuric chloride).[6] In order to prevent losses, the samples are irradiated frozen and wet ashed under reflux using aqua regia. However, for most heavy metal elements this does not appear to be a problem.[7]

The ashing of the sample before irradiation obviates the wet-ashing of the samples when they are radioactive and also allows the separation to be carried out much sooner.

Radiochemical Separations

The details of the scheme used for radiochemical separations have been published elsewhere.[8] A diagram of one of the semiautomatic ion-exchange columns is shown in Figure 2. A recent modification to the scheme has been the addition of a short column of hydrated antimony pentoxide (HAP) ahead of the column of Dowex 1-X8 to remove sodium from the feed solution. The feed solution is in 9M HCl and under these conditions only sodium, protactinum, and tantalum are reported to adsorb on the HAP. However, these latter two elements are quantitatively eluted from this column by 7 M HCl + 0.3 M HF. At this time the small HAP column is removed, and elution continues from the larger column of Dowex 1-X8 only. The eluents used and the elements found in each are summarized in Table 1. At present the columns are operated automatically. Fractions (5 ml) are collected automatically, but an operator is required to change eluents.

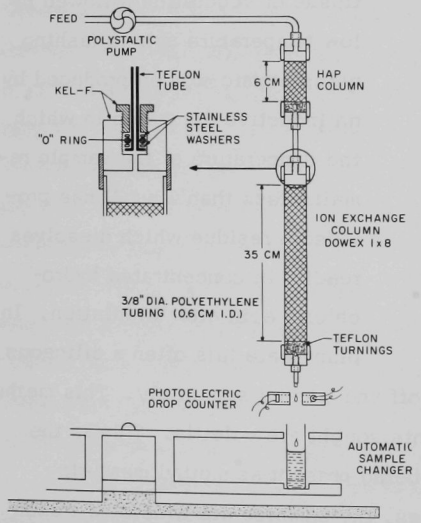

FIG. 2.--Line drawing of one of the semiautomatic ion exchange columns.

The fraction collectors were built in the Argonne shops to our design; the only metallic part is the motor which is enclosed in a polymethacrylate shield. Indexing of the turntable is achieved photoelectrically, and the main shaft is locked by an internal relay when the motor is not energized. The unit is controlled using solid-state devices and has proved to be very reliable.

TABLE 1. Elements Found in the Various Fractions from the Ion-Exchange Separation Scheme

Eluent	Elements found*
9 M HCl	Alkali, alkaline earths, rare earths, As (as As V), Sc, Cr (as Cr^{3+}), Mn, Ni P (as phosphates), $SO_4^{=}$
7 M HCl, 0.3 M HF	Pa, Np, V, Zr, Nb, Hf, Ta
4 M HCl	Co, Cu, Cr, As (as As III), Se, W
1 M HCl	Fe, Ga, Mo
1 M NH_4NO_3	Zn, Cd, In, Sb (as Sb V), Re
Resin	Tc, Ag, Sb (as Sb III), Te (as Te IV), Au, Hg

*Bromine appears in all fractions unless it is removed prior to absorbing the activity onto the column.

The columns are fabricated of 1-cm polyethylene tubing. The small column contains approximately 2 ml of a slurry of 40-to 60-mesh hydrated antimony pentoxide (prepared by the method of Morrison[9]); the larger column contains approximately 8 ml of 100- to 200-mesh Dowex 1-X8 resin. The connections between the peristaltic pump and the columns and between columns are made with Teflon tubing using pressure-tight connectors made of Kel-F to withstand the strong acids. Eluents are pumped through these columns at approximately 0.75 ml/min. The separation procedure

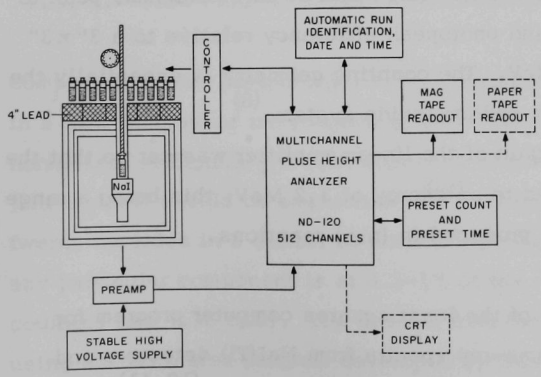

FIG. 3.--Line and block diagram of the gamma-ray spectrometer.

is completed in less than six hours.

Gamma-Ray Spectrometry

A block diagram of the automatic gamma-ray spectrometer is shown in Figure 3. The sample changer unit was supplied by Nuclear Chicago and adapted for our use. The data reported in this paper were obtained using a 4" X 2" (NaI(Tl) crystal. Details of the electronics and the low-background counting room have been given elsewhere.[8] The gamma-ray spectra are read out of the analyzer directly onto computer-compatible magnetic tape together with our identifying tag word which includes run number, year, day of year, and time of start of accumulation of count. The sample is changed while the data are transferred to magnetic tape.

An essential feature of the system is the ability to change the duration of count depending upon the count rate. The analyzer was modified by adding a countdown scaler ahead of the analog-to-digital converter which can be preset to different values of total counts. A maximum counting time or number of counts is set and the analyzer goes to the read-out mode when either of these preset conditions is exceeded.

The high-resolution gamma-ray spectra were obtained using a counting system consisting of a 22-cc Ge(Li) detector (Ortec), an Ortec preamplifier, an active filter amplifier, and a Geoscience 4096 multichannel analyzer. The resolution was 2.9 keV full width at half maximum, peak to Compton continuum was 21, and photopeak efficiency relative to a 3" x 3" NaI crystal was 3% at 1.33 MeV. The counting geometry is essentially the same as that described for the sodium iodide system.[8]

In both systems, the gain of the linear amplifier was set so that the maximum channel corresponded to an energy of 3.2 MeV, this being a range which includes most nuclides produced in (n,γ) reactions.

Data Processing

A detailed description of the least squares computer program for the resolution of complex gamma-ray spectra from NaI(Tl) detectors and a discussion of its capabilities has been given elsewhere.[10,11] The program utilizes a weighted non-linear least squares technique with

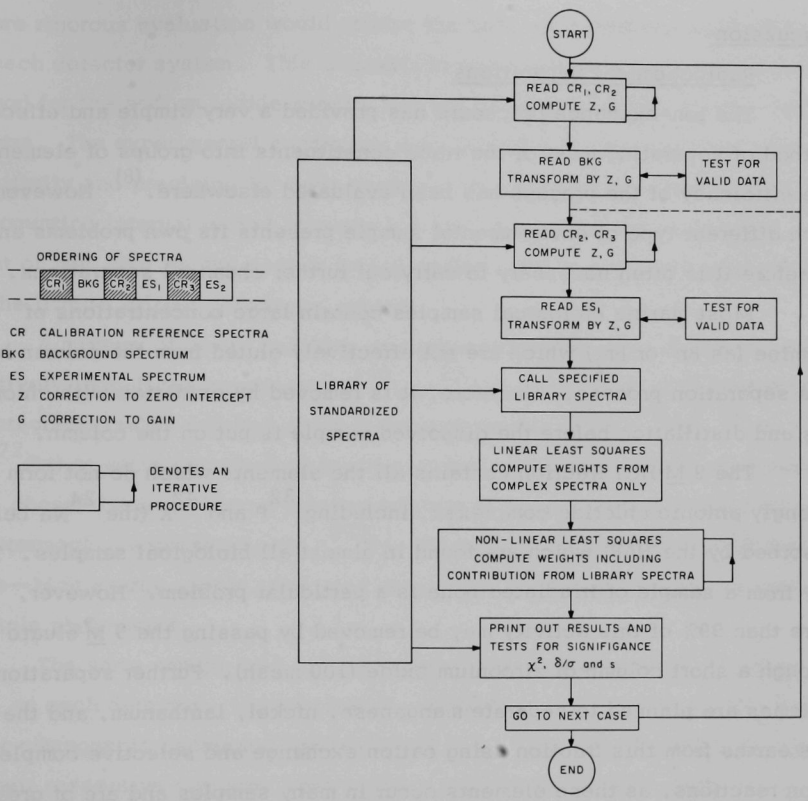

FIG. 4.--Flow diagram of the salient features of the least squares program.

compensation for instrumental drift. The salient features are summarized in a flow diagram of the program given in Figure 4. The importance of the normalized residuals δ/σ (del/sigma) in assessing the goodness of fit χ^2 (chi-square) should be emphasized.[11] The program can handle up to twenty nuclides in a gamma spectrum, and the lower limit of detection of any particular component is at 0.5-1% of the total or 10% of the background counting rate (136 cpm). The spectra from the Ge(Li) detector were analyzed using the peak area program developed by Gunnink.[12]

Discussion

Radiochemical Separations

The ion-exchange procedure has provided a very simple and effective method of separating most of the trace constituents into groups of elements. The efficiency of the process has been evaluated elsewhere.[8] However, each different type of environmental sample presents its own problems and therefore it is often necessary to carry out further chemical separations.

Most marine biological samples contain large concentrations of bromine (as Br^- or Br_2) which are not effectively eluted from the column by this separation process. Therefore, it is removed by oxidation with chlorine gas and distillation before the dissolved sample is put on the column.

The 9 M HCl fraction contains all the elements which do not form strongly anionic chloride complexes, including ^{32}P and ^{42}K (the ^{24}Na being adsorbed by the HAP) which are found in almost all biological samples. The ^{32}P from a sample of irradiated bone is a particular problem. However, more than 99% of this activity may be removed by passing the 9 M eluate through a short column of zirconium oxide (100 mesh). Further separation schemes are planned to separate manganese, nickel, lanthanum, and the rare earths from this fraction using cation exchange and selective complexation reactions, as these elements occur in many samples and are of great interest.

Gamma-Ray Spectrometry

The least squares method of resolution of complex gamma-ray spectra is a very reliable technique if the individual components have been recognized. However, it is possible to obtain incorrect answers which appear to give an acceptable χ^2 (chi-square) value and a good fit to the experimental spectrum when using a large ($\simeq 20$) randomly selected list of standard spectra. It is, therefore, good practice to know which nuclides are likely to be present in each spectrum before attempting an analysis.

A careful comparison of the capabilities of the two detector systems was made in order to assess their role in routine environmental analysis. Voigt has made a comparison using the peak area evaluation technique.[13]

A more rigorous evaluation would utilize the best computational technique for each detector system. This comparison was made using the least squares method for the sodium iodide spectra and the peak area method for the Ge(Li) spectra. The experimental conditions were selected to give equal accuracy, sensitivity and precision for each system when counting the same sample. The counting interval varied between 1.6 and 15 minutes (for an integral count of 200,000) for the sodium iodide system, and was always 1000 minutes for the lithium drifted germanium system.

A mixture of seven nuclides was prepared which contained three comparatively long-lived components (^{140}La, ^{233}Pa, and ^{60}Co) at low relative disintegration rates and four short-lived components (^{82}Br, ^{24}Na, ^{64}Cu, and ^{72}Ga) at much greater disintegration rates. The three minor components were chosen because they are representative of three spectral shapes which are commonly encountered, viz, ^{233}Pa--X rays and photopeaks at low energy; ^{60}Co--high energy simple photopeak spectrum; ^{140}La--extremely complex, multiple photopeaks.

The same sample was counted several times over a period of seven days on each detector. In this time the activity due to the four short-lived major components decreased by a factor of ten. The spectra were analyzed by their respective computer techniques. The amount of each minor component had been determined previously, and it was possible to calculate not only the precision but also the accuracy of the results. The accuracy and precision of the determination was not substantially different for the NaI and Ge(Li) systems as the mean ratio of the observed to the true result was 0.99 ± 0.05 and 1.06 ± 0.06, respectively.[14] A higher accuracy and precision are attainable for low energy gamma ray emitting nuclides in NaI(Tl) least squares system. In contrast, for the Ge(Li) system, the expected increased sensitivity at low energy was not observed. This was attributed to the effect of the high energy continuum on the counting statistics. Since the counting times required by the NaI(Tl) system were considerably less than required for the Ge(Li) system to obtain the same sensitivity and accuracy, the NaI(Tl) system is the one of choice.

Applications

Pollution in the Great Lakes has received considerable attention in recent years. This interest was greatly increased after the exceptionally heavy die-off of the alewife (Alosa pseudoharengus) in the spring and early summer of 1967 which made most of the beaches of Lake Michigan unsuitable for recreation. There were many theories proposed to explain this die-off and most of them involved chemical pollutants or lack of essential elements for survival. However, it was obvious that there was a great interest in a subject about which little was known--the concentration of trace elements in the waters and biota of the Great Lakes.

The concentration of seventeen trace elements in seventy-five samples of fish has been analyzed by these neutron activation techniques.[15] The concentration of cobalt showed the least variation among different species and lakes (0.01-0.1 ppm wet tissue) and between the concentration in muscle and liver. The concentrations of copper were more variable, for muscle between 0.4 and 8, and for liver between 1.0 and 128 ppm, respectively. The concentration of copper is 4 to 70 times greater in the livers of predators at the top of the food chain than in those lower down. Cadmium is concentrated in the liver, 0.5-4 ppm,

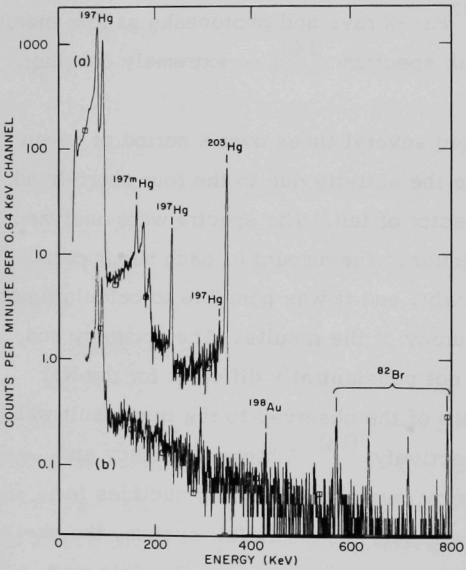

FIG. 5.--Gamma-ray spectra of (a) 50 μg mercury standard and (b) the ion exchange resin fraction for the separation of mercury from a herring caught in Lake Superior.

rather than in the muscle, 0.02-0.4 ppm, but there are no large differences between species. The arsenic levels showed the greatest variation, 0.002-1.0 ppm, but there was little difference among muscle and liver. The large differences found suggest that arsenic is quite variable in the environment or subject to considerable individual variation in uptake and retention.

There is a considerable interest in the concentration of mercury in the environment, and the techniques described in this paper are fast and accurate. Mercury is quantitatively adsorbed on the resin with a few other elements (Table 1) and may be determined with no interferences. The Ge(Li) spectra of a 50-μg mercury standard, and the activity found on the ion-exchange resin in the analysis of a freshwater herring are shown in Figure 5. The spectral lines observed are identified, and it is evident that the spectrum from the herring, which contained 0.25 ppm of mercury, shows this element and weak lines due to gold and bromine.

Mercury levels in fish caught in the Great Lakes vary between 0.02 and 0.5 ppm, but those taken from the St. Clair River near Detroit contain up to 15 ppm. Those caught in Lake Michigan appear to contain less than those from the other lakes.

A parallel study involves the determination of trace elements in lake sediments and water. An area of special interest in Lake Michigan is Green Bay, where the quality of water varies from highly polluted at the southern end with an anoxic grey sludge bottom to an almost pristine condition at its northern end with a clean sandy bottom covered with manganese nodules.[16] About thirty trace elements, including nine rare earths, were detected.[17] These nodules were found to have a composition similar to those found in the oceans, except that the concentration of heavy metals like cobalt and tungsten is much lower. Arsenic, however, is an exception. Large concentrations were found in all samples except in sediments taken from the polluted area. As manganese nodules form only under oxidizing conditions, it is interesting to speculate as to what would happen if further pollution increased the area of the anoxic sludge.

References

1. Allaway, W. N. Trace Analysis--Physical Methods, Ed. G. H. Morrison. Interscience, New York, Ch. 3. (1965).
2. Mariscotti, M. A., A method for automatic identification of peaks in the presence of background and its application to spectrum analysis, Nucl. Instr. Methods 50, 304 (1967).
3. Yule, H. P. Computation of experimental results in activation analysis. Modern Trends in Activation Analysis, Ed. J. R. DeVoe. National Bureau of Standards Special Publication 312 (1969) p. 1155.
4. Guinn, V. P. The current status of neutron activation analysis applications. Modern Trends in Activation Analysis. Ed. J. R. DeVoe. National Bureau of Standards Special Publication 312 (1969) p. 679.
5. Dooley, J. A. Measurement and comparison of detector efficiencies. Modern Trends in Activation Analysis. Ed. J. R. DeVoe. National Bureau of Standards Special Publication 312 (1969), p. 1043.
6. Sjöstrand, B. Simultaneous determination of mercury and arsenic in biological and organic materials by activation analysis. Anal. Chem. 36 (4), 814 (1964.
7. Gleit, C. E. and W. D. Holland. Use of electrically excited oxygen for the low temperature decomposition of organic substances. Anal. Chem. 34 (11), 1454 (1962).
8. Edgington, D. N. and H. F. Lucas, Jr. A system for the neutron activation analysis of trace elements in samples of biological and environmental interest. J. Radioanal. Chem., (in press).
9. Peterson, S. F., A. Travesi, and G. H. Morrison. Rapid group separation method for neutron activation analysis of geological materials. Modern Trends in Activation Analysis, Ed. J. R. DeVoe. National Bureau of Standards Special Publication 312 (1969), p. 624.
10. Parr, R. M., H. F. Lucas, Jr. A rigorous least-squares analysis of complex gamma-ray spectra with partial compensation for instrumental instability. IEEE Trans. Nucl. Sci. NS-11 (3), 349 (1964).
11. Lucas, H. F., Jr. and D. N. Edgington. Computer analysis of gamma-ray spectra: validity of the results. Modern Trends in Activation Analysis, Ed. J. R. DeVoe. National Bureau of Standards Special Publication 312 (1969), p. 1207.
12. Gunnink, R., H. B. Levy, and J. B. Niday. Identification and Determination of Gamma Emitters by Computer Analysis of Ge(Li) Spectra. U.S. Atomic Energy Commission Report UCID-15140 (1967).
13. Voigt, A. F., D. E. Becknell, and L. Menapace, Sr. Comparison of solid state and scintillation gamma ray spectrometry in analysis. Modern Trends in Activation Analysis, Ed. J. R. DeVoe. National Bureau of Standards Special Publication 312 (1969) p. 1035.
14. Lucas, H. F., Jr. and D. N. Edgington. Unpublished data.
15. Lucas, H. F., Jr., D. N. Edgington, and P. J. Colby. Distribution of trace minerals in Great Lakes fishes. J. Fisheries Research Board Can. 27 (4), 677 (1970).

16. Rossmann, R. and E. Callender. Manganese nodules in Lake Michigan, Science 162, 1123 (1968).
17. Edgington, D. N. and E. Callender. Minor element geochemistry of Lake Michigan ferromanganese nodules. Earth and Planetary Sci. Letters 8 (2), 97 (1970).

AN AUTOMATIC SEQUENTIAL RAIN SAMPLER*

D. F. Gatz, R. F. Selman, R. K. Langs,
and R. B. Holtzman

A sequential rain sampler has been developed that collects up to 70 samples from 35 to 70 mm of rain. Each sample has a volume of 500 to 1000 ml and represents 0.5 mm to 1.0 mm of rain. After all bottles are filled, any additional rain is automatically discharged. The area of the collector is 1 square meter. All surfaces touched by the rain water, including the bottles used to contain the samples, are polyethylene or Teflon. After every sample, an event mark is recorded on a strip chart; at the first mark, the chart speed increases from 3.8 cm/hr to 3.8 cm/min. This provides adequate resolution between event marks for the computation of rainfall rate. If a time reference is provided while the chart is on fast speed, the starting and ending times of individual samples are known within 1 sec.

*Abstract of paper presented at the 1970 Precipitation Scavenging Meeting, Richland, Washington, June 1-4, 1970, and to appear in the proceedings of that conference in the AEC Symposium Series. Also accepted for publication in Journal of Applied Meteorology.

THERMAL NEUTRON ACTIVATION ANALYSIS OF PURIFIED BIOLOGICAL MEMBRANES*

S. S. Brar, D. M. Nelson, Y.-E. Rahman[+] and E. A. Cerny[+]

Purpose and Methods

Biological functions of some trace elements have been extensively studied in recent years. These elements play essential roles in many intracellular catalytic reactions, and a few are essential components of many enzyme molecules.[1]

Although trace elements are widespread in animal and plant tissues, their intracellular distributions are poorly known because subfractionation of tissues usually yields amounts inadequate for chemical analyses. Because neutron activation analysis has proved valuable in quantitative determinations of minute samples, experiments were initiated to apply this method of analyzing subcellular fractions, with emphasis on purified intracellular membranes. Although we used rat liver in this preliminary study, we intend to extend the study to other tissues as the technical aspect of the program becomes well established.

Female rats of SD/Anl (Anl 66) strain were used throughout these experiments. Lysosomes were prepared by the flotation method described by Trouet;[2] membranes were further isolated from these particles by the method described previously.[3] Mitochondria also were purified by a previously described method.[3] They were further subfractionated into inner and outer membranes according to a method described by Jones and Jones.[4] Endoplasmic reticulum and their subfractions, i.e., smooth membranes, rough membranes, and free polysomes, were purified by a method of Bloemendal et al.[5] Nuclei were purified by the method of Blobel and Potter.[6]

---

*This report also appears in Argonne National Laboratory, Division of Biological and Medical Research Annual Report, ANL-7770 (1970).

[+]Division of Biological and Medical Research.

The purity of each of these subcellular fractions was confirmed by electron microscopy and by the determination of marker enzymes.

Samples were dried at 90° C in an oven for 24 to 36 hours. A known quantity of each sample was placed in a polyethylene capsule, which was irradiated at Ames in the Iowa State University reactor (flux approximately 1×10^{13} n/cm^2/sec). The irradiation time for all samples was 13 hours and 35 minutes. Except for ^{140}La, this analysis was restricted to "long-lived" nuclides. Gamma-ray spectrometry was done in conjunction with a 35-cc Ge(Li) detector and a 4096-channel analyzer. The first analysis began about 10 days after irradiation, with each sample counted for 20,000 seconds. The analysis was repeated (except for ^{140}La) approximately 53 days after irradiation, with each sample counted for 60,000 seconds (1000 minutes). Gamma-ray analysis was by a peak integration method furnished by Henry Lucas of Radiological Physics Division.

Progress Report

Table 1 is a summary of gamma-ray emitting nuclides in various samples under study. As the concentrations of these elements have not been quantitated, results should be read as relative values and compared from one category of preparations against the others.

Conclusions

1. Iron, zinc, cobalt, chromium, antimony, rubidium, selenium, and lanthanum were found in the samples tested. The first 4 elements were found in all samples, while the last 4 elements were absent from some.

2. Lysosomal membranes have the highest content of iron, zinc, cobalt, and chromium per unit dried weight. The content of zinc and chromium varied widely from one preparation to the other; this might be due to a difference in food intake and absorption.

3. Mitochondria have a relatively high zinc content, and this element seems mainly to be localized in the inner membranes. The inner membranes, however, had only a small fraction of the iron, chromium, and

TABLE 1. Gamma-ray Emitting Nuclides in Tissue Samples.

		Half-life, days							
		45.00	245.0	19.21	27.80	60.20	18.66	120.0	1.667
		^{59}Fe	^{65}Zn	^{60}Co	^{51}Cr	^{124}Sb	^{86}Rb	^{75}Se	^{140}La
Sample[a]	Dry sample weight, mg	Counts/100 min/10 mg dry sample							
Lysosomal membranes (1)	14.2	1,700	42,000	260	1,100	3	-	180	-
Lysosomal membranes (2)	20.0	1,900	6,000	110	350	8	33	180	16
Lysosomal membranes (3)	16.7	1,300	1,400	71	3,500	4	130	55	-
Lysosomal membranes (4)	13.3	1,300	790	220	2,000	-	46	89	21
Unfractionated mitochondria	80.7	110	700	38	160	5	120	140	14
Mitochondrial inner membranes	155.2	53	670	33	41	5	6	86	-
Unfractionated endoplasmic reticulum (1)	146.5	540	290	5	46	-	32	17	-
Unfractionated endoplasmic reticulum (2)	85.4	1,500	450	7	120	1	98	38	-
Smooth membranes of endoplasmic reticulum (1)	51.4	140	57	1	37	12	19	6	10
Smooth membranes endoplasmic reticulum (2)	112.0	180	160	2	18	3	120	27	7
Nuclei	142.4	22	140	2	63	1	3	-	-

[a]The number in parentheses represents separate preparations from different groups of animals.

rubidium, compared with the concentrations of these elements in the whole mitochondria.

4. Endoplasmic reticulum has a high concentration of iron and zinc, and a very low concentration of cobalt. Concentrations of these first two elements, however, were much lower in the smooth membranes, compared with the whole endoplasmic reticulum fraction.

5. Purified nuclei have few trace elements, and their concentrations are low; the concentration of zinc is highest among elements.

6. The above results indicate that neutron activation analysis is valuable for the studies of purified biological membranes. Work is in progress to quantitate these elements, and it is intended to apply this

method to other biological membranes, including those from normal and pathological human tissues. Other biologically important elements, including arsenic, mercury, calcium, magnesium, vanadium, manganese, copper, and nickel, will also be included in this study.

References

1. Bowen, H. J. M. Trace Elements in Biochemistry, Academic Press, New York, 1966.
2. Trouet, A. Arch. Int. Physiol. 72, 698-700 (1964).
3. Rahman, Y.-E., J. Verhagen, and D. F. M. v.d. Wiel. Biochem. Biophys. Res. Commun. 38, 670-677 (1970).
4. Jones, M. S. and O. T. G. Jones. Biochem. J. 113, 507-514 (1969).
5. Bloemendal, H., W. S. Bont, M. de Vries, and E. L. Benedetti. Biochem. J. 103, 177-182 (1967).
6. Blobel, B. and V. R. Potter. Science 154, 1662-1665 (1966).

PUBLICATIONS

Brar, S. S., D. M. Nelson, E. L. Kanabrocki, C. E. Moore, C. D. Burnham, and D. M. Hattori. Thermal Neutron Activation Analysis of Particulate Matter in Surface Air of the Chicago Metropolitan Area. One-Minute Irradiations. J. Environ. Sci. Tech. 4, 50-54 (January 1970).

Brar, S. S., D. M. Nelson, J. R. Kline, P. F. Gustafson, E. L. Kanabrocki, and C. E. Moore. Instrumental Analysis for Trace Elements Present in Chicago Area Surface Air. J. Geophys. Res. 75 (15), 2939-45 (1970).

Carson, J. E. and H. Moses. The Validity of Several Plume Rise Formulas. J. Air Poll. Control Assoc. 19, 862-866 (1969).

Carson, J. E. and H. Moses. Plume Rise Formulas. J. Air Poll. Control Assoc. 20, 476-477 (1970).

Edgington, D. N. and E. Callender. Minor Element Geochemistry of Lake Michigan Ferromanganese Nodules. Earth Planetary Sci. Letters 8, 97-100 (1970).

Edgington, D. N. and H. F. Lucas, Jr. A System for the Neutron Activation Analysis of Trace Elements in Samples of Biological and Environmental Interest. J. Radioanalyt. Chem. 5, 233-250 (1970).

Gustafson, P. F. Nuclear Power and Thermal Pollution: Zion, Illinois. Bull. Atom. Sci. 26, 17-23 (March 1970).

Jordan, Carl F. Derivation of Leaf Area Index from Quality of Light on the Forest Floor. Ecology 50, 663-666 (1969).

Jordan, Carl F., J. J. Koranda, J. R. Kline, and J. R. Martin. Tritium Movement in a Tropical Ecosystem. BioScience 20, 807-812 (1970).

Kline, J. R. and S. S. Brar. Instrumental Analysis of Neutron Irradiated Soils. Soil Sci. Soc. Am. Proc. 33 (2), 234-238 (March-April 1969).

Kline, J. R. and S. S. Brar. Instrumental Analysis of Neutron-Irradiated Soils. Isotopes Radiat. Technol. 7 (3), 319-324 (Spring 1970).

Lucas, H. F., Jr., D. N. Edgington, and P. J. Colby. Concentrations of Trace Elements in Great Lakes Fishes. J. Fish. Res. Bd. Canada 27, 677-684 (1970).

X

ARGONNE NATIONAL LAB WEST
3 4444 00010935 5

B